ALKALINE IGNEOUS ROCKS OF THE COASTAL BELT, SOUTH OF LUDERITZ, SOUTH WEST AFRICA: A PETROLOGICAL STUDY

JULIAN SAVILLE MARSH

Thesis submitted for the degree of
Ph.D. in the Faculty of Science,
University of Cape Town

Department of Geology
University of Cape Town
September, 1973.

INDEX

ABSTRACT

The Luderitz Alkaline Province, as it is at present known, comprises the subvolcanic central complexes of Drachenberg, Pomona, and Granitberg. An attendant dyke swarm strikes NE-SW and crops out between the latitudes of 27°00' and 27°30' S. Stratigraphic indications (now confirmed by a K/Ar age from Granitberg) are that the Luderitz Province is early-Cretaceous in age and therefore older than the Klinghardt phonolites (Eocene) as well as the smaller melilitite and nephelinite intrusions.

Granitberg is a circular foyaite complex, in the centre of which is preserved a large fragment of sedimentary rocks that originally formed the roof of the intrusion. The foyaites have been emplaced into the feldspathic sandstones and dolomites of the Bogenfels Formation, and three major intrusive phases can be recognised.

The first phase produced chilled nepheline syenites beneath the roof of the intrusion. These chilled rocks grade downwards into coarse-grained foyaites. The second phase was the emplacement of the Inner Foyaite which crystallized as a cylindrically zoned plug, capped by a zone of layered, laminated, and xenolith-rich foyaites. The third phase was the emplacement of the Outer Foyaite, into which the Roof Zone and the Inner Foyaite foundered. The Outer Foyaite is zoned with a miaskitic core, and an agpaitic outer zone.

The Outer Foyaite interfingers repeatedly with thinly bedded sediments at the contact zones. Assimilation - fractional crystallization processes operating at these sandstone-foyaite contacts have generated a suite of pulaskites, peralkaline nordmarkites, and peralkaline granites, which intrude the sedimentary rocks as thin sheets. Similarly, at dolomite-foyaite contacts, melteigite-ijolite-urtite and shonkinite-pulaskite suites have been generated.

Metasomatic effects accompanying the foyaite emplacement are also evident. The Roof Zone sediments have undergone fenitization, giving rise to aegirine- and arfvedsonite-bearing fenites. At the West Ridge contact, Ca-Mg metasomatism has dominated over alkali metasomatism, resulting in the production of diopside-quartz-perthite and diopside-perthite metasomatites. In the NE contact zone the dolomitic sediments have been metamorphosed under conditions of high fH_2O/fCO_2 and at T = 450° to 525°C, to produce forsterite- and diopside-bearing assemblages.

The Pomona complex is a well developed ring complex, with a distinct radial dyke pattern. Successive intrusion of the Outer Syenite, the Inner

Syenite, the Hub Syenite, and the Outer Ring Dyke define a silica-oversaturated, peralkaline trend which culminates in the widespread development of quartz-bostonite dykes. Quartz-feldspar porphyry dykes are associated with explosively emplaced igneous breccias at the NE edge of the complex. Tinguaite dykes and a small plug of nepheline syenite intrude the Inner Syenite in the core of the complex. Exposures of Biotite-rich Monzonite occur within the Inner Syenite outcrop area, and possibly represent a cumulate developed during the evolution of the suite of syenites.

The Pomona syenites intrude granitic and granodioritic gneisses of pre-Gariep age, and assimilation processes in the contact zone have generated silicic liquids which manifest themselves as numerous nordmarkitic and granitic veins and dykelets that anastomoze through the gneisses in the contact zone.

The Drachenberg complex is poorly exposed. A number of saturated and oversaturated syenites outcrop through thick sand cover which obscures the relationships between these various syenite types. No feldspathoid-bearing rocks are present, nor are any of the syenites peralkaline. The silica-oversaturated trend defined by the Drachenberg syenites has culminated in the intrusion of quartz-bostonite and quartz-feldspar porphyry dykes.

The complex is emplaced into pre-Gariep schists and granites. The contact, where exposed, is sharp, and orthopyroxene- and cordierite-bearing hornfelses occur in the contact zones, indicating metamorphic temperatures of about 600°C at the prevailing pressures (estimated less than 1,5 Kb).

Chemical analyses of the syenites from the complexes have been carried out using X-ray fluorescence spectrometry. Consideration of the major elements plotted in the system Na_2O-K_2O-Al_2O_3-SiO_2 suggests that alkali feldspar fractionation has been dominant control in the evolution of the syenites, especially the nepheline syenites. Trace element abundances and inter-element ratios confirm this and also indicate that the syenites from each complex have an independent origin and evolution. The silica undersaturated suite is similar to typical trachybasanite - phonolite suites which have evolved from a basanite parent. The Drachenberg and Pomona syenites are typical trachyte - alkali rhyolite suites and probably evolved from alkali basalt parents. None of these suites can, however, be reconciled to a common parent.

The "normal" behaviour of several elements appears to break down in peralkaline liquids, and the behaviour of these elements in silica over- and under-

saturated environments appears also to be different. Ca is capable of extreme depletion in silicic liquids, but it appears to stabilize in the residual liquids in undersaturated suites so that it is always significantly present, regardless of degree of fractionation. Rb is often considerably enriched in silicic liquids, but only rarely so in silica-undersaturated liquids, due possibly to the ease with which Rb enters nepheline.

Zr and Nb have a complicated behaviour in peralkaline liquids. The Zr/Nb ratio may remain unaffected by fractionation, and a genetically related suite of peralkaline rocks usually possesses a characteristic value of this ratio. Under extreme fractionation the ratio does vary but there appears to be no rule governing the direction or magnitude of the variation. Absolute abundances of Ba and Sr, and the ratios K/Ba and Pb/Sr, are sensitive indicators of fractionation in peralkaline felsic suites, whereas K/Rb is not.

Microprobe analyses of mafic minerals from rocks from Pomona (oversaturated suite) and Granitberg (undersaturated suite) have been carried out. The dominant feature of these analyses is the Mn-enrichment exhibited by these minerals. In the undersaturated suite, the mineral and whole rock data indicate a regular increase in the Fe/(Fe+Mg) ratio with fractionation. In contrast, the oversaturated suite exhibits Mg-enrichment which can be explained by abundant and early precipitation of magnetite under conditions of high fO_2. Biotite, amphibole, and Na-pyroxene composition trends are markedly different for the two suites. The pyroxene composition trend in the Ac - Di - Hd system is strongly influenced by fO_2 and not by the bulk chemistry of the liquid from which they crystallize. It appears that Mg-enrichment trends in salic liquids could be more common than is generally held.

Calculated oxygen fugacities for the Pomona and Granitberg suites confirms the interpretations of the mineral chemistry. Phonolitic liquids crystallize under lower oxygen fugacities than do liquids in the trachyte-rhyolite spectrum, which in turn have lower oxygen fugacities than calc-alkaline rhyolites. This refutes the commonly held notion that nepheline syenites crystallize under high fO_2 conditions.

The petrography of perovskite-bearing nepheline syenites at Granitberg, together with thermochemical considerations, indicate that a number of factors influence the relative stabilities of sphene and perovskite. Perovskite may crystallize in equilibrium with alkali feldspar and other phases in a peralkaline liquid at relatively high silica activities. Under such conditions low fO_2

favours the precipitation of sphene, whereas higher fO_2 favours crystallization of perovskite.

A no-oxide field in fO_2 - T space, in which aenigmatite crystallizes at the expense of an Fe-Ti oxide, exists in undersaturated liquids. The field is more restricted in fO_2-T space in these liquids than in their oversaturated counterparts. In the case of the aenigmatite-bearing foyaites at Granitberg, the lower termination of the no-oxide field is almost certainly the stability field of Na-amphibole. It appears that astrophyllite has a stability field similar to that of these Na-amphiboles.

The origin and evolution of the Luderitz Province must be considered in the context of the Karroo tholeiitic volcanism and the South America - Africa split leading to the formation of the South Atlantic. It is postulated that the alkaline rocks evolved by crystal fractionation from alkali basalt and basanite parental magmas. These magmas have been tapped at depths greater than 35 km beneath the edges of the continental crust by fracturing associated with the formation of transform faults and fracture zones. The disposition of a number of alkaline complex lineaments in Africa and South America is shown to be related to these transform fractures. The ascent into the upper crust, and the eventual eruption of these alkaline basic magmas and their derivatives, appears to be controlled by gross regional structures in the upper crust.

ABBREVIATIONS

A number of abbreviations have been used in the text of this thesis. Most of them are standard, but some are specific for the purpose for which they are used here. To avoid confusion a full list is presented below.

PCNS - Porphyritic Chilled Nepheline Syenite from Granitberg

m, cm, mm - meter, centimeter, milimeter

km - kilometer

Kb - kilobars (pressure)

my - million years

msl - mean sea level

fO_2 - oxygen fugacity

fH_2O - fugacity of steam

fCO_2 - fugacity of carbon dioxide

$a^{pyroxene}_{acmite}$ - activity of acmite in the pyroxene

$x^{pyroxene}_{acmite}$ - mole fraction of acmite in the pyroxene

ΔG^{o}_{r} - standard free energy of the reaction

ΔG^{o}_{f298} - standard free energy of formation from elements at 298,15°K

ΔG^{o}_{fT} - standard free energy of formation at temperature T°K

S^{o}_{298} - standard Third Law entropy at 298,15°K

ΔS^{o}_{fT} - standard entropy of formation from the elements at temperature, T

ΔH^{o}_{f298} - standard enthalpy of formation at 298,15°K

R - Gas constant per mole

D - distribution coefficient of a given element between crystal and liquid

NOMENCLATURE

For the alkaline rocks studied in this thesis, it has been found convenient to adopt a broad and rather imprecise nomenclature. The details of texture and mineralogy of the various rocks are however recorded in the petrographic descriptions. It must be noted that for the Luderitz Province rocks, textural attributes are of secondary importance in the classification scheme outlined below.

(a) Nepheline syenite and Foyaite are used interchangeably.

(b) Pulaskite refers to a leucocratic syenite with a few percent modal nepheline.

(c) Nordmarkite refers to a leucocratic syenite with a few percent modal quartz, and is used interchangeably with quartz syenite.

(d) Tinguaite is the dyke equivalent to a nepheline syenite.

(e) Bostonites and quartz-bostonites are the dyke equivalents of extremely leucocratic syenites and quartz-syenites.

(f) Grorudite is an aegirine-rich quartz-bostonite.

CHAPTER 1

INTRODUCTION

1.1. GENERAL STATEMENT

In 1926 Erich Kaiser published a two-volume memoir - "Die Diamantenwuste, Sudwestafrikas" - which was the result of many years detailed mapping and investigation into the geology of the area covered by the diamond claims of the Vereinigten Diamantminen in the coastal area south of Luderitz, S.W.A. The memoir contains maps and a comprehensive petrographic account of the felsic alkaline rocks of the Granitberg complex and the Pomona complex (which is called the Signal-Schlueberg Massif in the memoir) as well as all the dykes and minor plugs in the claim areas. Brief mention is also made of the occurrence of similar rocks at Drachenberg to the east of the claim areas.

In the same memoir, a chapter contributed by W. Beetz mentions the occurrence of syenites in the Naras Hills, south of the Klinghardt mountains (p. 175). This chapter had appeared earlier in English as a separate paper (Beetz, 1924).

The 1:1 000 000 Geological Map of South West Africa (1963) shows the Granitberg, Pomona, and Drachenberg intrusions as well as an occurrence at Marmora, near Angras Juntas. No other reference to this occurrence exists.

Kaiser (1926) also describes the widespread occurrence of phonolites which build the Klinghardt Mountains. He found these phonolites to be of Tertiary age, and considered the Granitberg suite of rocks to be older. These suggestions have since been substantiated by isotopic age determinations (see chapter 2).

1.2. THE PRESENT INVESTIGATION

The purpose of the present investigation is to confirm the existence of all reported occurrences of pre-Tertiary alkaline rocks, and to undertake a thorough investigation of the mineralogy and petrology of the major intrusive complexes, in an attempt to define their origin and evolution.

Field work was conducted during 1970 and 1971 and it was soon established that the reported intrusion at Marmora did not exist. Apart from the map in Beetz's (1924) paper, the Naras Hills is recorded on no other map of the Sperrgebiedt. A careful airphotograph study of the

supposed locality south of the Klinghardt Mountains revealed extensive sand dune cover with very little hard rock outcrop. Access to these outcrops by vehicle proved impossible, and the existence of any syenites in the dune belt remains unsubstantiated. If the Naras Hills syenite does exist, there is some evidence that it is older than the Luderitz Province rocks (see chapter 2).

The name Luderitz Alkaline Province is proposed to refer to the Cretaceous alkaline rocks in the southern Namib. As it is presently known the province comprises the syenite-foyaite complexes of Granitberg, Pomona, and Drachenberg and the attendant dyke swarm which has an ENE trend and outcrops extensively between Prinzenbucht and Bogenfels (Figure 1). The area to the east of that mapped by Kaiser is at present geologically unknown, and it does not seem unlikely that extensions to the Luderitz Province may yet be found to the east of Drachenberg. In this respect consideration should be given to the occurrences listed by Kaiser (1926, p. 217 - 218), especially those of the Koviesberg, the Tsirub area, and the Dicken Willem or Garubberg, all east of Luderitz, in the vicinity of Aus. The carbonate rocks at Dicken Willem have recently been interpreted as magmatic in origin, i.e. carbonatitic (De Villiers, 1971, p. 49), an interpretation which is supported by the presence of tinguaite dykes there (Kaiser, 1926, p. 218, 242), and it seems possible that the Dicken Willem (Garubberg) is a carbonatite - alkaline rock complex. De Villiers (1971) correlated this occurrence with the Klinghardt phonolites, but since the outcrops have been exposed by the "African" erosion cycle (King, 1951, p. 249) and occur above the End-Cretaceous erosion surface (Hallam 1964), this correlation cannot be supported, and it is more likely that this "carbonatite" is related to the Granitberg-Pomona-Drachenberg suite of rocks.

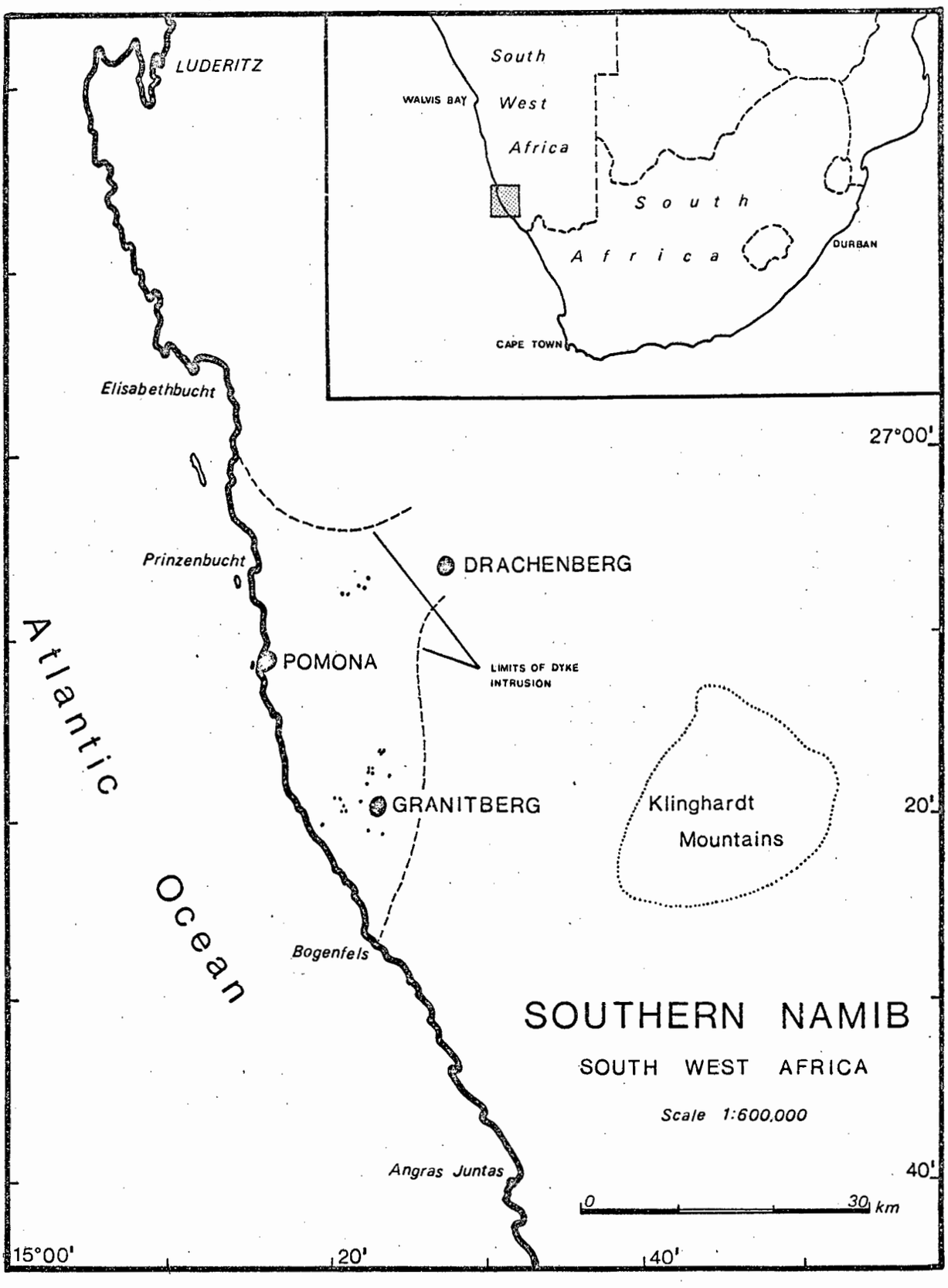

Figure 1. Locality map showing the distribution of the major intrusive complexes, minor bostonite plugs, and the limits of the dyke swarm.

CHAPTER 2

THE AGE OF THE LUDERITZ ALKALINE PROVINCE

The intrusive relationship between igneous rocks of the Luderitz Province and the Bogenfels Formation has never been doubted, thus fixing the lower limit for the age of these intrusive rocks. Kaiser (1926) found the upper limit more difficult to define. Beetz (1924, p. 16) observed that the syenites in the Naras Hills, which he correlated with the Granitberg-Pomona-Drachenberg suite of rocks, outcrop at the same level as the extrusive Klinghardt phonolites, and deduced that the syenite is older than the phonolite. At Swartkop the phonolites are reported by Kaiser (1926) to overlie, and to have baked, the Eocene quartzites of the Pomona Beds. K/Ar (whole rock) age determinations on two samples of this phonolite give ages of 37 $\pm$ 1 my and 35,7 my (G.C. Stocken, private communication) confirming the paleontological findings of Kaiser (1926). Provided Beetz's correlation is correct the Luderitz province rocks would appear to be older than Oligocene. However, this correlation can be questioned in the light of Kaiser's (1926, p. 218) statement that the Naras Hills syenite is similar to the syenite at Namtib, 50 km NE of Garub. The latter occurrence has recently been described by Von Brunn (1967) as a facies of the GT Granites of that area. These granites have been dated by the Rb/Sr (whole rock) method at 1290 $\pm$ 80 my (Von Brunn, 1969), and by inference the age of the syenite must be similar. If the Naras Hills syenites are correlates of the Namtib syenite, then they do not belong to the alkaline rocks which are the subject of this study.

The relationship between alkaline rocks of the Luderitz province and the Pomona Beds, and the End-Cretaceous erosion surface (Hallam, 1964) on which the latter lie, may be seen at the Chalcedontafelberg, which is capped by a thick silcrete of Tertiary age. None of the bostonite and syenite porphyry dykes in the area intrude the silcrete, and although the silcrete is not seen to overlie the alkaline rocks directly, the latter are deeply weathered to many metres below the erosion surface (Kaiser, 1926, p. 297). Kaiser relates this weathering to the End-Cretaceous erosion cycle and concludes that the bostonites must be pre-Tertiary in age.

Further evidence with regard to the age of the Luderitz alkaline rocks and particularly Granitberg, is afforded by the summit height of Granitberg and the height of the End-Cretaceous erosion surface as it is measured at Chalcedontafelberg, the various tafelberge east of Pomona, and the Buntfeldschuh escarpment. Kaiser (1926, p. 252) gives the following heights:-

Granitberg..... 225 m
Chalcedontafelberg..... 204 m
Tafelberg E of Pomona ... 206 m
Buntfeldschuh..... 234 m

Verwoerd (1968, p. 244), using these heights, and incorrectly identifying the erosion surface as pre-Cretaceous, argued that Granitberg is older than Cretaceous in age. In fact the heights given by Kaiser are themselves incorrect. The latest 1:50 000 topo sheet, LUDERITZ SHEET 2715 AD, issued by the Government Printer assigns the following heights:-

Granitberg..... 252 m
Chalcedontafelberg..... 214 m

Granitberg is some 40 - 50 m higher than the End-Cretaceous erosion surface and therefore cannot be younger than this surface. During the present investigation some thin calcareous sandstones and pebbly limestones were found at Granitberg, in a small outcrop in the sand cover of the Roof Zone, due west of the trig beacon and about 40 m below it. This outcrop is correlated with the Tertiary Pomona Beds, and thus confirms the pre-Tertiary age for Granitberg. Furthermore the syenites at Drachenberg outcrop on the erosion surface and must therefore be older.

Several instances of dyke rocks of the Luderitz Province cutting dolerite dykes correlated with the Karroo basic volcanicity, have been noted by Kaiser (1926). Kaokoveld (Karroo) lavas and dolerites in Damaraland are Late-Jurassic to Early-Cretaceous in age (Siedner and Miller, 1968), and a similar age for the dolerites south of Luderitz can be expected. This would appear to confine the age of the Luderitz alkaline rocks to the period between the dolerite intrusions at the end of the Jurassic, and the formation of the erosion surface at the end of the Cretaceous.

Recently all these stratigraphic ages for the Luderitz alkaline rocks have been confirmed by an isotopic age determination for Granitberg.

Biotite from a foyaite yielded a K/Ar age of 130 $\pm$ 2 my (G.C. Stocken, private communication). To date no other determinations are available from the other complexes.

The ages of the minor intrusions of ultrabasic and basic alkaline rocks (limburgite, nephelinite, and melilite basalt at Dreyerrucken, Chalcedontafelberg and Schwarzenberg) are more problematical. No isotopic ages are available for these rocks. Kaiser (1926, p. 497) correlated them with the syenitic intrusions of the Luderitz province, but both he (1926, p. 297) and Beetz (1924, p. 16) recorded that both the limburgite and melilite basalt cut the silcrete capping the Chalcedontafelberg. This implies that these rocks are post-Eocene and should possibly be correlated with the Klinghardt volcanism. During the present investigation the outcrops at the Chalcedontafelberg were examined but the relationships are largely obscured by rubble and could not be determined with any certainty. Accepting Kaiser and Beetz's record one must conclude that these basic rocks are not related to the Luderitz alkaline suite. With regard to the correlation with the Klinghardt phonolites one must note Beetz's (1924, p. 16) observation that there may be two phases of basic igneous activity - one at least younger than the Klinghardt volcanicity.

CHAPTER 3

3.1. INTRODUCTION

The Granitberg Foyaite Complex lies 11 km north of the abandoned mining camp of Bogenfels in Diamond Area No. 1, South West Africa. Access to the intrusion is provided by the remaining sections of the original Pomona - Bogenfels road and a narrow gauge railway line embankment, both dating back to pre-World War 1 days. The near-circular complex is 2,5 km in diameter and forms a peak 252 m above msl, the highest in the coastal area between Bogenfels and Pomona. The name Granitberg originates from the early reconnaissance exploration of the Namib Desert. Apparently the Foyaite was originally identified as granite, purely on the texture of the rock, and hence the peak which it builds was christened Granitberg (Kaiser, 1926, p. 253).

The complex and the surrounding country rocks are well exposed, the result of excavation by a post-Eocene erosion cycle (Congo cycle? of King 1951). It is estimated that about 70% of the complex outcrops through a cover of wind-blown sand and deflation gravels. The quality of outcrop is excellent. Constant sand blasting by strong southerly winds removes any altered or oxidised rock surfaces, leaving fresh, polished exposures.

The foyaitic rocks which form most of the complex are intrusive into thinly bedded feldspathic sandstones, dolomites and minor shales and phyllites of the Bogenfels Formation of the Gariep Group. Some of these sediments are also preserved in the centre of the intrusion as part of the Roof Zone. On the eastern border of the complex the foyaites are in intrusive contact with granite-gneiss, etc., which underlies the Bogenfels formation.

3.2. PREVIOUS WORK

The foyaitic nature of the rocks at Granitberg was originally established by Wagner (1910). Shand (1915) gives a more complete petrographic description of some of the rock types and dykes. Attracted by the excellent exposure and fascinating contact phenomena in the contact and roof zones, Kaiser made a detailed petrographic study of the various

alkaline rocks and included these descriptions in his memoir on the diamond fields (Kaiser, 1926). Kaiser also lists some chemical analyses but it is clear that most of them are of the more unusual rock types and are of little use in elucidating the petrological development of the complex.

It is not intended here to summarise Kaiser's findings - instead they will be referred to at the relevant places in the following text. Since Kaiser's account is largely descriptive much of it is in agreement with this work, though differences in interpretation naturally do exist.

3.3. EARLY PORPHYRITIC SYENITES

Outcrops of the early porphyritic syenites are confined to two large tongues lying to the SW and NW of the complex, and to a few small scattered plugs S of the main body of intrusive rocks. Field relationships indicate that they are probably the earliest phase of intrusion in the complex. They are cut by all the dyke rocks of the complex, the alkali granite and nordmarkite bodies related to the intrusion of the Outer Foyaite.

Individual outcrops of these rocks differ somewhat in their form and field characteristics. The poorly exposed occurrences in the south are vertical plug-like bodies that develop a narrow chilled facies at the contact. They are typical rhomb porphyries with square phenocrysts of alkali feldspar enclosed in a fine-grained groundmass displaying a high degree of alteration. The phenocryst-groundmass ratio in these rocks is generally 1 : 5. The plugs are for most part in contact with dolomites which only show minor effects of recrystallization within 1 - 2 cm of the contact. Contacts with the feldspathic sandstones are largely obscured by rubble.

The largest outcrop of syenite porphyry occurs west of the railway embankment, SW of the complex. The exact form of the occurrence is unclear. It appears to be a sheet of limited extent, which dips slightly to the south, and from which the cover rocks have been stripped by erosion. In outcrop the rock is dark grey to brown depending on the extent of oxidation. It differs petrographically from the plugs in the south in two striking respects.

(a) The phenocryst:groundmass ratio is high, and is generally of the order of 50 : 50 and occasionally 70 : 30. In places the rock is tightly packed with alkali feldspar phenocrysts.

(b) The rock encloses a large number of inclusions and xenoliths. The size of the xenoliths varies from <1 mm up to fragments of 1,0 m across, and may be both angular and rounded. The inclusions are fragments of country rock and recognisable syenitic and foyaitic rocks.

Fragments of the country rocks are mostly dolomite, sandstone and minor shales. The alkaline igneous rocks are generally coarse to medium grained rocks which exhibit textures and mineralogy reminiscent of the various rock types of the Roof Zone. Despite the designation of these porphyries as the earliest intrusive phase of the complex, the nature of the inclusions indicate that they might be immediately post- or contemporaneous with the emplacement of the Roof Zone rocks.

The only other outcrop of syenite porphyry occurs between the railway embankment and the jeep track to the NNW of the complex. It is in the form of a narrow tongue, some 900 m long and up to 60 m wide, intruded into feldspathic sandstones. The exact form of this intrusive body is difficult to determine, but it appears to be a vertical dyke-like body. It is a dark porphyritic rock and in appearance in the field is very similar to the SW Tongue. Only a few xenoliths are however present. The southern end of the tongue lies close to the main outcrop of the Outer Foyaite of the complex, and is intruded by several alkali - granite - nordmarkite - pulaskite bodies which are related through assimilation to the Outer Foyaite (see section 3.6.3.).

3.3.1. Petrographic Features

All specimens of the syenite porphyry examined in thin section are highly altered. The rocks are porphyritic, or occasionally glomeroporphyritic, with a high phenocryst/groundmass ratio, estimated to be from 1 to 4. The phenocrysts range in size from 0,2 to 0,5 mm up to 8 to 10 mm.

Alkali feldspar is the dominant phenocryst phase and occurs as heavily altered, euhedral crystals which occasionally display simple Carlsbad twins. Pseudomorphs after euhedral mafic minerals form about

5 to 10% of the rock. They are strongly oxidised and consist largely of intergrowths of opaque oxide, carbonate, and an unidentifiable dark brown mineral. Their well preserved prismatic form indicates that they may have originally been pyroxene or amphibole. Occasional square phenocrysts, possibly originally nepheline, are now largely occupied by colourless phyllosilicates of which, it is assumed, paragonite is dominant.

Of the minor constituents the only identifiable mineral is apatite. It occurs as eu- to subhedral, clear, unaltered crystals up to 0,1 mm in length.

The groundmass material is highly altered and apart from a peppering of opaque oxides, the intergrown minerals are too small to identify. Calcite is commonly seen filling veins, and may occur in the groundmass as well, and is most likely of secondary origin.

3.4. THE ROOF ZONE

3.4.1. Introduction

The Roof Zone is a petrographically complex, circular structural entity occupying a position SW of the centre of the complex. Kaiser (1926) noted sediments and "hybride Mischgesteine" in the central portion of the intrusion, but his mapping was too generalised for him to appreciate the structural significance of these rocks. He did however recognise that the sediments must have formed part of the roof of the intrusion and deduced (p. 256) "dass hier das Dach des Injektionskorpers nahe uber der Heutigen Denudationsflache gelegen hat" (that the roof of the intrusive body must have lain close above the present erosion surface). Kaiser also gives petrographic descriptions of most of the rock types in the roof zone, but failed to recognise the often subtle relationships between them - a feature which is the key to unravelling much of the development of the complex as a whole.

In a gross way the Roof Zone can be thought of as a horizontally layered unit built up of successively crystallized, intrusive nepheline syenites, of diverse textural type. The exact sequence of rocks varies considerably, and at any one place in the Roof Zone the succession may differ from the next. The Roof Zone has also suffered faulting and

fragmentation. The faults are now largely occupied by dykes (tinguaites), many of which do not extend beyond the boundaries of the Roof Zone. Vertical movements on the faults and tilting of faulted units has resulted in a mosaic-like pattern whereby rocks from different stratigraphic horizons now lie adjacent to one another. Generally the vertical throw on the faults is small, and since many are marked by sand-filled depression features, possible faulted boundaries and contacts are difficult to distinguish from intrusive and the relatively rapid gradational contacts between the various igneous rocks. No attempt has been made to depict possible faulted contacts on the 1:10 000 map.

The Roof Zone outcrops on a gentle SW-facing slope which provides an adequate 80 - 100 m section through the essentially horizontal sequence. The sequence of rock types and their relationships is summarised diagrammatically in Figure 2 and is discussed below.

To facilitate description of the various features in the Roof Zone two topographically prominent features have been given the names Central Massif and East Massif. Their location is illustrated in Figure 3.

3.4.2. Sedimentary rocks of the Bogenfels formation

Sedimentary rocks of the Bogenfels Formation - assumed to be the original roof of the intrusion - crop out at various places in the Roof Zone. The largest occurrence of sedimentary rocks underlies the northern sector of the Roof Zone, though the exposures are poor. Here thinly bedded, low-grade schists and phyllites, felspathic sandstones and quartzite crop out with a regular NW strike and variable southerly dips. Similar rocks are found in smaller exposures on the Central and East Massifs. Kaiser (1926) correlated these sediments with the Kuibis quartzite of his "Folded Nama" i.e. the arenaceous rocks which crop out along the SW contact zone. No attempt was made to substantiate this correlation during this investigation, but this correlation is undoubtedly correct though these sediments are no longer regarded as folded Nama (Martin, 1965; Kroner, 1972). Kaiser also recorded the existence of extensive areas of Bedded Dolomite in the Roof Zone. During the present investigation only one small outcrop of dolomitic rocks was found a few metres east of the jeep track in the NW section of the Roof Zone. Here dolomites, arkoses, and phyllites form a small roof pendant, or raft, surrounded and intruded by dark, fine to medium grained, contaminated

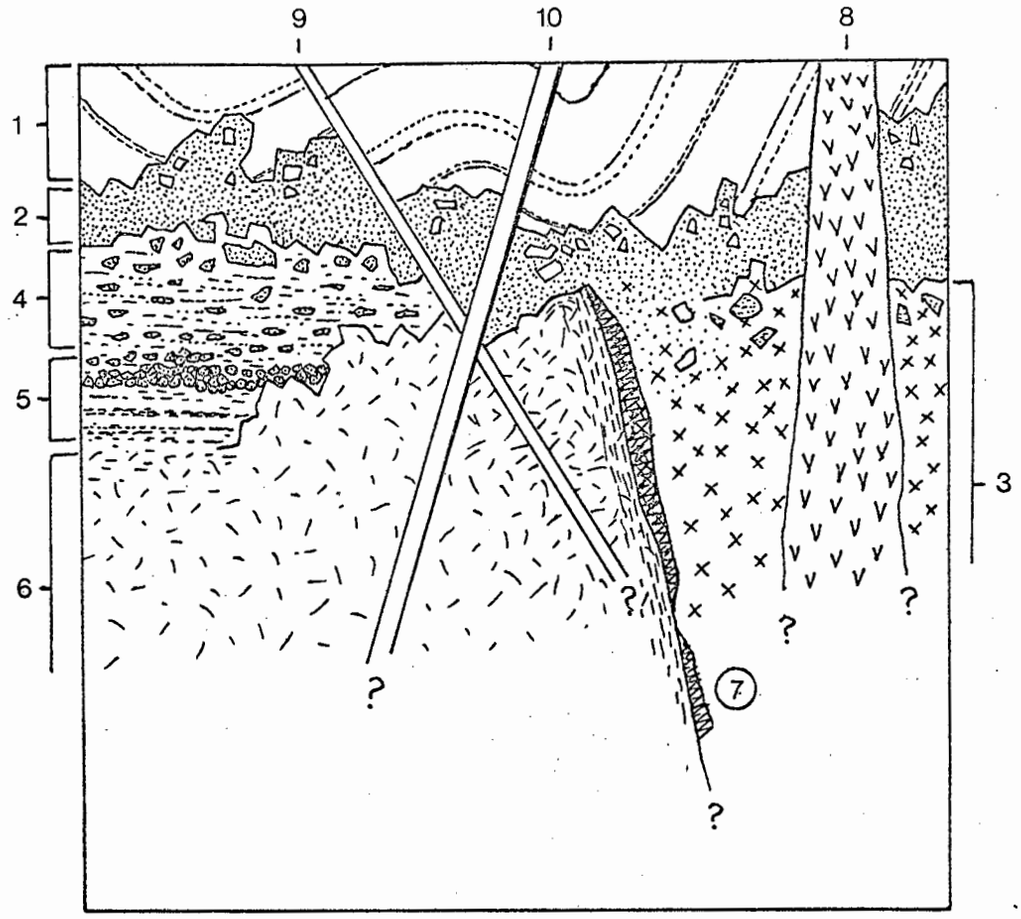

Figure 2. Schematic diagram illustrating relationships in the Roof Zone. 1 - Bogenfels Formation sediments; 2 - PCNS; 3 - coarse grained nepheline syenites; 4 - Laminated Foyaite unit; 5 - Xenolith Cumulate and the Layered Foyaites; 6 - Inner Foyaite; 7 - igneous breccia; 8 - bostonite plug; 9 - tinguaite dykes; 10 - quartz-bostonite dykes.

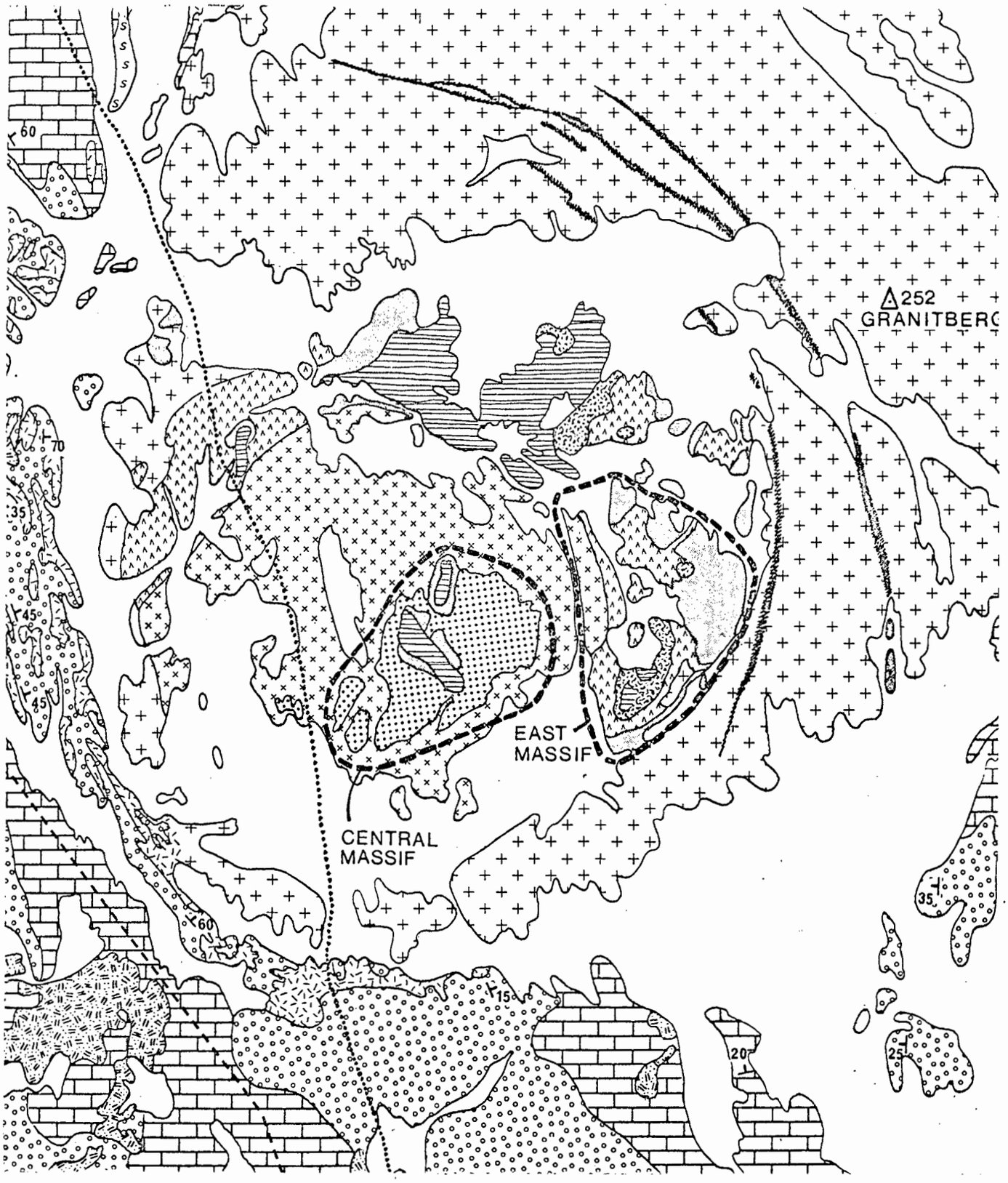

Figure 3. The location of the East Massif and the Central Massif in the Roof Zone, Granitberg.

magmatic rocks. Numerous fragments of similar rocks occur as xenoliths in the vicinity, and in places these rocks are packed together and resemble breccias. Verwoerd (1968) suggested that these roof zone dolomites recorded by Kaiser should be reappraised with the view to proving them carbonatites. This investigation indicates that the dolomites are not as widespread as was previously thought, and furthermore the field characteristics of the single small occurrence does not support in any way the contention that it is magmatic in origin.

The sedimentary sequence is underlain by the intrusive Porphyritic Chilled Nepheline Syenite (PCNS). The contact is well exposed in the northern sector of the Roof Zone and in places on the Central Massif. Close to this contact the sedimentary rocks are fragmented and intruded by numerous magmatic bodies. Many of these magmatic bodies are pegmatitic pulaskites and nordmarkites. Near the contact the sediments show the effects of thermal metamorphism - sandstones show little alteration but the phyllites and shales have been converted to hornfels. Close to the contact, and adjacent to magmatic and hydrothermal veins, the rocks show the effects of strong alkali metasomatism or fenitisation. The rocks take on a greenish tint due to growth of aegirine/alkali amphibole. Those that are strongly affected by fenitisation are dark green, almost black in colour, so that there seems to be a direct relationship between intensity of the green hue (which is itself related to the proportion of aegirine/alkali amphibole in the rock) and the intensity of fenitisation which the rock has suffered. There is little or no change in grain size in the fenitized rocks, original bedding and other delicate sedimentary textures are preserved even in rocks showing the strongest effects of fenitisation. Detailed descriptions of the characteristics of the fenites and the fenitization are given in section 3.6.3.

3.4.3. The Porphyritic Chilled Nepheline Syenite (PCNS)

Immediately underlying the sedimentary rock sequence and intrusive into it are dark, porphyritic nepheline syenites. The fine-grained and porphyritic nature of these rocks, together with their position in the stratigraphy of the Roof Zone, indicates that they are probably the earliest intrusive phase of the central complex, and represent nepheline syenites that chilled immediately below the sedimentary roof of the intrusion.

The PCNS are dark rocks and are easily distinguished against the paler colours of the other rocks in the complex. They crop out extensively in the East Massif, and again in the N sector of the Roof Zone (see map). More limited outcrops are found associated with the sedimentary rocks on the Central Massif, and near the jeep track in the NW sector of the Roof Zone. Beyond the boundaries of the Roof Zone these rocks are found as xenoliths in the Outer Foyaite, e.g. W of the jeep track, NW of the Roof Zone, and S of the East Massif.

In outcrop the PCNS are massive and exhibit no preferred orientation of phenocryst or groundmass minerals. Close to the overlying contact with the sedimentary sequence, xenoliths derived from the latter are commonly found in the PCNS. More rarely xenoliths of fine-grained igneous rocks are also present. Whereas the sedimentary fragments may be up to 50 to 60 cm across, the size of the igneous rock fragments are much smaller - generally no larger than 3 to 4 cm. The fenitisation effects in the sedimentary rock xenoliths described in the previous section apply equally to the igenous rock xenoliths.

The PCNS unit is of variable thickness, with gradational or truncated lower contacts. In many places the PCNS forms only a thin horizon, 2 to 3 m thick, between the sedimentary roof rocks and the coarse grained nepheline syenites. Elsewhere the thickness probably never exceeds 10 to 12 metres.

In many places in the Roof Zone the PCNS grade downwards into coarse-grained, equigranular or porphyritic nepheline syenites. Similar rocks show intrusive relationships to the PCNS and often enclose xenoliths of the latter rocks. These features may be seen on the East Massif and the outcrops to the north, as well as in the vicinity of the jeep track in the NW sector of the Roof Zone. This dual relationship between the PCNS and the underlying coarse-grained nepheline syenites is a common feature amongst other igneous rock associations in the Roof Zone and reflects on the quasi-stability of many parts of the Roof Zone during its development.

3.4.3.1. Petrographic Features

The petrographic features of the PCNS are variable. Most specimens are porphyritic, with phenocrysts of alkali feldspar, nepheline, clinopyroxene,

and biotite, set in a finer-grained groundmass of essentially the same mineralogy but including sphene, Ti-magnetite and apatite. Size of the phenocrysts ranges from 1 to 8 mm, whereas the groundmass phases are less than 0,3 mm in size.

Alkali feldspar phenocrysts ($Ab_{80}Or_{20}$) are euhedral and perthitic. In some specimens the perthite exhibits a vermicular intergrowth with nepheline, similar to that described by Davidson (1970). Nepheline occurs as compositionally homogeneous euhedral grains which are sparsely distributed in most specimens. The composition of the nepheline phenocrysts is $Ne_{81}Ks_{19}$ (analyses in Table 25).

Biotite ($Ann_{56}Phlog_{36}MnBi_2TiBi_6$) occurs as sparse phenocrysts, but is the dominant mafic mineral in the groundmass. Clinopyroxene ($Ac_8Di_{70}Hd_{22}$) is similarly rare as phenocrysts but is abundant in the groundmass. The phenocrysts have narrow rims of Na-rich pyroxene, and the composition of the groundmass pyroxenes appears to be similar to these rims.

Ti-magnetite is confined to the groundmass, but does occur as microphenocrysts in some specimens. Sphene is likewise common in the groundmass and may occur mantling grains of magnetite. Apatite is also a common accessory, occuring as microphenocrysts and in the groundmass.

3.4.4. The coarse-grained nepheline syenite

This section deals with a variety of coarse-grained feldspathoidal rocks, the majority of which are situated immediately below the PCNS in the Roof Zone. They crop out extensively on the East Massif, and occur in the scattered exposures north of the East Massif, and in the NW sector of the Roof Zone. On the 1:10 000 map of the Granitberg Complex they are marked "Various intrusive foyaites (undifferentiated)".

These nepheline syenites display both the gradational and transgressive relationships to the PCNS described in the section above, and are interpreted as being the products of the same magma pulse which resulted in the formation of the PCNS as a thin crust at the roof of the conduit. After emplacement the nepheline syenites appear to have undergone non-uniform, in situ differentiation to produce rather mottled rocks, and

although rapid variations in grain-size are uncommon (most of the rocks display an average grain-size of 4 to 8 mm), variation in the proportion of essential minerals in the rock is often marked. Feldspathoid-rich and -poor varieties are common and mafic mineral abundances are also variable. This rapid but irregular variation in mineral content of the rocks is confusing, especially in the scattered outcrops of the sand covered areas. It is therefore possible that some of the nepheline syenites classified in this section are related to the later major intrusive pulses, i.e. those of the Inner and Outer Foyaite.

The point that is being stressed here is that there exists in the Roof Zone a wide and often confusing variety of coarse-grained nepheline syenites, which carry indications of being crystallization products of the same magmatic pulse that gave rise to the PCNS, but whose ultimate classification and correlation remains obscure.

3.4.5. The Inner Foyaite and the Layered Sequence

3.4.5.1. General

The largest petrographic entity in the Roof Zone is the Inner Foyaite and the related rocks of the Layered Sequence. The Inner Foyaite forms a near circular body intrusive into all other rocks of the Roof Zone, and crops out in the central-SW portion of the Roof Zone (see map). The Inner Foyaite is overlain by the Layered Sequence - a 20 to 30 m thick succession of nepheline syenites, rich in xenoliths, and characterised by the development of igneous lamination and to a lesser extent, rhythmic layering. The Layered Sequence is confined to the Central Massif, the relatively steep SE face of which provides an excellent section through the layered rocks.

The Layered Sequence and the overlying PCNS are separated by an intrusive contact, distinguished by sharp contacts and the abundance of PCNS xenoliths in the foyaites of the Sequence. The relationship between the Layered Sequence and the underlying Inner Foyaite is more ambiguous, with both transgressive and gradational contacts being common. These relationships are summarised in Figure 2. It must be emphasised that the relationships between the various rock units on the Central Massif are more complicated than is shown on the 1:20 000 map. In the central and western sectors of the Central Massif considerable faulting and tilting of the faulted

blocks has occurred and some of the contacts shown on the map are most likely faulted contacts (see section 3.4.1.). Both the Inner Foyaite and the Layered Sequence are believed to be the products of a complex crystallization history of a single major magmatic pulse.

3.4.5.2. The Layered Sequence

The Layered Sequence is divided into two distinct units for descriptive purposes:-

(a) The xenolith-rich Laminated Foyaite Unit, including the Xenolith Cumulate,

(b) The Layered Foyaite Unit.

3.4.5.2. (a) The Xenolith-rich Laminated Foyaite

This unit forms the bulk of the Layered Sequence and underlies the PCNS. Since the two sedimentary rock outcrops and associated PCNS on the Central Massif appear to be down-faulted blocks, their relationship to the Laminated Foyaite is not well displayed. Instead, a thin veneer of PCNS is rather irregularly distributed on the highest points of the eastern side of the Central Massif. Here the foyaite, intrusive into the PCNS and occurring immediately below it, does not show igneous lamination nor chilling at the contact. The foyaite is crowded with xenoliths of PCNS stoped from the roof of the intrusive chamber. Immediately below the contact the xenoliths are poorly sorted and large (2,0 to 4,0 m) angular slabs are associated with smaller, well-rounded xenoliths, typical of the lower zones of the Laminated Foyaite unit. (Plate 1.)

Descending through the Laminated Foyaites, the xenoliths decrease in size and number, and become more rounded. Moreover there is a corresponding gradation from non-laminated foyaite, through weakly laminated foyaite, to a foyaite displaying a strongly developed igneous lamination. There is an associated tendency for the xenoliths to orient themselves with their long axes parallel to this lamination (see Plate 2). Thus in the central zone of the Laminated Foyaite the xenolith/foyaite ratio is of the order 10 to 20%, and the xenoliths are well rounded and well sorted i.e. they are in the size range 3 - 5 cm. The xenoliths may be of any shape,

but strongly flattened spheroidal fragments are most common.

The foyaite itself is a medium to coarse-grained grey rock, with a pronounced lamination due essentially to the parallel alignment of euhedral, tabular or bladed alkali feldspar crystals, which are seldom more than 1 mm thick but which may be up to 10 mm long. Subhedral, equidimensional crystals of grey to pink nepheline, 2 to 3 mm in diameter, are packed together with alkali feldspar. Dark mafic minerals - consisting of small (< 1 mm) crystals of euhedral alkali pyroxene, and to a lesser extent alkaliamphibole and flakes of biotite, 1 to 3 mm in diameter, fill the interstices of the rock, with the biotite invariably aligned parallel to the lamination.

Towards the base of the Laminated Foyaite unit, the foyaite maintains its textural and mineralogical features, but the xenoliths increase gradually in size and abundance and individual fragments take on a more equidimensional shape. Aggregates of xenoliths have developed and where a number of xenoliths are packed together they are often distorted around each other. The preferred orientation of the feldspar crystals is usually disturbed in the vicinity of the aggregates, and the 'lamination' is draped and distorted around the xenoliths.

The base of the Laminated Foyaite Unit is marked by the xenolith cumulate. This is a graded zone, 2 to 3 m thick, which shows all the characteristics of having accumulated on a floor as a result of settling. This zone is generally marked by a xenolith/foyaite ratio > 1, and has a sharp lower contact with the xenolith-free rocks of the Layered Foyaite Unit (Plate 3). The xenoliths in the cumulate are well-rounded, nearly spherical in shape, and show a very limited size range, seldom exceeding 10 cm in diameter. The xenoliths at the base of the cumulate are usually tightly packed and the lower 1 m of this zone may have a xenolith/foyaite ratio of 2 to 4 or greater. The interstitial foyaite within the xenolith cumulate shows little or no igneous lamination. It is coarse-grained with an equigranular texture (Plate 4).

3.4.5.2. (b) The Layered Foyaite

The Xenolith Cumulate is underlain by the Layered Foyaite Unit. This unit has a maximum thickness of 3 to 4 m and is characterised by igneous lamination and rhythmic mineral graded layering in a medium to coarse-grained, xenolith-free foyaite. The contact between the Xenolith Cumulate and the

Layered Foyaites is sharp, and may be one of two types:-

(a) the contact interface is marked by the sudden appearance of abundant xenoliths with the interstitial foyaite in the Xenolith Cumulate being of the same modal composition, colour, and texture as the underlying foyaite of the Layered Unit;

(b) the interface is marked by the sudden appearance of xenoliths with the interstitial foyaite in the xenolith cumulate differing markedly in mode, colour, and texture from the foyaite below (see Plate 3).

The former type of contact is generally confined to regions where the xenolith/foyaite ratio is high, and the xenoliths large and particularly closely packed. The latter occurs where the ratio is low, and the interstitial foyaite is darker, possibly due to contamination through resorption, disaggregation, and dispersion of mafic minerals of many of the smaller xenoliths. In all cases the base of the Xenolith Cumulate and the Laminated Foyaite Unit is marked by the lowermost concentration of xenoliths of PCNS.

Due to its position at the base of the Layered Sequence, the Layered Foyaite Unit is only exposed in intermittent outcrops around the eastern and northern edges of the Central Massif. Layering is irregular, and it is not possible to trace individual layers from one outcrop to the next. In some places only two layers are present, each layer being 15 to 20 cm thick. In other exposures up to fifteen layers of 2 to 3 cm may occur. All the layering is mineral graded, and in any one sequence individual layers may vary considerably in thickness. All the layers are composed of the same cumulus minerals - alkali feldspar and aegirine (it is uncertain whether nepheline was also a cumulus phase). The contact between individual layers may be knife sharp or diffuse, the latter being most common where a large number of closely spaced layers are present.

The whole Layered Unit displays planar igneous lamination. The layering is accomplished through rhythmic density grading, size grading not being noted anywhere in the unit. The Layered Unit passes gradually downwards into the typical Inner Foyaite, first by cessation of the mineral graded layering, then by gradual decrease in the preferred orientation of the constituent minerals, especially the bladed alkali feldspar.

Around the southern margin of the Central Massif the Layered Foyaite Unit is absent below the Xenolith Cumulate, instead the latter displays a sharp horizontal contact with a non-laminated foyaite.

PLATE 1. Angular slabs of PCNS enclosed by intruding foyaite, near the roof of the Laminated Foyaite Unit, Roof Zone, Granitberg.

PLATE 2. Preferred orientation of rounded PCNS xenoliths in the middle zones of the Laminated Foyaite Unit, Roof Zone, Granitberg.

PLATE 3. Sharp contact between the xenolith-rich Laminated Foyaite Unit and the underlying Layered Foyaite Unit, Central Massif, Granitberg.

PLATE 4. Tightly packed PCNS xenoliths near the base of the Laminated Foyaite Unit, Central Massif, Granitberg.

1

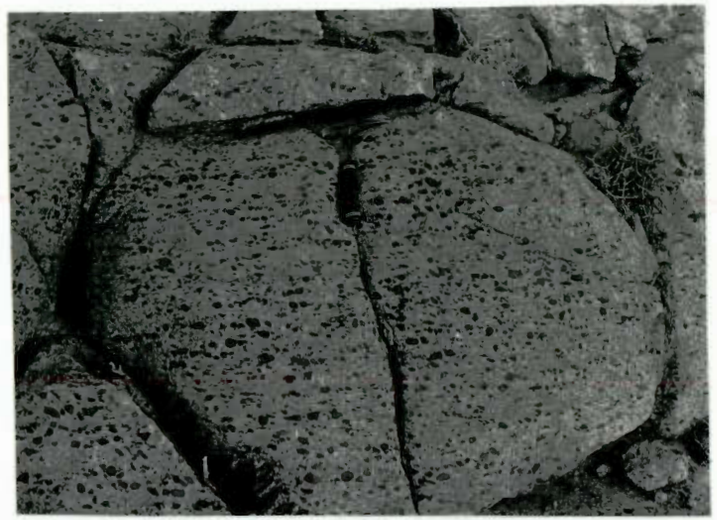

2

3

4

Furthermore, offshoots from this foyaite vein the Xenolith Cumulate. The horizontal nature of the contact interface suggests that the non-laminated foyaite formed the floor on which the xenoliths and the laminated foyaites accumulated. However the uniform texture and the presence of veins of the foyaite intruding the Laminated Foyaites indicates that the foyaite was possibly intruded from below after consolidation of the cumulate rocks. The relationship of this non-laminated foyaite to the rocks of the Layered Foyaite Unit is unknown. It seems that the relationship between the rocks in question is similar to the ambiguous relationship between the PCNS and the Coarse-Grained Nepheline Syenites of the East Massif.

In the central and western sectors of the Central Massif considerable disturbance of the sequence of layered rocks, as discussed above, has occurred. Whereas in the eastern portion of the Central Massif, where an ideal section through the Layered Sequence exists, the igneous layering and lamination is essentially horizontal with slight inward dips of 5^{o} to 15^{o} around the periphery, the lamination and horizons to the west often show very steep and highly irregular dips - up to 70^{o} in places. Traversing from E to W across the Central Massif the slight westward dip in the lamination increases as one approaches the large fragment of PCNS and roof sediments, and the Xenolith Cumulate splits into two layers. The upper layer of Xenolith Cumulate is rather poorly developed and remains essentially horizontal, whereas the lower layer appears to dip beneath the sedimentary rock-PCNS fragment, though the actual relationship is obscured by the presence of a wide bostonite dyke occupying a possible fault. Similar seam splitting is observed in layers of the Layered Foyaite Unit around the NW periphery of the Massif. Another notable feature is that in the central sector, xenoliths of fenitized sandstone and phyllite join those of PCNS in the upper zones of the Laminated Foyaite Unit.

In the western sector of the Central Massif the Xenolith Cumulate is poorly sorted, and rounded boulders of PCNS up to 1,5 to 2,0 m in diameter are packed together with xenoliths of a much smaller size (2 to 3 cm). Here also fragments of PCNS are joined by rounded fragments of coarse-grained foyaite in the xenolith population. The xenolith-rich rocks rest with a sharp, NE-dipping contact on the normal Inner Foyaite. No transgressive effects along this contact were noted.

Other confusing features in the disturbed part of the Massif are the presence of dykes of material identical to the xenolith-rich laminated

foyaites, cutting the normal Inner Foyaite in the vicinity of the Central Massif. Furthermore a similar dyke of leucocratic foyaite packed with well rounded, well sorted xenoliths of PCNS cuts the upper zone of the Laminated Foyaite Unit just east of the large sedimentary rock fragment.

It appears that on the Central Massif there are preserved rocks which indicate that the massif was the site of a domed, basin-shaped chamber, below the roof of the intrusion, in which magmatic sediment accumulated under relatively quiet, stable conditions. Although most of the tilting and disturbance of the Layered Sequence in the western and central parts of the Central Massif can be ascribed to brittle fracture and movement, there are a number of features in the Layered Sequence which are consistent with, and are best explained by, a certain amount of pre-consolidation instability, in the form of warping and fracturing of the floor of accumulation and also the roof of the chamber. These features which have been described above, are:-

(1) The poor sorting in the Xenolith Cumulate of the western sector compared with that in the eastern sector;

(2) The polymictic nature of the xenolith-rich rocks in the western sector compared with the oligomictic xenolith-rich rocks of the eastern sector;

(3) The dykes of xenolith-rich foyaite intrusive into both the Laminated Foyaite and the normal Inner Foyaite;

(4) Seam-splitting in the Xenolith Cumulate and the Layered Foyaites.

It must be pointed out that no igneous breccias or slump structures, which would be expected to develop under the conditions described above (see Wadsworth 1973, p. 29, 31), have been encountered on the Central Massif. This does not however erode the support, given by the features listed above, to limited, pre-consolidation faulting and tilting.

3.4.5.3. The Inner Foyaite

The Inner Foyaite is a cylindrical shaped zoned intrusion and has the largest outcrop area of any rock type in the Roof Zone. It underlies the Layered Sequence and is intrusive into all other rock types of the Roof Zone. Around the NW and E boundaries it is in contact with the coarse-grained, mottled nepheline syenite that lies below the PCNS, and along the

N boundary it is in contact with the PCNS and, though not exposed, with the sedimentary rocks. Along the W and SW boundary it is in contact with the Outer Foyaite, though the actual contact is only exposed in two small outcrops.

3.4.5.3. (a) Contact with the Roof Zone rocks

From the 1:10 000 map it can be seen that the contact with the Roof Zone rocks is only exposed on either side of the jeep track in the NW, and also on the W side of the East Massif. Only on the East Massif, however, is the actual contact interface exposed - in the scattered NW exposures the actual contact is obscured by sand and gravels.

On the East Massif a foliated, slightly chilled, Inner Foyaite intrudes coarse-grained mottled nepheline syenites, the actual contact being exposed over several metres. The contact is very regular with only minor veining and disruption of the nepheline syenites.

In the N-NW contact areas an igneous breccia is present along much of the contact zone, and a similar breccia is also found in places along the East Massif. The igneous breccia is followed on its inner edge by foliated Inner Foyaite, though nowhere is the contact between the two actually exposed, despite the fact that outcrops of the two rock types occur within a metre of each other.

The igneous breccia is a dark, unsorted, polymictic rock, consisting of fragments, both rounded and angular, of variously textured magmatic and sedimentary rocks, packed together and cemented by a medium- to fine-grained porphyritic groundmass, strongly resembling the foliated Inner Foyaite. Individual rock fragments range in size from 1 mm up to large 'boulders,' 0,5 to 1,0 m in diameter, and many show reaction rims.

Lying immediately within the envelope of igneous breccia, is a dark, porphyritic, zone of vertically foliated nepheline syenite some 2 to 3 m wide. The foliation is everywhere parallel to the contact, and a parallel banding of light and dark constituents is well developed in many places, but is often very weakly developed or altogether absent. Banding is regular, and each band is of the order of 3 to 5 cm wide. Contacts between individual bands are never sharp, but gradational over

0,25 to 0,5 cm. The foliation is very similar to the marked igneous lamination of the Layered Sequence, though the word "foliation" is preferred in this description as "igneous lamination" is well entrenched in the literature where crystal settling is the dominant process responsible for the foliation/lamination.

The dominant constituent of the rock and that most responsible for the marked foliation, is white to pink alkali feldspar, the 1,5 to 2,0 cm bladed or tabular crystals showing a strong preferred orientation. Less commonly, 2 to 3 mm plates of black biotite lie in the foliation. Nepheline occasionally occurs as large 5 mm rounded crystals with a distinctive red-brown colour, but is more common as an interstitial mineral in the groundmass. Finely disseminated mafic minerals - aegirine and biotite - have crystallized in the interstices between the feldspar laths. These mafic minerals are seldom larger than 0,5 mm, and their distribution and nature of occurrence impart the distinctive dark grey, mottled appearance to the rock.

Frequently occurring in the foliated contact rocks are 'pods' of darker, more mafic-rich material. These 'pods' are lens-shaped in section and aligned parallel to the foliation and show both sharp and diffuse contacts with the foliated foyaite. They resemble in texture and mineralogy the groundmass in the darker bands in the banded sections of the foliated foyaite in which they are enclosed. The foliated foyaite grades inwards into the non-foliated Inner Foyaite.

3.4.5.3. (b) Contact with the Outer Foyaite

The contact between the Inner Foyaite and the Outer Foyaite is poorly exposed in a few scattered outcrops between the West Ridge and the jeep track. The contact relationships are ambiguous though the indications are that the Outer Foyaite crystallized against the Inner Foyaite. No igneous breccia is present, nor is there banding in the grey foliated zone of the Inner Foyaite which is present in all the contact exposures. The contact is sharp, and the Outer Foyaite is somewhat contaminated and mottled against the foliated Inner Foyaite, and in one outcrop develops a pegmatitic facies at the contact. At the northern most point of contact between the Inner and Outer Foyaite, a wide tongue of Outer Foyaite is intrusive into the contact between the Inner Foyaite and the other nepheline syenites of

the Roof Zone. Veins of foyaite from this tongue cut across the banding and foliation in the Inner Foyaite along this contact.

This, and the pegmatitic development of the Outer Foyaite at its contact with the Inner Foyaite further south, is strongly indicative that the Outer Foyaite crystallized against an already crystalline, rigid mass of Inner Foyaite, although a superficial glance at the foliated zone Inner Foyaite lying against apparently non-transgressive Outer Foyaite can easily be misinterpreted in favour of the reverse situation.

3.4.5.3. (c) Petrographic Features

The Inner Foyaite is petrographically zoned and can be divided into a foliated marginal zone, an intermediate zone, and a core zone. The mineralogy of these zones is summarised in Table 1. These zones are similar with respect to their major mineralogy, but differ considerably in the minor minerals present.

The foyaites are leucocratic and coarse-grained, with hypidiomorphic granular textures in the intermediate and core zones, whereas the marginal zone displays a trachytic texture. Perthite ($Ab_{64}Or_{36}$) occurs as euhedral laths 7 to 8 mm long, and displays a coarse 'patch' type exsolution intergrowth of twinned albite and altered K-feldspar. The structural state of the K-feldspar is intermediate between orthoclase and microcline (see section 7.8.1.).

In the intermediate and marginal zones nepheline ($Ne_{80}Ks_{20}$) occurs as anhedral, poikilitic grains measuring 20 x 20 mm in some specimens. In the core zone nepheline is more abundant and more restricted in size. Although most of the nepheline in this zone is interstitial to the feldspar laths, the presence of varying amounts of sub- to euhedral grains indicates that some nepheline did crystallize early with the alkali feldspar. Nepheline in all the zones is commonly altered to cancrinite, sodalite, and paragonite. However, some of the sodalite may be primary.

Biotite and alkali pyroxene are the dominant mafic minerals in the foyaite. In the marginal and intermediate zones individual grains are euhedral, 0,2 to 0,3 mm in size, and occur interstitially between the feldspar laths, enclosed by the poikilitic feldspathoid minerals. In

TABLE 1

Mineral assemblages in the Inner Foyaite

	foliated foyaite				intermediate zone					core zone			
	301	302	305	319	350	344	303	304	300	320	321	333	334
Perthite	x	x	x	x	x	x	x	x	x	x	x	x	x
Nepheline and alteration prods.	x	x	x	x	x	x	x	x	x	x	x	x	x
Aegirine	x	x	x	x	x	x	x	x	x	x	x	x	x
Biotite	x	x	x	x	x	x	x	x	x	x	x	x	x
Na-Amphibole	x	x	-	-	x	-	-	x	x	-	-	-	-
Opaques	-	x	x	x	x	-	-	-	-	-	x	-	-
Apatite	x	x	x	x	(x	x	x	x	x)?	x	x	x	x
Sphene	x	x	x	x	x	x	x	x	x	-	-	-	-
Perovskite	-	-	-	-	x	x	x	x	x	x	x	x	x
Astrophyllite	-	-	-	-	-	-	-	-	-	x	x	x	x
Zircon	-	-	-	-	-	x	x	x	-	x	x	x	-
Calcite	-	-	-	-	-	-	-	-	x	-	x	-	-

the core zone the mafic minerals are much larger, averaging 1 to 3 mm in size. Biotite ($Ann_{68}Phlog_{22}MnBi_{8}TiBi_{2}$) occurs as stubby, euhedral books, exhibiting strong pleochroism (γ'(black brown)$>\alpha'$ (red brown to yellow brown)). Na-pyroxene ($Ac_{56-75}Di_{17-12}Hd_{27-13}$) is slightly zoned, but some crystals with cores of colourless augite do occur, especially in the marginal zone. Na-amphibole is rare, but occurs in the cores of some pyroxene crystals, again particularly in the marginal zone. Amphibole is however absent from the core zone.

Apatite is the most ubiquitous minor constituent, occurring throughout the Inner Foyaite, and is associated with, or is enclosed by biotite. Ti-magnetite is common in the marginal zone where it may be intergrown with sphene - possibly indicating a reaction relationship. In the intermediate and core zones Ti-magnetite is extremely rare, and is always enclosed by biotite or pyroxene. Sphene occurs as sub-to euhedral grains in the marginal zone, and as corroded remnants in the intermediate zone, but is absent from the core zone. In contrast, euhedral perovskite is found in the intermediate and core zones but is absent from the marginal zone.

Zircon occurs as large anhedral grains which have crystallized interstitially between the feldspar laths in the intermediate zone, but is absent from the marginal zone. In the core zone, either zircon or eudialyte-eucolite may be present. Bright yellow, pleochroic astrophyllite is ubiquitous in the core zone, but has a variable abundance.

The core zone, therefore, has agpaitic affinities, whereas miaskitic mineral assemblages are found in the intermediate and marginal zones. It must be stressed that the boundaries between the various zones are gradational, especially that between the intermediate and core zones. Chemical analyses of intermediate zone Inner Foyaites are presented in Table 12.

3.4.5.5. Crystallization development of the Inner Foyaite

From the evidence presented in the previous section it is likely that the Inner Foyaite, was emplaced as an inhomogeneous magmatic body. At the present level of erosion the outer zones of the intrusive magma must have been semi-crystalline and have possessed enough sheer strength

to break off slabs and fragments of wall rock as it moved upwards into its present position. These fragments were then crammed into the outermost zones of the magma and solidified into an envelope of igneous breccia. Further evidence of the nature of the marginal zone is given by the foliation and banding in the foyaite which was most likely produced by viscous flow in a semi-solid medium.

The non-foliated Inner Foyaite was probably emplaced in a largely liquid condition, the crystallization details of which are discussed in section 8.5.

The Inner Foyaite specimens also present excellent evidence as to the order of crystallization - an important feature in the consideration of fractionation schemes. In all cases alkali feldspar, was the first mineral to crystallize, followed by the mafic minerals with biotite preceeding the alkali pyroxene, whose initial composition was augite - aegirine-augite. There is no evidence to suggest that nepheline was ever an important liquidus mineral in the Inner Foyaite composition range.

3.4.5.6. Crystallization development of the Layered Sequence

Field evidence is consistent with the Layered Sequence being the last liquid in the Inner Foyaite chamber to crystallize, and it is interesting to reconstruct the development of this peculiar sequence of rocks. The field evidence suggests that the Layered Sequence was deposited on a relatively stable floor which lay close to the roof of the magma chamber. A simple model reconstructing the situation in the chamber is one in which the magma crystallizes from the bottom of the chamber upwards and develops a "wet top," i.e. the upper zones are enriched in the volatiles. This concentration of volatiles lowers the liquidus in this zone, and their presence can be manipulated to account for the relevant density and viscosity of the liquid, and crystallization sequence of minerals, necessary to produce the igneous layering. The "wet top" development in a cylindrical magma chamber is similar to that envisaged by Kennedy (1955), but in this case we follow Burnham (1967, p. 45) in ascribing the "wet top" to concentration of volatiles by crystallization in the lower portion of the magma chamber, and not to the Soret effect, though it is clear that an initial concentration of volatiles at the top of the chamber is necessary to lower the liquidus temperature there so that crystallization does take place from the bottom up. ?

Once a floor and a volatile-rich magma was established near the roof, the nature of the crystallization was disturbed in order for minerals to crystallize at the top of the chamber and settle on the established floor. The mineral grading of the individual layers is consistent with sedimentation through crystal settling from above and the rhythmic repetition of the layers indicates some cyclic operation of the crystallizing or settling process. This writer favours intermittent crystallization and differential settling of the crystals to account for the layered foyaites lying below the Xenolith Cumulate.

Intermittent crystallization could be caused by a variety of processes, all discussed by Sorensen (1968). These are:-

(1) Variation of vapour pressure in the chamber by periodic expulsion of volatiles through the volcanic conduit;

(2) periodic nucleation in a supersaturated magma;

(3) progressive concentration of volatiles in the uppermost parts of the magma chamber;

(4) seismic activity triggering off crystallization in supersaturated horizons in the magma.

The variable nature of the layering suggests that the relative abundance of minerals in the supply varied during sedimentation and constraints can be applied to the points listed above to satisfy both the rhythmic supply of the minerals and a change in the relative abundance of minerals in the supply. Melting experiments conducted by Sood and Edgar (1970) on a foyaite from Ilimaussaq, Greenland, show that at 1030 bars P_{H_2O}, feldspar and nepheline crystallized before clinopyroxene as was the case in the dry melting at 1 atm. However at 1030 bars with $f\theta_2$ in the melt controlled by the HM buffer, clinopyroxene was the first mineral to appear on the liquidus followed shortly by beldspar and nepheline. It follows that the variation of $f\theta_2$ in the magma could account for an abnormal supply of either felsic or mafic minerals. Since $f\theta_2$ imposed on the magma, i.e. controlled by an external buffer (Nicholls and Carmichael 1967, p. 4673) would be controlled by the surroundings, or, more likely, the volatile phase of the magma, variation in the volatile content of the magma, and therefore variation in the vapour pressure, would result in variation in $f\theta_2$, and hence the species of minerals first on the liquidus, and the supply of cumulus minerals. Thus points (1) and (3) above are considered most

likely to have controlled the crystallization of the minerals from the magma. Case (3) is actually only part of (1) as the former only becomes operative under the conditions of the latter, i.e. variation of vapour pressure by periodic expulsion of volatiles through the roof followed by concentration of volatiles below the roof, followed by expulsion, etc.

More problematical is the development of the Xenolith Cumulate and the xenolith-rich laminated foyaite. This unit can be considered as a single, thick, xenolith-graded layer in which no mineral grading or layering is present. It is therefore best ascribed to a single event of continuous sedimentation. The absence of xenoliths from the Layered Unit suggests that they were not in existence in the liquid during sedimentation of this unit, as they would have certainly settled along with the cumulus minerals.

The abrupt and concentrated appearance of xenoliths above the Layered Foyaite Unit indicates that some event was responsible for the introduction of a large number of xenoliths in the upper part of the chamber and they "showered" down with the crystallized alkali feldspar, aegirine and nepheline, and accumulated rapidly on the floor. No cyclic process seems to have operated during the sedimentation of the Laminated Foyaite unit. It seems possible that after a series of periodic and limited expulsions of volatiles through the roof, a major outburst of volatiles occurred, severely fracturing the PCNS roof and introducing a large number of PCNS fragments into the liquid. The volatiles in the liquid escaped either in the one major outburst, or following it, continuously and steadily through the permanently ruptured roof. In either event the remaining, relatively dry (witness the paucity of hydrous minerals in the laminated rocks) liquid crystallized rapidly but steadily and continuously at the roof, the crystals settling with the xenoliths. It is almost certain that the xenoliths were subjected to temperatures which were above their solidus (see section 8.4), and the presence of an interstitial melt in the otherwise coherent xenoliths facilitated rounding and deformation of these fragments, as described in section 3.4.5.2. (a).

Differential settling and the production of layering in the Laminated Foyaite could have been disrupted and prevented by "mixing" of the settling crystals by the downward passage of relatively large xenoliths, or by rapid settling. The latter case requires a settling medium of low viscosity and density, properties of the magma which would be operated against by the escape of dissolved volatiles.

After sedimentation a substantial amount of interstitial liquid remained in the pile of laminated foyaites, and also apparently in the underlying non-laminated Inner Foyaite. It is then possible to postulate that during subsequent tilting, warping or even fracturing, these semi-consolidated rocks, lubricated by the interstitial liquid, were able to flow and produce the transgressive contact between the Xenolith Cumulate and the underlying foyaite, as well as the dykes of xenolith-rich foyaite observed cutting the Inner Foyaite and the laminated Foyaite (see section 3.4.5.2. (b).)

It was hoped that it would be possible to make a minimum estimate of the H_2O content of the magma which crystallized the Layered Sequence, by considering the relative densities of the magma and settled crystals. Using the method outlined by Bottinga and Weill (1970) as well as mineral data recorded in Clark (1966), it is possible to estimate with accuracy the densities of the settled minerals, ρ_s, and the anhydrous magma, ρ_f. If $(\rho_s - \rho_f)$ is negative, then ρ_f could be decreased by adding H_2O to the magma until the density of the magma is less than that of the settled minerals, and thus a minimum estimate of the H_2O content of the magma could be obtained.

The analysis of Inner Foyaite sample GM 350 was used in the calculation and the result for the anhydrous melt and the density data on the cumulas minerals is presented in Table 2. The results indicate that the anhydrous melt is less dense than any of the minerals in the T range 800° - $1000^\circ C$. Bottinga and Weill (1970) estimate the accuracy of their method as $\pm$ 1%, and taking this into account does not alter the density relationships. This result does not allow, therefore, an estimate of H_2O to be made, but does indicate that although a considerable H_2O content of the magma is postulated to account for the pattern of crystallization, none is required to condition the magma for gravity settling of the mineral species.

It is possible to make one further calculation in connection with the Layered Sequence, that is to calculate the viscosity of the magma and hence deduce the settling rate of crystals during sedimentation of the Layered Unit. The viscosity calculation is that devised by Bottinga and Weill (1972), and the result for the anhydrous magma melt of GM350 is given in Table 3. Bottinga and Weill (1972) do not make any quantitative allowances for the effect of dissolved H_2O on the viscosity of the magma and this has to be estimated in a semi-quantitative way.

TABLE 2

Density data for rocks and minerals from the Inner Foyaite

DESCRIPTION	TEMP	DENSITY	REMARKS
GM350 melt (P_2O_5 and H_2O free)	800°C 1000°C	2,457 2,429	Calculated using the method of Bottinga and Weill (1970) and extrapolated to the lower temperature.
Nepheline	800°C	2,528	Densities from Clark (1966) except aegirine which is from Deer et al (1966). Densities have been corrected for T using volume expansion data listed in Clark (1966)
Alkali Feldspar $Ab_{50}Or_{50}$	800°C 1000°C	2,536 2,518	
Aegirine	800°C 1000°C	3,50 3,48	

TABLE 3

Viscosity data for GM350 melt (anhydrous)

	TEMPERATURE	VISCOSITY (poises)
Calculated	1500°C	$10^{2,97}$
	1200°C	$10^{3,99}$
Extrapolated	1000°C	$10^{4,98}$
	900°C	$10^{5,62}$
	800°C	$10^{6,32}$

However, using the anhydrous data in Tables 2 and 3, and Stoke's Law:

$$V = \frac{D^2(\rho_s - \rho_f).g}{18\eta}$$

— for spherical bodies only

where: V = settling velocity (cm sec^{-1}); D = diameter of particle (cm); ρ_s = density of particles; ρ_f = density of liquid; g = acceleration due to gravity; and η = viscosity of the fluid; V is calculated to be $1{,}269 \times 10^{-5}$ cm sec^{-1} for alkali feldspar, and $1{,}496 \times 10^{-4}$ cm sec^{-1} for aegirine at 1 000°C, both crystals being 0,5 cm in diameter. This means that the alkali feldspar would take 3 to 4 years to settle from the roof of the chamber, to the floor, a distance of 15 to 20 m. An unrealistic result here could still allow an estimate of the H_2O content of the magma to be made, but with far less accuracy than the density calculations would have allowed.

The result is not, however, unrealistic, considering that the calculations were made on an anhydrous basis. Shaw (1963) has provided curves by which it is possible to estimate the viscosity of melts containing H_2O. These curves show the drastic effect of dissolved H_2O on the viscosity of the melt, i.e. it decreases the viscosity enormously. If H_2O were taken into account in the calculation above, much faster settling rate would have resulted. However, it should be remembered that Stoke's Law applies only to strictly spherical bodies, and the results for the anhydrous calculation are much higher than they are in fact, due to the tabular nature of the settled minerals.

The discussion above is based on a very simple model which does not take into account a large number of influencing factors - density and viscosity gradients, disruption of settling by boiling of volatiles in the magma through pressure release, variation in shape and size of the settling minerals, etc. In summary, petrographic evidence suggests that the Layered Sequence owes its origin to magmatic sedimentation of minerals crystallizing from a magma. This suggestion is fully supported by the estimates of density and viscosity for the anhydrous magma.

3.5. THE OUTER FOYAITE

The Outer Foyaite builds the bulk of the Granitberg Complex and is

responsible for the physiographic prominence of the peak. It is well exposed and appears in the field as an attractive, pale grey rock, of remarkably even texture and colouring. The Outer Foyaite completely surrounds the Roof Zone in plan, as is well displayed on the accompanying 1:10 000 geological map. Small dykes and tongues of the Outer Foyaite occur within the Roof Zone, and can be seen on the East Massif, and in the area W of the jeep track (see section 3.4.5.3. (b).). Detailed petrographic work indicates that the Outer Foyaite is a zoned body with a miaskitic core zone and an agpaitic outer zone.

3.5.1. Petrographic Characteristics

The foyaite is a coarse-grained, hypidiomorphic granular rock, whose essential constituents are alkali feldspar, nepheline, and the mafic minerals, biotite and Na-pyroxene. Chemical analyses, norms, and modes of Outer Foyaite specimens are presented in Table 12.

Alkali feldspar ($Ab_{65}Or_{35}$) is the dominant constituent of the rock, and occurs as euhedral laths 6 to 7 mm long. The feldspar is coarsely perthitic, with an irregular 'patch' type intergrowth of clear, twinned plagioclase and altered K-feldspar. The exsolved plagioclase may form a continuous rim that surrounds the whole perthite crystal, but more often is concentrated around the (001) terminations of the crystals.

Nepheline ($Ne_{78}Ks_{22}$) is the second-most abundant constituent of the foyaite and occurs as subhedral and euhedral crystals. In most samples the euhedral nature of nepheline indicates that it was a primary phase on the liquidus along with alkali feldspar. However, it invariably also occupies an interstitial, and occasionally poikilitic, position in relation to the feldspar laths, indicating that it was a late crystallizing phase as well. Sodalite is nearly always present as a minor interstitial phase, but occasionally it may dominate the feldspathoid population as large poikilitic crystals enclosing perthite, nepheline, and mafic minerals. Only rarely is sodalite euhedral and it appears that in all cases nepheline preceded sodalite in the crystallization sequence.

Cancrinite is commonly present as a minor interstitial mineral, or it occurs intergrown with nepheline. In the latter instance it can be regarded as an alteration product of the nepheline, but its interstitial nature in many rocks suggests late crystallization from residual fluids enriched in CO_3^{--}. As

noted by Kaiser (1926) the mineral is ubiquitous in the foyaites close ~~from~~ to the dolomite contact-zones, and this is probably indicative of local introduction of CO_3^{--} into the magma, due to limited assimilation of the carbonate country rocks by the intruding foyaite.

Zoned alkali clinopyroxene is an essential constituent in the foyaite. Individual crystals are subhedral to euhedral and are zoned from $Ac_{14}Di_{48}Hd_{38}$ to $Ac_{62}Di_{10}Hd_{28}$. These pyroxene crystals are host to many inclusions which include apatite, sphene, fluorite, biotite, and magnetite. Biotite ranges in composition from $Ann_{71}Phlog_{16}MnBi_8TiBi_5$ to $Ann_{76}Phlog_{12}MnBi_4TiBi_8$. It is present as subhedral individuals but may also be intergrown with pyroxene. The significance of this intergrowth is unclear but the writer favours co-crystallization as an explanation. In some specimens biotite is rimmed by granular aggregates of magnetite and this could well be due to the breakdown of biotite in the presence of O_2 to give K-feldspar and magnetite (Wones and Eugster, 1965).

There are a large number of minor constituents in the Outer Foyaite, and Kaiser (1926, p. 255) reported apatite, arfvedsonite, zircon, lavenite, eudialyte-eucolite, astrophyllite, sphene, magnetite, and epidote. All these except zircon and epidote were found in collected specimens, and in addition aenigmatite, fluorite, and perovskite were identified. Not all of these minor minerals are present together in any one specimen. On the basis of the minor mineral contents it is possible to divide the Outer Foyaite into foyaites with miaskitic affinities, and those with agpaitic affinities (Sorensen, 1960). The agpaitic foyaites are consistently located in the outer zones of the Inner Foyaite body.

The Ti-magnetites are anisotropic in reflected light, and an analysis (Table 24) indicates that they are Mn-rich. They have a composition of $Usp_{34}Mt_{66}$. Fe-Ti oxides are absent from the agpaitic foyaites except where they are enclosed by biotite or Na-pyroxene. This feature is considered in more detail in section 8.6. Sphene occurs in aggregates with magnetite and biotite, or as individual subhedral to euhedral crystals in the miaskitic foyaites. Sphene is absent or very rare in the agpaitic rocks. Apatite is nearly always present in all the foyaites, but only in trace amounts. It is generally enclosed by biotite or aegirine, indicating that it is an early crystallizing phase in the foyaites.

Arfvedsonite has a restricted occurrence and is found only in the agpaitic zone. It occurs as large anhedral, sometimes poikilitic, grains and apparently crystallized late in the solidification history of the foyaites. Analyses of arfvedsonite are presented in Table 20.

Aenigmatite occurs as large euhedral crystals with a deep red colouring and pleochroism, and is likewise restricted to those foyaites with agpaitic affinities. In reflected light the aenigmatite is seen to enclose skeletal grains of Ti-magnetite. The crystallization of aenigmatite is dealt with more fully in section 8.6. Analyses of the aenigmatite are presented in Table 23.

Members of the eudialyte-eucolite solid solution series also occur in the agpaitic zone. A similar spatial distribution of eudialyte-eucolite-bearing foyaites was also noted by Kaiser (1926, p. 258), who believed that the distribution of these minerals were related to the foyaite-dolomite contacts. The inference from Kaiser's description is that the presence of carbonate rocks and their possible reaction with the foyaite magma affected the crystallization of eudialyte-eucolite. This inference is somewhat supported by the experiments of Christophe-Michel-Levy (1961). The eudialyte-eucolite minerals may be colourless or pleochroic in various shades of pink and red. Individual crystals are anhedral and extensively zoned, and are always found in the interstices between feldspar and nepheline grains.

Lavenite occurs as small, pale yellow, pleochroic crystals, and is found in trace amounts in some of the agpaitic foyaites. Fluorite is found as minute mauve-tinted crystals enclosed in clinopyroxene in both the miaskitic and agpaitic foyaites, and is possibly an early crystallizing phase in these rocks. Perovskite has been identified in only one sample collected from the SE dolomite contact zone. It occurs as a few euhedral grains in close proximity to large sphene crystals, and one perovskite crystal is enclosed by the sphene. Perovskite is absent from all other specimens of the Outer Foyaite which have been examined, and probably owes its presence to a favourable micro-environment that developed in the contact foyaitic rocks.

Kaiser (1926) reported zircon in the foyaites he examined. No zircon was found in the Outer Foyaite, and since Kaiser did not recognise the division of the foyaites as described in this work, the zircon mentioned by him could well have been from some other foyaite in the complex. The mineralogy of the Outer Foyaite is summarised in Table 4.

TABLE 4

Mineral Assemblages in the Outer Foyaite

Specimen No.	103	67	101	145	69	137	171	284	286	147	167	141	135	133	112	285	136	129	142
Perthite	x	x	x	x	x	x	x	x	x	x	x	x	x	x	x	x	x	x	x
Nepheline	x	x	x	x	x	x	x	x	x	x	x	x	x	x	x	x	x	x	x
Aegirine	x	x	x	x	x	x	x	x	x	x	x	x	x	x	x	x	x	x	x
Biotite	x			x	x	x	x	x	x	x	x	x	x	x	x	x	x	x	x
Sodalite			x								x	x	x	x			x	x	x
Cancrinite	x										x								
Sphene		x				x	x			x	x	x	x	x	x	x	x	x	x
Magnetite	x	x	x	x						x	x	x	x	x	x	x	x	x	x
Aenigmatite					x	x	x	x	x										
Arfvedsonite					x	x	x	x	x										
Astrophyllite					x	x	x												
Eucolite		x	x	x	x	x		x	x										
Lavenite	x				x			x		x									
Apatite	x			x				x				x				x		x	x
Fluorite							x	x	x				x						
Perovskite																x			
	AGPAITIC										MIASKITIC								

3.6. CONTACT RELATIONS

3.6.1. Introduction

Foyaite-dolomite contacts are well exposed in the NE and to a lesser extent around the SE and NW edges of the intrusion. Foyaite-sandstone contacts occur on the West Ridge along the W-SW margin of the intrusion, and again in the N-NE. A small outcrop in the E reveals the foyaite-granite-gneiss contact.

Assimilation and metamorphic phenomena at the contacts attracted a great deal of attention from Kaiser (1926) who recorded the petrographic features of the wide variety of rocks occurring in these contact zones. He also commented on the nature of the contact - the interfingering of sedimentary rocks and foyaite, and the complete lack of intrusion breccias - a feature that led him to describe the intrusion as a "diskordanten Durchschmelzkorper."

3.6.2 Contact with the Granite-Gneiss

This is the least spectacular of the foyaite-country rock contacts, and is only exposed in one small outcrop on the eastern boundary of the intrusion. The granite-gneiss shows the effects of contact metamorphism/fenitization 50 to 60 cms from the contact. In this zone quartz is absent or present in minor amounts, and there is a sporadic growth of alkali clinopyroxene in the rock.

The foyaite is typically coarse-grained, almost pegmatitic, the grain-size increasing as one approaches the contact. With the grain-size increase the abundance of nepheline and mafic minerals decreases in the foyaite and against the contact a leucocratic, coarse-grained rock composed largely of feldspar with a little interstitial nepheline and alkali clinopyroxene is developed. In places there is evidence of a little chilled foyaite along the contact, but the chilling is only sporadically developed and only 5 to 10 cm thick.

3.6.3. Contact with the feldspathic sandstones

Contacts between the foyaites and the feldspathic sandstones are well developed on the West Ridge and in the N-NE contact zone. Sedimentary

rocks show contact metamorphic/metasomatic effects and the foyaite has assimilated siliceous material to produce medium- to coarse-grained pulaskites, nordmarkites and alkali granites.

3.6.3.1. Physical nature of the contact

Along the southern contact, in the vicinity of the jeep track, the strike of the contact is at right angles to the strike of the sedimentary rocks. Along the West Ridge the strike of the contact and the sediments is parallel, and moreover the sedimentary rocks dip steeply towards the contact. In the NE, dolomites lie adjacent to the foyaite, but beyond the immediate contact zone, sandstones, etc., are intruded by a number of minor plugs or sheets of pulaskite, nordmarkite and alkali granite.

The thinly bedded nature (often with thin intercalated argillaceous beds), and the steep eastward dips of the arenaceous sediments of the West Ridge, has resulted in complex and repeated interfingering of sediments and magmatic rocks. Thus on the West Ridge the contact is represented by a 30 to 40 m wide zone of alternating sedimentary rocks and intruded magmatic rocks. Similar features are found in the S and NE contact zones but are less well developed.

The dominant form of the magmatic intrusions is a sheet-like body emplaced concordantly with the bedding. These sheets may pinch or swell along their length and can vary from thin veinlets 1 to 2 mm thick, to larger bodies 3 to 4 m thick. Lenticular bodies are also common but irregular or circular plugs are more rare. The latter occur sporadically in the contact zone and may range up to 5 to 8 m in diameter. Xenoliths of sedimentary rock are common occurrences in the intrusive bodies. Figure 4 is a section through the West Ridge, illustrating all the main features of the contact zone.

The nature of the contact owes its origin to the intrusion of magmatic material along favourably oriented bedding planes in the sedimentary sequence. Stopping of thinly bedded units has evidently occured to a certain extent, and there is evidence that dilation and assimilation have also facilitated intrusion. Figure 5 illustrates three types of sedimentary rock - igneous rock relationships observed in the contact zones:

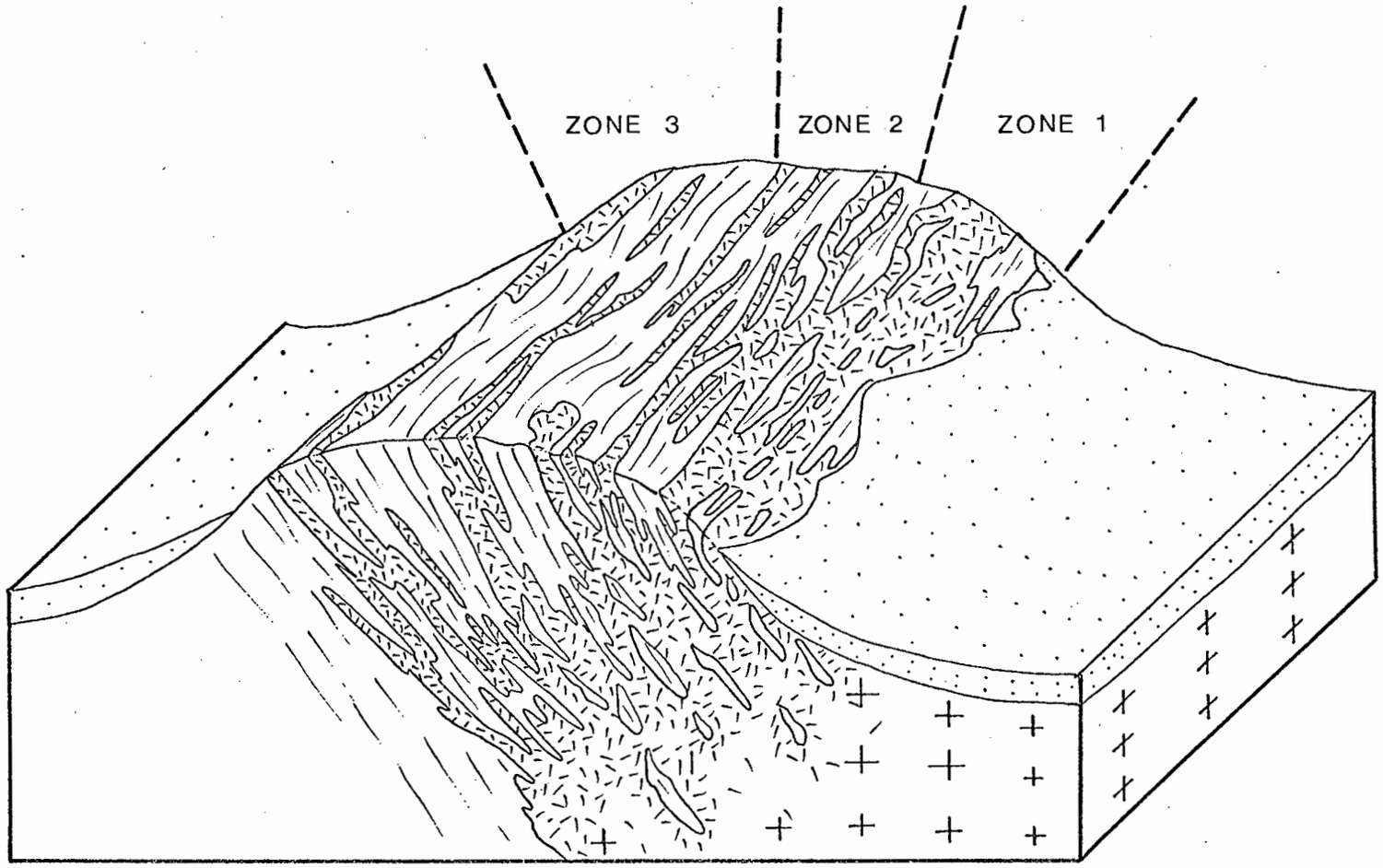

Figure 4. Relationships in the West Ridge contact zone, Granitberg. Speckled - sand cover; crosses - Outer Foyaite; hatchures - derivative magmatic rocks; lines - feldspathic sandstones.

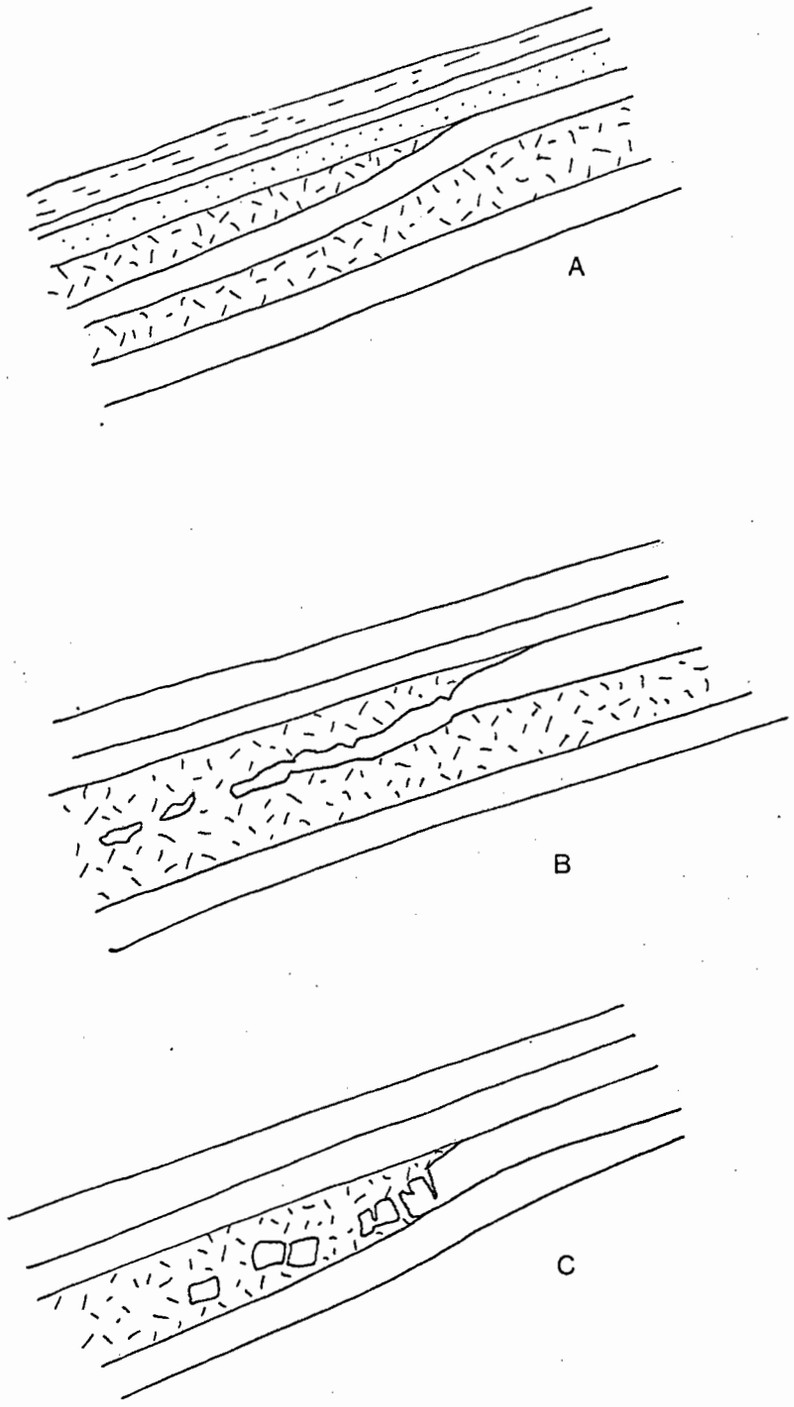

Figure 5. Intrusive relationships between magmatic sheets and bedded feldspathic sandstones, West Ridge, Granitberg.

A - intrusion facilitated by dilation

B - intrusion facilitated by assimilation

C - intrusion facilitated by dilation and stoping

PLATE 5. Alternating sedimentary beds and intrusive magmatic sheets, NE Contact Zone, Granitberg.

(a) illustrates intrusion facilitated by dilation,

(b) illustrates intrusion dominated by assimilation though the isolated sedimentary rock fragments may indicate an initial stage of minor dilation and stoping,

(c) illustrates a dominant stoping process aided by minor dilation.

It is clear that all gradations between types a, b and c may exist and that intrusion is facilitated by all three processes, with dilation and stoping being a precursor to assimilation. Notwithstanding the above, the sediment-magmatic rock contacts parallel to the bedding planes are regular and sharp.

In the NE contact zone the sandstone-arkose sequence is somewhat removed from the Outer Foyaite and the contact features are somewhat different to those described above. The sediments display shallow dips both towards and away from the intrusion. Intrusive plugs are absent, and intrusive sheets are less abundant and much thinner though in some places regular alternation of sedimentary rocks and magmatic rocks similar to those seen on the West Ridge occurs (see Plate 5). In one occurrence there is a very regular, bed for bed alternation of sediments and intrusive magmatic material. The thickness of the sedimentary and magmatic units varies from 10 to 50 cm. The thicker sheets occasionally enclose large stoped xenoliths of sedimentary rock with numerous 1 to 15 mm veins of syenitic material intruded parallel to the bedding.

In another similar occurrence at the SE end of the NE contact zone, alternations of intrusive magmatic sheets and thinly bedded dolomites, sandstones, and argillaceous rocks crop out over several metres. Here individual intrusive sheets are seldom more than 15 to 25 cm thick on a gross scale. On a finer scale argillaceous rocks have been intimately veined parallel to bedding by syenitic material. Kaiser (1926, p. 261) described these rocks as 'neophelingneiss' and discussed them in detail. In the writer's experience, nepheline is seldom present in these veins and Kaiser's name is therefore misleading.

One of the outstanding features in the NE contact zone is the persistence over considerable distances of thin syenitic sheets often no more than 2 cm in thickness. In one case one of these veins, emplaced along a bedding plane in the arkose was traced for over 40 m.

Another feature in the NE contact zone is the presence of a number of thin vertical, (20 to 30) cm alkali granite dykes, which trend SW-NE away from the contact. They cut across the bedding in the sandstones and fragments of sandstone commonly occur as xenoliths in the dykes. A thin 1 to 2 cm zone of fenitization occurs in the sandstone wall rock and xenoliths adjacent to the contact.

3.6.3.2. Magmatic contact rocks

In the contact area there is a zonal arrangement of contact magmatic rocks as indicated in Figure 4. All the magmatic rocks in the contact area are medium- to coarse-grained. In zone 1 the dominant type is a coarse grained, almost pegmatitic leucocratic pulaskite. This pulaskite is strongly altered and susceptible to weathering, thus accounting for the poor exposures of this rock, and the sand-filled depression that occurs just inside the contact around the S-W-NW side of the complex. Zone 1 is characterised by a high pulaskite/country rock ratio, with the fenitised sedimentary rocks occurring as thin screens or xenoliths.

Occasionally in zone 1 remnants of a fine grained pulaskitic chill may be seen between the country rock and the coarse grained pulaskite. The latter shows a sharp contact with the chill, and similar chilled rocks occur as xenoliths in the coarse-grained pulaskite. It appears that an initial intrusion of magma chilled against the country rocks, and was then disrupted by the major magmatic pulse which is responsible for the main features of the contact zone. The xenoliths of chilled rock often display segregations of pegmatitic material within them (see Figure 6). This might be due to partial melting of the chilled rocks during injection of the main pulse, or to injection of magmatic material into the chilled rocks. Occasionally a nordmarkitic or granitic facies is developed on the edges of pulaskite bodies immediately adjacent to the feldspathic sandstones.

Zone 2 is characterised by roughly equal volumes of country rock and magmatic rocks, the latter being dominantly a medium to coarse grained nordmarkite. In many places the quartz content of the nordmarkite increases and the latter passes into alkali granites. The nordmarkites are generally fresh and show little alteration. Some of the more leucocratic varieties display a sacharoidal texture and are difficult to distinguish from arkoses and feldspathic sandstones in hand specimen.

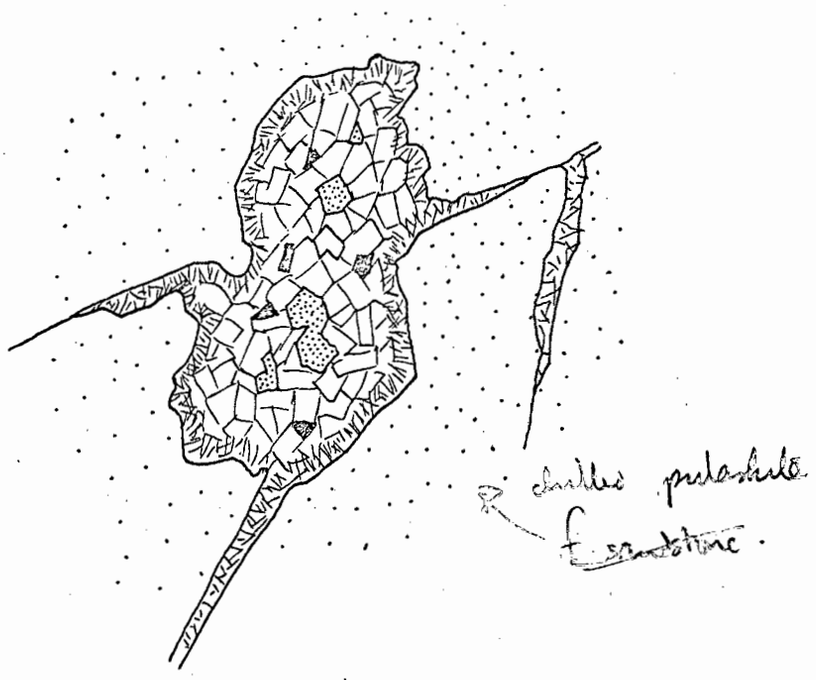

Figure 6. Pulaskitic segregation in xenolith, West Ridge contact zone. The segregation exhibits a fine chilled margin, and a coarse grained core of feldspar, mafic minerals(black), and nepheline(speckled).

Away from the foyaites, the abundance of nordmarkite intrusive bodies decreases and one passes into zone 3, which is characterised by large expanses of undisturbed country rock with few intrusive bodies. Here the main intrusive rock type is an alkali granite which forms thick 1,0 to 1,5 m sheets or lens shaped bodies emplaced parallel to the bedding. The alkali granites are medium to coarse grained hypidiomorphic granular rocks, but within a single sheet they may show a zonal variation in grain size or mineralogy. This may take the form of developing a leucocratic pegmatitic facies at the top of the sheet, or at the top and bottom of the sheet. Similar pegmatites develop at the wedge-shaped terminations of lensoid sheets. Mafic mineral content is likewise variable and higher concentrations at the bottom of some sheets is common. In one case weakly developed phase layering and igneous lamination was noted in the central portion of a sheet.

3.6.3.2. (a) Petrography and Mineralogy

Typical modes of various types of contact magmatic rocks are given in Table 5, together with chemical analyses and CIPW norms.

Pulaskites of Zone 1

These are very coarse-grained, almost pegmatitic, hypidiomorphic granular rocks. The average grain-size is 1,0 to 1,5 cm, but may range up to 3,0 to 4,0 cm in patches. Perthite forms 90 to 95% of the rock as subhedral crystals displaying coarse ribbon-type exsolution intergrowth of K- and Na-feldspar. Nepheline is present in large, generally euhedral, crystals, and as an interstitial mineral between the feldspar laths. The distribution of nepheline is highly irregular - in some places nepheline has congregated into large clots 10 to 15 cm across; elsewhere rapid and irregular alternations of nepheline-poor and nepheline-free rocks occurs.

Mafic minerals are sparse and are found irregularly scattered through the pulaskites. Sphene, biotite and oxidized augite are the commonest species, but oxides and epidote also occur.

Pulaskitic injections or segregations in xenoliths and in the country rock in zone 1 show interesting features. The segregations may be from 1,0 to 10,0 cm across, and tend to be irregular in shape (see Figure 6). Around the

walls of the segregation is a thin narrow chilled zone consisting of a fine grained mass of feldspar laths, free of nepheline and mafic minerals, and in some cases a little interstitial quartz may occur. The interior is coarse grained, consisting of perthite and a little nepheline, the latter occuring as euhedral or interstitial crystal confined to the centre of the segregation.

Nordmarkites of Zone 2 .

The nordmarkites and alkali granites of this zone are leucocratic, medium to coarse grained hypidiomorphic granular rocks with an average grain size of 0,1 to 0,3 cm. Subhedral perthite is the dominant constituent of these rocks, and occurs as 1,0 to 2,0 mm laths which show a rounding, possibly due to limited resorption and which is well developed in the more quartz-rich rocks. Some specimens show completely anhedral perthites with interlocking dentate boundaries. Ribbon-type exsolution intergrowths are well developed in all the perthites, and many crystals display thin albite rims. Twinning on the Carlsbad law is common.

Quartz is present in varying amounts in these rocks, and generally fills the interstices between feldspar grains, or it occurs as large poikilitic crystals continuous for 6 to 10 mm enclosing loosely packed feldspar grains. Myrmekitic intergrowths are occasionally developed.

The dominant mafic mineral is zoned aegirine which occurs as small ($< 0,5$ mm) euhedral grains enclosed by both poikilitic quartz and perthite. The aegirine is zoned from Na-augite (core) to aegirine (rim). Pale blue arfvedsonite may be intergrown with aegirine especially in the core of the pyroxene, or it may occur as discrete crystals. Euhedral sphene is a common minor constituent, but biotite and apatite are rare, and opaque oxides are very seldom present. With increasing quartz content the nordmarkites pass into alkali granites, with features very similar to the alkali granite sheets from zone 3.

Alkali granites of Zone 3

These rocks are medium- to coarse-grained (average grain size 2,0 to 5,0 mm) and display a hypidiomorphic texture. A pegmatitic facies with crystals

TABLE 5

Contact magmatic rocks, West Ridge, Granitberg;
Analyses, norms (CIPW) and modes

	GM169	GM232	GM174	GM175	A	B
SiO_2	63,36	64,24	75,41	73,34	56,70	87,95
TiO_2	0,32	0,35	0,25	0,27	0,31	0,07
Al_2O_3	18,36	17,22	11,51	12,90	21,60	5,99
Fe_2O_3	1,25	1,27	0,94	0,97	1,21	0,41
FeO	0,47	0,43	0,25	0,33	1,09	0,37
MnO	0,10	0,11	0,08	0,08	0,19	0,00
MgO	0,25	0,86	0,25	0,25	0,20	0,48
CaO	1,25	1,16	0,26	0,55	0,85	0,22
K_2O	6,72	7,48	5,89	6,88	5,91	3,70
Na_2O	6,38	5,84	3,72	3,91	9,82	1,23
P_2O_5	0,10	0,09	0,00	0,00	0,01	0,02
H_2O	0,09	0,12	0,65	0,05		0,09
LOI	0,73	0,34	0,30	0,31	1,11	0,31
	99,38	99,54	99,51	99,84		

CIPW NORMS				
or	39,71	44,20	34,81	40,66
ab	50,96	46,72	26,42	28,06
an	1,62	-	-	-
ne	1,64	-	-	-
q	-	0,12	32,32	24,95
ac	-	2,18	2,72	2,81
ns	-	-	0,46	0,43
di	1,34	4,02	1,03	1,94
hy	-	-	0,33	-
ol	-	0,20	-	-
il	0,60	0,66	0,47	0,51
mt	0,94	0,75	-	-
hm	0,60	-	-	-
ap	0,24	0,21	-	-

GM169 Pulaskite
232 Nordmarkite
174 Alkali Granite
175 Alkali Granite
A Ave Outer Foyaite
B Ave Sandstone

TABLE 5 (cont.)

MODES

93,6	92,9	63,2	67,9	Feldspar
-	1,7	34,5	27,2	Quartz
0,7	-	-	-	Nepheline
-	4,3	2,1	3,7	Aegirine
3,2	-	-	-	Augite
0,8	-	-	-	Biotite
-	0,8	0,1	1,1	Na-amphibole
-	0,3	0,1	0,2	Sphene
1,7	-	-	-	Other

up to 5 to 6 cm in size is present in a number of intrusive sheets.

Perthite is the dominant constituent and occurs as euhedral laths displaying well developed ribbon or a coarse patch-type exsolution intergrowth. Plagioclase commonly forms a semi continuous rim around the laths and in some specimens small discrete crystals of twinned albite occur sandwiched between larger feldspar grains. The Na-rich phase in the coarse 'patch'-type perthites is often twinned on the Albite law and compositions estimated by the method of Michel-Levy lie between Ab_{98} and Ab_{83}.

Quartz occurs as anhedral semi-poikilitic grains up to 1 cm in diameter. In one specimen, GM42, quartz occurs as clear equidimensional grains displaying slight strain extinction, as well as rounding and crushing. The feldspars in this section show a distinct preferred orientation. All these features suggest that the sheet from which the specimen was collected was emplaced in a near solid condition.

Euhedral aegirine, often with arfvedsonite in the core, is the dominant mafic mineral in the alkali granites. The arfvedsonite often occurs as discrete crystals, pleochroic in pale shades of blue (α') to mauve (γ'), and exhibits anomalous interference colours. Euhedral sphene is ubiquitous, but biotite and opaque oxides are absent.

3.6.3.3. The origin of the magmatic rocks in contact with the sandstones of the West Ridge

Kaiser (1926, p. 257) was in no doubt that the alkali granites of the West Ridge were products of assimilation of quartzites by the intruding foyaite. Field relations provide strong support for Kaiser's suggestion, but to what extent assimilation occurred is examined here.

Chemical analyses and CIPW norms of the alkali granite, nordmarkite and pulaskite specimens from the West Ridge are presented in Table 5, together with the average data for 4 Outer Foyaites and 3 feldspathic sandstones.

It seems clear that the initial silication of the foyaite magma, to produce saturated or slightly saturated syenitic liquids, must have been accomplished to a certain extent by the assimilation of quartz-rich rocks. However, once a slightly oversaturated syenitic liquid is produced it is

possible that the subsequent development of the nordmarkite - alkali granite suite could have been achieved by crystal fractionation. It is therefore desirable that this possibility be tested first before examining the role of assimilation.

To this end the CIPW normative compositions of the relevant rocks from Table 5 have been plotted in the 'granite' system, the plane SiO_2 - $NaAlSi_3O_8$ - $KAlSi_3O_8$ on to which has been projected the positions of the minimum melting compositions in the 'wet' system for P_{H_2O} of 0,5, 1,0, 2,0 Kb and the axial traces of their respective thermal valleys (Tuttle and Bowen, 1958). Also plotted are the minimum melting compositions, and their respective 'thermal valleys' for peralkaline liquids at 1 000 gm/cm^2 $P(H_2O)$, where peralkalinity is expressed in terms of excess Na (Carmichael and MacKenzie, 1963). For peralkalinity in terms of excess K the low-temperature zone lies close to the $NaAlSi_3O_8$ - SiO_2 side line (Thompson and MacKenzie, 1967). Bailey and Schairer (1964) have pointed out the dangers of using this type of normative plot for peralkaline rocks, but the errors in projection for the rocks in question are small, and do not affect the discussion that follows (Figure 7).

From the Figure 7 it is obvious that all the compositions lie well to the right (Or-rich side) of the 'thermal valleys.' If a liquid line of descent, controlled purely by crystal fractionation of alkali feldspar, connects GM232 to the two granites, GM174 and GM175, it is unlikely that it could maintain its 'displaced' position and not be constrained towards the thermal valleys and the minima on the two-phase boundary. Figure 8 shows furthermore, that the compositions lie far above the thermal minimum surface in the feldspar volume for peralkaline compositions (i.e. excess Na). A liquid, originating at GM232, and fractionating alkali feldspar would be forced down on to the surface and would then travel along it to the minimum. Granitic compositions derived in this way would be expected to lie on the surface. Clearly then GM174 and GM175 are not related through alkali feldspar fractionation to GM232.

Alkali clinopyroxene is the only other mineral besides alkali feldspar that is capable of contributing significantly to the development of the alkali granites. The nordmarkite contains only a few per cent clinopyroxene (see Table 5), and is thus incapable of playing a dominant role in any crystal fractionation process. Moreover fractionation of alkali clinopyroxene would

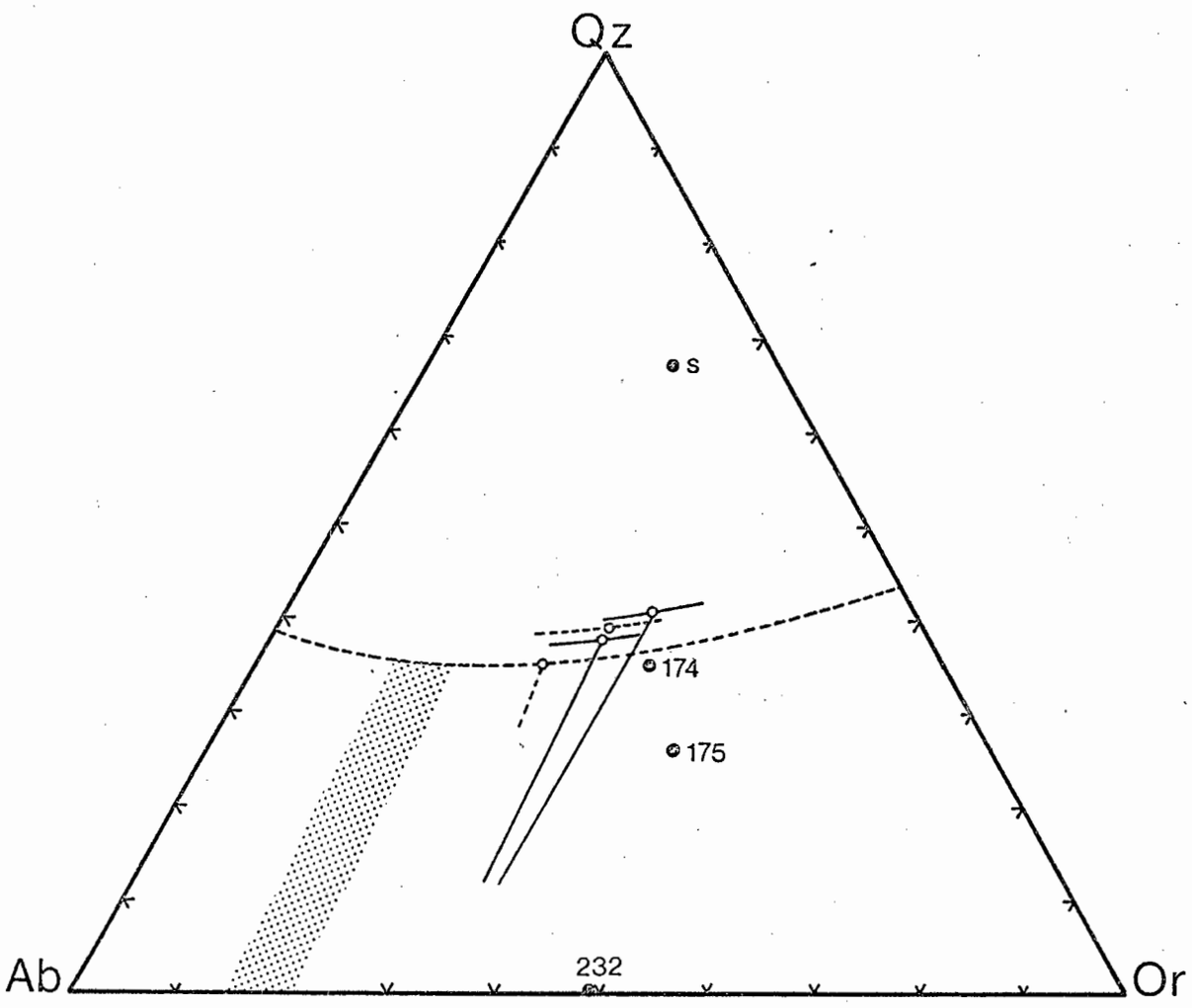

Figure 7. Projections onto the Qz - Ab - Or plane of the 'Granite System'. S - average feldspathic sandstone; 174,175 - alkali granites; 232 - nordmarkite. Also plotted are the minimum melting compositions and thermal valley axial traces for granites at 500 and 1000 bars P_{H_2O} (dashed lines)(Bowen and Tuttle, 1958), and the minimum melting compositions of peralkaline granites with 4,5(ac + ns) and 8,3(ac + ns) with their respective axial traces of their 'thermal valleys' (solid lines) (Carmichael and McKenzie, 1963). The speckled zone marks the position of the thermal valleys in the peralkaline granite system, where peralkalinity is expressed in terms of excess K (Thompson and McKenzie, 1967).

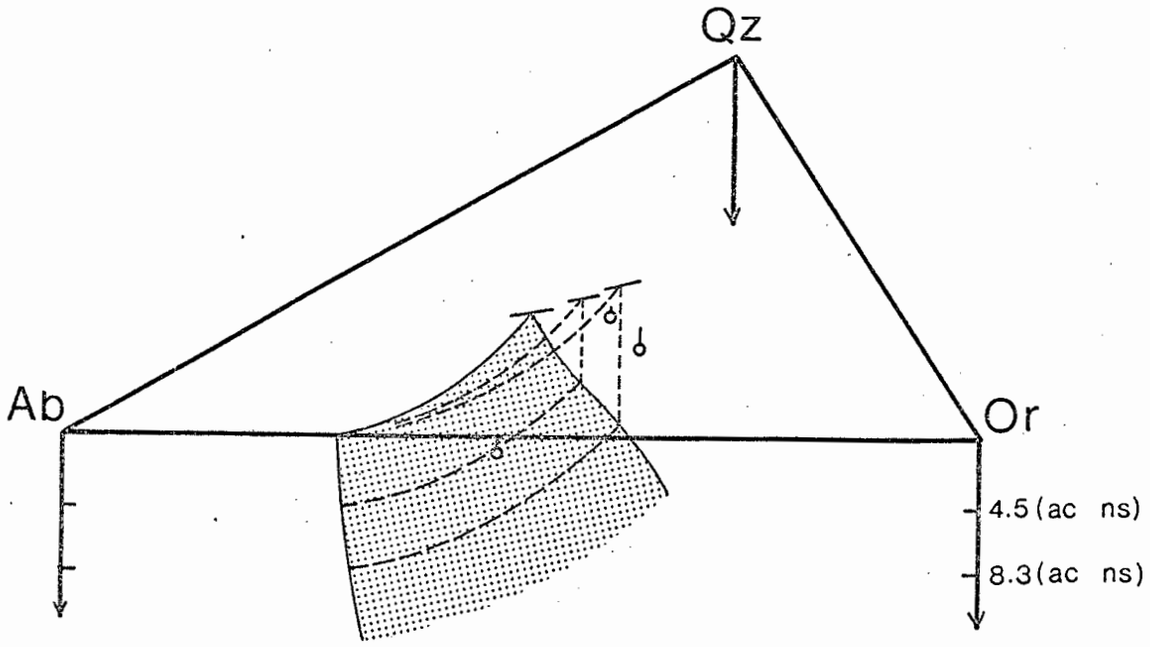

Figure 8. Schematic diagram of the peralkaline volume(in terms of excess Na) of the 'granite system' (modified after Bailey and Schairer, 1964). The diagram shows the relationship between the nordmarkite - alkali granite compositions and the peralkaline thermal minimum surface at 1 Kb P_{H_2O}.

tend to drive the liquid into Al_2O_3 -rich compositions, and could hardly promote the distinct peralkalinity of the alkali granites.

To test the validity of the assimilation Figure 9 has been constructed. It is a simple addition-subtraction diagram employing mole SiO_2 plotted against mole oxides but it can be used in the same manner as a conventional SiO_2 vs oxides weight % plot. The advantage of using the molecular plot is that it illustrates peralkalinity ratio, and estimates of mineralogical additions and subtractions are more easily made. Two scales have been used on the ordinate; one for the oxides Na_2O, K_2O, and Al_2O_3, and one for the minor oxides CaO, Fe_2O_3 + FeO, and MgO.

Two features emerge from the diagram:

(a) Although it is assumed above that the nordmarkite is derived from the Outer Foyaite by assimilation, it is clear from the diagram that assimilation <u>alone</u> (i.e. simple addition of the composition of the average feldspathic sandstone to the Outer Foyaite magma) could not produce the nordmarkite. This is particularly marked for the oxides K_2O, Na_2O, CaO, and MgO. Even considering that the composition of a crystalline rock is not necessarily the same as the composition of the magma from which it crystallised (especially in alkali content), this observation still holds.

(b) Assimilation of the country rocks (feldspathic sandstones, composition $\overset{S}{X}$) <u>can</u> explain the derivation of the alkali granites from the nordmarkite (compositions G and N respectively). This is particularly so for the oxides $FeO + Fe_2)_3$, TiO_2, Al_2O_3, and Na_2O, and to a lesser extent K_2O. MgO and CaO require some other explanation, but these are present in amounts of $< 1\%$, and a slight amount of removal through some process like crystal fractionation could account for the trend in their abundances. Furthermore assimilation would not destroy the peralkalinity in the derivative rocks and it is also capable of reversing the mol Na_2O/mol K_2O ratio, which is $> 1{,}0$ in the nordmarkite and $< 1{,}0$ in the alkali granites, (see Figure 9).

However, the nordmarkite would be required to assimilate feldspathic sandstone of composition $\overset{S}{X}$ to the extent of 70% of its own volume, in order to produce the required alkali granite composition! No magma has the superheat to accomplish assimilation to this extent. Clearly then, pure assimilation

Figure 9. Mole SiO_2 variation diagram for the oxides. F - average Outer Foyaite; N - nordmarkite; G - alkali granite; S - average feldspathic sandstone.

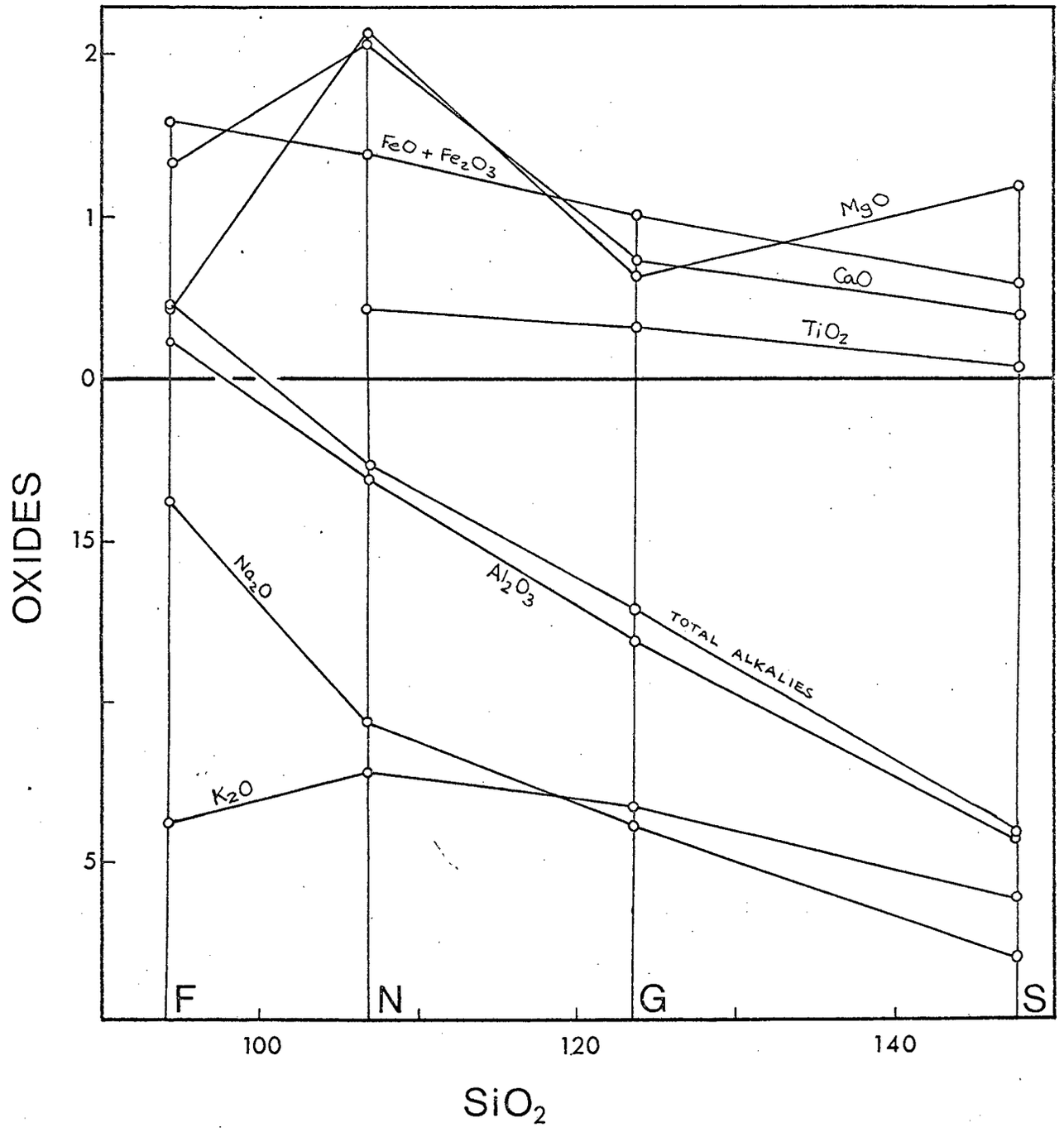

as considered here is chemically possible but physically impossible, and must be discounted as being the sole control in producing the derivative rocks in the contact zone.

Accepted petrogenetic theory does not count assimilation as a major process in igneous rock formation, and Bowen (1928) and other workers have argued convincingly against large-scale assimilation, and even moderate scale assimilation as envisaged here. In this respect it was perhaps naive to have entered into the preceding discussion at such length. However the discussion is useful in that it serves to draw attention to the chemical features of the rock types in question, and, more important, to show that for the special case of the contact rocks at Granitberg, neither crystal fractionation alone, nor assimilation can account for the development of the derivative rocks in question. From this stand we can postulate their probable origin.

Firstly, it must be established that some assimilation has occurred in the contact zone. Elsewhere it has been assumed that the nordmarkites have been derived from the foyaite by assimilation of siliceous material. There seems no other feasible mechanism to bring about this change, and all the field evidence supports this contention. Once assimilation has produced the nordmarkite there is no reason for it to cease being effective, and it is therefore likely that assimilation played some part in the production of all the derivative rocks in the contact zone.

Assimilation of solid material by a magma is a result of (a) melting of the solid, and (b) solution of the melt in the magma. In most situations this melting and solution occur simultaneously, and both are endothermic processes. In order for the magma assimilate material it must provide heat, and since magmas possess little or no superheat, it must crystallize in order to supply heat. If the crystals sink away, or are otherwise removed from the residual liquid, a crystal fractionation system develops. Continuous crystallization, melting, and solution controls the compositional path, the liquid moves along and hence the composition of the rocks crystallizing from it. This compositional path could be predicted with a knowledge of the composition and amounts of the fractionating phases, and a similar knowledge of the added material.

For the change foyaite → nordmarkite the fractionation/assimilation process produced marked changes in the chemistry of the residual magma → a

large decrease in Na_2O, a slight increase in K_2O, and a marked increase in CaO and MgO. This can be attributed to the fractionation of a relatively Na-rich feldspar and initially also some nepheline and aegirine/aegirine-augite, the latter removing Na and Fe, and concentrating Ca, and Mg. The composition of the added material would be the initial melting product of the sandstones, which would be the approximate composition of the minimum in the granite system. At 500 bars this is $Qz_{39}Ab_{30}Or_{31}$, but as melting proceeds more K-rich and more siliceous compositions would be added to the residual liquid. Obviously as the composition of the residual liquid changes, so does the composition of the phases fractionating from it. The composition path of the residual liquid is therefore controlled by a complex interplay of what is removed, and what is added. The actual liquid path is impossible to predict with the evidence available. It is clear that though nepheline and aegirine may have initially been precipitated, they soon ceased to appear on the liquidus and alkali feldspar dominated the fractionation control. The end result was that the nordmarkites that developed reveal a large concentration of K relative to Na, compared with the foyaite.

For the change nordmarkite - alkali granite, near straight line relationships exist between the composition $\overset{S}{\chi}$ and the nordmarkite and granite composition (see Figure 9). It would therefore appear that the liquid added to the residual liquid by assimilation was similar in composition to the residual liquid developed through crystal fractionation, at each stage of the transition nordmarkite - alkali granite. This is not surprising considering the compositions involved. The residual magma would be initially feldspathic with steadily increasing SiO_2 content as it fractionates feldspar. The composition of the melt derived from melting of the sandstones would be granitic with increasing amounts of silica, depending on the degree of partial melting.

The development of alkali granite from the nordmarkite is marked by a depletion of CaO and MgO and an increase in K_2O in a proportion greater than would be the case if crystal fractionation controlled the development. This is apparent from Figure 9 and Figure 7, and the discussion concerning them.

From Figure 7 it is obvious that the feldspar fractionated from any liquid lying between GM232 and GM175, would be Or-rich, because the tendency would be to drive the liquid towards the thermal valley, i.e. to more Ab-rich compositions. From a perusal of the feldspar - liquid

tie lines for the compositions studied by Tuttle and Bowen (1958), Carmichael and MacKenzie (1963) and Thompson and MacKenzie (1967), the composition of the precipitating feldspar would be in the region $Or_{55}Ab_{45}$ to $Or_{65}Ab_{35}$, i.e. the K_2O/Na_2O of the precipitating feldspar is 1,22 to 1,85, and may be even more Or- or K-rich for more granitic compositions. This tendency to deplete the residual magma in K by feldspar fractionation was discussed in consideration of a purely crystal fractionation model for the origin of the derivative rocks. But by all the evidence the residual magma followed a K-rich liquid path, an important feature that must be accounted for, i.e. there must be a mechanism which offsets the feldspar fractionation trend.

K-depletion can be offset by (a) continually adding K_2O-rich material to the residual magma, or (b) fractionating Na_2O-rich phases. Concerning the latter, the only possible phase which could remove Na from the liquid is aegirine or aegirine-augite. In relation to feldspar, Na-clinopyroxene is not at all abundant, and is therefore not capable of offsetting the effects of feldspar fractionating. Marked depletion shown by Ca and Mg can be ascribed to clinopyroxene fractionating, which would have also removed some Fe. Since FeO + Fe_2O_3 shows a steady decrease from the nordmarkite to the granites, it is clear that it was not involved in any large scale fractionating of any phase like alkali clinopyroxene.

Concerning the addition of material to the magma, the composition of the melt derived through assimilation ranges from $Qz_{39}Ab_{30}Or_{31}$ (the minimum melting composition in the granite system at 0,5 Kb P_{H_2O}) to approximately $Qz_{42}Ab_{18}Or_{43}$, and then to more siliceous compositions.[2] The K_2O/Na_2O ratio of material added, therefore, lies between 1,03 and 2,38. Clearly then assimilation can play an important role in maintaining the K-rich liquid path by supplying the residual magma with melts rich in K.

3.6.3.3. (a) Summary

Pulaskites, nordmarkites, and alkali granites are widespread along the foyaite-sandstone contacts. Field evidence suggests that the magmatic contact rocks were derived from the foyaite by assimilation of Quartz-rich material. It is shown that large scale assimilation of up to 135% is required if assimilation alone is envisaged as the mechanism by which the derivative rocks originated. Furthermore, given a nordmarkitic magma,

derived from the foyaite by an assimilation process, it is not possible to derive the alkali granites from the nordmarkite by crystal fractionation alone. These rocks are K-rich and although there is no direct evidence, other than initial and final compositions, it appears that the liquid path joining the nordmarkite and alkali granites lies well to the Or-rich side of the 'thermal valleys' in the conventional and peralkaline 'granite' systems, and could not develop through crystal-liquid equilibrium in a closed system.

It is postulated that the derivative rocks were produced by a continuous fractional crystallization and assimilation process, from the foyaite magma. The residual magma path was controlled by the nature of the partial melt added to it from melting of the country rock, and the nature of the phases crystallizing from it. The development of the magma change from foyaite to nordmarkite was controlled by fractionation of Na-rich alkali feldspar, and (initially) a little nepheline and aegirine and aegirine-augite, and the solution of melts with the composition $Qz_{39}Ab_{30}Or_{31}$ to $Qz_{42}Ab_{18}Or_{43}$ to more siliceous compositions and the solution of siliceous melts with a K_2O/Na_2O ranging from 1,03 to 2,38. Assimilation was more important than fractional crystallization at this stage since feldspar fractionation would tend to drive the residual liquid towards more under-saturated compositions, i.e. it would work against assimilation. Once oversaturation is achieved, the residual liquid trend controlled by feld-spar fractionation and that controlled by assimilation is similar.

The liquid path from nordmarkite to granitic compositions was controlled by fractionation of alkali feldspar, initially of composition Or_{55} to Or_{65} but becoming more Or-rich in the later stages, and the solution of partial melts of highly siliceous nature and K_2O/Na_2O of 1,03 to 2,38. Minor fractionation of clinopyroxene also occurred but was not important in controlling the liquid path. The dominance of fractionation over assimilation, or vice versa, is impossible to establish, but it is suggested that both played an equally important role.

3.6.3.4. Metasomatism at Foyaite-sandstone contacts

Mineralogical transformations seen in the siliceous country rocks can be ascribed to a process of metasomatism. Metasomatism accompanying

alkaline rock intrusions is normally an alkali metasomatism or fenitization.

Fenitization has been described from a number of alkaline rock - carbonatite complexes where typically wide aureoles of strongly fenitized rocks are present. Less commonly fenitization is described from non-carbonatitic complexes of the agpaitic type, and even from calc-alkaline rock intrusions (Anderson, 1963). Recently reference to fenitized rocks associated with faulting but with no apparent igneous activity have appeared in literature (Tanner and Tobisch, 1972; Deans et al, 1972). 1971

Summaries of fenites and fenitization processes in general, and in relation to specific intrusions, have appeared in recent years (McKie, 1966; Verwoerd, 1966; Heinrich, 1966; Currie and Ferguson, 1971; Currie and Ferguson, 1972). It is becoming increasingly evident that each occurrence of fenitized rocks possesses its own characteristics and arises through a unique process which can only generally be described as alkali metasomatism. Granitberg is no exception. It will be shown that the metasomatism at Granitberg is of such an unusual nature that "fenitization" in the commonly used sense is a misnomer for the Granitberg process. To avoid confusion the general term metasomatism is used hereafter to denote the Granitberg process.

3.6.3.4. (a) Evidence for metasomatism

The evidence for metasomatism is most striking at places where the magmatic rocks of the intrusion are in contact with the feldspathic sandstones of the Bogenfels Formation, particularly along the W-SW boundary of the intrusion. Adjacent to magmatic rocks, the pale grey- to cream-coloured feldspathic sandstones have been transformed to green, perthite + clinopyroxene and perthite + clinopyroxene + quartz rocks with minor amounts of sphene, biotite, and amphibole. Original sedimentary structures and even textures are preserved in all these rocks.

The intensity of the metasomatism falls off rapidly as one moves away from any particular sandstone - magmatic rock contact, though signs of metasomatism are exhibited in rocks several tens of metres from any contact. Metasomatism at Granitberg is therefore a short range process, giving rise to the "patchy" development of metasomatized rocks. This coupled with repeated interfingering of sediments and magmatic rocks gives

the impression of a substantial metasomatic aureole. However it is clear that the Granitberg aureole is not comparable to those developed at the well described classic areas (e.g. Alnö).

Xenoliths of country rock in the magmatic rocks exhibit the strongest effects of metasomatism. In the sedimentary rocks in situ the extent of metasomatism is controlled by the availability of discontinuities and other "passage ways" in the rock (joints, bedding planes, fractures or schistosity). Thus the patchy nature of the metasomatism can be directly ascribed to the well bedded, jointed nature of the sandstones and the absence of extensive shattering which seems to be a prerequisite to the development of extensive fenitization aureoles (Heinrich, 1966, p. 74).

3.6.3.4. (b) Petrographic and mineralogical features of metasomatism

The mineralogy of the metasomatic rocks is simple and is summarised in Table 6 ~~where visual estimates of the abundance of various phases is given.~~ * Not Also, 3 unaltered sandstones and 6 metasomatized rocks have been analyzed for major elements. Modes, chemical analyses and CIPW norms for these 9 rocks are presented in Table 7.

Non-metasomatised feldspathic sandstones are medium grained, well sorted rocks exhibiting non-clastic textures, though the detrital characteristics of the rocks are well preserved. Many of the rocks possess a distinctly oriented fabric, emphasised by the preferred orientation of elongated grains and the "streaming out" of fine grained recrystallized material. Kaiser (1926) gives a complete account of these sandstones - all that is summarised here are those features which are involved in the metasomatic process.

Modes of the 3 analyzed specimens are given in Table 7. The alkali feldspar occurs as well-rounded, spherical grains up to 1 mm in diameter. Quartz exhibits complete recrystallization and occurs as clear unstrained grains with clear interlocking grain boundaries. Fine grained intergrowths of quartz, alkali feldspar, and serecite fill the interstices and occur in bands or lens-shaped aggregates which display a preferred orientation.

The first signs of metasomatism in the rock is the appearance of skeletal, poikiloblastic crystals of pale blue amphibole. With increasing

TABLE 6

Mineral Assemblages in metasomatized sandstones, Granitberg.

	West Ridge Contact							NE Contact Zone						Roof Zone						
specimen no.	210	221	211	203	220	32	38	240	260	250	247	94	72	292	308	166	165	295	312	31
Perthite	x	x	x	x	x	x	x	x	x	x	x	x	x	x	x	x	x	x	x	x
Quartz	x		x			x		x		x	x			x	x		x		x	
Diopside	x		x			x		x	x	x	x		x							
Zoned Diopside		x		x	x		x					x								
Aegirine														x	x	x	x	x	x	x
Alk-Amphibole			x			x		x		x				x	x	x	x	x	x	x
Sphene				x		x	x		x	x		x								
Biotite		x		x	x		x						x							

no visual estimates of abundance — x only indicates presence or absence.

TABLE 7

Feldspathic sandstones and metasomatic sandstones; Granitberg.

Major element analyses and CIPW NORMS.

	GMA1	GMA2	GMA3	GMA4	GMA5	GMA6	GMA7	GMA8	GMA9
	Feldspathic Sandstones			metasomatized sandstones					
SiO_2	87,58	87,15	89,13	85,56	75,75	59,80	59,70	64,32	57,79
TiO_2	0,05	0,09	0,06	0,06	0,11	0,16	0,30	0,15	0,37
Al_2O_3	6,03	6,32	5,56	6,21	5,48	12,99	11,27	4,78	8,12
Fe_2O_3	0,18	0,10	0,13	0,16	0,42	1,25	1,52	1,01	2,06
FeO	0,39	0,36	0,35	0,30	0,85	1,56	2,14	1,82	2,04
MnO	0,00	0,00	0,00	0,04	0,05	0,27	0,22	0,12	0,16
MgO	0,56	0,47	0,41	1,08	5,01	6,15	6,52	9,82	8,95
CaO	0,29	0,16	0,21	0,99	6,89	8,65	9,36	14,17	12,82
Na_2O	1,07	1,28	1,35	1,61	2,37	6,17	4,67	1,25	4,13
K_2O	4,10	4,02	2,97	3,82	2,52	2,68	4,05	2,61	2,96
P_2O_5	0,02	0,02	0,03	0,02	0,06	0,03	0,11	0,31	0,39
H_2O	0,10	0,07	0,09	0,07	0,01	0,26	0,15	0,14	0,13
LOI	0,41	0,27	0,25	0,21	0,41	0,72	0,56	0,44	0,50
	100,78	100,51	100,87	100,13	99,93	100,69	100,57	100,96	100,42
CIPW NORM									
or	24,23	23,76	17,45	22,57	14,89	15,84	23,93	15,42	17,49
ab	8,19	10,13	11,32	11,32	14,16	40,59	29,93	10,26	21,83
an	-	-	0,67	-	-	-	-	-	-
q	64,55	63,53	69,33	60,20	39,88	-	-	16,51	-
ne	-	-	-	-	-	6,13	2,98	-	1,88
ac	0,52	0,29	-	0,46	1,36	0,27	3,60	0,27	5,96
ns	0,06	0,09	-	0,56	1,01	-	-	-	0,67
di	1,05	0,54	0,14	3,80	26,56	33,73	36,34	53,84	48,25
hy	1,52	1,43	1,39	1,42	1,18	-	-	1,79	-
ol	-	-	-	-	-	1,12	1,87	-	2,11
il	0,09	0,17	0,11	0,11	0,21	0,30	0,56	0,28	0,69
mt	-	-	0,19	-	-	1,68	0,40	1,33	0,00
ap	0,05	0,05	0,07	0,05	0,14	0,07	0,26	0,73	0,92
MODES									
Feldspar	36,5	30,7	27,4	34,5	26,0	59,4	49,5	13,6	37,4
Quartz	60,4	66,5	70,8	64,9	40,4	-	-	19,0	
Cpx	-	-	-	-	33,2	38,0	48,4	66,2	60,7
Biotite	-	-	-	-		2,3	1,6	-	1,1
Sphene	-	-	-	-	0,4	0,3	0,5	0,4	0,4
Amphibole	-	-	-	-	0,1	-	-	-	
Other	3,1	2,8	1,8	0,6	-	-	-	0,8	0,6

metasomatism the sandstone begins to loose its detrital characteristics. Alkali feldspar exhibits marked recrystallization or replacement in the development of clear exsolution lamellae and rims of albite, the latter often extending and partially enclosing some of the adjacent quartz grains. Large, clear and unaltered poikiloblastic perthites may also develop (see Figure 10 (b)) and commonly enclose well rounded quartz grains much smaller in size than those in the rest of the rock. Although these poikiloblastic feldspars may be partially ascribed to recrystallization of fine, intergranular feldspathic material, the diminished size of the enclosed quartz grains suggests that they possibly originated by reaction of quartz with the alkali-rich solutions. Skeletal amphibole persists in these rocks and may be rimmed by green aegirine-augite (see Figure 10 (a)).

More intensive metasomatism is indicated by an increase of alkali feldspar and mafic minerals at the expense of quartz. Colourless diopside (< 0,1 mm) forms sinuous, tightly packed aggregates concentrated along grain boundaries. (Figure 10 (c)). Amphibole is only rarely present. Increasing metasomatism produces granoblastic texture in the rocks and all indications of the original fabric of the rock, except for gross features like bedding, are lost. Quartz may or may not be present. Perthite forms large anhedral crystals (1,0 to 1,5 mm) which may show Carlsbad or the typical microcline cross-hatched twinning. Zoned clinopyroxene occurs in aggregates somewhat more dispersed than in the lower grade rocks (Figure 10 (d)). Individual crystals are less than 0,1 mm in diameter, exhibit rounded euhedral forms, and are rimmed by green aegirine-augite. The more dispersed nature of the clinopyroxene aggregates results in poikiloblastic texture in the high grade rocks, where alkali feldspar (and quartz if present) enclose scattered pyroxene grains. Sphene is a common minor constituent and poikiloblastic biotite may also be present.

The presence or absence of quartz in the high grade metasomatic rocks appears to be controlled by the mineralogy of the adjacent magmatic rocks. Where these are pulaskites the metasomatic rocks are devoid of quartz. Where the magmatic rocks are granitic, the metasomatic rocks are quartz-bearing. This appears to indicate that the metasomatizing fluids are variable in composition with respect to Si, but are in equilibrium with the adjacent magma.

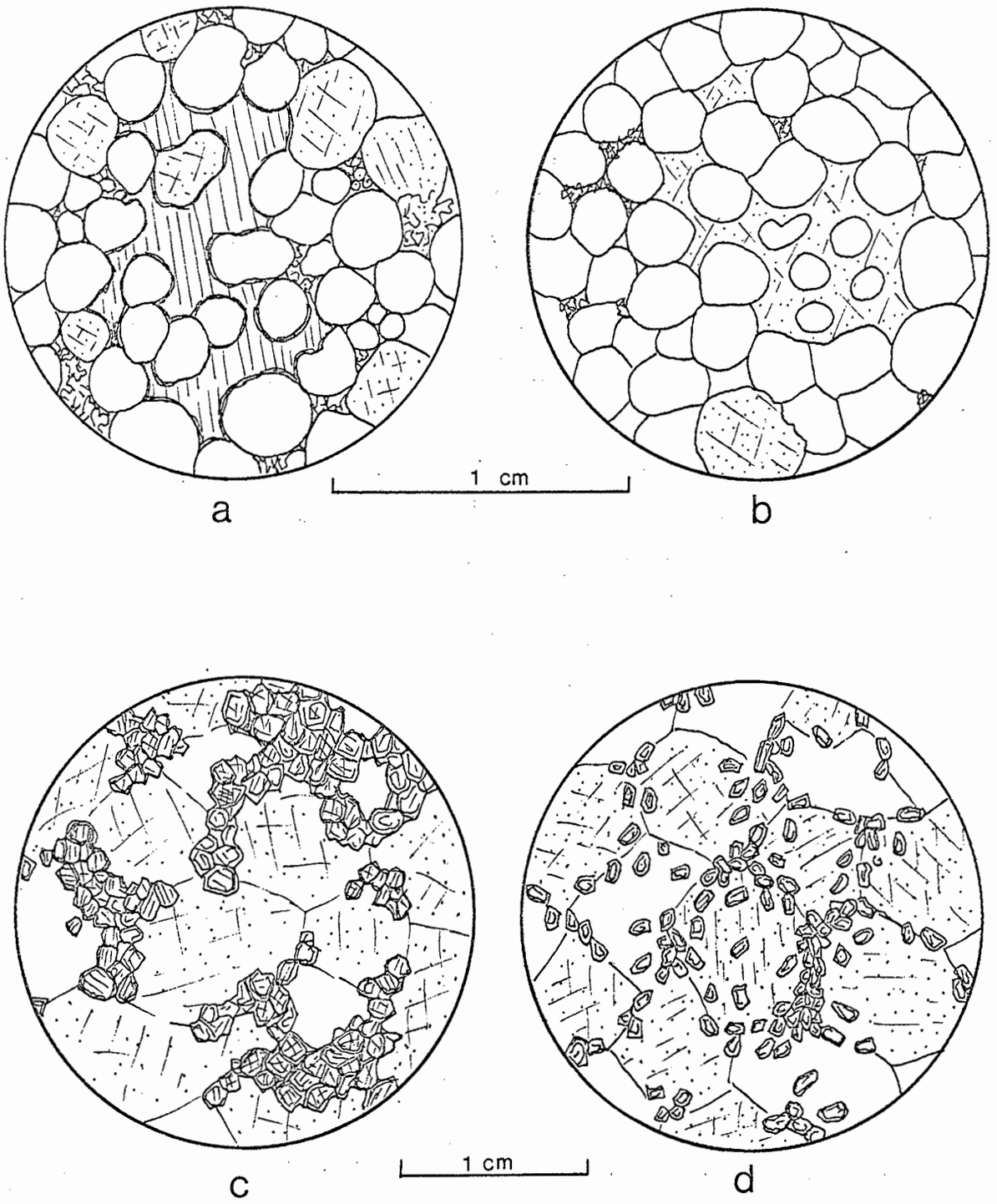

Figure 10. Microdrawings of metasomatites, West Ridge contact zone

(a) - poikiloblastic amphibole

(b) - poikiloblastic alkali feldspar

(c) - sinuous diopside aggregates

(d) - dispersed diopside aggregates

The main features of the metasomatic rocks are:-

1. there is a distinct bimodal distribution of grain size in all the metasomatic rocks. Perthite and quartz have grain sizes in the region 0,5 to 4 mm whereas clinopyroxene is always less than 0,1 mm.

2. Amphibole is present in the low grade rocks but absent from the strongly metasomatized rocks.

3. Clinopyroxene crystallizing in the early stages of metasomatism is diopside, but becomes zoned to aegirine in strongly metasomatized rocks.

4. The zoning in the pyroxenes may be progressive or an abrupt mantling of core by margin.

It is clear from the metasomatic products in the sandstones that a true alkali metasomatism (fenitization) is only evident to any extent in the high grade rocks. Otherwise the production of large amounts of diopside is a striking variation to the normal fenitization process.

3.6.3.4. (c) The chemistry of metasomatism

In order to assess the nature of the metasomatism at Granitberg, major element analyses of 9 rocks have been made and assembled in Table 7. Diagrams illustrating the chemical variation in the analyzed rocks are presented in Figures 11, 12 and 13. These are standard ternary diagrams and Si variation diagrams of the number of ions in a standard cell of 100 oxygens (Currie and Ferguson, 1971).

The triangular plots illustrate that metasomatism is a desilication process with slight enrichment in Na, K, and Fe, and spectacular enrichment of Ca and Mg. This is confirmed by the standard cell Si variation diagrams. These show two trends in reference to the three unaltered feldspathic sandstones (GMA1, GMA2, GMA3). Initially, with decreasing Si there is a parallel and sharp increase in Ca and Mg and a slight increase in Fe, while Al, Na, and K remain essentially constant. Then with a further, but slight, decrease in Si, there is a sharp decrease in the trend of Ca and Mg, and a sharp rise in K, Na, and Al with no change in Fe.

Despite the widely differing modes of GMA6, GMS7, and GMA8, they all plot with near constant number of Si ions (34 - 35) in the unit cell. This may be in indication that the metasomatism works towards reducing the number of Si ions in the rock to constant values, although many more analyses are needed to confirm this.

In all the classical fenetization studies, alkali-iron metasomatism over-shadows other metasomatic effects, though there are many cases where addition of Mg, and more commonly Ca, has occurred, but not in the spectacular manner as the petrographic and chemical data presented here indicate.

The other possibility is that the effects of "metasomatism" are in fact simply the effects of thermal metamorphism of sandstones carrying large but varying amounts of Ca and Mg, possibly as dolomite, $CaMg(CO_3)_2$, i.e. the "fenites" are simply due to recrystallization of dolomitic sandstones at high temperature. From the analyses, this implies from 15% (GMA5) to 30 to 35% (GMA6 - GMA9) dolomite in the sandstones. Such large amounts of Carbonate are not reflected in the analyses of the three feldspathic sandstones (GMA1, GMA2, GMA3) nor do any of the sandstones examined in thin section and in the field indicate more than a trace of carbonate ($< 1\%$) nor any other Ca-Mg mineral. Indeed, Kaiser (1926) does not report any dolomitic sandstones in the sequence. It is also difficult to believe that sampling was so biased that all the "fenites" sampled were originally dolomitic sandstones whereas all the non-metasomatic rocks are not. Given then that large amounts of Ca and Mg were not present in the original sediments, it can only be concluded that they were introduced by metasomatism.

3.6.3.4. (d) Composition of the metasomatic fluids

Ca and Mg have always been considered as insoluble, immobile elements in comparison with the alkali elements. This is true in a pure aqueous phase, but chloride-bearing solutions may contain high concentrations of Ca and Mg (Burnham, 1967). Similar considerations led Currie and Ferguson (1971) to postulate that fenitizing solutions are chloride rich brines. However the chemical and petrographic evidence indicates that alkalies were unimportant in the fenitization process except in the highly fenitized rocks. This suggests that if a chloride metasomatizing fluid is postulated for the

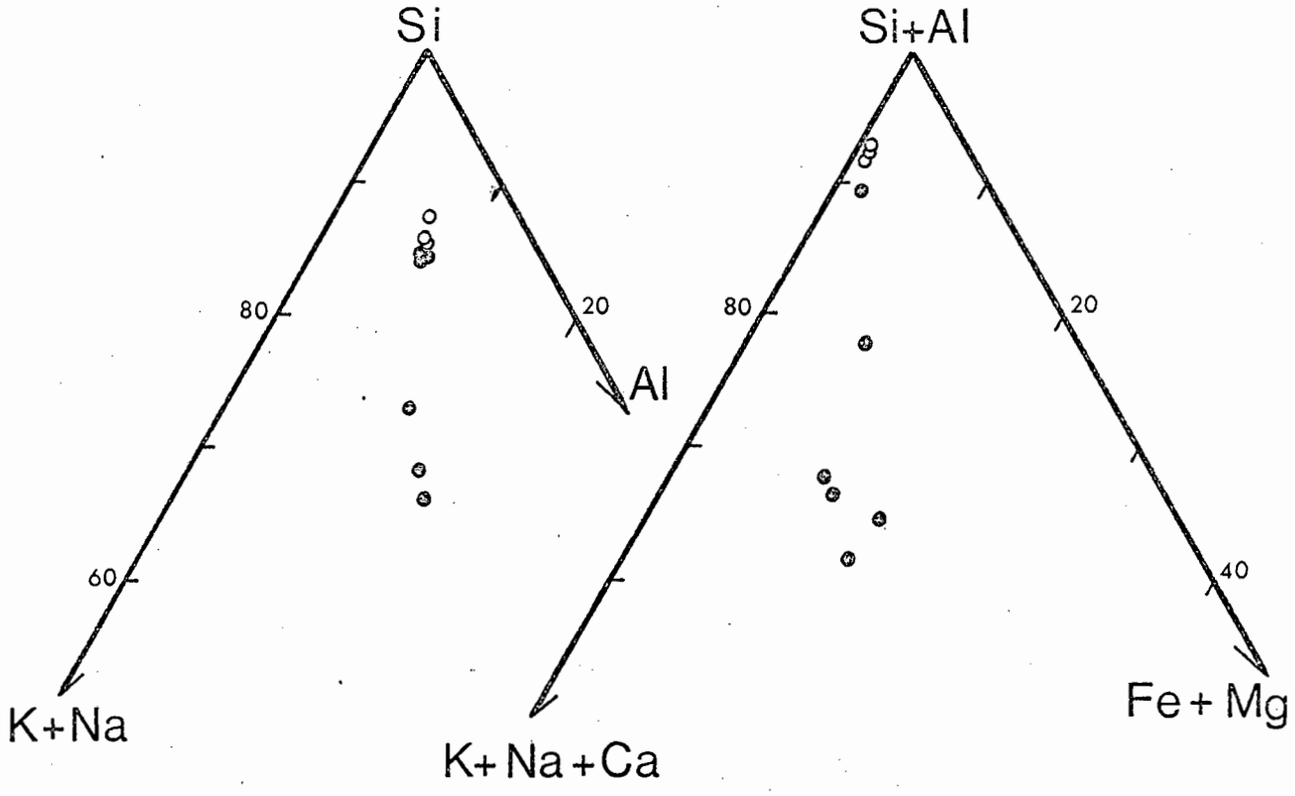

Figure 11. Chemistry of the metasomatites: composition in terms of Si - K+Na - Al and Si+Al - Fe+Mg - K+Na+Ca.

o - feldspathic sandstones

● - metasomatites

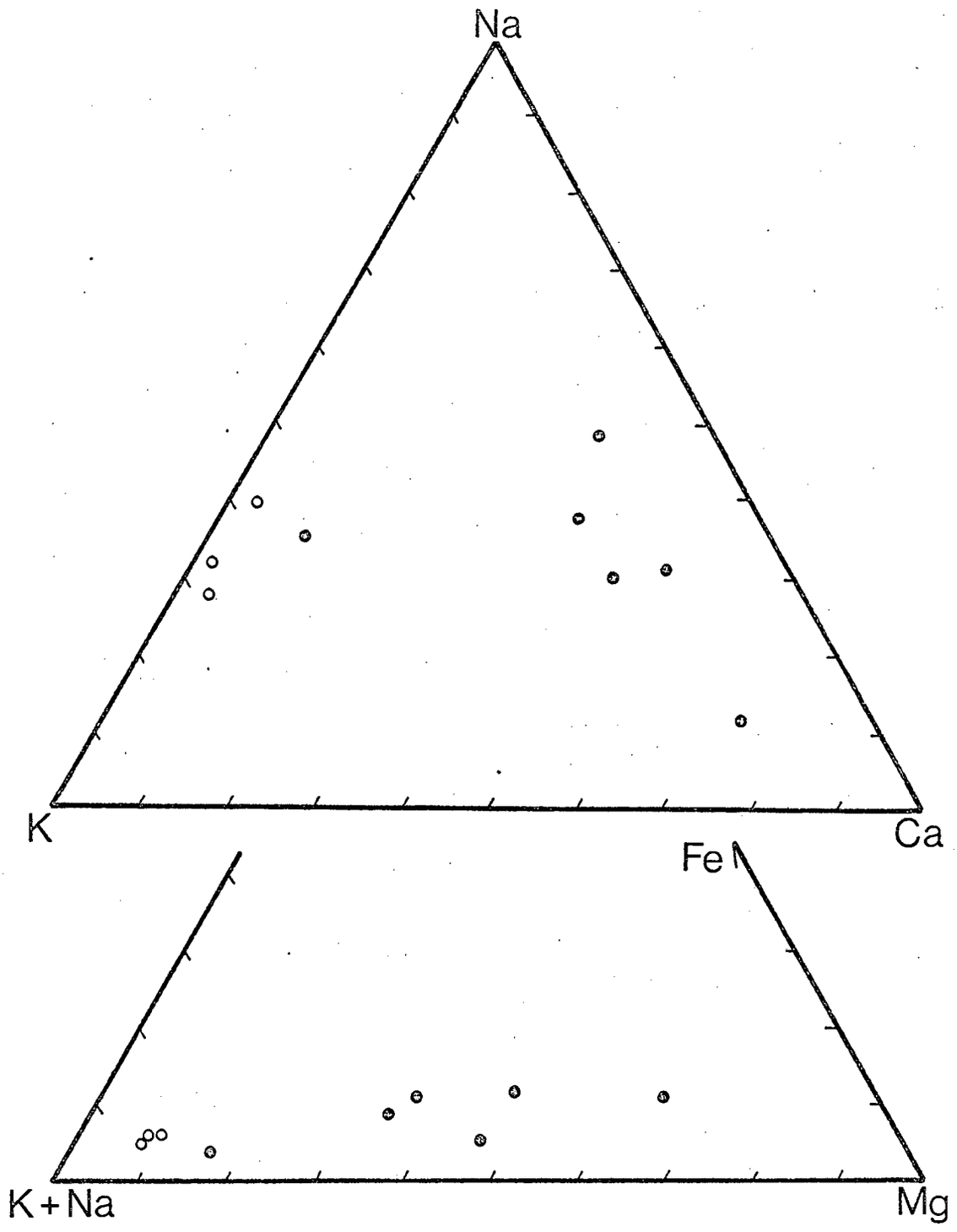

Figure 12. Chemistry of the metasomatites: KNC and FMA plots. Symbols as in Figure 11.

Figure 13. Chemistry of the metasomatites: Si variation diagram. Symbols as in Figure 11.

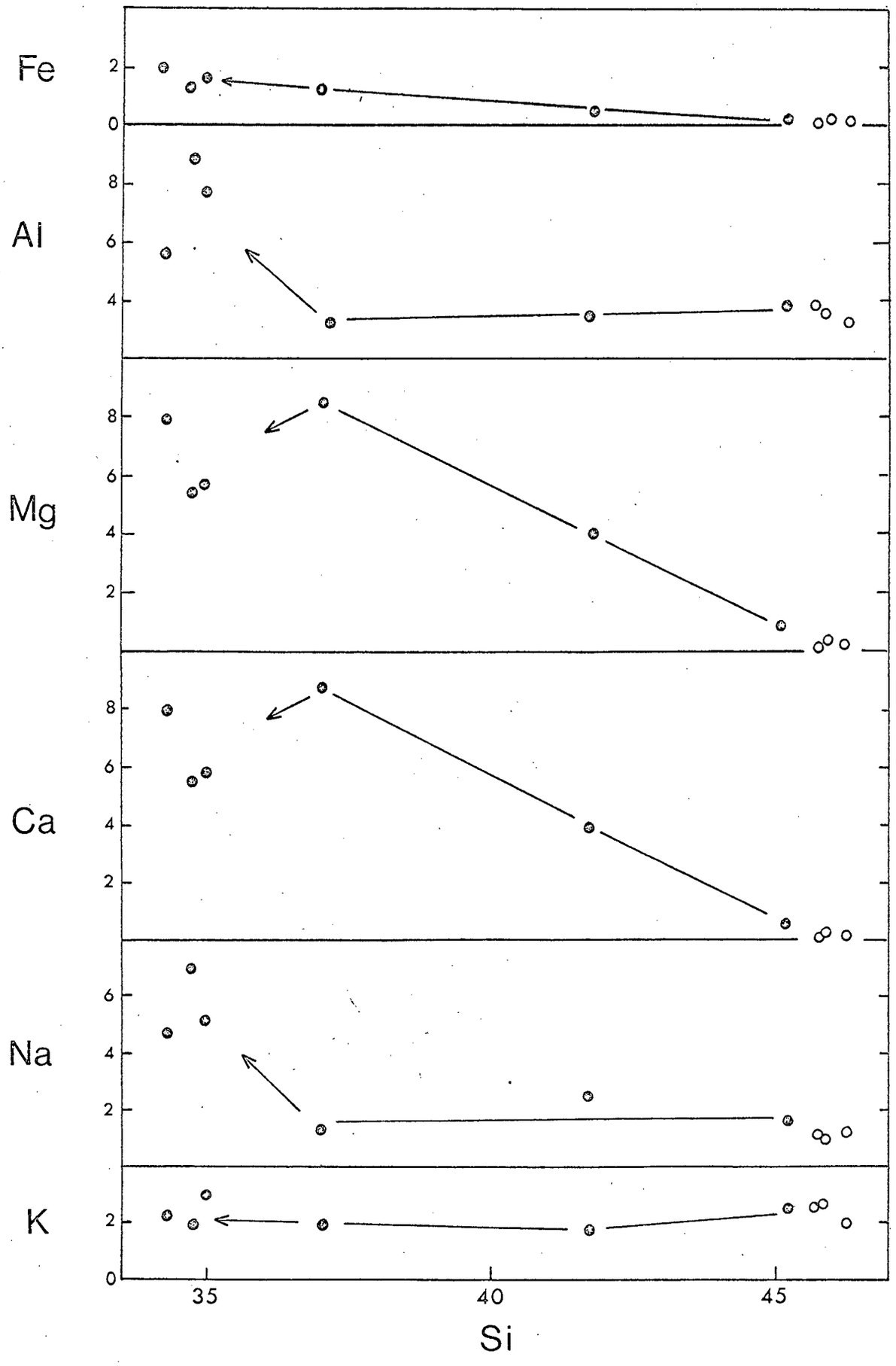

Granitberg rocks, it was poor in alkalies but rich in Ca and Mg! This is difficult to believe, especially if one postulates that the solutions are emanations from, and were in equilibrium with, an alkaline magma.

It is important to note the presence of dolomitic rocks in considerable thickness lying stratigraphically above and below the sandstones. It is perhaps possible that reaction of the magma, or fluids accompanying the magma, with these dolomites produced a fluid phase rich in Ca and Mg compared to the alkalies. This suggestion is not supported by experimental evidence especially if the fluid is also (as seems likely) enriched in CO_2. Burnham (1967) states that in such a fluid, Ca would be far less soluble than the alkalies - contradictions whichever way one turns!

In conclusion it is well to summarise the points of conflict. There is ample evidence to suggest that any metasomatising fluid was in equilibrium with a silicate magma. Yet the chemistry of the metasomatic rocks indicates that the fluid was of highly unusual character, rich in Ca and Mg, and it is doubtful from experimental evidence whether such a fluid could ever be in equilibrium with a magma such as that which crystallized at Granitberg.

3.6.3.5. Fenitization accompanying minor intrusions and fenitization in the Roof Zone

Despite the indications that unusual metasomatism occurred at the contacts at Granitberg there is abundant evidence that "normal" fenitization does occur. It is common to see narrow fenitization zones surrounding intrusions of nordmarkitic and alkali granitic veins and dykes well away from the contact zones. In these cases dykes no more than 20 to 30 cm wide exhibit fenitization "aureoles" 2 to 3 cm wide. These "aureoles" are marked by a greenish colour and thin section examination reveals abundant growth of clear albite, blue, poikiloblastic alkali amphibole and green aegirine in acicular and stubby, prismatic crystals. The aureoles are zoned, with an inner zone of alkali pyroxene and an outer zone of alkali amphibole.

Likewise the metasomatic effects in the Roof Zone sedimentary rocks is different to that of the flanking contact zones. The Roof Zone rocks exhibit strong fenitization effects with preservation of detailed

TABLE 8

Mineral Assemblages in metamorphosed Carbonate rocks

Specimen no.	248	259	255	243	236	254	80	93	242	257	278	175	74	85
Dolomite/Calcite	x	x	x	x	x	x	x	x	x	x	x	x	x	x
Spinel	x		x	x					x	x				x
Forsterite			x	x	x	x			x	x		x		x
Diopside	x						x	x						
Phlogopite	x		x	x										x
Brucite													x	
Periclase							x	x					x	

From Table 8 it is noticeable that spinel and phlogopite are invariably found together - the latter as poikiloblastic grains that frequently enclose the former. Both these minerals are aluminous, indicating the argillaceous nature of the original dolomites. Rocks which are composed largely of diopside (GM248, GM80, GM93) must originally have been highly siliceous dolomites, whereas those that carry forsterite or serpentine pseudomorphs after forsterite (never forming more than 30 to 40% of the rock) were of a less siliceous nature. In the latter the forsterite is concentrated in distinct bands, attesting to the original bedded nature of the dolomites.

From Table 8 a number of features which reflect on the conditions of metamorphism are apparent. These are:-

(1) the most widespread assemblage is spinel + forsterite + dolomite $\pm$ phlogopite.

(2) The assemblage diopside $\pm$ spinel $\pm$ phlogopite $\pm$ periclase + dolomite/calcite is confined to certain siliceous rocks in the immediate vicinity of an intrusive body.

(3) Forsterite and diopside are never found together and there is no evidence to suggest that forsterite follows the development of diopside. In fact forsterite is often present in dolomites that appear to have undergone little recrystallization.

(4) Brucite in GM74 occurs in rounded cavities in the dolomite that has suffered little crystallization. Clear dolomite lines the cavaties in many instances. Despite Kaiser's statement (1926, p. 266) that brucite is a pseudomorph after periclase, textural evidence suggests that the brucite formed directly from the dolomite.

(5) Phlogopite and brucite are the only hydrous minerals found in the contact dolomites.

3.6.4.2. Estimation of metamorphic parameters

Turner (1968, p. 150) is of the opinion that the appearance of the forsterite + carbonate assemblage before the diopside + carbonate assemblage indicates reaction at low fCO_2 and at temperatures less than 490° to 500°C. Under such conditions hydrous minerals (tremolite etc.) would be expected.

The only commonly occurring hydrous mineral in the contact rocks is phlogopite which seldom exceeds 5% of the rock. The occurrence of brucite, the formation of which from dolomite, without prior formation of periclase, requires an essentially aqueous environment at temperatures greater than 470°C (Turner, 1968, p. 141), gives supporting evidence of a low CO_2 content of the fluid phase. Therefore despite the lack of direct petrographic evidence, experimental and thermochemical data indicate that high fH_2O low fCO_2 conditions prevailed during metamorphism. Temperatures were in the range 470° to 525°C, and P total is considered to be low, not greater than 0,5 Kb, though there is no direct evidence for this (see section 8). The bedded nature of the dolomites and their complex interfingering with the magmatic rocks, increases the possibility that within the contact zone microenvironments, with conditions somewhat different to those established above, might have prevailed. Certainly the diopside and periclase assemblage indicate higher fCO_2 (and possibly T) conditions than is required for the generation of the forsterite and brucite bearing assemblages.

One of the interesting features of the coarsely crystalline marbles in the inner zones of the contact zones, is the presence of aegirine or aegirine-augite in the marbles close to intrusive veins of foyaite. The aegirine may or may not be associated with altered nepheline or cancrinite, and aggregates of crystals tend to be concentrated in bands, indicating original bedding in the dolomite. When not located in bands, individual crystals may occur at carbonate grain boundaries, or may even be enclosed in individual carbonate grains.

These features could be accounted for by involving the injection of magmatic material along bedding planes and grain boundaries, followed by crystallization in situ. Schists and siliceous rocks interbedded with these rocks have been converted to alkali feldspar and aegirine bearing assemblages through the process of fenitization, and the aegirine in the dolomites is more likely to have originated by reaction of these fenitizing fluids with siliceous or argillaceous impurities on bedding planes in the dolomite.

The important feature here is that the fenitizing fluids seem to have reacted only with the siliceous and/or argillaceous material and not with the carbonate component of the rock. This has interesting petrological implications, since it is clear support for the experimental evidence (Watkinson and Wyllie, 1971) that alkali-rich fluids responsible for the fenitization accompanying carbonatite intrusions can exist in equilibrium with the carbonatite. Elsewhere it was suggested that the fenitizing fluids at Granitberg were in

equilibrium with a silicate melt of foyaitic composition (section 3.6.3.4. (b)). This suggests that the fenitizing fluids present at carbonatite - alkali rock complexes are possibly in equilibrium with both the carbonatite and the silicate rock melts.

3.6.4.3. Assimilation effects at dolomite - foyaite contacts

Even more spectacular than the contact metamorphic effects in the NE contact zone, is the assimilation of dolomitic material by the foyaite magma. Since the exact nature of the assimilated material is unknown (apart from the pure carbonate rocks, assimilated material includes siliceous dolomites, argillites, and marls), the assimilation processes were not treated quantitatively. Due to the variable nature of the assimilated material, and the extent to which it is incorporated into the magma, a wide range of assimilation products are produced.

The mineralogical effects of assimilation on the foyaite are twofold:-

(a) reduction of the feldspathoid/feldspar ratio in the derivative rocks, i.e. the production of saturated rather than undersaturated rocks;

(b) increase in the mafic/felsic mineral ratio in the derivative rocks.

Despite this tendency for assimilation to produce mafic rocks, veins and small plugs of leucocratic pegmatites and pulaskites are common in the contact zone. This is a reflection of the variable nature of the assimilated material, and also suggests that a crystal fractionation system operates in conjunction with assimilation. Within several of the intrusive bodies the grain size is also highly variable and may range from fine grained ($< 0,5$ mm) to pegmatitic (> 2 cm) over a few centimetres.

Despite these inhomogeneities, the most widespread rock type in the contact zone is a medium- to coarse-grained, even-textured shonkinite. The dominant constituent of the shonkinite is anhedral perthite that poikilitically encloses the mafic minerals of which biotite is the most abundant. The biotite itself is host to apatite and opaque oxides (Ti-magnetite). Clinopyroxene occurs as euhedral augite, zoned towards aegirine-augite at the rims. Sphene is common as large (1 to 3 mm) euhedral crystals. Altered nepheline and sodalite occur in minor amounts in the interstitial positions in the rock. Table 9 lists the mode of a typical shonkinite.

The shonkinite grades into a more mafic facies in which slightly zoned subhedral aegirine-augite and minor amounts of Ti-magnetite and biotite form 60 to 70% of the rock together with accessory sphene and apatite. Nepheline and perthite, the former often dominant to the exclusion of the latter, occur as large poikilitic crystals enclosing the mafic minerals. These rocks have the textural characteristics of cumulates and can be described mineralogically as feldspar-bearing members of the ijolite-melteigite seies.

It is significant that the association ijolite - nepheline syenite - dolomite in the NE contact zone is analogous to the association ijolite - nepheline syenite - carbonatite found in many alkaline rock complexes, and the origin and evolution of which, are the cause of much speculation. The evidence from Granitberg suggests that reaction between carbonatite and nepheline syenite could produce rocks of the ijolite-melteigite series.

Besides the mafic rocks, there are many smaller intrusions which show only slight degrees of dolomite contamination. This contamination is indicated by alteration of the nepheline (surprisingly cancrinite is not at all common), decrease in the acmite component of the clinopyroxenes, precipitation of abundant sphene, and breakdown of the Ti-magnetite to produce sphene. Biotite, and less commonly pyroxene display dark reaction rims. Plagioclase does not crystallize.

The chemical changes accompanying the assimilation are best illustrated by comparing analyses of the shonkinite with the average for the Outer Foyaite (Table 9). Assimilation has produced decreases in Si, Al, and Na, whereas marked increases in Mg, Ca, Fe and Ti have occurred. K remains essentially constant, probably due to it being fixed in the biotite. The magnitude of the change with respect to the Outer Foyaite is also indicated in Table 9.

Considering the chemistry, mineralogy, and textural features of the derivative rocks, it is clear that if crystal fractionation operated in the foyaite - dolomite assimilation zone, then undersaturated residual liquids enriched in Na and volatiles can be produced. This is the liquid which has crystallized in the interstices in the various shonkinites and other mafic rocks. The widespread pegmatites, poor in mafic minerals but commonly rich in nepheline, found in the contact zone, may be the crystallization products of these residual liquids generated by assimilation -

TABLE 9

Mode, Wt% analysis, CIPW Norm and Standard Cell of Shonkinite GM88.

Mode		Wt% Analysis		CIPW Norm		Cations in standard cell*			
							1	2	
Perthite	55,4	SiO_2	51,36	or	31,20	Si	30,4	32,8	
Felspathoids	2,9	TiO_2	1,89	ab	31,60	Ti	0,9	0,2	
Biotite	21,9	Al_2O_3	14,97	an	3,53	Al	10,4	14,7	
Clinopyroxene	12,4	Fe_2O_3	5,37	ne	5,07	Fe^{3+}	5,5	1,1	(5x)
Opaques	3,4	FeO	6,16	di	5,75	Mn	0,2	0,1	
Sphene	2,1	MnO	0,48	ol	7,24	Mg	2,8	0,2	(14x)
Apatite	2,2	MgO	3,22	mt	7,79	Ca	2,4	0,5	(5x)
		CaO	3,73	il	3,55	K	4,0	4,4	
		K_2O	5,28	ap	2,87	Na	5,6	11,0	
		Na_2O	4,84			P	0,6	-	
		P_2O_5	1,21						
		H_2O	0,21						
		L.O.I.	0,98						
			99,70						

* Standard cell based on 100 oxygen atoms.

1 Shonkinite

2 Average outer foyaite

crystal fractionation.

The alkali-rich fluid phase accompanying these residual liquids may be responsible for the fenitization evident in some of the siliceous sediments in the contact zone. A similar suggestion was made for the SW contact zone in order to account for the unusual nature of the metasomatism there. This implies that although the fenitizing fluids may not accompany the foyaite, they may be generated at contact zones by assimilation reactions between country rock and magma. It is thus possible that the nature of the assimilation reactions can control the chemistry of the fenitizing fluids.

Kesler (1968) has described assimilation reactions between quartz-monzonite and marble at Haiti, in which syenodiorite and pockets of syenite and nepheline syenite have been produced. The latter he ascribes to metasomatic replacement of plagioclase by orthoclase, i.e. a K-metasomatism. At Haiti the assimilation products show a progressive decrease in K_2O/Na_2O, i.e. Na_2O was fixed in early formed crystals (plagioclase) and a K-rich liquid and fluid were generated. Although Kesler did not comment on the origin of the K-rich metasomatic fluids it seems possible that they originated in this way. As discussed above, a parallel situation exists at Granitberg, except that the shonkinite shows an increase in K_2O/Na_2O compared with the Outer Foyaite. Therefore K is fixed in the crystallizing solids and a liquid and fluid phase rich in Na is generated.

In summary, reactions between the dolomites and an alkaline silicate magma can produce a wide range of derivative rock types, especially if crystal fractionation accompanies the assimilation process. In this way a full range of alkaline rocks, from melteigite-ijolite (cumulate) through shonkinite, to undersaturated leucocratic pegmatites may develop. Alkali-rich fenitizing fluids may also be generated, even where none existed before.

3.7. DYKE ROCKS

Dykes are extremely common in the vicinity of Granitberg. Unlike at Pomona, no radial pattern is developed; instead the dykes strike dominantly in a ENE direction (see Kaiser, 1926, p. 313). Petrographically the dykes can be divided into several different types. These are:

(a) orthophyric tinguaites;

(b) trachytic textured tinguaites;

(c) quartz-bostonites and grorudites;

(d) breccia dykes;

(e) lamprophyres.

3.7.1. Tinguaite dykes

These are the most abundant dyke rocks in the vicinity of Granitberg. Two ages of intrusion can be recognised, but they show no difference in their petrographic characteristics. Several thin dykes intruding the Roof Zone rocks are not continuous into the Outer Foyaite and are inferred to predate the Outer Foyaite emplacement. The majority of dykes, however, intrude both the Outer Foyaite and the Roof Zone.

The dykes vary in width from thin veins less than 5 cm wide to long, persistent dykes 2 to 3 m wide. Occasionally the dykes may swell out and form plug-like bodies. Two different textural types can be recognised in the tinguates, and these are discussed below. In addition, the chemical analyses (Table 12) of two tinguaites indicates that chemically diversity also exists, and a more comprehensive study on these dykes could prove a profitable undertaking.

3.7.1.1. Orthophyric tinguaites

These are the least abundant of the two types and are confined to the S parts of the complex. They are fine-grained with an orthophyric texture and are invariably banded due to *in situ* differentiation.

Equidimensional nepheline and stubby alkali feldspar are the dominant constituents of the rock. However, the characteristic feature of these dykes is the presence of magnetite and its antipathetic relationship with aegirine. Magnetite occurs as partially resorped microphenocrysts, and the area immediately surrounding these aggregates is devoid of aegirine. The latter mineral occurs as subhedral, or large poikilitic crystals, which may be concentrated in bands. Thus, these dykes have a banded or blotchy appearance,

and can be considered to consist of the following contrasted assemblages:

(a) nepheline+ perthite + aegirine

(b) nepheline + perthite + magnetite

Eudialyte-eucolite and lavenite are accessory minerals.

The petrographic features of these dykes indicate crystallization under static conditions. The tinguaite initially crystallized perthite, nepheline, and magnetite, and these phases underwent a limited amount of crystal settling. With increase of peralkalinity in the residual liquid with cooling, the magnetite became unstable, was partially resorped, and aegirine crystallized. There is no direct evidence of the reaction relationship between magnetite and aegirine, i.e. aegirine is not seen mantling magnetite.

3.7.1.2. Trachytic-textured tinguaites

These dykes are characterized by a well developed trachytic texture and the absence of Fe-Ti oxides. Nepheline and alkali feldspar are the dominant constituents, and acicular aegirine is the dominant mafic mineral. Biotite is invariably present and may form microphenocrysts. Accessory minerals are lavenite, fluorite, cancrinite, and eudialyte-eucolite, the latter being particularly abundant in some tinguaites and easily identified in hand specimen. These accessory minerals are not present in all the dykes.

It is postulated that magnetite initially crystallized in these tinguaites but non-static conditions facilitated complete resorption of the magnetite, prevented in situ differentiation, and produced the distinct trachytic texture.

3.7.2. Quartz-bostonite and grorudites

Quartz-bostonites are less abundant in the vicinity of Granitberg than elsewhere in the Luderitz Province. They occur as wide (2 to 5 m), yellow-brown to red-brown fine-grained dykes and sheets, particularly in the northern part of the intrusion. Most of the wider dykes are extremely persistent and may be traced for several miles. They apparently represent the latest phase of magmatic activity in the province as they cut across all

other dykes and intrusions.

The grorudites (perthite + aegirine + little quartz) are dark fine-grained rocks exposed as gently dipping sheets to the NE of the complex. The bostonites grade into grorudites by increase in the Na-pyroxene content, and all gradations between the two probably exist, though the extreme alteration common to many of these oversaturated dykes is responsible for the apparent paucity of mafic minerals.

3.7.2.1. Petrographic Features

These rocks are fine-grained porphyritic rocks, with a ground mass that displays well developed orthophyric, and less commonly, bostonitic textures. Perthite occurs as euhedral phenocrysts (< 5% of the rock) and is the dominant constituent in the groundmass. The structural state of the alkali feldspar is close to maximum microcline (see section 7.8.1.). Quartz is found in the interstitial positions in the rock and never exceeds 5%. Aegirine is abundant in the grorudite, but is rare or absent in the bostonites. In the latter it may be accompanied by alkali amphibole.

Chemical analyses, CIPW norms and modes of these rocks are presented in Table 12

3.7.3. Breccia Dykes

Two wide, semicircular breccia dykes intrude the Outer Foyaite to the E and N of the Roof Zone. The dykes dip SW at angles of 60° to 70° and are dark-coloured rocks, packed with angular fragments of fine- and coarse-grained magmatic rocks, as well as fragments of sandstone, schists, and gneisses, although the latter types are comparatively rare. The fragments range in size from microscopic to large blocks 30 to 40 cm in diameter. Most of the fragments display narrow reaction rims at their contacts with the groundmass.

The dykes are concentric about a point in the centre of the Roof Zone, and to the south and north west must eventually encounter the Oyter Foyaite - country rock contact zones, although this is not observed in the field due to sand cover. However, the evidence suggests that they die out before or at the contacts (see the 1;10 000 geological map). The breccia dykes cut across

the tinguaite dykes, but are themselves intruded by the late bostonite dykes.

The interpretation of the breccia dykes ~~are~~ is problematical. They appear to be incomplete cone sheets focussed at a point below the central portion of the Roof Zone. Instability in this zone could have resulted in fracturing of the Outer Foyaite and emplacement of the brecciated material. To the S and W the stresses resulting from this instability were probably relieved by the discontinuities at the contact zones, and no fracturing and breccia emplacement occurred there.

3.7.4. Lamprophyre dykes

None of the lamprophyres recorded by Kaiser (1926) were found during this study. From Kaiser's work they appear to be numerically rare in the vicinity of Granitberg in comparison with the other types.

3.8. INTRUSIVE HISTORY OF THE COMPLEX

1. Emplacement of sheets and dykes of Perphyritic Syenite.
2. Intrusion of a vertical plug of undersaturated trachytic magma. The upper portion of the magma chills below the roof of Bogenfels Formation sediments to form the PCNS.
3. Intrusion of the Inner Foyaite as a vertical plug into the PCNS. During crystallization, a liquid, volatile-rich top was maintained in the magma chamber. Crystallization at the top of the chamber results in crystal settling and the production of a thin band of layered foyaites. Explosive escape of volatiles disrupts the PCNS roof and introduces a large number of xenoliths into the magma. Crystallization and settling of crystals and xenoliths results in the formation of the Xenolith Cumulate and the Laminated Foyaite.
4. Intrusion of tinguaite dykes.
5. Ring fractures form due to upward movement of the Outer Foyaite magma, and result in the detachment of the Inner Foyaite - Roof Zone segment from the roof. The Roof Zone segment founders in the rising Outer Foyaite magma.
6. The Outer Foyaite crystallizes. Assimilation - metasomatic

reactions at the contacts results in the production of a wide variety of exotic rock types in the contact zones.

7. The main mass of tinguaite dykes are intruded. Movement below the Roof Zone segment fractures the Outer Foyaite and brecciated material is injected along the fractures.

8. Intrusion of the quartz-bostonites and the grorudite sheets.

CHAPTER 4

POMONA SYENITE COMPLEX

4.1. INTRODUCTION

The Pomona Syenite Complex lies on the coast between Pomona Island and Jammerbucht, due west of the abandoned mining town of Pomona. One half to two thirds of the complex is exposed, the remainder lies below the present day sea level.

The complex is 2,5 to 3,0 km in diameter, and along its eastern edge reaches a height of 80 m above msl, forming the Schlueberg. Syenites of the complex are intrusive into Precambrian gneisses of Pre-Gariep age. The total outcrop area of the complex and the basement rocks is high, though proximity to the coast has resulted in most of the exposed rock surfaces being highly weathered and of poor quality.

Ring structures in the complex are accentuated by the concentric pattern of ridges and valleys - particularly evident on air photographs - within the syenite outcrop area. A strong radial dyke pattern is also well developed.

4.2. PREVIOUS INVESTIGATION

The only published account of the syenites is that of Kaiser (1926, p. 224 - 227). He referred to the complex as the Signalberg-Schlueberg Massif, but it has been renamed the Pomona Complex here, due to the proximity of the Pomona mining area which appears on most published maps. Kaiser (1926) discerned an inner and a marginal division to the intrusion, and noted the presence of nepheline-bearing rocks in the inner portion. He also gave a brief account of the contact zones, and attempted to account for the presence of nepheline in some of the rocks by considering Daly's limestone assimilation hypothesis.

4.3. THE PRECAMBRIAN BASEMENT GNEISSES

The basement rocks into which the complex is intruded are biotite gneisses ranging from granitic to granodioritic in composition. They consist

essentially of quartz, perthite, plagioclase, muscovite and biotite, with minor amounts of sphene, zircon, apatite and chlorite. Coarsely porphyroblastic green gneisses and even-grained grey gneisses are the most common textural varieties, and they display a strong NNW trending foliation.

Although not radiometrically dated, the gneisses must be pre-Gariep in age as they are overlain by the Bogenfels Formation further to the east. The Bogenfels Formation is part of the Gariep Group (Kroner, 1972) which is late-Precambrian in age. It is possible that the gneisses can be correlated with the Kheis System which is older than 1850 my.

4.4. SYENITES OF THE INTRUSIVE COMPLEX

4.4.1. Introduction

Structurally the complex consists of two concentric rings of syenite, the Inner and Outer Syenites, arranged about a central plug of nordmarkite, the Hub Syenite. Minor intrusions of syenite porphyry and nepheline syenite also occur in the central part of the complex, whereas a nordmarkite ring dyke and breccia bodies associated with quartz-feldspar porphyries occur in the gneisses beyond the contact.

The syenite-gneiss contact on Pomona Island has been interpreted from air photographs and by examination from the mainland. It was not possible to visit the island during this study, so the presence of a contact as indicated on the 1:10 000 geological map remains unconfirmed. Kaiser also indicated that a contact existed here, but he did not visit the island (p. 225).

4.4.2. The Outer Syenite

The Outer Syenite covers the largest area in the complex and, as its name implies, it occurs in the outer zones where it is everywhere in contact with the gneisses. Towards the centre of the complex it grades into the Inner Syenite.

Essentially the Outer Syenite is characterised by the presence of augite and occasional zoned feldspar crystals with cores of untwinned oligoclase and rims of perthite. Both augite and the zoned feldspars are absent

TABLE 10

Comparative modes of the Inner and Outer Syenites, Pomona

	Felsics	Mafics
Inner Syenite		
PM 150	94,1	5,9
PM 146	91,7	8,3
Outer Syenite		
PM 31	78,5	22,5
PM 157	76,4	23,6

from the Inner Syenite, and in general the abundance of mafic minerals in the Outer Syenite is greater than in the Inner Syenite (see modes in Table 10). The petrographic differences between the two syenites are therefore slight, though the mineral and whole rock chemistry is distinctive (see chapters 6 and 7).

The gradational boundary between the Inner Syenite and the Outer Syenite is indicated on the 1:10 000 map. Its position is only approximate and was fixed by petrographic classification of syenites collected along radial traverses across the complex. In some respects the designation 'Inner Syenite' and 'Outer Syenite' is artificial, and a continuous gradation in composition possibly exists. Such a gradation would be difficult to prove petrographically, and an extensive geochemical investigation of the problem is beyond the scope of this work. There is however evidence that the two syenites evolved separately and an intrusive relationship exists between them (see below and section 4.7).

4.4.2.1. Petrographic features

The Outer Syenite is coarse-grained (ave. grain size 4 to 8 mm) and leucocratic with a hypidiomorphic granular texture. Anhedral alkali feldspar is the dominant constituent and exhibits a coarse 'patch' type exsolution texture. Migration of exsolved phases has occurred, such that grain boundaries are highly sutured and interpenetrative. It is not uncommon to find blebs of albite, exsolved from one alkali feldspar grain, included in an adjacent grain. The result is a distinctive interpenetrating exsolution texture (see Figure 14). The Na-rich phase in the perthites is less altered than the K-rich phase, and commonly displays albite twinning.

The zoned feldspar crystals form less than 2% of the rock. The cores of these grains are untwinned, or exhibit only a very faint repeated twinning. The optical properties of these cores indicate that they range from sodic oligoclase to anorthoclase in composition. There is generally a regular gradation in composition from the cores to the normal perthitic rims in these grains, but occasional examples of abrupt mantling, i.e. sharp contact between mantle and core, are seen. The perthites have a bulk composition of $Ab_{66}Or_{34}$. X-ray diffraction data (see section 7.8.1.) indicate that the structural state of the potassic phase is intermediate between orthoclase and microcline.

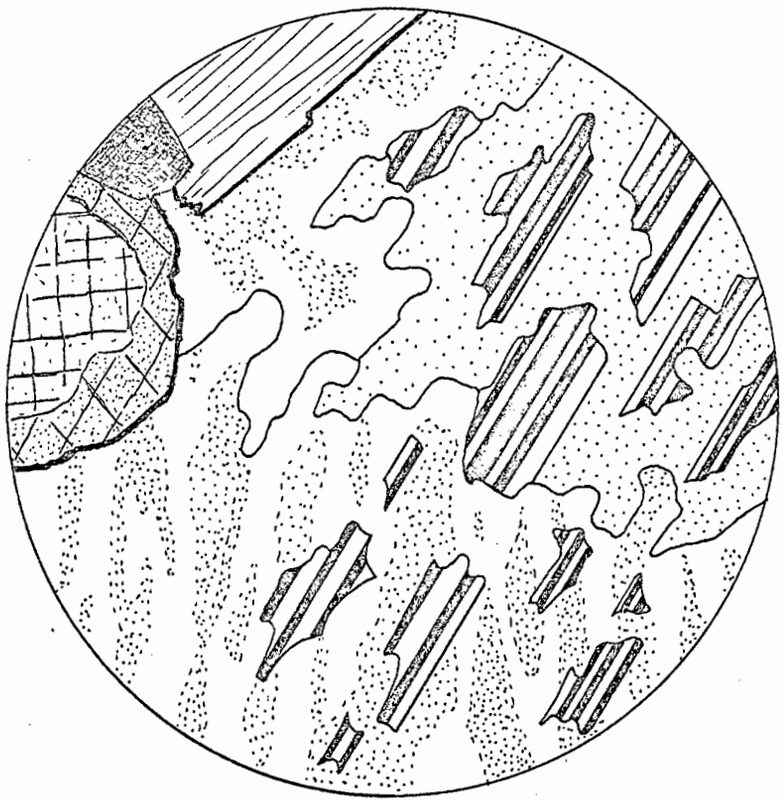

Figure 14. Interpenetrating exsolution texture in alkali feldspars from the Outer Syenite, Pomona. Stippled – K'feldspar clear, twinned – albite

Key – stippling – alteration?

Mafic minerals are sparsely distributed through the rock in aggregates. Euhedral biotite is the most abundant mafic constituent and ranges in composition from $Ann_{56}Phlog_{40}MnBi_2TiBi_2$ to $Ann_{52}Phlog_{43}MnBi_2TiBi_3$ (see Table 19). No zoning was detected in the grains during analysis.

Augite ($Di_{63}Hd_{29}Ac_8$ - $Di_{59}Hd_{31}Ac_{10}$) is rimmed by amphibole in the composition range Fe-edenite to Fe-hastingsite. (Analyses are presented in Table 20). During analysis a slight zoning towards Fe-rich and Mn-rich margins was detected, although this was not determined quantitatively.

Euhedral sphene, Ti-magnetite ($Usp_{14}Mt_{86}$) and apatite are accessory minerals. Sphene occurs as large crystals up to 4 mm in length and is easily recognised in hand specimen. Ti-magnetite is presently seen as an intergrowth of magnetite and ilmenite, the latter exsolved through oxidation (Buddington and Lindsley, 1964). A chemical analysis of a bulk separate is presented in Table 24. In many instances the Ti-magnetite may display narrow rims of biotite or amphibole where it is in contact with alkali feldspar. Apatite is abundant as euhedral crystals (up to 0,1 mm in diameter) commonly enclosed in mafic minerals especially biotite.

Within the Outer Syenite there is considerable variation in mafic mineral abundances. Schlieren of more mafic syenites are common, their darker appearance in the field being due to 'dusting' of the perthite by abundant small crystals ($< 0{,}01$ mm) of opaque oxide and biotite. However in grain-size and texture they do not differ from the normal syenite. In contrast, more leucocratic segregations and schlieren are commonly pegmatitic with individual perthite crystals up to 5 cm in size.

4.4.2.2. Possible evidence for a transgressive Inner Syenite - Outer Syenite relationship

On the coast N of Signalberg, and just N of the Inner Syenite - Outer Syenite contact as indicated on the 1:10 000 map, the Outer Syenite reveals a distinct banding of more mafic syenite alternating with more leucocratic syenite. The banding is irregular along strike and dips steeply to the SW. Individual bands average 5 to 8 cm in width. The mafic syenite generally shows a diffuse or gradational contact with the leucocratic syenite, but in many places the contact is sharp. In the same area the leucocratic syenites may enclose numerous inclusions of more mafic syenite. These inclusions range in size

from 5 to 10 cm, up to several tens of metres in diameter, and usually display gradational contacts with the enclosing syenite.

These features are similar to features displayed at the Inner Syenite - Hub Syenite contact (see section 4.4.3), and provide the only field evidence for a transgressive contact between the Inner and Outer Syenites. Elsewhere the contact between the two syenites appears to be gradational, indicating in situ differentiation of a single magmatic pulse. The mineralogical and chemical evidence, however does not explicitly support either of these suggestions.

4.4.2.3. Outer Syenite - gneiss contact

The intrusive contact between the Outer Syenite and the gneisses is well exposed over wide areas. The contact is complex, with repeated interfingering of syenite and gneiss forming a 30 to 40 m wide contact zone. In the N, on the coast, the contact gneisses are dark green and coarsely porphyroblastic, whereas further south, in the vicinity of Schlueberg, the gneisses are more leucocratic and equigranular and may be difficult to distinguish from the syenites in the field.

The southern contact, N of Kreuzberg, is poorly exposed due to extensive chemical alteration of the gneisses and the syenites. Nevertheless the trace of the contact is easily discerned due to the contrasting colour of the weathered products of the gneisses and the syenites. W of Kreuzberg, a wide dune belt covers all exposures and the contact only appears again at the coast.

4.4.2.3. (a) Contact metamorphism in the gneisses

Macroscopic metamorphic effects are only observed in the gneisses within 5 to 10 m of the contact. These effects are most marked in the green porphyroblastic gneisses which are sheared at the contact and display extensive recrystallization to produce leucocratic porphyroblastic gneisses with an aplitic groundmass. The more leucocratic gneisses have also suffered extensive recrystallization, though this is not apparent in the outcrops. Microscopically the result of this recrystallization is the development of extensive trails of fine grained intergrowths of clear alkali feldspar and quartz. Kaiser (1926, p. 226) reported cordierite and andalusite from some of the contact gneisses though none were observed in this study.

4.4.2.3. (b) The Outer Syenite contact facies

Within the contact zone the various tongues and bodies of syenite show the effects of contamination/assimilation to varying degrees. The commonest sign of contamination is the development of coarse clots of mafic minerals, especially biotite, and the sporadic appearance of quartz. The latter frequently occurs in pegmatitic segregations, where quartz grains 1 to 2 cm in diameter are surrounded by large 2 to 4 cm grains of perthite.

Evidence that the quartz content in the syenites arises through limited assimilation of the siliceous gneisses, is seen where xenoliths of gneiss occur in the syenite. In such situations the syenite develops a nordmarkitic zone immediately surrounding the xenolith.

The presence of coarse-grained, almost pegmatitic, leucocratic syenites, similar to those described along the W-SW contact zone at Granitberg, is another marked feature of the contact zone. As at Granitberg, chilled magmatic contact rocks are either absent or of very minor importance. At Pomona the only rocks which could be regarded as chilled syenites are grey, medium-grained porphyritic syenites which occur as intrusive tongues and plugs in the vicinity of Schlueberg.

Another feature of the contact zone is the large number of medium-grained nordmarkitic and granitic bodies intrusive into the gneisses beyond the contact. These are in the form of irregular, inpersistent dykes, sheets, and veins, seldom more than 50 to 75 cm wide, which do not penetrate the gneisses for more than 100 to 150 m beyond the contact. They appear to have arisen in the contact zone through processes of assimilation/fractionation, similar to that described for the origin of the quartz-bearing intrusives in the W-SW contact zone at Granitberg (section 3.6.3.3.), and must be distinguished from the regular, persistent bostonite dykes that intrude both the syenites and the gneisses.

All of the Pomona contact zone intrusives display similar petrographic features, with euhedral perthite as the dominant constituent and interstitial quartz in varying amounts. An Fe-Ti oxide is generally the sole mafic constituent, but in a few instances may be accompanied by accessory biotite. Alkali amphibole and Na-pyroxene were noted in some of the intrusives.

A particularly strong concentration of these dykes and veins occur at Kreuzberg where they anastomoze through the gneisses over a wide area.

4.4.3. The Inner Syenite

The Inner Syenite crops out as a broad ring around the centrally situated Hub Syenite. The relationship between the Inner and Outer Syenites has already been discussed. The contact between the Hub Syenite and the Inner Syenite is exposed only over a few metres on the coast SW of Signalberg, everywhere else the contact is marked by a sand-filled, arcuate depression, in which sporadic outcrops of a biotite-rich monzonite are found.

At the contact exposure mentioned above there is a complex interfingering of the two syenites, with the frequent occurrence of xenoliths of Inner Syenite enclosed by the Hub Syenite. These xenoliths may display sharp or diffuse boundaries. The Hub Syenite is not chilled against them, nor against the main mass of Inner Syenite. The latter syenite develops a more mafic-rich facies at the contact and is typically darker than the intrusive Hub Syenite.

4.4.3.1. Petrographic Features

The petrographic distinctions between the Inner and the Outer Syenite have been discussed (see section 4.4.2.2.). The Inner Syenite is leucocratic, coarse-grained and has a hypidiomorphic granular texture. Perthite ($Ab_{61}Or_{39}$) occurs as euhedral to subhedral crystals displaying a fine to medium exsolution intergrowth of Na- and K-rich phases. Some specimens do however display the interpenetrating intergrowths so characteristic of the Outer Syenite. The structural state of the feldspar is intermediate between orthoclase and microcline. Anhedral to subhedral alkali amphibole, intermediate in composition between a richterite and arfvedsonite (analysis in Table 20) is the dominant mafic mineral. Biotite ($Ann_{38}Phlog_{50}MnBi_5TiBi_6$) -(analysis in Table 19), varies in abundance and may only occur in trace amounts in some specimens. Subhedral sphene is common, as is Ti-magnetite, the latter having suffered oxidation in many specimens. Accessory minerals include zircon and euhedral apatite.

4.4.4. The Biotite-rich Monzonites

Outcrops of the Monzonite are consistently confined to the sand-filled depression which marks the contact of the Hub and Inner Syenites, except for two occurrences lying wholly within the Inner Syenite. These are just NNE of Signalberg, and inland from the coast, opposite Pomona Island. However at only one locality is the Monzonite actually seen in contact with any of the syenites - this is on the coast NW of Signalberg. Here the Hub Syenite intrudes the Monzonite. The contact is sharp, and leucocratic veins emanating from the syenite intrude the monzonite. Within 10 to 20 cm from the contact the Monzonite has recrystallised as an even-textured, medium-grained monzonite. Further from the contact the Monzonite displays the typical texture and mineralogy described below. A weak vertical orientation of biotite flakes is evident, and a few small (< 10 cm) xenoliths of fine grained porphyritic syenite within the Monzonite show a similar preferred orientation.

As one approaches the contact with the Inner Syenite the Monzonite becomes gradually more leucocratic. At this contact the Monzonite grades rapidly over 1 m into normal syenite. A suite of samples taken across the Monzonite show a steady decrease in the size and abundance of biotite and sphene, the gradual disappearance of plagioclase and the development of amphibole at the expense of augite as the Inner Syenite is approached.

The occurrences within the Inner Syenite are poorly exposed, but similar leucocratic trends towards the contacts (not exposed) can be discerned.

In summary, the Monzonite is confined to areas near, or at, the contact between the Hub and Inner syenites. It is intruded by the Hub Syenite but shows a gradational contact with the Inner Syenite. Its distinctive mineralogy and chemistry preclude it from being a product of reaction or metamorphism between the Inner and Hub syenites.

4.4.4.1. Petrographic Features

The Monzonite is mesocratic, coarse-grained with a hypidiomorphic granular texture. The dominant feature of the rock are the large (1,0 to 1,5 cm) plates of biotite ($Ann_{46}Phlog_{49}MnBi_1TiBi_5$ - analysis in Table 19) which form about 20% of the rock. Zoned feldspar with plagioclase cores (An_{40-45}) rimmed by perthite occur as subhedral crystals of 4 to 8 mm. The

composition of the perthite was estimated from the whole rock and mafic mineral analyses and the mode to be $Or_{20-25}Ab_{25-75}$ and X-ray studies indicate that its structural state is orthoclase. Sphene is abundant as euhedral crystals up to 3 mm long, as is Ti-magnetite (Usp_8Mt_{92} - analysis in Table 24). Pale green augite occurs as subhedral crystals and is slightly zoned from $Di_{77}Hd_{19}Ac_4$ to $Di_{67}Hd_{25}Ac_8$ (analyses in Table 22). Incipient alteration/reaction to a dark green amphibole may be seen along cracks in some of the augite grains. Modes and a chemical analysis of the Monzonite are presented in Table 13.

4.4.5. The Hub Syenite

The Hub Syenite is a well exposed, circular intrusion in the centre of the complex, and it forms the topographically prominent Signalberg. The relationships between the Hub Syenite and the Inner Syenite and Monzonite have been described above. In addition the Hub Syenite is intruded by the Syenite Porphyry and associated agglomerate pipes.

4.4.5.1. Petrographic Features

The Hub Syenite is leucocratic and coarse grained and possesses a hypidiomorphic granular texture. A whole rock analysis (PM127) and modes are presented in Table 13. Macroscopically the Hub Syenite is distinguished from the Inner Syenite by its distinctive brown grey colour, and the presence of interstitial quartz, which although forming $< 1\%$ of the rock, is readily identified in hand specimen.

Perthite ($Ab_{60}Or_{40}$) occurs as subhedral grains and is the dominant constituent of the rock. The fine to medium intergrowth of Na- and K-rich phases in the perthite is similar to that in the Inner Syenite. In many specimens the mafic minerals are strongly altered and oxidised. Where fresh they are alkali amphibole, alkali clinopyroxene, biotite, sphene and Ti-magnetite. The amphibole is Mg-arfvedsonite (analysis in Table 20) and may be intergrown with clinopyroxene. The latter also occurs as individual prismatic crystals and is zoned from $Di_{52}Hd_{33}Ac_{15}$ to $Di_{32}Hd_{39}Ac_{29}$ (analyses in Table 22). The Mg-arfvedsonite displays a patchy pleochroism, and a patchy anomalous extinction, and during analysis was found to be compositionally

inhomogeneous with respect to the minor elements, especially Al.

Biotite is less common than the amphiboles and pyroxenes and exhibits a relatively pale pleochroism. The composition of the biotite is $Ann_{37}Phlog_{56}MnBi_3TiBi_4$ (analysis in Table 19).

Sphene and Ti-magnetite occur in large (up to 1,5 mm grains) grains and may be intergrown. Where occurring as individual crystals, the Ti-magnetite is now seen as a coarse intergrowth of ilmenite and magnetite which has a bulk composition of Usp_7Mt_{93} (analysis of bulk separate in Table 24).

Accessory constituents are zircon, quartz, calcite, and riebeeckite. Zircon forms large prismatic crystals up to 0,5 mm in size. Quartz fills the interstices in the rock where it is often associated with calcite and trace amounts of blue, fibrous riebeeckite.

4.4.6. The Syenite Porphyry and associated Agglomerate

An irregular body of grey, coarse-grained feldspar porphyry intrudes the Hub Syenite SW of Signalberg. The Porphyry is chilled against the syenite and is host to numerous xenoliths of the latter. A dyke-like extension of the Porphyry intrudes the Biotite-rich Monzonite S of Signalberg and continues into the Inner Syenite. It therefore post-dates all these rocks in the intrusive sequence. Its relationship to the nepheline syenite is unknown, but tinguaite dykes cut the Porphyry and it probably predates the undersaturated rocks. A smaller Porphyry body crops out on the coast opposite the southern tip of Pomona Island.

Associated with both these occurrences are vertical pipe-like bodies of agglomerate. These bodies are in sharp contact with the Porphyry and are located at Porphyry-syenite contacts. The agglomerate contains numerous fragments (up to 20 cm across) of both syenite and gneiss, set in a fine grained grey-green matrix.

4.4.6.1. Petrographic Features

Large 1 cm perthite phenocrysts are the dominant feature of the Syenite Porphyry. They display a rounded form and are markedly zoned, especially towards

the margins. Smaller phenocrysts of perthite (euhedral), biotite, augite, and magnetite also occur.

The groundmass has an average grain-size of less than 0,1 mm and is composed of the same minerals as in the phenocryst population, as well as apatite and sphene. The relative abundances of the mafic minerals is variable, and sphene and magnetite dominate to the exclusion of augite in some specimens. In most instances biotite and augite are the most abundant minerals in the mafic population.

A chemical analysis of the Syenite Porphyry (PM63) is presented in Table 13.

4.4.7. The Gneiss Breccia and associated Quartz-Feldspar Porphyry

Large breccia bodies (200 to 300 m in diameter) occur in the gneisses along the NE edge of the complex. The breccia bodies consist of various sized slabs and angular fragments of gneiss with minor amounts of syenite, packed tightly together so that large areas of the breccia have no obvious cementing material. Associated with these breccia bodies are quartz-feldspar porphyry intrusives, which are found only in the immediate vicinity of the breccia bodies, i.e. between the coast and Schlueberg. The quartz-feldspar porphyries occur in the form of dykes, sheets, and veins, and apparently also form the cementing material in some parts of the breccia.

The breccia bodies are funnel- or pipe-shaped, and are probably explosion vents now filled with fall-back, and intersected at a high level by the present erosion surface. They are almost certainly associated with the emplacement of the porphyry, whose only expression at this high level are irregular dykes, veins, and sheets.

Complicated relationships exist between the breccia bodies, the quartz-feldspar porphyries, and the syenitic rocks of the complex. Quartz-feldspar porphyry cements the breccia and occurs as dykes cutting through the latter. However, short dykes of agglomeratic and brecciated material cut the quartz-feldspar porphyry dykes in some instances.

As already noted the breccia contains fragments of syenite, and the northernmost breccia body transgresses across the Outer Syenite - gneiss con-

tact, suggesting that the breccias post-date the intrusion of the Outer Syenite. Yet numerous syenite dykes and the Outer Ring Dyke intrude the breccias. Some of these syenite dykes are in turn cut by quartz-feldspar porphyry dykes. The only reasonable interpretation of these relationships is that the emplacement of the breccia bodies and related rocks was contemporaneous with the emplacement of the syenite complex.

4.4.7.1. Petrographic Features

The breccia bodies are composed almost entirely of accidental lithic ejecta, and, despite the lack of cementing material, are tightly compacted. Individual fragments range up to a metre in diameter, though the average size is 20 to 30 cm. Fine-grained agglomeratic dykes are similarly composed of xenocrysts and numerous fragments derived from the gneisses, seldom more than 2 to 3 cm in size, cemented by a fine grained sub-microscopic material.

The quartz-feldspar porphyries are fine grained leucocratic rocks in which the phenocrysts average 2 to 3 mm in size. The groundmass grain-size is less than 0,05 mm. Most specimens are altered and the mafic minerals oxidized beyond recognition. Apart from the euhedral quartz and feldspar, an Fe-Ti oxide may also form phenocrysts. The groundmass is essentially a quartz-feldspar intergrowth sparsely peppered with opaque oxides and oxidized mafic minerals. An analysis (PM177) is presented in Table 13.

4.4.8. The Outer Ring Dyke

This dyke is a quartz syenite or nordmarkite that crops out in a ring around the complex, some 100 to 200 m beyond the Outer Syenite - gneiss contact. The dyke dips outwards at a consistent angle of 50° to 65°, and cuts all other magmatic rocks of the complex.

The Outer Ring Dyke is best developed around the NE and E sides of the complex where it forms a wide (20 to 30 m), persistent body. Along the SE side in the vicinity of Kreuzberg, it splits into a number of narrower dykes which pinch and swell along strike. The dyke does not appear between the sea and the dune belt on the S margin of the complex.

Field evidence and chemistry indicate that the Outer Ring Dyke intrusion was one of the final events in the emplacement history of the Pomona complex.

4.4.8.1. Petrographic Features

The dyke is a medium grained leucocratic nordmarkite, which develops a more coarse grained facies in places. Subhedral perthite of microcline structural state (with vein-type intergrowth of Na- and K-rich phases) is the dominant constituent. Quartz occurs interstitially, as does fluorite. Mafic minerals are arfvedsonite (analyses in Table 20) and magnetite, which shows extensive oxidation to goethite in more altered specimens. A chemical analysis (PM66) and mode are presented in Table 13.

4.5. UNDERSATURATED ROCKS OF THE COMPLEX

4.5.1. Introduction

Kaiser (1926, p. 225) noted the presence of nepheline syenites on the promontory immediately opposite Pomona Island, though he did not mention any contacts with non-nepheline rocks. In fact he states that the complex consists of a nepheline-bearing inner portion, and a nepheline-free marginal portion, but ascribes the absence of nepheline in the marginal portion to the secondary breakdown of nepheline to produce miarolitic textured nepheline-free syenites.

During this investigation the presence of nepheline syenites on the promontory were confirmed, but it is clear from the preceding sections that Kaiser's views on the possible widespread occurrence of nepheline in the syenites, and the reason for its absence in some rocks, are unfounded. Tinguaite dykes are also present and cut all the syenites of the complex.

4.5.2. The Nepheline Syenite

A small plug of nepheline syenite on the promontory opposite Pomona Island is intrusive into the Inner Syenite. Tinguaite dykes related to the nepheline syenite are intrusive into the Hub Syenite, the Monzonite, the

Syenite Porphyry. The undersaturated rocks therefore post-date all these syenites and, by inference, the Outer Syenite as well.

The contact between the nepheline syenite and the Inner Syenite is exposed in altered outcrops at sea level and in occasional sporadic outcrops protruding through the sand cover. The nepheline syenite develops a fine-grained, darker, chilled facies which interfingers with the Inner Syenite over a width of 5 to 10 m.

4.5.2.1. Petrographic Features

The nepheline syenite is coarse-grained and leucocratic, and is composed essentially of subhedral alkali feldspar, displaying a fine perthitic intergrowth, and interstitial nepheline. The latter is commonly altered to paragonite. A little sodalite and cancrinite are also present. The dominant mafic mineral is aegirine occurring as subhedral, green-brown pleochroic grains which are occasionally intergrown with small amounts of biotite. Ti-magnetite also occurs with this association.

One of the outstanding features of the nepheline syenite is the presence of abundant zircon in crystals up to 0,5 mm in size. Zircon has crystallized as zoned euhedral crystals as well as large interstitial grains between feldspar laths. In one specimen of chilled nepheline syenite, Ti-magnetite and zircon, in that order, are the most abundant minerals, after perthite, in the rock.

Fluorite and calcite are accessory minerals. The former is common as inclusions in aegirine, and as an interstitial mineral. Calcite is interstitial and is possibly primary.

Apart from their grain size the chilled nepheline syenites show petrographic features similar to the normal nepheline syenites, except that they contain less nepheline.

The tinguaite dykes are fine grained porphyritic rocks with a pronounced trachytic texture. The dominant member of the phenocryst population is microperthite occurring as slender euhedral laths, displaying Carlsbad twinning and a fine perthitic intergrowth. Minor amounts of sphene, Na-pyroxene, and biotite also occur as phenocrysts. Na-pyroxene phenocrysts

commonly rim corroded grains of magnetite.

The groundmass is mainly composed of aegirine-augite, alkali feldspar, and nepheline, together with small amounts of zircon, fluorite, lavenite, biotite, and sphene.

4.6. THE DYKE ROCKS OF THE COMPLEX

4.6.1. Introduction

Dyke rocks of the complex form a distinct radial pattern (see Figure 15) which penetrates beyond the confines of the intrusion, into the gneisses. Several different types of dyke rock are present. These are:-

(a) quartz-feldspar porphyry dykes associated with the explosion breccias;

(b) the Outer Ring Dyke;

(c) tinguaite dykes associated with the nepheline syenite;

(d) syenitic and granitic dykes associated with the contact zones;

(e) lamprophyres;

(f) the bostonites and quartz-bostonites.

Types (a) to (d) have already been discussed under the relevant sections.

4.6.2. The Lamprophyric Dykes

Lamprophyric dykes are found throughout the outcrop area of the Luderitz Alkaline Province, but are rare in relation to the other dykes near the intrusive complexes. They have been largely excluded from this study for two reasons. Firstly, they are generally highly altered, and yield few satisfactory specimens for petrographic examination, let alone chemical analysis. Secondly, they have no intrinsic importance in the development of the complexes (which are the main subject of this study), although their evolution is connected with the evolution of the province as a whole.

Recently the importance of lamprophyres in alkaline rock genesis has been emphasised (Philpotts and Hodgson, 1968; Ferguson and Currie, 1971), and it is perhaps an oversight that they have been somewhat ignored. However their

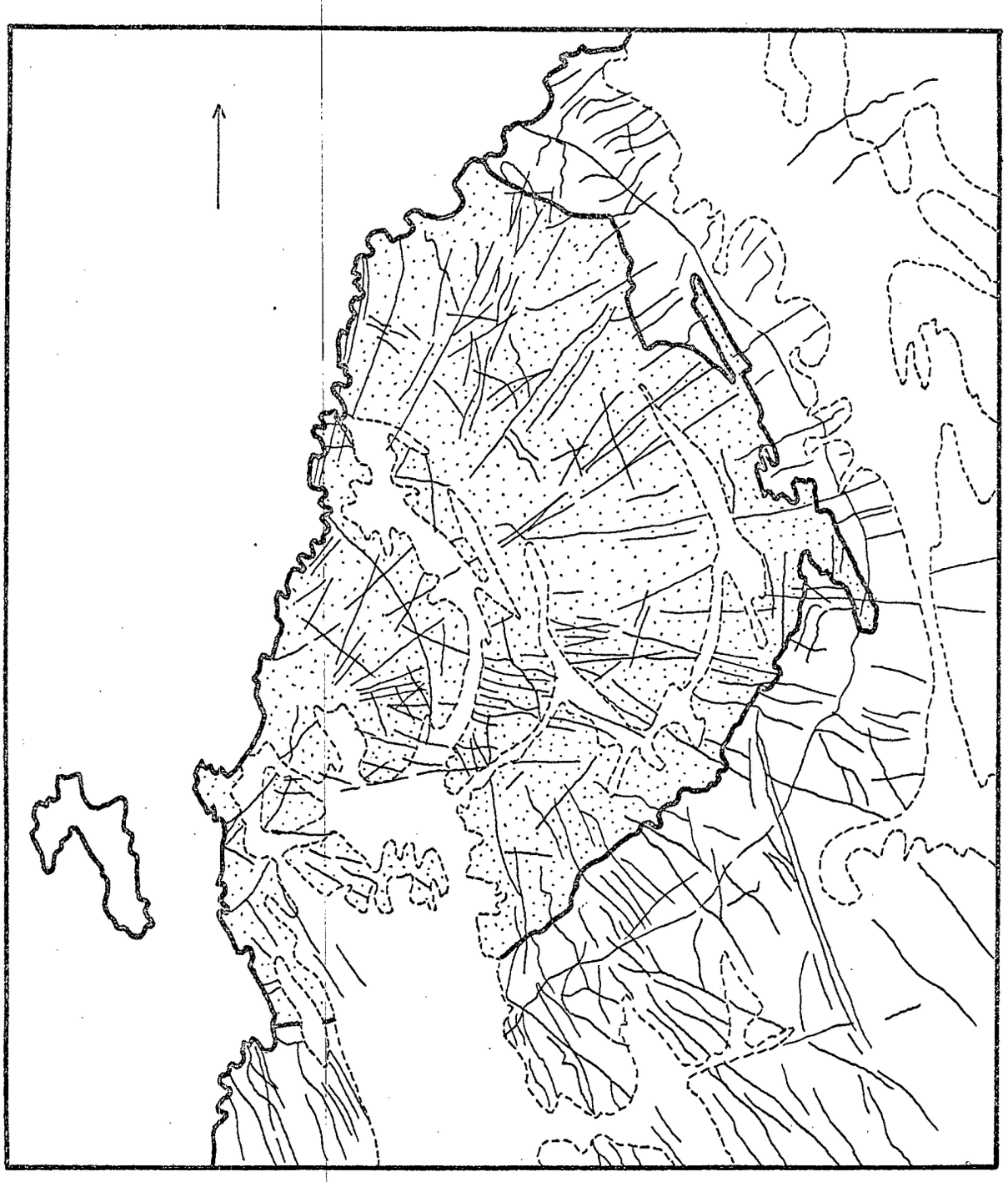

Figure 15. Radial dyke pattern, Pomona Syenite Complex.

relevance is discussed in later sections of this account (see chapter 9).

Kaiser (1926) described the lamprophyres as monchiquites, camptonites, fourchites and alnoites. Of the three specimens collected at Pomona, none were of these types. Two of the specimens are composed of biotite, augite, magnetite, interstitial alkali feldspar, and occasional serpentine pseudomorphs after olivine phenocrysts. The other specimen consists of biotite, magnetite and augite in a glass groundmass. On this basis all the specimens would be classified as minette or vogesite.

4.6.3. The Bostonites and Quartz-bostonites

These dykes are the most abundant of all the different dyke rock types, both at Pomona, and throughout the Luderitz Province. They occur as fine-grained, cream to reddish brown, rocks, but in rare unaltered outcrops they are grey to green-grey.

At Pomona the bostonites form a distinct radial pattern in the complex (see Figure 15) which persists into the country rock especially to the S of the complex where the NW-SE trending radial dykes parallel the regional foliation in the gneisses. In contrast, the E-W trending dykes do not continue beyond the immediate vicinity of the complex, and are rare in the gneisses E of the complex. In this region the E-W trending dykes strike at right angles to the regional foliation in the gneisses.

Although dyke patterns in the vicinity of an intrusive complex reflect fracture patterns developed during emplacement, the evidence from Pomona is that structures in the country rocks are capable of influencing dyke patterns to the extent that certain trends may be enhanced, whereas others may be all but suppressed. Thus NS-SE dykes are well developed in the gneisses in the vicinity of Pomona, whereas E-W dykes are rare.

4.6.3.1. Petrographic Features

The bostonites show little petrographic variation. The dominant texture is orthophyric, but bostonitic textures do occur. Euhedral alkali feldspar phenocrysts are invariably present but seldom exceed 5% of the rock. In the groundmass alkali feldspar is the dominant phase. It is perthitic,

and X-ray investigations indicate that their structural state is close to maximum microcline. Interstitial quartz and the oxidized remnants of sparsely scattered mafic minerals form less than 5% of the groundmass. In fresh specimens the mafic minerals are alkali amphibole or Na-pyroxene. Some bostonites are enriched in mafic minerals especially aegirine and grade into grorudites. These are well developed near Granitberg, but none occur at Pomona.

4.7. INTRUSIVE HISTORY OF THE COMPLEX

1. Intrusion of the Outer Syenite into Precambrian gneisses. Assimilation of gneissic material gives rise to quartz-bearing syenites and minor intrusions in the contact zone.

2. The Inner Syenite was possibly emplaced shortly after the Outer Syenite, before the latter had solidified, or it is a result of *in situ* differentiation of a single magma pulse of Outer Syenite composition. The writer favours the former suggestion, as it readily explains the anomalous contact (section 4.4.2.2.) which shows features which can be ascribed to magma mixing. Furthermore the Inner Syenite is chemically highly fractionated in comparison with the Outer Foyaite Syenite, and this could not be achieved by *in situ* fractionation without the generation of extensive feldspar cumulates.

3. The Biotite-rich Monzonite is probably a cumulate associated with the development of the Inner Syenite. This is supported by its irregular occurrence in the field and by its chemistry (see Chapter 6). The Inner Syenite crystallized under high fO_2 conditions (section 8.4) which implies that the H_2O content of the magma was also high. Thus crystal fractionation was rapid and efficient (due to lowered density and viscosity in the magma), and the Inner Syenite liquid developed rapidly and was emplaced soon after the Outer Syenite. Under such conditions, portions of semi-consolidated cumulates (Biotite-rich Monzomite) may well have been caught up in the Inner Syenite liquid and emplaced with it at higher levels.

4. Intrusion of the Hub Syenite.

5. Explosive emplacement of the Syenite Porphyry and agglomerates in the core of the complex, and the emplacement of the igneous breccias and quartz-feldspar porphyries N of Schlueberg.

6. Intrusion of the nepheline syenite and tinguaite dykes.

7. Intrusion of bostonite and quartz-bostonite dykes into radial fractures in the complex and surrounding gneisses.

8. Emplacement of the Outer Ring Dyke into ring fractures developed by settling of the consolidated syenites into the exhausted magma chamber below.

CHAPTER 5

THE DRACHENBERG SYENITE COMPLEX

5.1. INTRODUCTION

The Drachenberg Syenite Complex lies 2 km E of the Luderitz - Oranjemund main road, 160 km N of Oranjemund. It is the most poorly exposed of the three complexes, and it is estimated that more than 85% of the complex is covered by younger formations, mainly wind blown sand. A very generous impression of the extent of the outcrop is given on the 1:10 000 geological map.

The syenites of the complex occur as a series of scattered outcrops on the crests of low hills and ridges to the W and SW of the Drachenberg peak (435 m). The syenites are intrusive into various quartzites, quartz-mica schists, pelitic schists, and granitic rocks of pre-Gariep age. The size of the complex is similar to that of Pomona and Granitberg (i.e. 2 to 3 km in diameter), but is difficult to estimate due to poor exposure.

5.2. Previous Investigation

Kaiser (1926) does not record any details of the complex, though he was aware of its existence, and obviously visited the area (p. 230). He does however mention that the Drachenberg syenites display variations of texture over short distances, and a concentric disposition of syenites of different textural types. He also mentions the presence of abundant alkali syenite dykes.

Beetz (1924, p. 35) describes the Drachenberg intrusion as a "Durchsmelzungskorper," and noted there, "analogous assimilation phenomena to those described by Kaiser for the Granitberg." Beetz also records the presence of invaded country rocks in the centre of the intrusion, though whether he is referring to Granitberg or Drachenberg is unclear.

Both Kaiser and Beetz were impressed by the similarities between Drachenberg and the two complexes they studied in more detail - Pomona and Granitberg, and it is evident from their writings that they considered them to be of the same age. This account supports this contention and is discussed more fully in Chapter 2.

5.3 PRECAMBRIAN METAROCKS

Metarocks of pre-Gariep age (Kroner, 1972) appear sporadically through the sand cover in the mapped area. They are dominantly metasediments - quartzite, quartzmica schists and semi-pelitic schists. These rocks build the Drachenberg and the ridges to the W of this peak. Dolomites of the Gariep Group occur in the vicinity of the Luderitz-Oranjemund road, and to the W, NW, and S of the mapped area. Minor amphibolites occur to the S of the complex. The metarocks all display a marked foliation which trends NW - NNW and dips steeply to the E.

On the ridges W of Drachenberg the metarocks are intruded by an irregular body of even textured, medium grained granite. The granite-metarock contact is sharp with no interfingering, and the granite is strongly sheared within 3 to 4 m of the contact. Pegmatites which have accompanied the granite intrusion are also present.

5.4. SYENITES OF THE INTRUSIVE COMPLEX

5.4.1. Introduction

Drachenberg is the most perplexing of all the complexes in the Luderitz Province in that (a) the inter-relationships between the various syenites are unknown, and (b) the exposures give very little hint to any pattern in the distribution of the various syenites, and extrapolation from one outcrop to the next is not possible. From the meagre field, petrographic, and chemical evidence, the following age relationships for the syenites are proposed:-

Quartz-feldspar porphyry dykes
Bostonite dykes

Syenite Porphyry

Various syenites and nordmarkites
Quartz-free syenites
Biotite-rich syenite
Fine and coarse grained porphytitic syenites

Quartz monzonite

Although the position of some of the rock types in the scheme is unequivocal (e.g. the dyke rocks), the status of others is either unknown or ambiguous.

5.4.2. The Quartz Monzonite

This rock occurs in scattered outcrops at the S end of the exposed portion of the complex, SW of Black Cap Hill. Outcrops are in the form of large, red to grey coloured exfoliated boulders, protruding through the sand cover. A further occurrence, a single boulder, occurs due south of Black Cap Hill, south of the jeep track, and far removed from the other outcrops. This might indicate that the Quartz monzonite underlies large areas in the south of the complex. The monazite is host to a number of small, 3 to 5 cm rounded xenoliths, which are more fine grained than the monzonite, but appear to have the same mineralogical composition.

The relationship of the Monzonite to other syenites in the complex is ambiguous. A sharp contact between the Monzonite and a xenolith-rich biotite syenite, possibly related to the Biotite-rich Syenite (see section 5.4.6.) occurs just E of the western-most outcrop of Quartz Monzonite. The contact is sharp and regular and neither rock is chilled. Although the contact was carefully examined, no conclusion could be reached as to their precise relationship.

5.4.2.1. Petrographic Features

The Quartz Monzonite is a reddish, coarse-grained hypidiomorphic granular rock in which all the major mineral constituents are easily identified in hand specimen. Modes and a chemical analysis are given in Table 14.

Both plagioclase, zoned towards perthite, and alkali feldspar are present. The plagioclase is generally unaltered and in the cores has a composition An_{30-35}. Alkali feldspar in both discrete and zoned crystals is composed of a fine intergrowth of K- and Na-rich phases, the former being typically altered and giving the rock its reddish hue. The plagioclase is frequently host to tiny euhedral crystals of biotite and apatite.

Quartz occurs as interstitial grains dusted with numerous submicroscopic inclusions.

Strongly pleochroic biotite is the dominant mafic mineral, and is host to numerous inclusions of apatite and zircon. Hornblende (pleochroism: γ' (blue-green); α' (pale yellow-brown) occurs as ragged crystals frequently enclosing biotite, Ti magnetite and to a lesser extent apatite. Narrow rims of hornblende are often seen surrounding biotite, and can possibly be interpreted as reaction rims. Accessory minerals include euhedral apatite, sphene, and Ti-magnetite (now seen as intergrowths of magnetite and ilmenite).

5.4.3. Fine- and coarse-grained porphyritic syenites

These are dark grey to black syenites which crop out on Black Cap Hill. Less well developed exposures occur in the outcrops west of this hill. The coarse, porphyritic syenite intrudes the fine-grained porphyry, and despite their dissimilarity in texture, they have essentially the same mineralogy and chemistry, and may be different facies of the same intrusive pulse.

The porphyritic syenites are intruded by coarse-grained leucocratic syenites, some of which are quartz-bearing. The intrusive relationship is clearly exposed on several places on Black Cap Hill and in the outcrops to the west. The contacts are sharp and the leucocratic syenite encloses xenoliths and partially stoped blocks of the porphyritic syenites. The latter are also intruded by numerous veins which are offshoots from the leucocratic syenites.

5.4.3.1. Petrographic Features

The fine-grained porphyry consists of 5 to 8 mm perthite phenocrysts set in a fine groundmass whose average grain size is 0,05 to 0,10 mm. The perthite phenocrysts are rounded and display marked zoning, an effect which is enhanced by the concentration of numerous sub-microscopic inclusions in zones parallel to the grain outline. The cores of many of these phenocrysts display weak albite twinning or faint chessboard albite twinning, indicating that they have the composition of Na-plagioclase. Inclusions of biotite, augite, and magnetite are common in the phenocrysts.

The groundmass is composed dominantly of perthite in euhedral grains,

the outline of the latter being accentuated by the concentration of small grains of the mafic minerals along the crystal boundaries. The cores of these groundmass feldspars are dusted with submicroscopic inclusions. Mafic minerals in the groundmass are apatite, biotite, Ti-magnetite (consisting of exsolved intergrowths of magnetite and ilmenite), rounded grains of colourless clinopyroxene (augite), and a little sphene. These mafic minerals show a tendency to be associated in aggregates or clots which occasionally reach the size of 1,0 to 1,5 mm.

The coarse-grained porphyry displays a glomeroporphyritic texture, with 4 to 7 mm phenocrysts of perthite forming aggregates which attain sizes of 2,0 to 2,5 cm. The phenocrysts are subhedral and display a slight zoning. Perthitic intergrowths are well developed, and the Na-rich phase displays albite twinning.

The groundmass is coarser grained than in the fine-grained porphyry, with an average grain size of 0,2 to 0,3 mm. It is composed essentially of anhedral perthite with sutured, interlocking grain boundaries. Mafic minerals are biotite, hornblende, a little augite with reaction rims of hornblende, Ti-magnetite, apatite, and sphene.

5.4.4. The Biotite-rich Syenite

This coarse grained, dark grey rock has a distinctive texture, arising from the abundance of large 1,0 to 1,5 cm plates of biotite. Its field characteristics and hand specimen appearance are very similar to the Biotite-rich Monzonite of the Pomona Complex. It outcrops on the hill immediately N of Black Cap Hill, and on the ridge W of Drachenberg peak.

The Biotite-rich Syenite is frequent host to xenoliths of a porphyritic syenite, similar in appearance to the fine- and coarse-grained porphyries discussed above. These xenoliths are well rounded and range up to 20 cm in size, but occasional blocks 0,5 m in diameter are seen. Also present as xenoliths is a fine grained facies of the Biotite-rich Syenite. In places the xenoliths are concentrated to the extent that the xenolith/host rock ratio exceeds 50%. On the evidence of these xenoliths the Biotite-rich Syenite is younger than the porphyry rocks on Black Cap Hill, though these two rock types are not seen in contact.

The xenoliths occur in a zone some 30 to 40 m from the outer edge of the Biotite-rich Syenite outcrop area. Lack of outcrops and their sporadic nature does not allow this zone to be traced along its length, but radial sections across the outcrops reveal this consistent positioning of the xenolith-zone in the syenite.

The relationship between the Biotite-rich Syenite and the other syenites in the complex is perplexing. The outer-most contact of this Biotite-rich Syenite is seen in one small, badly weathered outcrop, at the northern most end of the complex. Elsewhere, along the length of the ridge crest W of Drachenberg peak, and in the outcrops further S, the actual contact lies beneath sand cover, even though exposures of the Biotite-rich Syenite and the leucocratic syenite lying on its outer edge, occur within a few metres of each other.

Relationships at the single exposure of the contact are difficult to interpret due to the weathered nature of the outcrop. The leucocratic syenite develops a pegmatitic texture at the contact, and veins of this syenite cut the Biotite-rich Syenite. On this evidence the outer, leucocratic syenite is interpreted as being intrusive into the Biotite-rich Syenite.

On the S side of the ridge west of Drachenberg peak (i.e. S of the contact described above), definite intrusive relationships between the Biotite-rich Syenite and a coarse-grained leucocratic quartz-syenite can be seen. The intrusive quartz-syenite develops a pegmatitic facies at the contact, and veining of the Biotite-rich Syenite by the latter is common. It is unlikely that the quartz-syenite is related to the outermost syenite mentioned above as the latter is devoid of quartz.

Elsewhere, towards the centre of the complex, the Biotite-rich Syenite becomes more leucocratic and more even-textured. In this way the Biotite-rich Syenite grades into more 'normal' syenites. This gradation is best observed in the outcrops to the N of Black Cap Hill. It must be emphasised that the sporadic nature of the exposures does not allow continuous observation of this gradation. However there is no evidence of intrusive or sharp contacts and the inferred gradational relationship appears to be the best explanation of the field evidence.

In summary, the Biotite-rich Syenite is a zoned body, intruded by leucocratic quartz-free syenites along its outer contact. Towards the centre of the complex the Biotite-rich Syenite grades through a xenolith-rich zone, then becomes progressively more leucocratic and apparently grades into quartz syenites of more 'normal' character which outcrop along its inner edge.

5.4.4.1. Petrographic Features

The Biotite-rich Syenite is a coarse grained hypidiomorphic granular rock, with gradations between mesocratic and leucocratic types. The average grain size is 3 to 4 mm, but the biotite and the occasional zoned feldspar phenocrysts may reach 1,5 to 2,0 cm in diameter.

Anhedral to subhedral perthite is the dominant constituent, and displays coarse exsolution features in common with most perthites from other syenites in this and the Pomona complexes. Clear, untwinned Na-feldspar occurs in the cores of some of the larger feldspar grains, and optical properties indicate that these cores may be as basic as oligoclase in composition. These grains show continuous zoning from oligoclase to normal perthite rims. The structural state of the feldspars is intermediate between orthoclase and microcline though the cell dimensions are anomalous (see section 7.8.1.).

Quartz is not present in the mesocratic facies of the syenite but appears in the leucocratic rocks towards the centre of the complex.

Biotite is the dominant mafic mineral and occurs as large plates. Pale green augite is ubiquitous, but shows varying degrees of replacement by hornblende. Thus in some specimens hornblende is absent, whereas in others hornblende is in greater abundance than pyroxene.

Accessory minerals are euhedral apatite, Ti-magnetite, and less commonly sphene.

5.4.5. Various Syenites and Nordmarkites

The differentiation and classification of the remaining syenites

(those NW and SW of Black Cap Hill and the outcrops SW of Drachenberg peak) is confusing. Exposures are poor, and the generous areas of outcrop designated on the map are in fact concentrations of scattered boulders protruding through the sand. No differentiation was possible on field characteristics and even the petrographic features of the collected specimens are somewhat ambiguous.

In hand specimen the syenite are all coarse grained and leucocratic. Alkali feldspar is the dominant constituent and all carry biotite. Quartz is present in some specimens, but is absent in others. Likewise zoned feldspars, with cores of Na-feldspar occur sporadically in some syenites and not others. A petrographic classification of these syenites on the basis of the presence or absence of quartz and zoned feldspars revealed the following:

(1) The syenites intrusive along the outer edge of the Biotite-rich Syenite are all quartz free.

(2) Similarly, quartz-free syenites are found in the central outcrops NW of Black Cap Hill.

(3) Quartz-syenites occur in a linear belt of outcrops SW of Drachenberg peak, in the scattered outcrops SW of the ridge west of this peak (i.e. within the belt of Biotite-rich Syenites), and in a similar position with respect to Biotite-rich Syenites N of Black Cap Hill, and in the outcrops to the west of this hill.

(4) Both quartz-free and quartz-bearing syenites intrude the porphyritic rocks on Black Cap Hill.

(5) Zoned feldspars may or may not be present in each of these occurrences.

On the basis of the presence or absence of Quartz it is possible, through extrapolation, to reconstruct the hypothetical structure over part of the complex with the sand cover removed. This reconstruction is illustrated in Figure 16. The fault positions indicated in the figure are supported by the offsets in the bostonite dykes. Extrapolation of the reconstructed features around the W and SW of the complex is confused by dissimilarity of rock types, and was not attempted.

Figure 17 is a hypothetical cross section through the N part of the complex, and is constructed from all the data available. The section also contains an interpretation of the intrusive development of the complex as is

Figure 16. Hypothetical reconstruction of the E portion of the Drachenberg Syenite Complex.

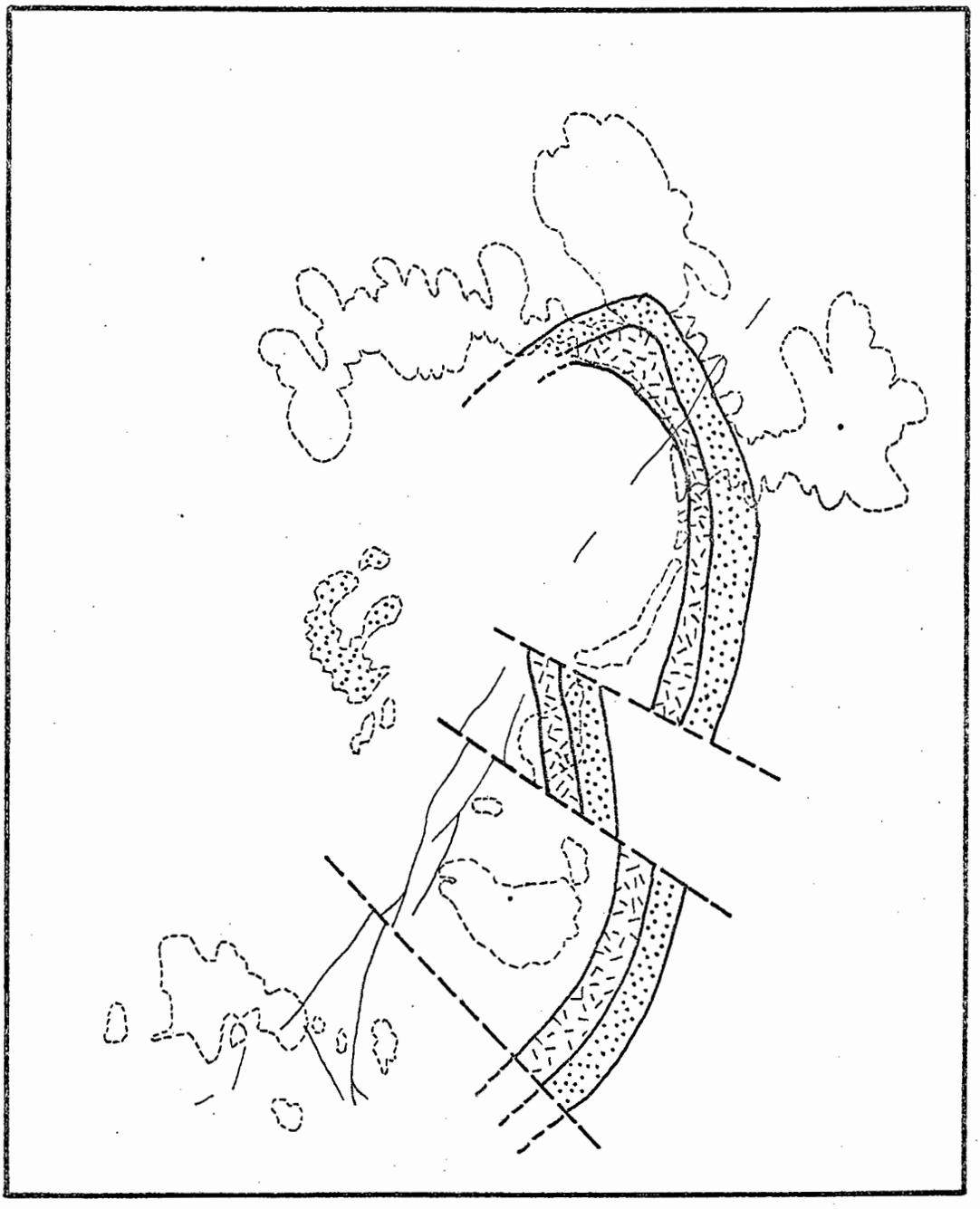

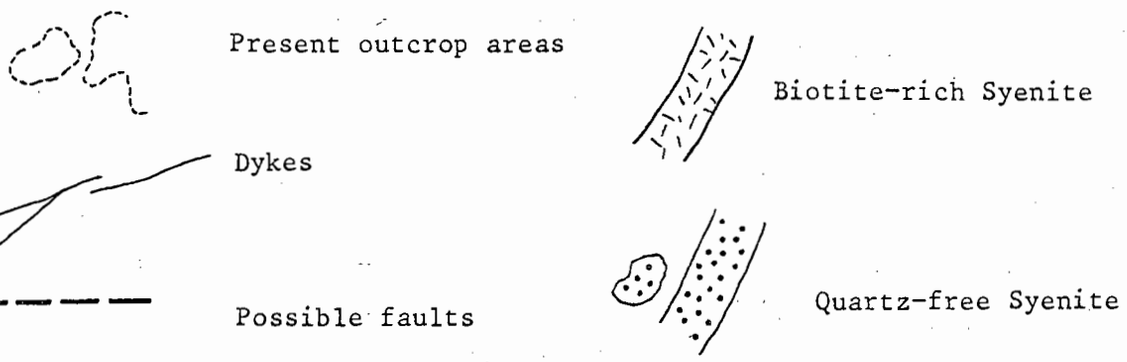

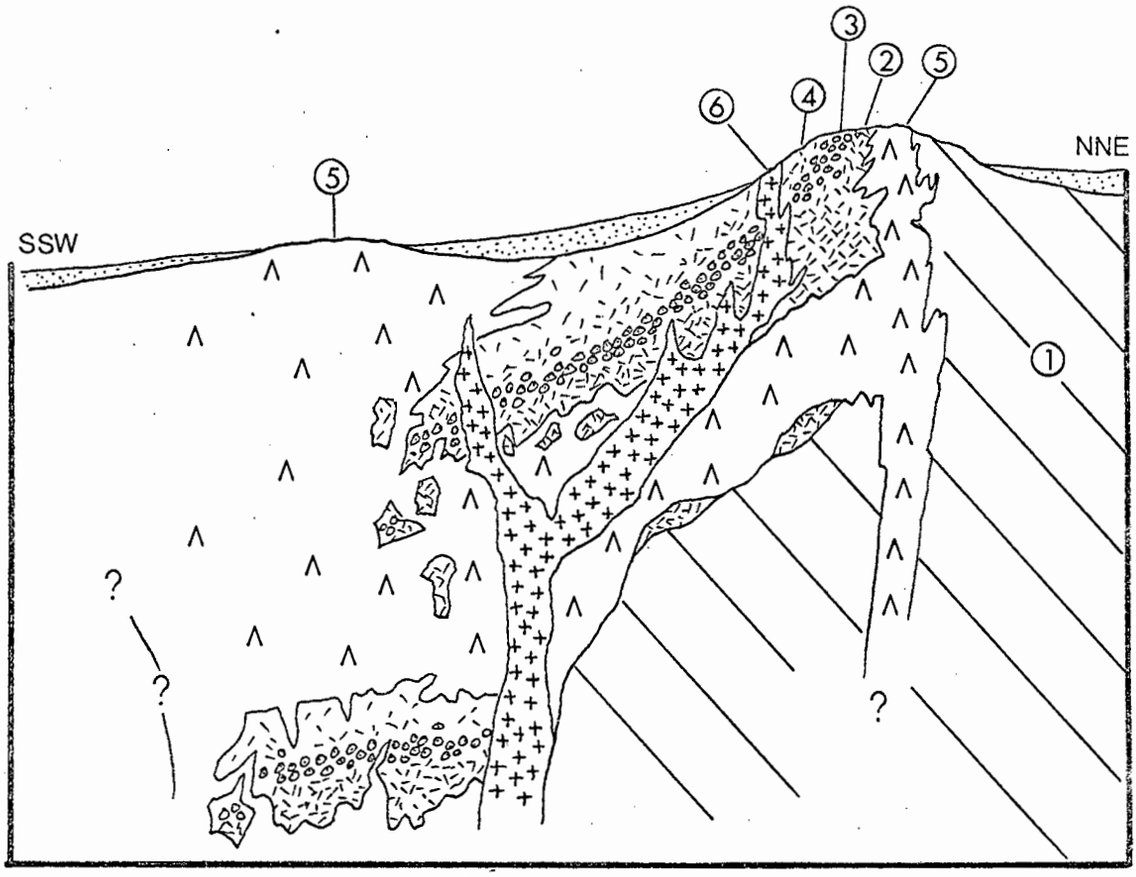

Figure 17. Hypothetical NNE - SSW section through the northern portion of the Drachenberg Complex. 1 - Basement schists; 2 - Biotite-rich Syenite; 3 - Xenolith-rich zone; 4 - Quartz-bearing, leucocratic facies of the Biotite-rich Syenite; 5 - Quartz-free Syenite; 6 - pegmatitic nordmarkite.

discussed in section 5.6.

5.4.5.1. Petrographic Features

(a) Quartz-free Syenites - These are coarse grained hypidiomorphic granular rocks whose dominant constituent is perthitic alkali feldspar. The perthite is subhedral and displays a coarse, 'patch' type exsolution intergrowth, with the Na-rich phase invariably showing albite twinning. Zoned feldspars may be present as noted above. The cores of these crystals are clear, unaltered, and untwinned, but optical properties suggest that some may be oligoclase. Tiny inclusions of biotite and opaque ore, and occasionally apatite, are invariably present in the cores. The zoning in these grains is progressive, and the perthite rims are indistinguishable from the homogeneous perthite grains in the rock. In some specimens there is evidence of abrupt mantling of the cores by perthite.

Mafic minerals generally form $<15\%$ of the rock, with biotite, dominant followed by brown hornblende. In some specimens pale green clinopyroxene occurs in the cores of the hornblende crystals. Accessory minerals are euhedral apatite, Ti-magnetite (now oxidised to magnetite-ilmenite intergrowths), and less commonly sphene.

Modes and chemical analyses of Two quartz-free syenites, DM110 and DM125 are presented in Table 14.

(b) Quartz-bearing Syenites - Apart from the presence of quartz, the petrography of these syenites does not differ much from the petrography of the quartz-free syenites discussed above.

Perthite is the dominant constituent exhibiting both patch and vein type exsolution intergrowths. The cores of the zoned feldspars may show faint albite twinning, and optical determinations indicate that they are oligoclase in composition. In all other respects - the presence of inclusions, the progressive zoning and the abundance of these feldspars in the rock - they are identical to the zoned feldspars in the quartz-free rocks.

Quarts never exceeds 5 to 10% of the rock and occurs in an interstitial position between the perthite laths.

The mafic mineralogy is the same as for the quartz-free syenites in all respects except that sphene is rare and zircon is usually present as inclusions in the biotite.

An analysis and mode of a typical quartz syenite, DM115, is presented in Table 14.

5.4.6. The syenites and quartz syenites intrusive into the porphyries of Black Cap Hill

Various syenites intrusive into the fine and coarse grained porphyries are similar to those already described, although their status in the structure and development of the complex is obscure. If the reconstruction in Figure 16 is correct, the intrusive syenites on Black Cap Hill should be quartz-bearing as they lie within the ring of Biotite-rich Syenite. However, only those syenites along the W side of the Hill carry quartz, and furthermore the easternmost outcrops have a field appearance and petrographic characteristics similar to the Quartz Monzonite!

In the exposures W of Black Cap Hill the porphyritic rocks are intruded by quartz syenites which grade westwards into a syenite similar in appearance to the more leucocratic facies of the Biotite-rich Syenite. The syenite encloses a number of zenoliths of porphyry and although it is not so delineated on the 1:10 000 map, it is possibly a correlate of the Biotite-rich Syenite. The relationship of this syenite to the Quartz Monzonite has already been noted (see section 5.4.2.).

Then again, the relationship of the coarse-grained leucocratic quartz syenite, which intrudes the Biotite-rich Syenite on the ridge W of Drachenberg peak (see section 5.4.4.), to the other syenites in the complex is obscure. Similar leucocratic quartz syenites with pegmatitic characteristics are found intrusive into the rocks on Black Cap Hill, and in minor exposures in the vicinity. These possibly represent fairly late stage magmatic activity in the complex.

A medium grained leucocratic granite in the form of a short dyke is apparently intrusive into the syenites W of Black Cap Hill. As there is evidence that the Drachenberg complex is composed of syenites showing progressive enrichment in quartz, this small occurrence of granite is possibly a late stage differentiate of the syenites of the complex.

5.4.7. The Dyke Rocks

The sporadic nature of the dyke rock outcrops is well illustrated on the 1:10 000 geological map. Two types are recognised - the feldspar-phyric quartz bostonites, and the quartz-feldspar porphyries, the former of which is more common.

The dykes are fine-grained with the phenocrysts rarely exceeding 2,0 to 2,5 mm in size. They are highly altered and appear in the field as orange-brown to cream coloured rocks, but the rare fresh exposures are grey-green in colour.

Related to these dykes is a large plug of Syenite Porphyry on the Luderitz - Oranjemund road, SW of Drachenberg. No outcrops, other than those revealed by the road cuttings are visible, but the extent of the plug is easily delineated as it forms a low positive feature in the topography, and is covered by chips of porphyry derived *in situ* by weathering. It is cut by a number of bostonite dykes.

5.4.7.1. Petrographic Features

The Syenite Porphyry is a reddish, coarsely porphyritic rock in which phenocrysts of perthite, up to 6 mm in length, form about 10 to 15% rock. The groundmass consists essentially of a felted mass of alkali feldspar laths 0,1 mm in size. Clear quartz occurs as an interstitial mineral but does not exceed 5 to 10%. Mafic minerals are heavily oxidised and unidentifiable.

The Quartz-Bostonites are similar to the syenite porphyry but much finer grained. Alkali feldspar phenocrysts are highly altered, as are those in the groundmass. The latter may show some preferred orientation which imparts an orthophyric texture to the rock, or they may occur in radiating aggregates giving rise to a bostonitic texture. Quartz is typically interstitial and

mafic minerals are rare, if present at all. Since most of the bostonites are strongly altered, only opaque reddish oxidation products (possibly limonite and goethite) of the mafics are present. Colourless muscovite is also invariably present in the groundmass, but it is uncertain whether it is primary or not.

Of the two samples of comparitively unaltered bostonite collected, one carried mauve-green arfvedsonite, whereas the other contained a few slender, green needles of aegirine. The former specimen also contained a few euhedral microphenocrysts of zircon.

Quartz-feldspar porphyries differ from the quartz-bostonites only in the presence of euhedral phenocrysts of quartz in the former. All gradations in composition between the two probably exist, and dykes with compositions intermediate between these two commonly display micrographic intergrowths of alkali feldspar and quartz.

5.5. CONTACT RELATIONSHIPS

Syenite-country rock contact relationships are sporadically exposed on the ridge W of Drachenberg peak. Exposures are poor but display enough features to allow a general description of contact phenomena.

5.5.1. Contact Metamorphism

The extent of the thermal metamorphic aureole surrounding the complex was not determined with any certainty due to the poor exposures and the complicating presence of the pre-syenite granite intrusion. From the limited study presented here a steep temperature gradient appears to have existed across the contact zone, and only those rocks within a few tens of metres of the syenites show any effects. This can be ascribed to thermal metamorphism accompanying the emplacement of the complex.

5.5.1.1. Petrographic evidence

The quartzites, feldspathic quartzites, and quartz-mica schists, show the effects of recrystallization and development of equigranular, non-

TABLE 11

Mineral Assemblages in contact metamorphic schists, Drachenberg

Specimen No.	53	54	56	57	61	62	64	65	69	70	71	84
Quartz	x	x	x	x		x	x	x	x	x	x	x
Alkali feldspar	x	x	x	x	x	x	x	x	x	x	x	x
Biotite	x	x	x	x	x	x	x	x				x
Garnet				x	x	x	x					
Orthopyroxene				x	x	x	x					
Cordierite			x	x	x	x	?					x
Spinel			x	x	x	x						x
Opaques			x	x	x	x						
Sillimanite			x			x						x
Zircon			x		x	x		x				
Sphene				x								x
Sericite								x	x	x	x	

oriented textures at the expense of the marked foliation of the original rocks. They remain mineralogically unaltered and are composed of perthite quartz and biotite.

In contrast, the darker, pelitic schists are metamorphosed to massive, medium-grained hornfelses. Garnet is often porphyroblastic, and the only constituent apparent in hand specimen. In thin section these rocks are medium-grained with granoblastic or porphyroblastic textures, although they still retain a certain degree of preferred orientation of their constituents. Anhedral quartz and clear microperthite are the dominant constituents, though the former may be absent. Mafic minerals are biotite, cordierite, magnetite, garnet, spinel, and orthopyroxene. Cordierite forms large anhedral porphyroblasts crowded with inclusions, especially dark green spinel and sillimanite. These spinel inclusions in the cordierite and in other minerals are probably responsible for the dark colour of the rocks. Orthopyroxene exhibits strong pleochroism (α'- pink; γ'- pale green). Zircon is a ubiquitous accessory.

Mineral assemblages are summarised in Table 11.

5.5.1.2. Conditions of metamorphism

Since the syenites at Drachenberg are believed to have crystallised in a sub-volcanic environment where P_{total} has not exceeded 1,0 Kb, the thermal metamorphism accompanying the intrusion must be of the low pressure type. The mineral assemblages of 4 samples (DM62, DM64, DM56, DM61) taken from close to the contact indicate that conditions typical of the low pressure, pyroxene-hornfels facies (Turner, 1968 p. 225) were achieved in the inner part of the aureole. This in turn suggests that temperatures at the P_{total} mentioned above could have reached 600° to 650°C.

5.5.2. Magmatic Assimilation

The poor exposures that thwarted proper observation of the contact metamorphism also allow only a cursory examination of the magmatic assimilation effects at the contact. The quartz-free syenites on the ridge W of Drachenberg peak display a clotting of mafic minerals and an increase in grain size as the contact is approached. At the contact the syenite develops a coarse grained pegmatitic facies which may contain a substantial amount of quartz. Magmatic

veins in the country rock beyond the contact are commonly granitic in composition, and may carry garnet. The latter may be xenocrystic, or they may have crystallised from a granitic liquid contaminated by pelitic material. Certainly the presence of quartz in the syenite contact facies indicates that some assimilation of quartz-rich metarocks has been accomplished.

There is a noticeable lack of interfingering of magmatic and country rocks. Xenoliths of metarocks in the syenite are equally rare. Despite this, assimilation/contamination mechanisms similar to those described at length for Granitberg (see section 3.6.3.3.) have probably operated at Drachenberg, but to a lesser extent.

5.6. INTRUSIVE HISTORY OF THE COMPLEX

1. Intrusion and crystallization of Fine-and Coarse-grained Porphyritic Syenites.
2. Intrusion of the Biotite-rich Syenite with disruption and incorporation of xenoliths of the Porphyry rocks in (1) above. Partial *in situ* differentiation to give gradation from the Biotite-rich Syenite at the base, through the xenolith-rich zone, to leucocratic quartz syenites at the top.
3. Ring faulting and collapse and tilting of large segments of the consolidated Biotite-rich Syenites. Quartz-free Syenites move up the central vent and up possible ring fractures around the edge of the complex.
4. Intrusion of coarse-grained quartz-syenites.
5. Intrusion of small bodies of late granitic differentiates.
6. Intrusion of bostonite and quartz-feldspar porphyry dykes.

The position of the Quartz Monzonites in this scheme is uncertain. Its mineralogy and chemistry indicate that it is one of the earliest rocks in the intrusive sequence.

CHAPTER 6

THE CHEMISTRY OF THE INTRUSIVE COMPLEXES

6.1. INTRODUCTION

Rock samples from the 3 complexes were collected for analysis by X-ray fluorescence (XRF) procedures. Analytical conditions and methods of sample preparation used, are the standard methods employed in the Geochemistry Department, University of Cape Town, and are summarised in the Appendix. In order to test the precision of the sample preparation and analytical techniques, 11 aliquots of one specimen, GM146, were analyzed for both major and trace elements. The results are presented in the Appendix and apart from 7,7% coefficient of variation (c.o.v.) for MgO, the c.o.v. for the other elements are less than 1,7%.

The elements analyzed for are the major elements Si, Ti, Al, Fe^{2+}, Fe^{3+}, Mn, Mg, Ca, Na, K, P, and the trace elements Ba, Rb, Sr, Zr, Nb, Y, Th, Pb, Ga. It was not the intention to provide extensive trace element data for the syenitic rocks of the complexes, rather the trace elements selected for determination were those which are of most use in monitoring any differentiation process.

Several elements that are perhaps important in alkaline rocks (Hf, Ta, Mo, Zn, Li, Sn, F, Cl) have not been determined for the purposes of this thesis. With regard to F and Cl it was felt that the abundance of these two elements in coarsely crystalline rocks would bare little relation to their abundances in the original magma. Furthermore F and Cl are susceptible to loss during alteration. Thus although analyses might have indicated any general differences between the over- and undersaturated suites, direct comparison between individual analyses would have been tenuous.

6.2. THE PETROGRAPHIC MODEL FOR THE LUDERITZ PROVINCE

Petrographic evidence indicates that the alkaline rocks in the complexes can be grouped into a silica oversaturated suite and a silica undersaturated suite (i.e. rocks with modal nepheline). Within these suites, the quartz or nepheline content of any rock varies sympathetically with its degree of differentiation, as is indicated by field relationships

Major and trace element analyses for nepheline syenites and bostonites Granitberg

	PCNS		Inner Foyaite		Outer Foyaite					Tinguates			Bostonites	
	GM128	GM146	GM131	GM350	GM129	GM136	GM142	GM147	GM171	GM130	GM77	GM160	GM339	GM340
% SiO_2	52,13	53,42	56,63	56,79	56,60	56,83	56,50	56,99	56,57	60,51	58,25	60,14	67,82	69,35
TiO_2	1,56	1,27	0,51	0,43	0,29	0,33	0,34	0,28	0,33	0,36	0,60	0,37	0,26	0,23
Al_2O_3	17,41	18,28	18,78	18,80	21,25	21,50	21,87	21,81	21,28	18,68	19,64	19,61	14,58	16,22
Fe_2O_3	2,27	1,92	2,67	2,26	1,37	1,19	1,13	1,06	1,32	2,45	1,69	2,20	2,54	0,54
FeO	4,80	4,23	2,11	2,18	0,91	1,29	0,87	1,17	1,22	1,01	1,76	0,69	0,91	0,09
MnO	0,21	0,23	0,33	0,41	0,18	0,21	0,17	0,18	0,23	0,31	0,20	0,26	0,34	0,07
MgO	2,85	2,24	0,90	0,86	0,25	0,12	0,16	0,29	0,19	0,33	0,51	0,09	0,19	0,17
CaO	3,83	3,03	1,48	1,52	0,96	0,82	0,70	0,81	0,75	0,87	1,31	0,73	0,12	0,005
K_2O	4,60	4,88	5,16	5,16	5,96	5,89	5,93	6,02	5,77	5,43	6,13	5,70	4,58	6,64
Na_2O	6,14	7,49	8,43	8,40	9,15	9,42	10,85	9,60	10,10	9,07	8,09	8,87	7,10	5,58
P_2O_5	1,32	1,01	0,33	0,29	0,00	0,00	0,00	0,01	0,00	0,04	0,16	0,00	0,02	0,05
H_2O	0,52	0,08	0,32	0,16	0,64	0,16	0,14	0,16	0,13	0,06	0,06	0,07	0,16	0,19
LOI	0,83	0,58	1,71	2,06	1,49	1,41	0,85	0,96	0,86	0,50	0,53	0,48	0,46	0,60
	98,47	98,66	99,36	100,32	99,05	99,17	99,35	99,34	98,75	99,62	98,93	99,21	99,08	99,74
FI	72,77	79,34	89,56	89,53	94,53	94,69	96,15	94,98	95,35	95,06	91,59	96,12	96,89	98,90
ppm Ba	1980	1586	528	381	52	4,2	6,5	16,2	*	101	313	*	20	98
Sr	1906	1596	436	395	78	7,7	11,7	22,0	4,5	88	281	9,4	13,3	17,6
Rb	101	152	198	211	165	177	181	166	197	232	162	240	758	364
Ga	20,03	22,9	26,7	26,6	24,1	23,8	25,2	22,9	26,6	28,9	24,6	30,8	38,1	28,7
Zr	586	843	1271	1200	555	535	420	539	732	2090	1125	1921	2902	544
Nb	135	199	281	289	158	167	155	135	222	414	241	379	1486	426
Th	*	9,9	41,8	38,2	17,9	30,2	13,4	13,1	29,1	44	26	39	178	62
Pb	*	11,0	27,1	39,2	13,7	6,5	6,5	*	6,7	38	11	19	98	20
Y	31,3	34,2	44	71	24,6	32	23	22	35,5	61	27	36	90	50

* below detection limit

TABLE 12 (contd.)

CIPW Norms and modes for nepheline syenites and bostonites, Granitberg

	GM128	GM146	GM131	GM350	GM129	GM136	GM142	GM147	GM171	GM130	GM77	GM160	GM339	GM340
or	27,18	28,84	30,49	30,49	35,22	34,81	35,04	35,57	34,10	32,09	36,22	33,68	26,95	39,00
ab	33,50	31,82	36,81	36,88	30,60	30,08	24,77	28,04	27,31	40,69	35,42	40,34	49,51	46,23
an	6,37	1,85	-	-	-	-	-	-	-	-	-	-	-	-
ne	9,99	17,09	16,83	16,85	24,66	25,86	29,64	27,43	27,11	13,64	17,05	15,06	-	-
Q	-	-	-	-	-	-	-	-	-	-	-	-	10,77	11,51
ns	-	-	-	-	-	-	2,00	-	0,88	0,66	-	-	0,69	-
ac	-	-	3,04	2,72	1,13	1,67	3,27	2,24	3,82	7,09	1,36	5,20	7,35	1,31
di	3,28	5,41	4,31	4,73	2,71	3,54	2,99	3,37	3,22	3,44	4,56	2,02	0,41	-
ol	7,52	5,48	1,80	2,05	-	0,14	0,18	0,60	0,71	0,69	0,46	-	-	-
wo	-	-	-	-	0,63	-	-	-	-	-	-	0,53	-	-
ap	3,13	2,39	0,78	0,69	-	-	-	-	-	0,09	0,38	-	0,02	0,12
mt	3,29	2,78	2,35	1,91	1,42	0,89	-	0,41	-	-	1,77	0,58	-	-
il	2,93	2,38	0,96	0,81	0,54	0,62	0,64	0,53	0,62	0,68	1,13	0,69	0,49	0,34
tn	-	-	-	-	-	-	-	-	-	-	-	-	-	0,11
Perthite	60,8	60,5	66,5	67,2	63,4	60,5	59,0	63,5	61,7				72,4	86,5
Nepheline	5,1	13,8	19,3	18,2	28,1	31,0	32,4	28,0	31,7				-	-
Quartz	-	-	-	-									5,0	12,9
Biotite	19,4	10,2	5,4	4,6	3,0	1,1	0,8	2,1	2,1				-	-
Clinopyroxene	7,0	8,1	7,4	8,1	3,5	5,6	4,7	5,9	3,7				22,4	-
Sphene	2,1	1,4	0,2	0,3	0,2	0,4	0,1	-	0,2				-	-
Opaque	3,2	2,1	-	-	0,7	0,5	0,9	0,2	0,4				-	-
Apatite	1,1	1,2	-	-	-	-	-	-	-				-	-
Other	1,3	1,7	1,1	1,6	1,1	0,9	2,1	0,3	0,2				0,2	0,6

TABLE 13

Major and trace element analyses for syenites and nepheline syenites, Pomona

	PM64	PM55	PM157	PM63	PM60	PM127	PM66	PM156	PM177	PM53	PM61
% SiO_2	49,35	59,54	60,96	59,88	62,51	62,99	66,77	68,05	75,02	60,49	58,36
TiO_2	2,41	1,01	0,83	0,74	0,57	0,74	0,33	0,26	0,12	0,25	0,32
Al_2O_3	17,45	18,59	18,72	17,53	17,38	17,14	16,08	17,46	12,46	19,22	20,29
Fe_2O_3	3,47	1,60	1,48	2,13	1,77	2,14	1,97	0,28	1,31	2,31	1,91
FeO	5,49	2,17	2,00	1,76	1,29	0,62	0,63	0,09	0,25	0,34	0,71
MnO	0,24	0,14	0,13	0,20	0,28	0,17	0,15	0,00	0,00	0,25	0,23
MgO	3,59	1,19	1,10	0,85	0,20	0,49	0,17	0,14	0,26	0,23	0,41
CaO	5,75	2,53	2,36	1,83	0,56	1,24	0,36	0,05	0,13	0,61	0,87
K_2O	3,62	5,71	5,50	6,00	6,55	6,33	4,98	6,32	7,07	5,28	5,75
Na_2O	4,58	5,66	6,07	5,76	6,23	6,25	6,99	6,49	3,26	9,04	9,06
P_2O_5	1,57	0,35	0,30	0,30	0,04	0,06	0,00	0,02	0,01	0,00	0,00
H_2O	0,10	-	0,12	0,10	0,37	,07	0,09	0,15	0,17	0,14	0,16
L.O.I.	1,48	0,53	0,40	0,99	0,90	,93	0,63	0,51	0,68	1,10	1,01
	99,10	99,02	99,97	98,07	98,65	99,17	99,15	99,82	100,74	99,26	99,08
Fl	59,24	82,22	83,82	86,68	93,99	92,41	96,82	99,00	98,26	96,84	94,87
ppm Ba	1880	1281	1312	1089	113	28	30	48	1010	*	12,1
Sr	2371	1167	1213	679	88	25	15	9,1	61	12,6	20,5
Rb	125	120	106	166	206	222	203	330	443	296	258
Ga	18,9	18,6	18,5	19,1	21,5	21,9	30,2	27,7	21,5	35,4	34,4
Zr	318	564	560	537	1050	1423	803	825	349	1255	1861
Nb	103	173	139	167	265	332	633	513	554	474	381
Th	7,7	12,3	12,2	nd	28	41	78	73	85	62	74
Pb	*	12,8	12,1	nd	15	25	15	*	*	45	29
Y	25	29	22	25	34	56	52	29	50	21	29

* below detection limit; nd - not determined

TABLE 13 (contd.)

CIPW Norms and modes for syenites and nepheline syenites, Pomona

	PM64	PM55	PM157	PM63	PM60	PM127	PM66	PM156	PM177	PM53	PM61
or	21,39	37,74	32,50	35,46	38,71	37,41	29,43	37,35	41,78	31,20	33,98
ab	33,58	46,46	50,27	48,45	52,71	52,88	54,99	54,63	24,73	43,44	34,78
an	16,37	8,46	7,60	4,26	0,12	0,03	-	-	-	-	-
ne	2,80	0,77	0,59	0,16	-	-	-	-	-	14,10	20,36
Q	-	-	-	-	0,11	0,43	7,22	5,95	29,14	-	-
ac	-	-	-	-	-	-	3,66	0,25	2,51	6,18	3,78
di	1,53	1,45	1,74	2,28	1,99	2,63	1,47	-	0,21	2,25	3,52
hy	-	-	-	-	0,02	-	0,02	0,35	0,44	-	-
ol	8,64	2,68	2,35	1,20	-	-	-	-	-	-	-
wo	-	-	-	-	-	0,98	-	-	-	0,12	-
mt	5,03	2,32	2,15	3,09	2,57	0,46	1,02	-	0,47	0,25	0,87
il	4,54	1,90	1,56	1,39	1,07	1,39	0,62	0,19	0,23	0,47	0,60
ap	3,72	0,83	0,71	0,71	0,09	0,14	-	0,05	0,02	-	-
tn	-	-	-	-	-	-	-	0,08	-	-	-
ru	-	-	-	-	-	-	-	0,12	-	-	-
hm						1,82	-	0,19	0,12	-	-
Plagioclase	17,6										
Perthite	47,3	78,1	76,4		95,7	91,1	90,0	94,6	17,2	79,7	
Quartz	-	-	-		-	1,2	6,1	2,0	11,1	12,0**	
Biotite	20,8	8,3	10,3		0,3	0,9				1,1	
Clinopyroxene	5,0	7,1	4,2		-	2,1				5,2	
Amphibole	-	4,3	5,7		1,7	2,7	3,1				
Opaque	2,7	1,8	1,5		1,1	1,4					
Sphene	4,0	0,4	1,5								
Other	2,6	-	0,8		1,0	0,6	0,8	3,4	71,7*	2,0	

* groundmass

** nepheline

TABLE 14

Major and trace element analyses of syenites from Drachenberg

	DM105	DM106	DM110	DM125	DM124	DM126	DM115	DM111
% SiO_2	60,10	59,09	60,58	60,35	60,56	57,39	65,10	75,52
TiO_2	0,86	0,77	0,67	0,62	0,94	1,24	0,49	0,04
Al_2O_3	17,92	18,18	19,01	17,99	17,11	17,65	16,69	12,35
Fe_2O_3	1,60	3,25	1,92	1,48	1,84	2,78	1,47	0,46
FeO	3,22	1,87	1,75	2,65	3,45	3,27	1,56	1,08
MnO	0,29	0,14	0,13	0,16	0,13	0,19	0,10	0,07
MgO	1,17	1,12	0,85	1,02	1,50	1,91	0,64	0,16
CaO	2,33	2,48	2,72	1,90	2,94	3,27	1,22	0,08
K_2O	5,98	6,08	5,37	6,54	5,41	5,44	6,24	4,60
Na_2O	5,52	5,34	5,81	5,39	4,36	5,17	5,20	4,01
P_2O_5	0,37	0,39	0,31	0,25	0,41	0,61	0,16	0,01
H_2O	0,13	0,06	0,07	0,08	0,12	0,07	0,19	0,19
LOI	0,20	0,27	0,44	0,33	0,36	0,38	0,43	1,06
	99,69	99,04	99,63	98,76	99,13	99,37	99,49	99,63
FI	82,29	82,11	81,60	85,06	78,90	76,40	89,54	96,12
ppm Ba	541	760	981	817	928	877	358	43
Sr	276	304	996	423	508	610	214	21
Rb	103	122	96	119	157	124	165	493
Ga	20,7	22,0	18,8	20,7	22,0	20,9	21,7	25,6
Zr	503	683	679	571	611	659	583	234
Nb	124	127	117	140	110	151	143	408
Th	6,8	14,2	*	9,4	nd	14,1	40	71
Pb	10,9	13,7	*	23	nd	46	32	9,1
Y	31	37	21,0	26	34	34	29	52

* below detection limit; n.d. - not determined

TABLE 14 (contd.)

CIPW Norms and modes for syenites from Drachenberg

	DM105	DM106	DM110	DM125	DM124	DM126	DM115	DM111
or	35,34	35,93	31,73	38,65	31,97	32,15	36,87	27,18
ab	46,10	45,05	49,16	44,33	36,89	43,05	44,00	33,93
an	6,46	7,69	9,94	5,58	11,14	8,89	3,78	0,33
ne	0,32	0,07	-	0,69	-	0,38	-	-
Q	-	-	-	-	7,83	-	7,65	33,45
di	2,24	1,61	1,23	1,83	0,68	2,70	1,00	-
hy	-	-	2,27	-	3,31	-	2,15	2,07
ol	4,11	1,43	0,03	3,37	-	3,99	-	-
ap	0,88	0,93	0,73	0,59	0,97	1,44	0,35	0,02
mt	2,32	4,31	2,78	2,15	2,67	4,03	2,13	2,78
il	1,61	1,45	1,26	1,14	1,76	2,33	0,92	0,08
hm	-	0,28	-	-	-	-	-	-
Plagioclase					34,7			
Perthite			87,4	90,2	46,2	76,3	87,1	12,3
Quartz			-		9,0	-	6,2	8,2
Clinopyroxene			2,1		-	6,3	-	
Amphibole			3,0	3,6	4,7	1,0	1,9	
Biotite			5,5	3,6	3,2	12,1	2,7	
Opaque			0,8	2,6	-	3,2	-	
Other			0,8		2,2	1,1	2,1	79,5 *

* Groundmass

and petrographic characteristics.

The Luderitz Province rocks are therefore analagous in nature, and perhaps in genesis, to the rhyolite-trachyte, and the phonolite-trachyte suites which have been well documented from localities throughout the world. Magma variation, or differentiation, in current petrological theory is largely ascribed to crystal fractionation and the evolution of the rhyolite-trachyte and phonolite-trachyte suites are no exception. With respect to the Luderitz Province, the development of quartz- and nepheline-rich syenites from a saturated syenitic parent by crystal fractionation is not only feasible, but is suggested by the field and petrographic evidence.

The hypothesis to be tested by the chemical data is that mentioned above, i.e. the over- and undersaturated suites are consanguineous, and have evolved through crystal fractionation processes. It is also intended to show which phases partake in the fractionation scheme.

It must be noted that it is becoming increasingly evident that the chemistry of crystalline peralkaline rocks does not necessarily reflect the composition of the magma from which they crystallized. MacDonald (1969), MacDonald et al (1970), Gill (1972) and Noble (1970) have all described the importance of the vapour phase in modifying magma compositions such that phenocryst-crystalline groundmass analyses do not reflect phenocryst-liquid equilibria and therefore cannot describe the differentiation path of the magma.

6.3. THE PROBLEM OF INVESTIGATING ALKALINE-PERALKALINE SALIC IGNEOUS ROCKS BY MEANS OF CHEMICAL VARIATION DIAGRAMS

Chemical variation diagrams have played a very important two-fold role in igneous petrological studies for over 70 years. Firstly, they have been invaluable aids in assisting investigators to interpret their chemical data, and secondly, they have provided a simple means by which authors may present data so as to be easily assimilated by the reader.

Molecular %, weight %, elemental values, and calculated normative constituents have been incorporated in a wide variety of variation diagrams which range from the simple (Harker diagram), to the more complex (Latent Vector diagram (Le Maitre, 1968)). Specific types of plots are applicable

to a wide range of rock compositions, whereas others have a more restricted application. Most diagrams are based on the hypothesis that crystal fractionation has been the sole or dominant process whereby variation in magma composition is achieved. Thus many of these general diagrams, e.g. those utilising the Differentiation Index or Crystallization Index (Thornton and Tuttle, 1960 ; and Poldervaart and Parker, 1964) are a quantitative and diagrammatic positioning of a rock composition in Bowen's reaction series.

With few exceptions most suites of salic alkaline rocks show little major element variation, and important features such as Na/K ratio, peralkalinity, and over- and undersaturation are obscured or even ignored in conventional plots. Even the CIPW Norm is not strictly valid for peralkaline and undersaturated alkaline rocks. It is for these reasons that the illustration of analyses of alkaline rocks, and especially the interpretation of such illustrations, must be carefully considered. A case in point is the misinterpretation of feldspar phenocryst - whole rock data for pantellerites (Carmichael and MacKenzie 1963) in which the conventional Granite system plot was used ignoring excess alkalies over alumina (see Bailey and Schairer 1964).

Illustration and interpretation of chemical variation in alkaline rocks has been treated in a number of different ways:-

1. Authors have modified the oxide-oxide plot of the Harker type by plotting diagrams of OXIDE v INDEX. INDEX is chosen because (a) it shows significant variation or "spread" for the compositions under consideration; and (b) it is known or assumed to vary sympathetically with fractionation, e.g. normative ne of Gill (1972), the Fractionation Index (FI) of MacDonald (1969), and Na + K/Al of Nash et al (1969).

2. Authors have used distortion-free diagrams which handle the chemical data rigorously, either in whole or in part. The simplest is the Molar Ratio diagram of Pearce (1968), and a more complex type is the Latent Vector diagram of Le Maitre (1968). There are also a large number of statistical methods of handling large numbers of analyses, but the petrological significance of any trends derived by the statistical manipulations is often obscure, e.g. the Factor analysis of the Hebridean tholeiitic magmas (Holland and Brown, 1972).

3. Authors have devised standard plots to test for specific fractionation

schemes for alkaline rocks. Of most value is that of Bailey and MacDonald (1969).

4. Authors studying porphyritic volcanic rocks have treated their rocks as crystal-liquid equilibrium systems, and by plotting phenocryst and whole-rock compositions onto suitable diagrams have analysed genetic trends in terms of fractional crystallization directly, e.g. Nash et al (1969).

In the Luderitz Province coarse grained equigranular rocks predominate and the methods outlined in (4) above are inapplicable. The other approaches outlined above are however of considerable use and the following scheme of evaluation is proposed:-

A. Use MacDonald's FI v Oxide plot to illustrate the chemistry of the rocks and the possible variation with fractionation.

B. Use the Bailey and MacDonald diagram to test for feldspar fractionation.

6.4. MAJOR ELEMENTS

Figures 18 and 19 are plots of Wt% oxide versus Fractionation Index (FI) (MacDonald, 1969). FI is the sum of the normative components q + or + ab + ac + ns. For undersaturated rocks a modified Fi; ne + or + ab + ac + ns is used. FI represents the experimentally determined path which fractionating peralkaline liquids follow (Bailey and Schairer, 1966), and increases with increasing differentiation. The FI for each rock type in the complexes agrees well with field and petrographic evidence. An important exception is that the Inner syenite at Pomona has a higher FI than the Hub Syenite. Field, petrographic and chemical evidence indicate the reverse, i.e. the Hub Syenite is more fractionated than the Inner Syenite.

The FI vs oxide diagrams are therefore a convenient method of illustrating chemical variation in an alkaline rock suite. Furthermore they may also be used in genetic interpretations with respect to crystal fractionation.

6.4.1. The Undersaturated Suite

With increasing FI the undersaturated rocks display increasing K_2O,

Na_2O, $K_2O + Na_2O$, $Fe_2O_3/FeO + Fe_2O_3$, and slightly increasing SiO_2 and Al_2O_3. Conversely CaO, MgO, TiO_2 and total Fe (as Fe_2O_3) decrease with increasing FI, whereas MnO remains essentially constant.

The other major feature in the diagrams is the considerable scatter in the abundance of certain oxides shown by rocks with high FI. This is especially noticeable for SiO_2, Al_2O_3, $Fe_2O_3/ (FeO + Fe_2O_3)$, and to a lesser extent Na_2O. In all cases the scatter can be attributed rock types. The tinguaite dykes and the Pomona foyaite all show higher SiO_2 and $Fe_2O_3/ (FeO + Fe_2O_3)$, and lower Al_2O_3 and Na_2O when compared with rocks of similar FI, the Granitberg Outer Foyaite. This scatter is a reflection of their mineralogy. The dykes and Pomona foyaite are lower in modal nepheline but higher in modal aegirine than the Outer Foyaite. Since FI is insensitive to nepheline/aegirine ratios a scatter in the major elements in these two minerals can be expected.

In general, the chemical variation depicted in the diagrams is typical of that which can be expected in a suite of nepheline syenites of this kind.

6.4.2. The Oversaturated Suite

Variation of oxide abundances with FI for the oversaturated rocks show many features in common with the undersaturated suite. SiO_2, K_2O, $Fe_2O_3/ (FeO + Fe_2O_3)$ and Na_2O all increase with increasing FI, whereas Al_2O_3, total Fe, MgO, CaO, and TiO_2 decrease and MnO remains constant.

More noticeable is the scatter in oxide abundances for high FI rocks, particularly in K_2O, Na_2O, SiO_2 and Al_2O_3. This would be expected in a suite of this kind where FI is insensitive to the normative quartz/feldspar ratio. Although a bostonite (< 5% quartz) and a quartz feldspar porphyry (30% quartz) can have the same FI they would differ considerably in their quartz/feldspar ratios and therefore in abundances of SiO_2, Al_2O_3, K_2O and Na_2O. The scatter mentioned above can be attributed to the "diluting" effect of quartz in the high FI, quartz rich rocks.

The implications of this is that the FI diagrams are useful to depict chemical variation controlled by fractionation of plagioclase and mafic minerals (other than aegirine), they are of little use in rock suites where alkali feldspar fractionation is dominant.

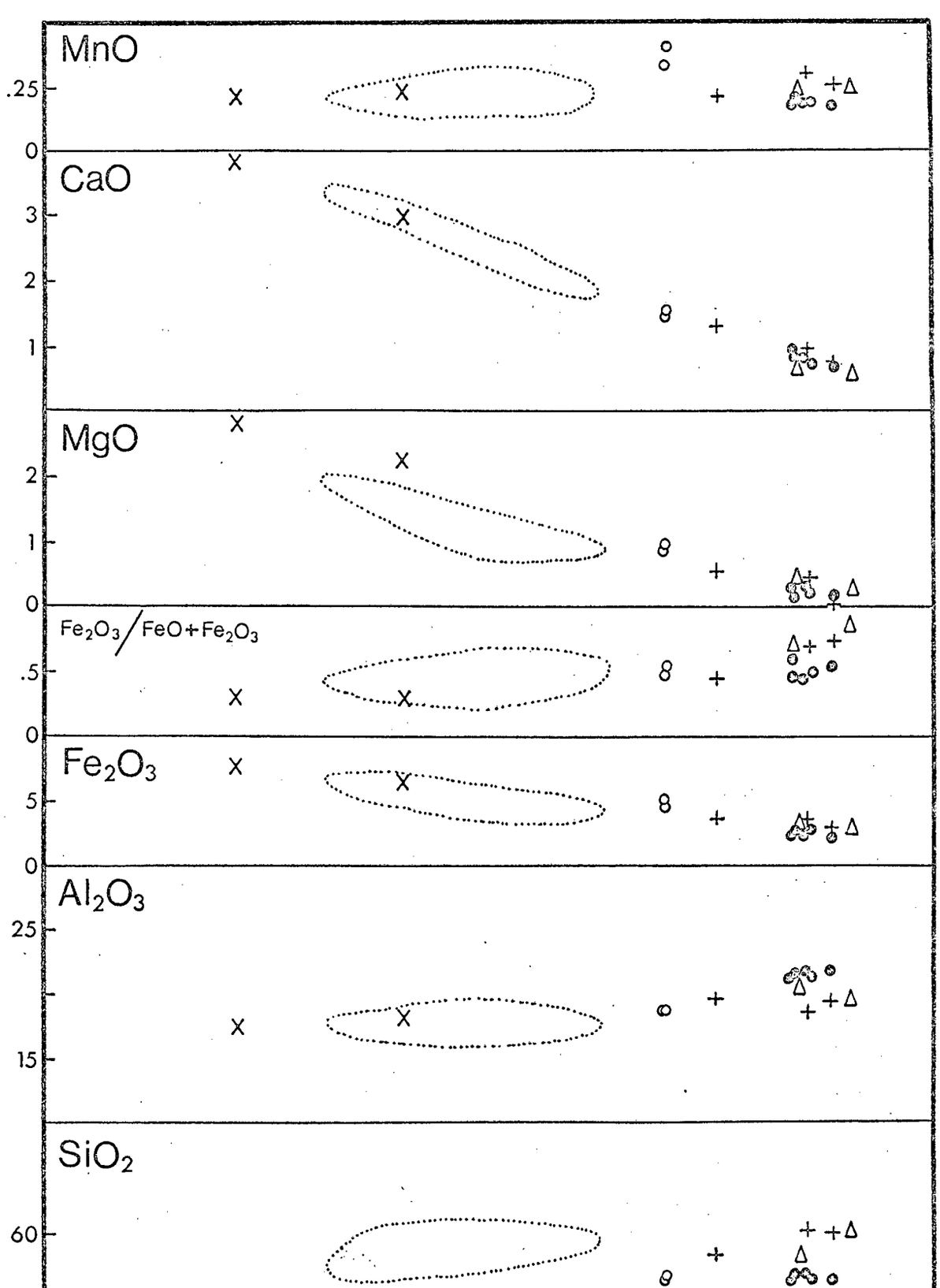

Figure 18. Plot of FI vs OXIDE for the undersaturated suite.
X - PCNS; o - Inner Foyaite; ⊙ - Outer Foyaite; + - tinguaite dykes and minor intrusions; Δ - Pomona undersaturated rocks.
Stippled fields indicate variation of element/oxide with FI for the oversaturated suite.

what are outlined areas?
explanation only follows on p.122!

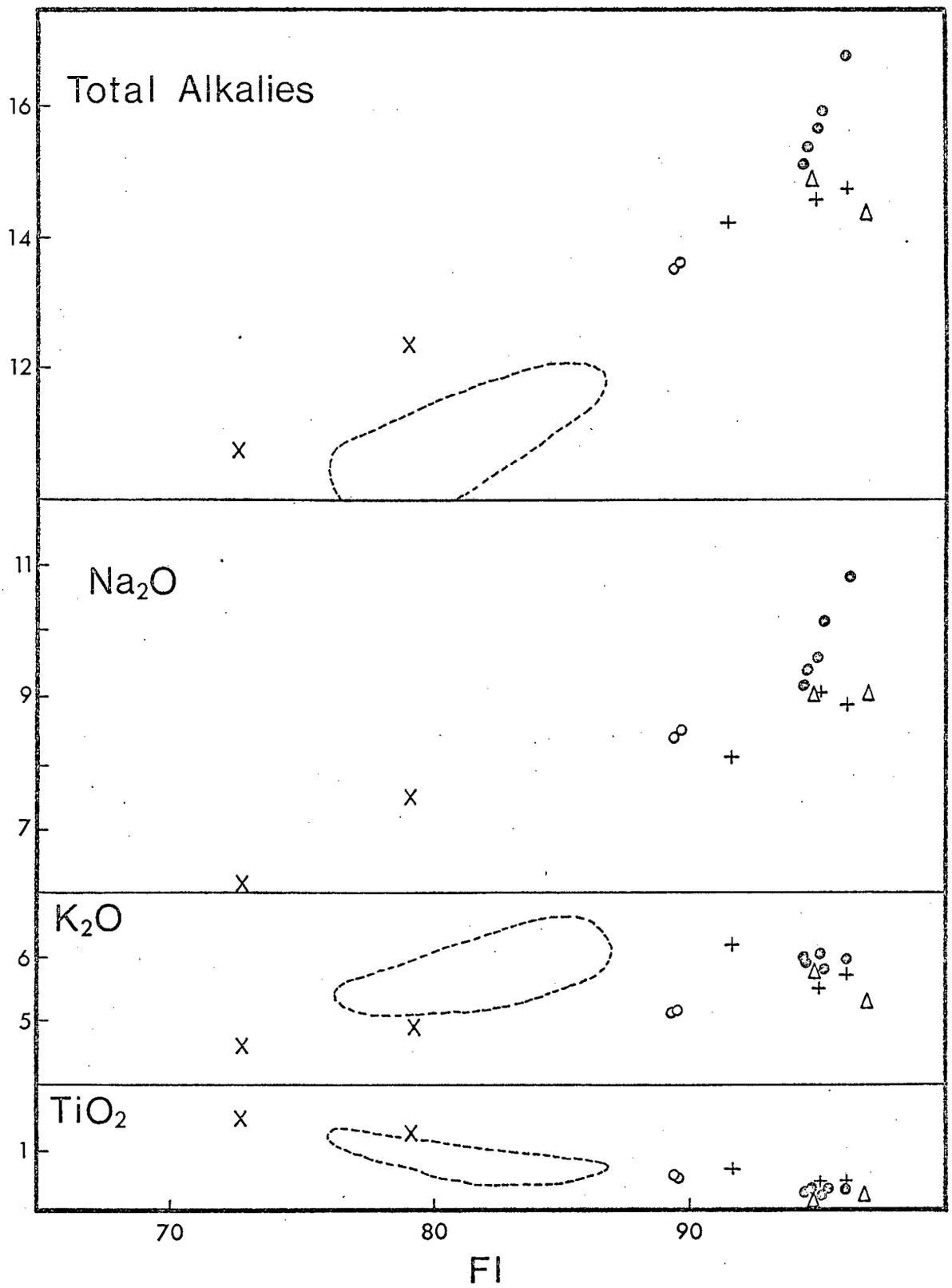
Total Alkalies
16
14
12
Na_2O
11
9
7
K_2O
6
5
TiO_2
1
70
80
90
FI

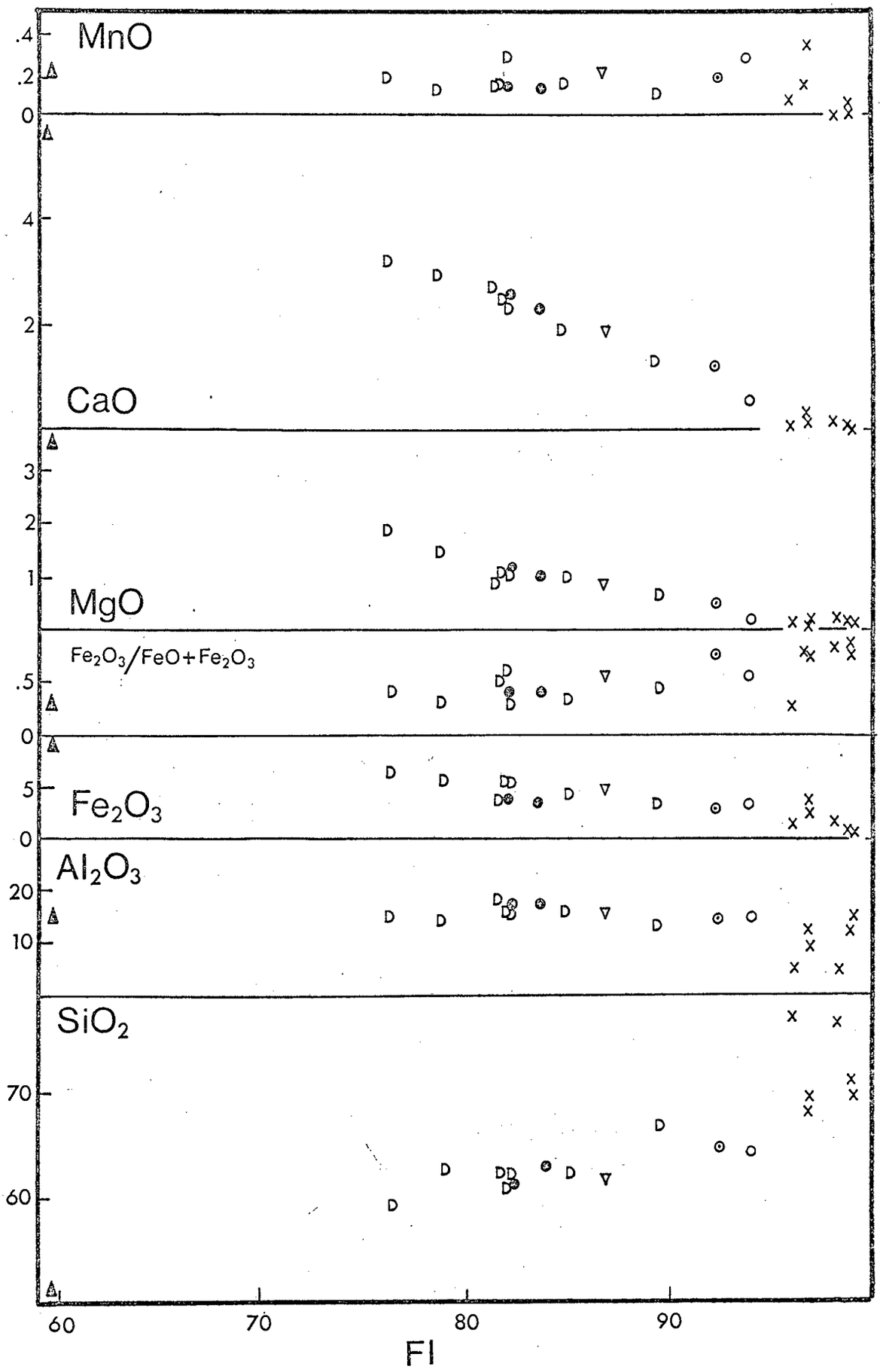

Figure 19. Plot of FI vs OXIDE for the oversaturated suite.

D - Drachenberg syenites; ▲ - Biotite-rich Monzonite, Pomona;
⊙ - Outer Syenite; ▽ - Syenite porphyry, Pomona; ⊙ - Hub Syenite;
o - Inner Syenite; x - bostonites, quartz-feldspar porphyries.

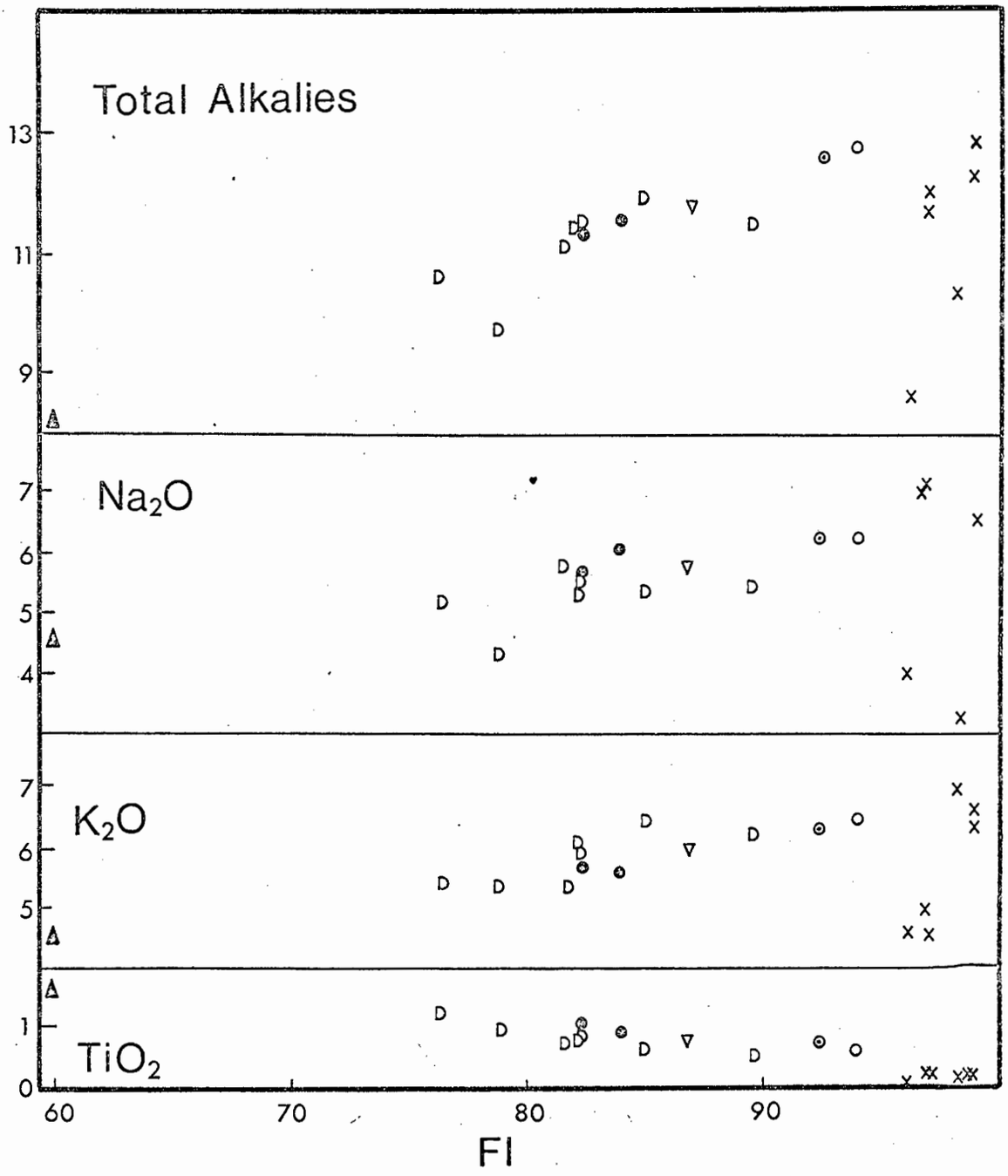
Total Alkalies
13
11
9
Na_2O
7
6
5
4
K_2O
7
6
5
TiO_2
1
0
60
70
80
90
FI

6.4.3. The behaviour of Ca and Mg in peralkaline liquids

One of the less obvious contrasts between the two suites is the extreme depletion of Ca in the oversaturated dyke rocks in contrast to the highly fractionated undersaturated rocks. An examination of the literature reveals that depletion of CaO to less than 0,10 Wt% is occasionally observed in acid alkaline rocks (MacDonald, 1969; Noble et. al., 1971) but never in undersaturated rocks where it appears to stabilize at about 0,5 to 0,4 Wt% (Gill, 1972 and this work). Of course Ca in greater amounts in both under and oversaturated alkaline rocks is commonly reported.

This distribution seems to be in contrast to observed partitioning of Ca between melt and alkali feldspar phenocrysts. Noble et al (1971) reported that Ca was preferentially partitioned into glass in certain sanidine phyric comendites from the Great Basin, U.S.A., and suggested that feldspar fractionation could result in an increase in Ca in residual liquids, and, regardless of degree of fractionation, slightly peralkaline silicic magmas will contain significant amounts of calcium. Nicholls and Carmichael (1969), noting the differences between peralkaline under- and oversaturated liquids, pointed out that sanidines from pantellerites and comendites contained much less anorthite molecules (0,1 to 0,2%) than do sanidines from phonolites (1 to 10%) (Nash et al 1969; Carmichael, 1964).

The other major phase in undersaturated liquids is nepheline. Heier's (1966) figures show that the ratio Ca (feldspar) /Ca (nepheline) ranges from 0,58 to 0,72 for coexisting feldspar and nepheline in a nepheline syenite. If Ca is already preferably entering the feldspar then the precipitation of nepheline would further deplete an undersaturated liquid in Ca.

The implications of the observed partioning mentioned above is that, if feldspar fractionation is the dominant mechanism by which peralkaline phonolitic and acid liquids are generated, the phonolitic liquids are more likely to show a marked Ca depletion than acid liquids. This, as has been noted, is in contrast to the Ca distribution in the Luderitz Province.

However, phases other than feldspar must also be considered. Na-pyroxene is a common mineral in all peralkaline rocks and generally carries notable amounts of Ca. In the writer's experience, undersaturated rocks are seldom completely depleted in mafic minerals. In addition in under-

saturated rocks crystallizing almost pure aegirine, significant amounts of fluorite, eudialyte, sphene, and rinkolite (all with Ca as a major constituent) are often present with textural evidence indicating that they crystallized interstitially from residual liquids. In contrast acid rocks are often entirely depleted in mafic minerals and in their absence the only possible minerals, with major amounts of Ca, likely to crystallize are fluorite, and sphene. In the Luderitz Province undersaturated dyke rocks carry abundant Na-pyroxene, sphene, fluorite, eudialyte whereas the bostonites and quartz feldspar porphyries are essentially quartz-feldspar rocks.

What is proposed here is that Ca in highly differentiated peralkaline over- and undersaturated liquids is controlled by processes in addition to feldspar fractionation, probably by fractionation of Ca-bearing mafic minerals. The incorporation of Ca into alkali feldspar as anorthite might be a strong influence in the early stages, especially in the development of the peralkaline condition. The common occurrence of late crystallizing fluorite, eudialyte, Ca-bearing arfvedsonite and rinkolite indicates that Ca is somewhat soluble in peralkaline undersaturated melts and is stabilized there so that significant amounts remain in the residual liquid regardless of degree of fractionation. In contrast, in oversaturated peralkaline liquids, Ca appears to readily enter mafic minerals and alkali feldspars, and may be depleted to very low concentrations by fractionation of these two phases.

Low Mg ($< 0,2$ Wt%MgO) is exhibited by the high FI rocks of both the over- and undersaturated suites. Low Mg is not unusual in strongly fractionated peralkaline rocks (e.g. Siedner, 1965; Noble 1968; Bailey and MacDonald, 1970; Ewart et al, 1968; MacDonald, 1969; Noble et al, 1969; Gill, 1972) but seems to be most commonly reported in acid rocks. What is noticeable in regard to the distribution of Ca mentioned above, is that extreme depletion of Mg is often recorded without similar depletion in Ca (see Noble et al, 1969). This supports the ideas expressed above, that crystal fractionation (which would deplete liquids in Mg) is not the sole control of the distribution and abundance of Ca in paralkaline liquids.

6.4.4. Feldspar fractionation and the development of the Luderitz Province Magmas

Since FI diagrams do not adequately test the chemical data for feldspar

fractionating, molecular % Na_2O, K_2O, SiO_2 and Al_2O_3 have been plotted in the relevant sections of the quarternary system Na_2O-K_2O-Al_2O_3-SiO_2 (Figures 20 and 21). These plots have been devised by Bailey and MacDonald (1969) to illustrate the degree of under- and oversaturation of salic rocks and their peralkalinity as well as to test if any peralkaline rock series could have evolved through feldspar fractionation.

These authors applied their diagrams to consider problems in the evolution of silicic peralkaline lavas and glasses, but there is no reason why they should not be applied to silica-undersaturated rocks. Indeed, Gill (1972) has recently done so.

6.4.4.1. Undersaturated Suite

Figure 20 (a) is part of the SiO_2-Al_2O_3-(Na_2O+K_2O) face of the SiO_2-Al_2O_3-Na_2O-K_2O volume in which the compositions of the nepheline bearing rocks have been plotted. Also plotted is the feldspar join (F), the undersaturated minimum in the system SiO_2-$NaAlSiO_4$-$KAlSiO_4$ (N) and the albite-nepheline cotectic (P-T). Compositions plotting to the left (Al_2O_3-rich side) of the line FR are meta- or peraluminous, whereas those to the right are peralkaline. Apart from the two PCNS specimens (GM128 and GM146) all the undersaturated rocks are peralkaline. Moreover these compositions lie with some scatter about a line originating at F, but projecting into the peralkaline field. The significance of such a line is that any composition lying on the line can be derived from a more siliceous composition on the line purely by feldspar fractionation. Any composition lying off the line cannot be derived from one on the line by fractionation of feldspar alone, but possibly by feldspar fractionation coupled with some other differentiation process.

In reality it would be naive to expect the compositions of a series of crystalline rocks, which have evolved solely by feldspar fractionation, to plot exactly on such a line, and a certain amount of scatter must be tolerated. It must also be noted that below the albite-nepheline cotectic considerable scatter can be expected as nepheline joins alkali feldspar on the liquidus and co-fractionation of these two phases will move the liquid composition sharply away from its original feldspar controlled path.

The disposition of the peralkaline rocks of the undersaturated suite suggests that their evolution could have been controlled by alkali feldspar fractionation.

The two PCNS specimens plot in the metaluminous field and a line joining them to the peralkaline nepheline syenites passes to the Al_2O_3-rich side of F. Gill (1972) has shown that an evolutionary trend of this orientation can be interpreted in terms of fractionation of an alkali feldspar with a small proportion of anorthite molecule. For the compositions as plotted a feldspar containing about 10 mole%. An is indicated. An alkali feldspar of this composition is well within the range reported by Scharbert (1966) (5 to 14%An) and Ridley (1970) (2 to 12,6%An), but greater than that 5,8% An determined by Carmichael (1964) for an alkali feldspar in equilibrium with an undersaturated liquid.

The trend could also have evolved through fractionation of an An-poor alkali feldspar together with some other alkali-poor, Al-bearing phase. Augite phenocrysts in the PCNS have 2,30% Al_2O_3 (Table 21), and co-fractionation of these with the feldspar could have generated the evolutionary path.

Figure 20 (a) does not show the alkali ratio of the plotted compositions, and although feldspar fractionation is indicated, it is not proven. The line connecting the plotted compositions is actually the projection of a plane in the SiO_2-Al_2O_3-Na_2O-K_2O volume with an alkali/alumina index of 54 : 46. Examination of the projected compositions on this plane involves the least distortion (except for the PCNS compositions) since the plane is the "best fit" to the compositions.

Figure 20 (b) is a plot of the compositions on this plane contoured for various values of molecular $Na_2O/(Na_2O+K_2O)$. Tie lines connect rock compositions to their bulk feldspar compositions plotted on the feldspar join.

The feldspar compositions for the Inner and Outer Foyaites are for bulk separates from coarse grained rocks and do not necessarily represent the composition of the liquidus feldspars. Such feldspars, i.e. those first appearing on the liquidus, would probably be more Na-rich than those plotted and would represent compositions involved in the fractionation. In contrast the PCNS feldspar composition is for phenocrysts and is more representative of the composition of the fractionating feldspar.

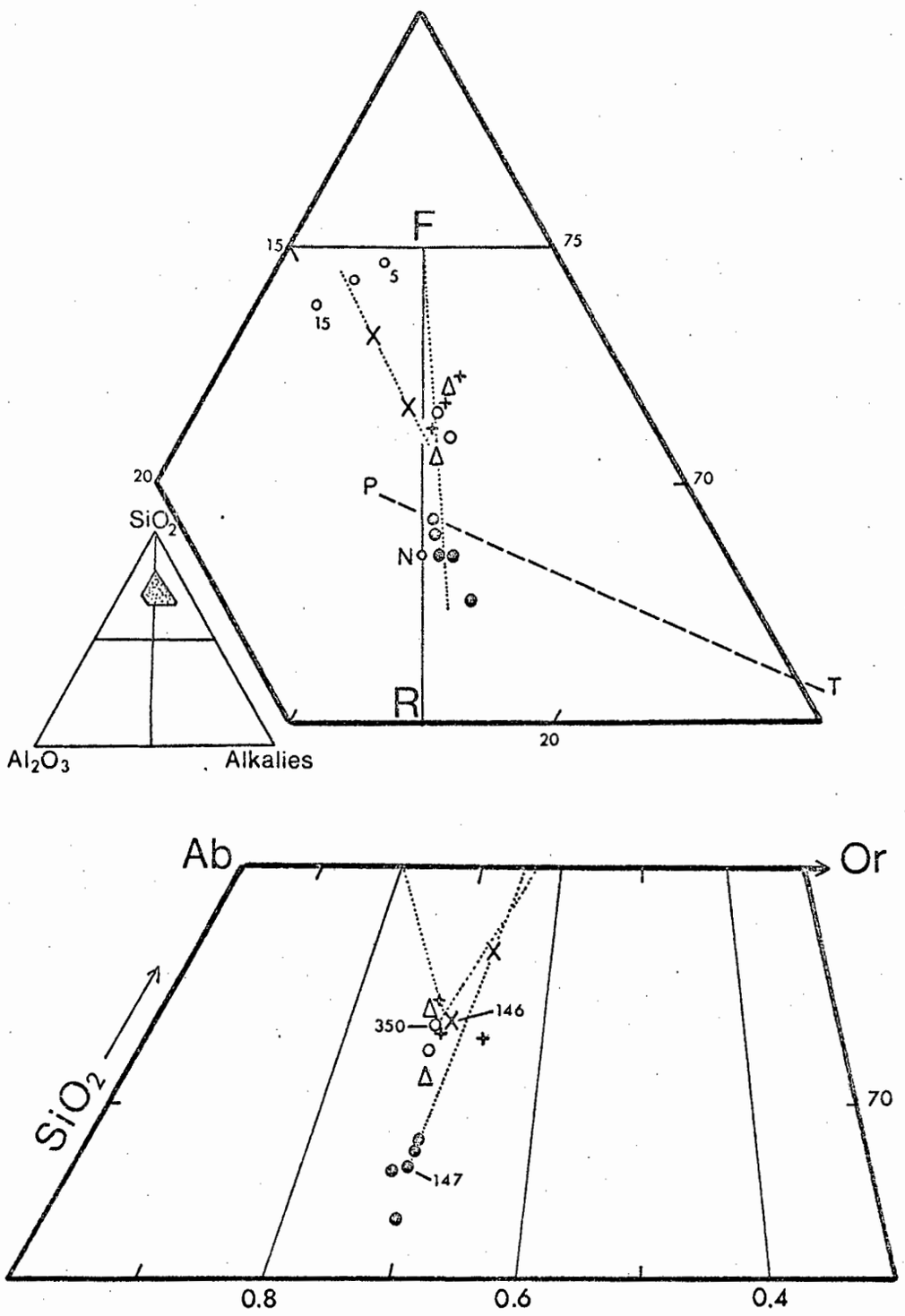

Figure 20. Composition of the undersaturated suite in terms of molecular % SiO_2, Al_2O_3, K_2O, and Na_2O (after Bailey and MacDonald, 1969). Symbols as in Figure 18; other features described in the text.

The whole rock compositions have near constant alkali ratio of 0,70 to 0,73 except for the two PCNS specimens which are more potassic. Clearly then, the main peralkaline development of the undersaturated trend could have been controlled by fractionation of an alkali feldspar with near-constant composition of $Ab_{70-72}Or_{30-28}$. This is slightly more Na-rich than the feldspar compositions determined for rocks in this series but it has already been explained that the liquidus feldspars could well have had this composition ($Ab_{70-72}Or_{30-28}$). This is convincing evidence that alkali feldspar was the dominating control in the evolution of the undersaturated suite.

The alternative to the above argument is that the liquids were initially more potassic than the analyses of their crystalline products indicates, and that they lost alkalies, especially K, on crystallization. Such a phenomenon is common, though Na is usually preferentially lost, and appears to be the chief reason for lack of sensible meaning between feldspar phenocrysts and their groundmass in peralkaline rocks.

The relationship between the PCNS specimen GM146 and its feldspar phenocrysts is more perplexing. Fractionation of the indicated feldspar composition would drive the residual liquid towards more K-rich compositions, away from the path of the undersaturated trend.

However, GM146 contains abundant biotite in the groundmass and as phenocrysts, in fact biotite is more common in these rocks than in any other nepheline syenite. Fractionation of biotite with its extremely high K/Na ratio, would offset any liquid trend controlled by fractionation of the feldspar phenocrysts, and steer it to more sodic compositions. Since biotite has the same alkali : Si : Al proportions as in alkali feldspar, biotite fractionation would be indistinguishable from feldspar fractionation when evaluated in the SiO_2-Al_2O_3-(K_2O+Na_2O) plane.

6.4.4.2. The Oversaturated Suite

The saturated and oversaturated syenites from Pomona and Drachenberg are plotted in Figure 21 (a) which is the oversaturated portion of the plane SiO_2-Al_2O_3-(K_2O+Na_2O). The various features of this portion of the plane have been given in detail by Bailey and MacDonald (1969) and are similar to its undersaturated analogue discussed above.

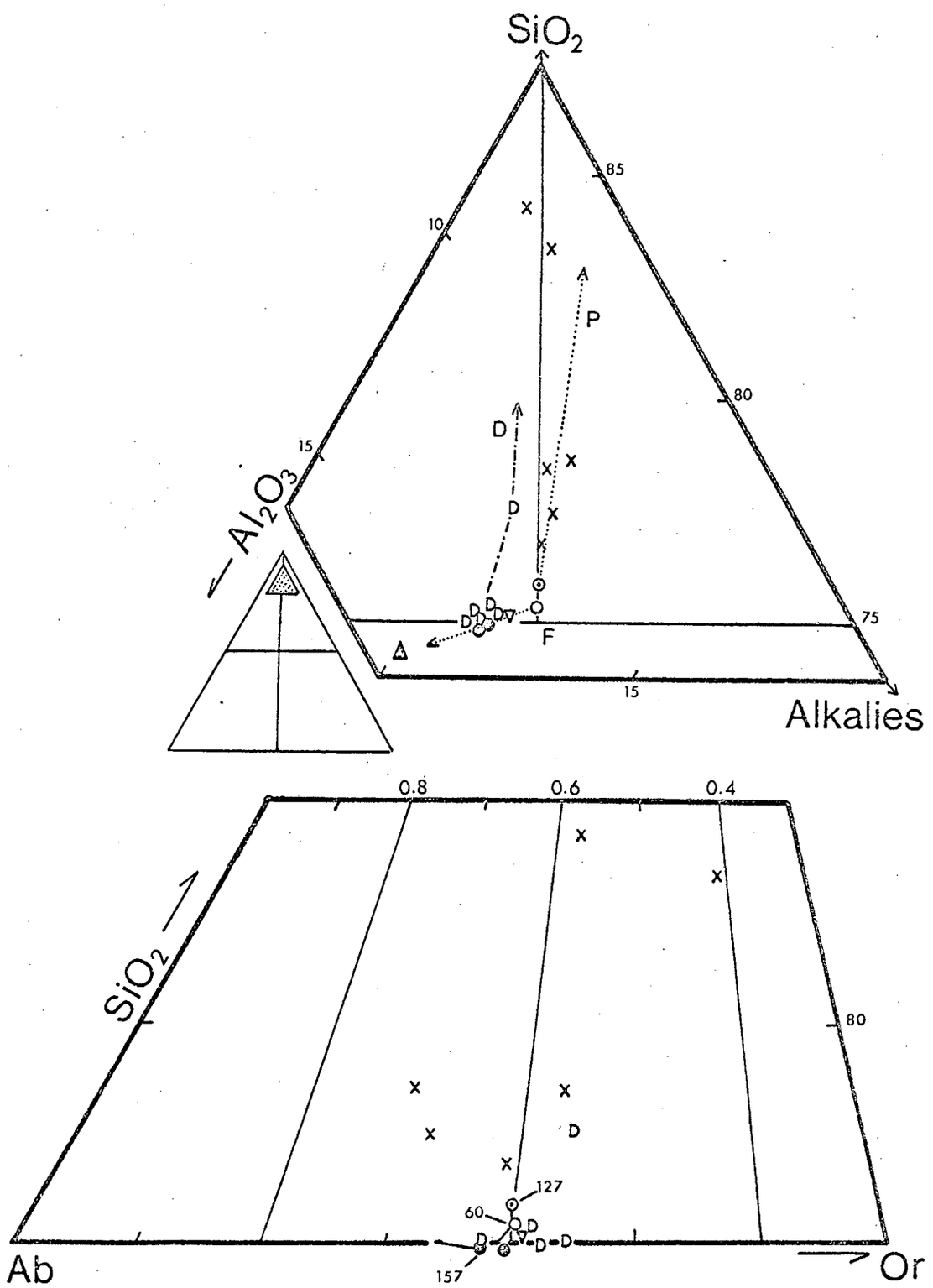

Figure 21. Composition of the oversaturated suite in terms of molecular SiO_2, Al_2O_3, K_2O, and Na_2O (after Bailey and MacDonald, 1969). Symbols as in Figure 19; other features described in the text.

Many of the syenites plot in a cluster on the critical line of saturation in the metaluminous field. The Biotite-rich Monzonite, PM64, plots well away from these syenites at a more Al-rich composition. Significantly the more siliceous Drachenberg rocks all plot in the metaluminous field whereas the more siliceous Pomona syenites and dyke rocks plot in the peralkaline field.

It appears that the Drachenberg suite of syenites could have developed by fractionation of a single feldspar containing about 7% An molecule. The constant appearance of zoned alkali feldspars with anorthoclase or sodic plagioclase cores in many of these syenites is evidence that such feldspars did crystallize. However, constant fractionation of such feldspars would soon deplete the residual liquid in Al_2O_3 and drive it into the peralkaline field. From the petrographic evidence more "normal" (An-poor) alkali feldspar followed soon on the precipitation of the An-rich feldspars, and successive liquids were probably steered along a metaluminous path by the buffering effect of the fractionation of these two feldspars. Although Al_2O_3 would initially be depleted in the residual liquid, prolonged fractionation of stochiometric alkali feldspars would offset the depletion enriching the liquid in Al. In this manner the Al_2O_3 content of the liquid is kept fairly constant, allowing for the appearance of a ternary feldspar in successive fractions.

Figure 21 (b) is part of the plane $Na_2O.Al_2O_3 - K_2O.Al_2O_3 - SiO_2$ showing the alkali ratio of the various syenites. The Drachenberg syenites and siliceous derivatives have very similar alkali ratios, i.e. $Na_2O / (Na_2O + K_2O)$ between 0,55 and 0,59, which is consistent with the fractionation scheme proposed above.

Feldspar fractionation in the Pomona syenites would initially involve a feldspar with a considerable proportion of An molecule in order to drive the residual liquid rapidly into the peralkaline field. The position of PM64 with respect to the Outer Syenite (PM157) and the Inner Syenite (PM60) is perhaps significant as it appears that it could be a cumulate arising through such a process. The molecular ratio $Al_2O_3/(Na_2O+K_2O)$ is greater than 1,0 for the mafic minerals in the Outer Syenite and their fractionation would assist in developing this peralkaline trend.

The Inner Syenite, Hub Syenite and the various dyke rocks lie close to a line passing through the projection of the feldspar join, F, and extending into the peralkaline field. Their evolution could therefore have been controlled by fractionation of alkali feldspar. The quartz-feldspar porphyry, PM177, is displaced to the left of the line, possibly due to alkali loss on crystallization (MacDonald, 1969).

Consideration of these compositions in the $Na_2O.Al_2O_3$ - $K_2O.Al_2O_3$ - SiO_2 plane (Figure 21 (b)) reveals that the alkali ratio for the syenites is similar (0,59 to 0,63) but varies widely in the dyke rocks. Bulk feldspars are more sodic than the rocks from which they are derived and the initial feldspars to crystallize were probably more so. It does not seem possible to account for the chemical features of the various rock types by feldspar fractionation ~~above~~ alone.

6.4.5. Summary of major element data

Major element data for the undersaturated suite and the Drachenberg syenites are consistent with the evolution of these rocks by a process of crystal fractionation dominated by alkali feldspar. The steady decrease in CaO, MgO, TiO_2 and total Fe with increasing FI confirms that mafic minerals (biotite, clinopyroxene and amphibole) were fractionated along with the alkali feldspar.

The data for the Pomona complex suggest a feldspar fractionation scheme for the evolution of the syenites and siliceous dyke rocks, but consideration of alkali ratios in the rocks indicates that some other process modified the evolutionary trend in the late stages. As with the Granitberg and Drachenberg rocks, mafic mineral fractionation accompanied feldspar fractionation at all stages of the evolution of these rocks.

6.5. TRACE ELEMENTS

Trace element abundances listed in Tables 12, 13, 14 are plotted against FI in Figures 22 and 23. Several element ratios are listed in order of increasing FI in Tables 15, 16, and 17.

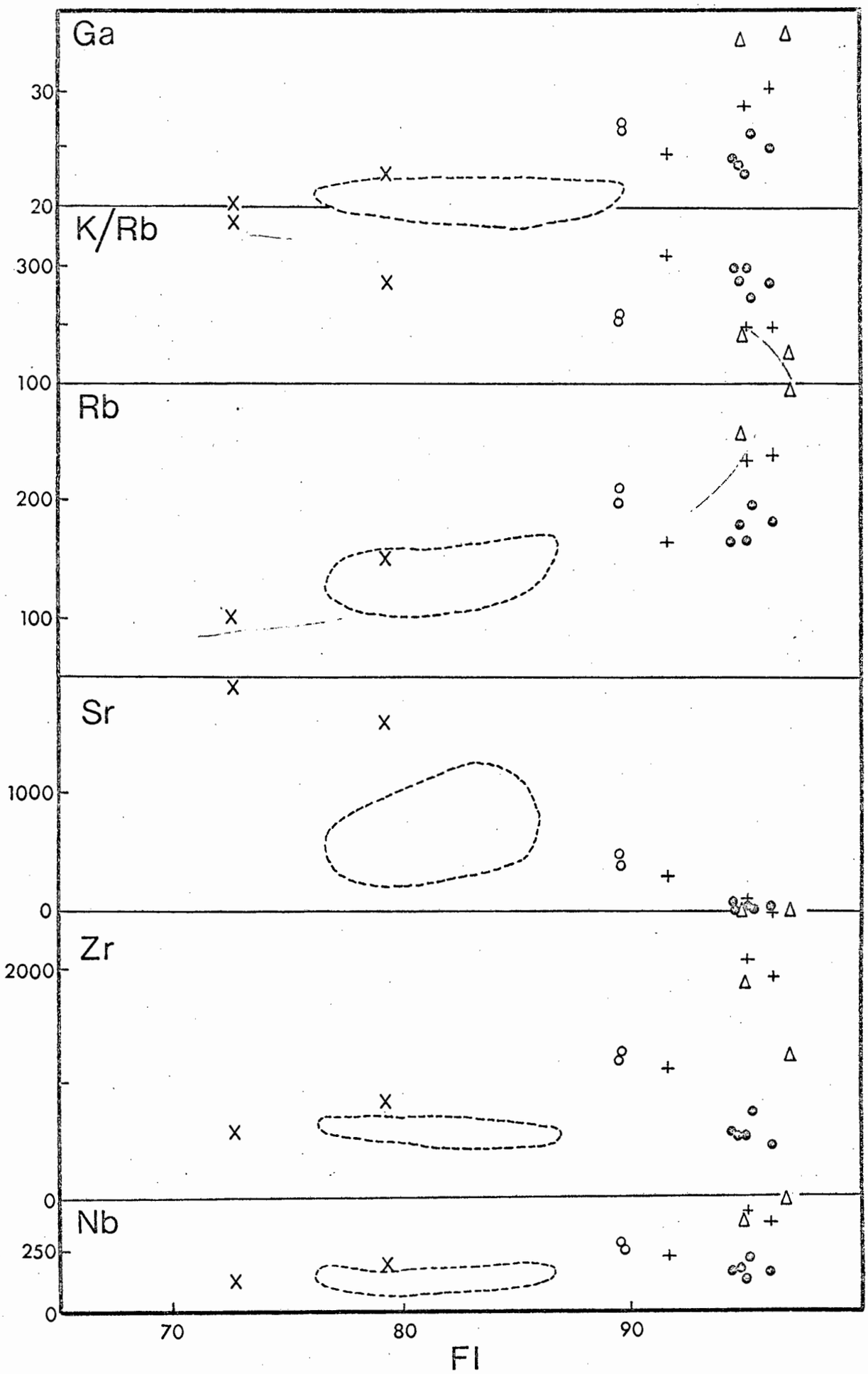

Figure 22. Plot of FI vs TRACE ELEMENT for the undersaturated suite. Symbols as in Figure 18.

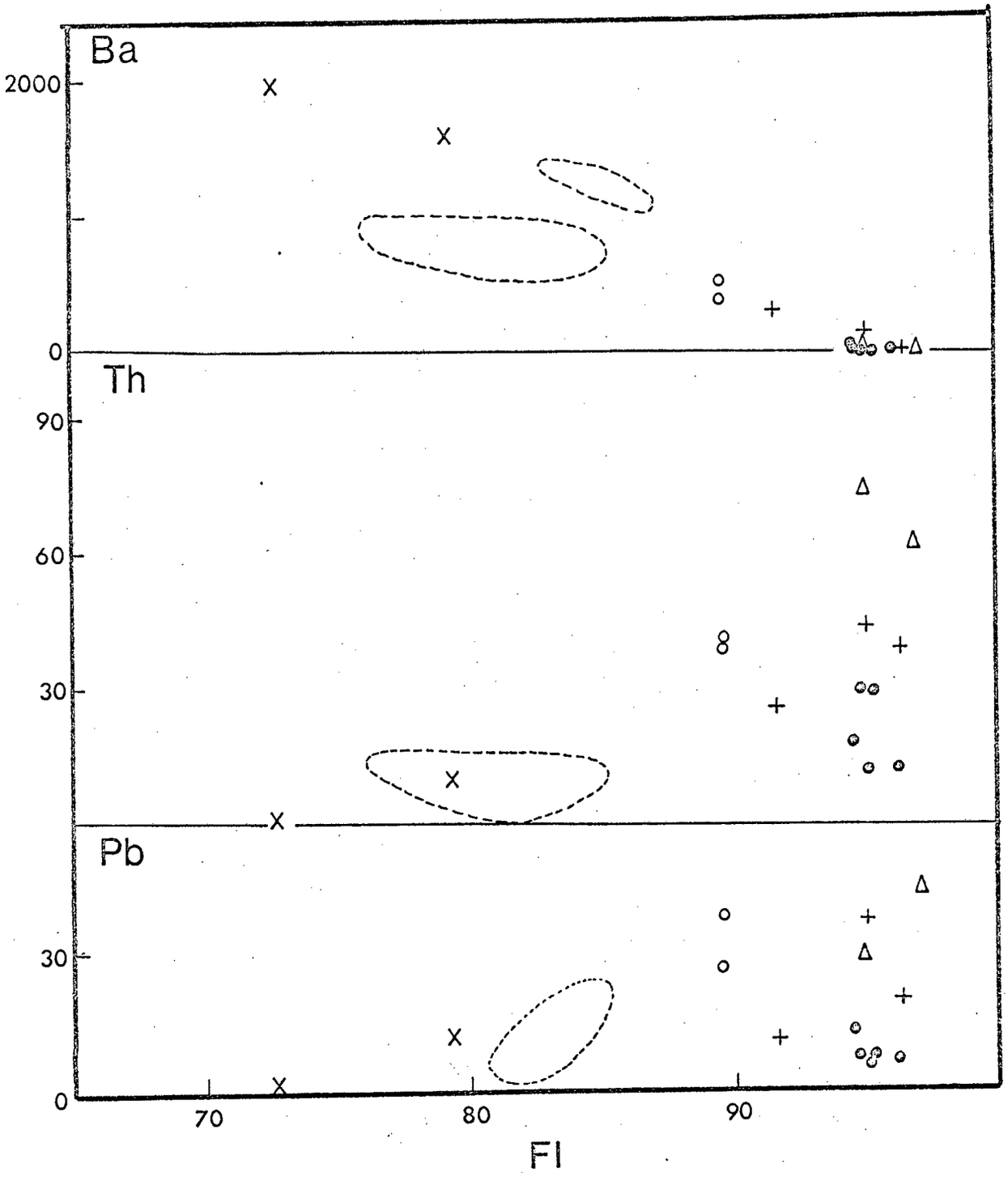
Ba
2000
0
Th
90
60
30
Pb
30
0
70
80
90
FI

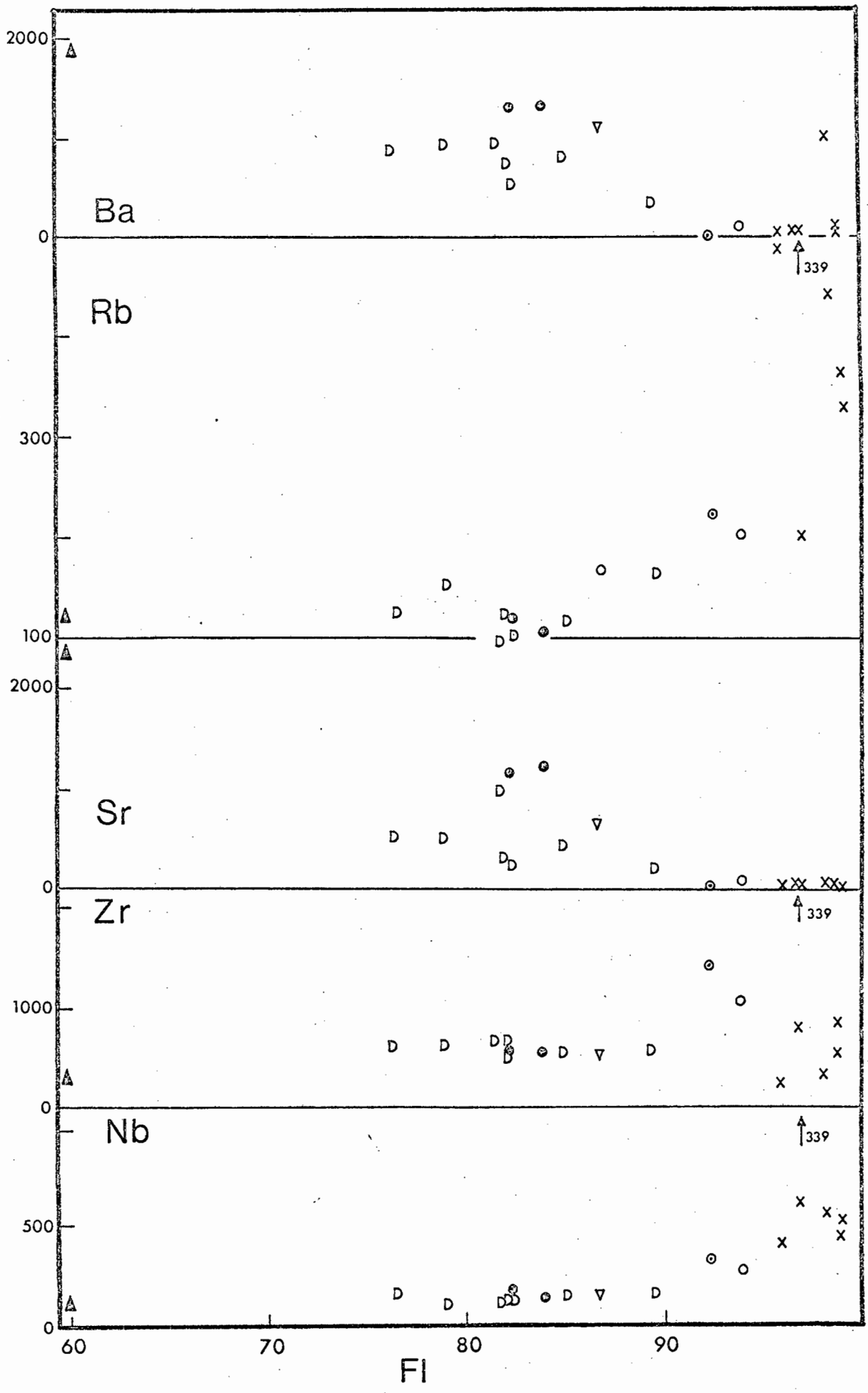

Figure 23. Plot of FI vs TRACE ELEMENT for the oversaturated suite. Symbols as for Figure 19.

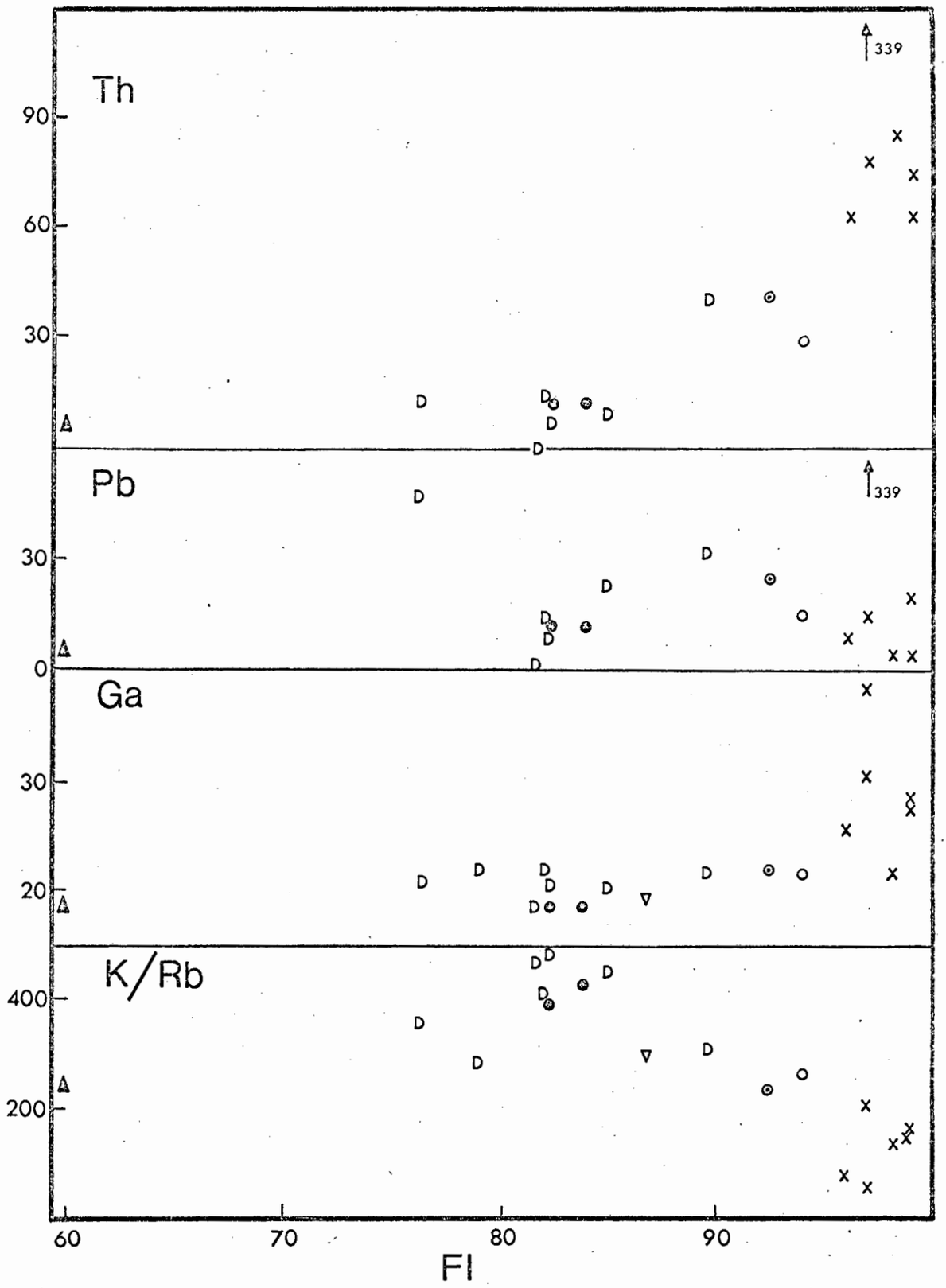
Th
339
90
60
30
Pb
339
30
0
Ga
30
20
K/Rb
400
200
60
70
80
90
FI

TABLE 15

Interelement ratios for the undersaturated rocks from Granitberg and Pomona

SAMPLE	FI	K/Ba	Ba/Sr	Ca/Sr	K/Rb	K/Th	Zr/Th	Zr/Nb	Ti/Nb	$Pbx10^2/Sr$	$Gax10^4/Fe^{3+}$	$Gax10^4/Al$
GM128	72,8	19	1,04	14,4	378	*	*	4,35	69,3	*	12,8	2,20
GM146	79,3	25	0,99	13,6	266	4091	85,2	4,24	38,2	17,4	17,1	2,37
GM350	89,5	112	1,81	27,5	203	1120	31,4	4,15	8,9	9,9	16,8	2,67
GM131	89,6	81	1,21	24,2	216	1024	30,4	4,52	10,9	6,2	14,3	2,68
GM77	91,6	160	1,11	33,3	314	1928	42,6	4,67	7,9	3,9	20,8	2,37
GM129	94,5	952	0,66	87,9	299	2765	31,0	3,51	11,0	175	25,2	2,14
GM136	94,7	11642	0,52	761	276	1630	17,8	3,21	11,9	844	28,6	2,09
GM147	95,0	3126	0,73	263	301	3817	41,1	3,98	12,4	*	30,9	1,98
GM171	95,4	*	*	1191	243	1646	25,2	3,30	8,9	1488	28,8	2,36
GM142	96,2	7027	0,60	427	271	3672	31,3	2,71	13,2	560	31,8	2,17
GM130	95,1	446	1,15	70,6	194	1025	47,5	5,05	5,2	43,3	16,9	2,92
GM160	96,1	*	*	555	197	1188	48,3	5,08	5,9	2063	20,0	2,96
PM61	94,9	3943	0,59	30,3	185	643	25,1	4,88	5,0	1434	25,8	3,20
PM53	96,8	*	*	346	148	699	20,0	2,65	3,2	3595	21,9	3,48

* denominator or numerator below detection limit

TABLE 16

Interelement ratios for the oversaturated rocks from Pomona and Granitberg

SAMPLE	FI	K/Ba	Ba/Sr	Ca/Sr	K/Rb	K/Th	Zr/Th	Zr/Nb	Ti/Nb	Pbx10^2/Sr	Gax10^4/Fe^{3+}	Gax10^4/AL	Y
PM64	59,2	15,9	0,79	17,3	240	4300	45,0	2,99	140	*	7,8	2,04	25,1
PM55	82,2	37,0	1,09	15,5	395	3854	45,8	3,26	35,0	1,01	16,6	1,89	29,3
PM157	83,8	34,8	1,08	13,9	450	3746	45,9	4,03	35,8	0,99	17,9	1,87	22,0
PM63	86,7	45,7	1,60	19,3	300	*	*	3,21	26,6	*	12,8	2,05	25,4
PM60	94,0	482	1,28	45,5	264	1888	36,4	3,97	12,9	17,0	17,4	2,34	33,9
PM127	92,4	1876	1,11	351	236	1284	34,8	4,29	13,4	101	14,6	2,42	56,0
PM66	96,8	1379	1,95	67,1	203	530	10,3	1,27	3,12	974	21,9	3,55	52,2
GM339	96,9	1893	1,50	59,0	50	213	16,3	1,95	1,05	13383	21,4	4,94	90,0
GM340	98,9	559	5,57	2,0	151	890	8,8	1,38	3,24	3517	75,9	3,34	49,8
PM156	99,0	1093	5,27	39,2	159	986	11,3	1,61	3,02	*	141,3	2,99	29,5
PM177	98,3	77,9	16,37	15,1	132	690	4,1	0,63	1,29	*	23,5	3,26	50,0
DM111	96,1	888	2,00	26,5	77	624	3,9	0,57	0,58	41,8	79,8	3,91	51,7

* denominator not determined; numerator or denominator below detection limit

TABLE 17

Interelement ratios for the Drachenberg Syenites

SAMPLE	FI	K/Ba	Ba/Sr	Ca/Sr	K/Rb	K/Th	Zr/Th	Zr/Nb	Ti/Nb	$Pbx10^2/Sr$	$Gax10^4/Fe^{3+}$	$Gax10^4/AL$	Y
DM124	78,9	48,4	1,83	41,3	286	*	*	5,55	51,2	*	17,1	2,43	34
DM126	76,4	51,5	1,44	38,3	364	3206	46,7	4,37	49,2	7,6	11,8	2,24	34
DM110	81,6	45,4	0,98	19,5	464			5,81	34,4	?	14,0	1,87	21
DM106	82,1	66,4	2,50	58,3	414	3556	48,1	5,38	36,4	4,51	9,7	2,28	37
DM105	82,3	91,7	1,96	60,3	482	7294	73,9	4,06	41,5	3,95	18,5	2,18	31
DM125	85,1	66,4	1,93	32,1	456	5776	60,7	4,08	26,6	5,58	19,9	2,17	26
DM115	89,5	144	1,67	40,7	314	1282	14,4	4,08	20,8	14,9	21,1	2,46	28
DM111	96,1	888	2,00	26,5	77	624	3,88	0,57	0,58	41,8	79,7	3,91	51

* denominator or numerator not determined
denominator below detection limit

6.5.1. Barium

Ba is one of the largest divalent cations and may substitute for K^+ and Ca^{++}, the former being the most important substitution. Ba is therefore concentrated in the two common K-bearing minerals alkali feldspar and biotite - a feature which has been repeatedly observed by several workers and emphasised by the recent compilation of data by Puchelt (1972). The important Ca-bearing minerals which Ba enters are plagioclase, pyroxenes and amphiboles.

There are many determinations of the distribution of Ba between phenocryst and melt for a number of different minerals in different rock types. Philpotts and Schnetzler (1970) found that the distribution coefficient, D, was greater than 1,0 only for K-feldspars and biotite - in all other minerals it was less than one. Berlin and Henderson (1969) reported data for phonolites and trachytes as follows:

Na plagioclase;	D	0,72 - 1,09
Sanidine;	D	1,17 - 8,95
Biotite;	D	1,6 - about 15.

Similar values are reported by Korringa and Noble (1971) and Lovering (1969) for silicic volcanic rocks. Heier (1966) found the ratio Ba (feldspar)/Ba (nepheline) to be about 80, and that K/Ba was higher in nepheline than feldspar.

These distribution coefficients readily explain the behaviour of Ba in a rock series related through crystal fractionation. Ba increases with fractionation from basic through intermediate compositions to those liquids where alkali feldspar and biotite become liquidus phases. With fractionation of one or both of these phases Ba will decrease in the residual liquid. Very low Ba in felsic igneous rocks is indicative of protracted crystal fractionation in which alkali feldspar and/or biotite have been important.

Such is the case with many recently described alkaline rock suites (e.g. Gill, 1972; Noble et al, 1972; Sceal and Weaver, 1971; Ewart et al, 1968; MacDonald and Edge, 1970; Upton, 1960; Upton, 1964; Abbott, 1968; Ridley, 1970; Bishop and Woolley, 1973). General statements that alkalic rocks are enriched in Ba (see Puchelt, 1972) are misleading when not considered within the context of their origin and evolution. This work, and those referenced above, provide ample confirmation of the carelessness of

such statements.

6.5.1.1. The Undersaturated Suite

Ba decreases progressively with increasing FI from the PCNS (2000 ppm) to the Outer Foyaites (< 2,5 ppm, the detection limit). This regular decrease in Ba and the extreme depletion of this element can only be ascribed to extensive feldspar fractionation and/or biotite fractionation. This confirms the findings of the major element data and also indicates the FI is a good measure of fractionation in an alkaline igneous suite.

K/Ba, as expected increase progressively with FI from 19 to values of about 12,000 (Table 15) although there is considerable variation amongst rocks with high FI due to the very low Ba levels in these rocks.

6.5.1.2. The Oversaturated Suite

Steadily decreasing Ba with increasing FI, is also exhibited in the oversaturated suite. As a group, the Drachenberg syenites are poorer in Ba than the Pomona syenites, for any value of FI. The quartz-feldspar porphyry has anomalous Ba concentration (1010 ppm) compared to rocks of similar FI in the suite.

K/Ba ratios (Tables 16, 17) range from 37 to about 1800 in the high FI specimens. As in the undersaturated rocks the variation of Ba and K/Ba indicate that the evolution of oversaturated suite can be ascribed to protracted alkali feldspar (or biotite) fractionation.

6.5.2. Strontium

The behaviour of Sr is complex. It substitutes for both Ca and K, however, the substitution is not only controlled by the presence of these two major cations but also by their co-ordination in various phases (Taylor, 1965). Thus Sr readily substitutes for Ca in plagioclase but not in pyroxene. Therefore in basic through intermediate liquids Sr decreases with fractionation, but Ca/Sr may vary depending on the proportion of Ca-pyroxene to plagioclase that is removed (Berlin and Henderson, 1968; Korringa and Noble, 1971; Brooke,

1968).

In felsic alkaline liquids Sr is strongly partitioned into the feldspars. D for sodic plagioclase is 3 to 4 (Berlin and Henderson, 1969) and for alkali feldspars is the same (Korringa and Noble, 1971). Sr is also more readily incorporated into these feldspars than Ca (Noble et al 1969; Berlin and Henderson, 1968, 1969) thus with minor pyroxene-amphibole fractionation in these liquids the Ca/Sr ratio increases in the residual liquids. In contrast to Ba, strontium does not enter biotite to any extent.

In coexisting feldspar the nepheline, Sr concentrates in feldspar relative to nepheline, and Rb/Sr and Ca/Sr for nepheline are greater than for alkali feldspar, whereas the reverse applies to the Ba/Sr ratio (Heier, 1966).

Variation in the Ba/Sr ratio with fractionation is discussed by Taylor (1965) and Berlin and Henderson (1969). In liquids where plagioclase is the fractionating feldspar, Ba/Sr will increase in residual liquids, but with precipitation of an alkali feldspar the behaviour becomes more complex. Concentration of Sr relative to Ba has been observed in pegmatites and strongly fractionated granitic rocks (Taylor, 1965; Rhodes, 1969), indicating that Ba/Sr should decrease with fractionation. Heier found Ba/Sr varied from 0,84 to 1,88 for alkali feldspars from nepheline syenites. In the absence of any other major Ba- or Sr-bearing phenocryst (biotite or plagioclase) it appears that Ba/Sr should remain nearly constant possibly decreasing in the late stages.

6.5.2.1. Undersaturated Suite

Sr decreases progressively with increasing FI, whereas Ca/Sr increases. This supports then the evidence of the major elements and the Ba distribution that the suite has evolved through feldspar fractionation.

The Ba/Sr ratio increases from the PCNS ($\sim$ 1,0) to the Inner Foyaite (1,8) then drops in the Outer Foyaite (0,5 to 0,7). This variation could be brought about by variation in Ba/Sr of the fractionating feldspar, or by the fractionation of abundant biotite (high Ba, low Sr) with alkali feldspar in producing the Outer Foyaite. The ratio Ba/Sr (feldspar)/Ba/Sr (nepheline) is about 5 (Heier, 1966), therefore the observed Ba/Sr variation in the suite

indicates that nepheline was never an important fractionating phase.

6.5.2.2. The Oversaturated Suite

Sr decreases progressively with increasing FI in a manner similar to Ba. This depletion of Sr is in keeping with the variation reported in many alkaline suites (Abbot, 1968; Siedner, 1965), and supports a feldspar fractionation model for the development of these suites. Ca/Sr (Table 15) increases with increasing FI to the Hub Syenite (PM127) then decreases in the dyke rocks but shows considerable scatter. This pattern reflects the extreme depletion of Ca in these rocks (see section 6.4.3.) in contrast to Sr. It is notable that PM177 has low Sr, emphasising the anomalous Ba concentration in this rock.

Ba/Sr fluctuates between 1,08 to 1,28 for the Pomona syenites and thereafter increases to values in excess of 5 in the strongly fractionated rocks as predicted by Taylor (1966).

The Drachenberg syenites are notably lower in Sr than the Pomona syenites and this is also reflected in the considerably different Ba/Sr and especially Ca/Sr ratios in comparison to the Pomona syenites (Table 15).

Plots of Ba vs Sr and Ca vs Sr for all the analysed rocks are presented in Figures 24 and 25, and illustrate the different behaviour of these elements in the two suites. Ca and Sr show covariance in the early stages of fractionation (high Ca and high Sr) but in the more fractionated rocks Sr is concentrated relative to Ca in the oversaturated suite, whereas the reverse is observed in the undersaturated suite. This contrasting behaviour in Ca/Sr reflects the contrasting behaviour of Ca in the two suites (see section 6.4.3.).

The marked covariance of Ba and Sr in Figure 24 is typical of strongly fractionated alkaline rock suites (Siedner, 1965). Some divergence is noticeable in highly fractionated rocks where Ba is enriched relative to Sr in the oversaturated suite, whereas the reverse is the case in the undersaturated suite. This implies that in undersaturated peralkaline liquids the ease with which trace elements enter crystallizing alkali feldspar is Ba > Sr > Ca, and in oversaturated liquids the order is Ca > Sr > Ba.

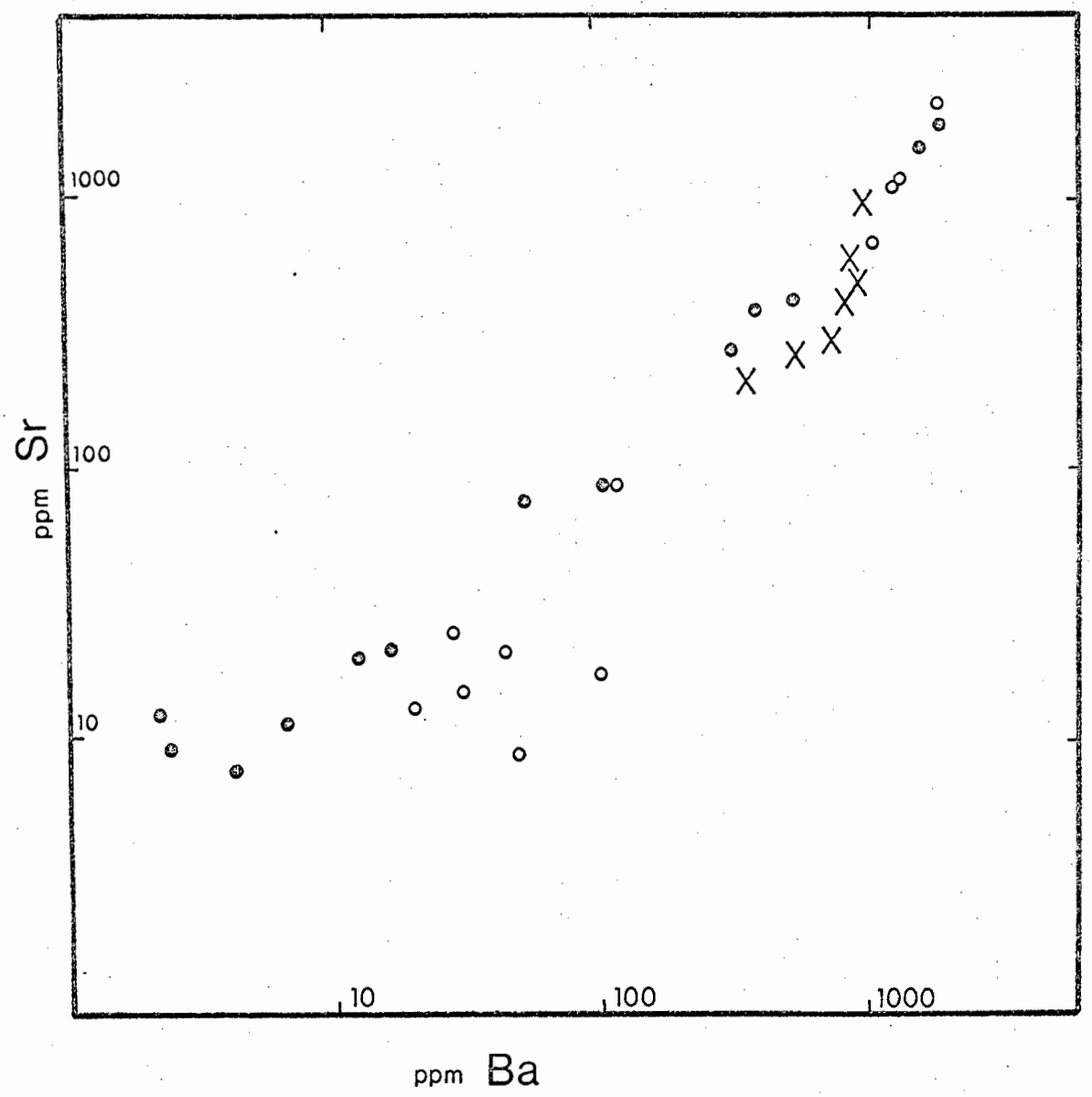

Figure 24. Log plot of Ba vs Sr for all Luderitz Province rocks.

o - Pomona oversaturated rocks

⊙ - Pomona and Granitberg undersaturated rocks

X - Drachenberg syenites

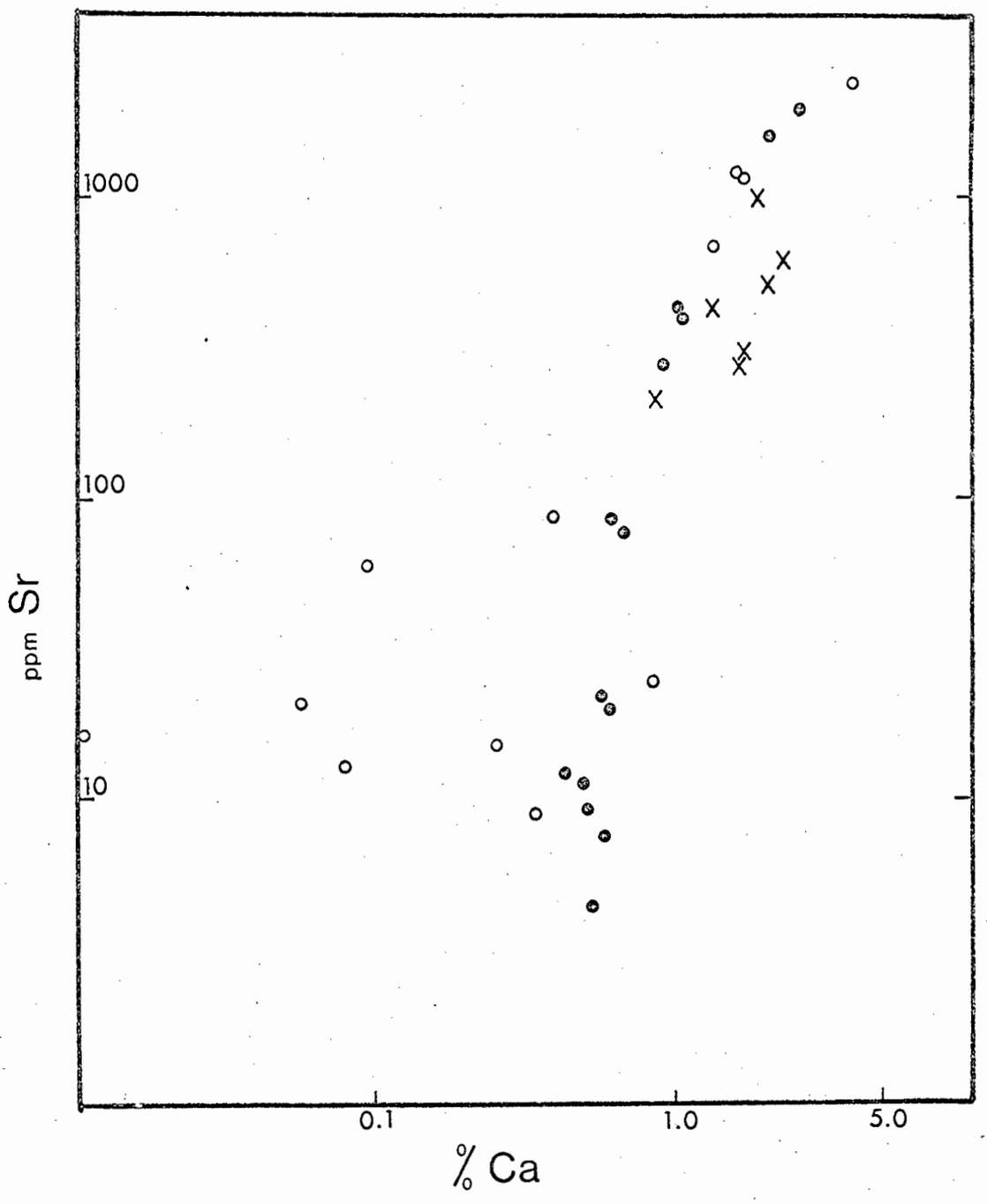

Figure 25. Log plot of ppm Ba vs %Ca for all Luderitz Province rocks. Symbols as in Figure 24.

Noble et al (1969) have emphasized that Sr and Ba are the two most useful elements by which fractionation in a felsic alkaline rock suite can be monitored. The data presented here confirm this emphasis. Furthermore the feldspar fractionation model for the evolution of the two suites which was proposed on consideration of the major elements, is fully supported by the data for Sr and Ba.

The data for the other trace elements can therefore be presented on the basis of this model.

6.5.3. Rubidium

The association of K with Rb, first noted by Ahrens et al (1952), is a well known phenomenon which has received extensive treatment (see reviews of Erlank (1968) and Shaw (1968)). Rb substitutes readily for K in alkali feldspars and biotites, both common minerals in felsic alkaline rocks, therefore distribution coefficient data for these phases are important in describing the behaviour of Rb in alkaline rocks.

Dupuy's (1968) data on ignimbrites indicate that D for sanidines vary from 0,66 to 0,83. D for biotites from the same rocks varies from 1,26 to 1,58. Noble and Hedge (1970) report D = 0,25 to 0,45 for sanidine in silicic lavas. These data indicate that protracted alkali feldspar fractionation would enrich residual liquids in Rb whereas fractionation of notable amounts of biotite could reverse this trend.

K-rich undersaturated volcanics in central Italy have D values for sanidine of 1,03; 1,15; 0,76 (Barbieri et al 1968), thus crystallization of these sanidines could deplete residual liquids in Rb.

K/Rb is a widely used fractionation and genetic indicator in petrology. Data from nature and experiment (see Dupuy, 1968; Barbieri et al 1968; Noble and Hedge, 1970; Phillpotts and Schnetzler 1970; Beswick, 1973; and Goodman 1972) all indicate that K/Rb (phenocryst)/K/Rb (liquid) is greater than unity for alkali feldspar, plagioclase, and clinopyroxene, but less than unity for biotite. Unless extensive fractionation of biotite has occurred successive liquids in a fractionation series should show decreasing K/Rb ratios.

Heier (1966) has reported that Rb enters nepheline more readily than coexisting feldspar and that K/Rb (nepheline) > K/Rb (feldspar).

6.5.3.1. The Undersaturated Suite

Rb behaves in a variable manner increasing from 101 ppm in the PCNS to 200 ppm in the Inner Foyaite, before decreasing in the Outer Foyaite. Apart from GM77, the dyke rocks and the Pomona syenite are enriched in Rb relative to the Outer Foyaite (Figure 22).

Variation of K/Rb with FI is a mirror image of the Rb variation, and K/Rb values are listed in Table 15. The Outer Foyaite therefore shows high K/Rb ratios in relation to the Inner Foyaite and the dyke rocks. The range in Rb and K/Rb is comparable to other undersaturated alkaline suites (e.g. Ilimaussaq - Ferguson, 1970). From a review of published data, undersaturated suites only rarely show K/Rb < 130, though low K/Rb ratios have been reported (e.g. the Vico Volcano, central Italy (Barbieri et al, 1968), phonolite dykes in the Gronnedal-Ika area of S. Greenland (Gill, 1972)). This could well be due to co-fractionation of nepheline whose effect on Rb and K/Rb is opposite to that of feldspar (Heier, 1966). Therefore Rb and K/Rb behaviour in undersaturated rocks appears to contrast to oversaturated suites where extreme Rb enrichment and resulting very low K/Rb ratios (< 100) are commonly reported (see section 6.5.3.2.).

It seems impossible to account for the K/Rb variation in the undersaturated suite. The comparatively high K/Rb ratios of the Outer Foyaites could be due to -

(a) biotite fractionation
(b) nepheline fractionation
(c) the possibility that the Outer Foyaite is a cumulate.

Ba and Sr data do not support (b) and (c) and to a certain extent (a). If biotite fractionation were to be responsible, large quantities are required to be fractionated to offset any feldspar induced trends. The mineralogical and petrographical evidence does not support this.

Also to be considered is any enrichment or depletion by a vapour phase. This does not seem to be a possibility as Beswick (1973) indicates that K/Rb distribution between crystals and vapour is the same as between crystals and

vapour is the same as between crystals and liquid.

6.5.3.2. The Oversaturated Suite

Rb increases sympathetically with FI showing a marked enrichment in high FI rocks. The saturated syenites at Pomona and Drachenberg have similar Rb abundances (100 to 130 ppm) whereas the siliceous syenites and dyke rocks have Rb concentrations of 300 to 800 ppm.

K/Rb decreases irregularly from the saturated syenites (K/Rb 400 to 500) to the siliceous dyke rocks (K/Rb < 200) two of which have very low K/Rb ratios of 50 (GM339) and 77 (DM111). The Biotite-rich Syenite (Drachenberg) and the Biotite-rich Monzonite (Pomona) have lower K/Rb ratios than their associated saturated syenites, due essentially to the abundance of biotite in these rocks. However, their feldspars may also contribute to these low K/Rb ratios, and support the proposal that these rocks are cumulates.

The pattern of high K/Rb in the syenites with an irregular scatter towards very low K/Rb quartz-bearing derivative rocks is typical of many oversaturated alkaline rocks (MacDonald and Edge, 1970; Abbott, 1967; Bowden et al 1962; Siedner, 1965). This pattern is strongly indicative of prolonged feldspar fractionation and therefore supports other chemical data in confirming that this process was the dominant control in the evolution of these rocks.

6.5.4. Gallium

Ga is a trivalent element with a low abundance in terrestrial rocks (generally < 50 ppm) but enriches in highly fractionated granites and nepheline syenites (75 to 100 ppm) (Burton and Culkin, 1972). Thus Ga appears to increase with increasing differentiation.

Ga may exhibit a covariance with both Al and ferric iron due to similarities in size and valency. Generally Ga is held to follow Al more closely than Fe^{3+} (Burton and Culkin, 1972) but Taylor (1965) and Goodman (1972) have suggested that Ga displays a closer coherence to Fe^{3+}, especially in six-fold co-ordinated sites.

Ga therefore enters feldspars, micas, magnetite and alkali clinopyroxene to much the same extent though micas and magnetite appear likely to concentrate Ga more than the other phases (Burton and Culkin, 1972). Goodman (1972) has determined D values for Ga in different phases in basic lavas. D for plagioclase ranges from 0,85 to 1,27 and increases in more sodic plagioclase. All other phases showed $D < 1,0$. Ga/Al ratios in plagioclase are always less than in the coexisting groundmass, but the reverse applies to olivine and pyroxene (Goodman 1972).

The behaviour of Ga and Ga/Al in felsic alkaline rocks can only be indicated by the extrapolation of Goodman's (1972) data. Extensive feldspar fractionation increase Ga/Al in the residual liquid. The effects of mafic minerals are largely unknown but it appears that magnetite, with very high Ga/Al ratios, is likely to counteract any feldspar induced trends.

6.5.4.1. The Undersaturated Suite

Ga is not notably enriched in these rocks varying from 20 to 35,5 ppm. In contrast Ferguson (1970) reports high Ga values (40 to 100 ppm) for the Ilimaussaq foyaites. The distribution of Ga in the FI variation diagrams is identical to Rb, being relatively depleted in the Outer Foyaites compared to the dyke rocks and the Inner Foyaite (Figure 22).

A plot of Ga vs Al (Figure 26) shows no coherence between these elements, and ignoring the Outer Foyaites, Ga/Al increases with increasing FI (Table 15). A plot of Ga vs Fe^{3+} also shows a similar lack of coherence (Figure 27) and Ga/Fe^{3+} increases with increasing FI (Table 15).

In the light of the poor knowledge of Ga in crystallizing alkaline liquids the trends illustrated above are difficult to interpret in terms of crystal fractionation.

6.5.4.2. The Oversaturated Suite

The distribution of Ga in the FI plots (Figure 23) is almost identical to Rb. Ga increases steadily with increasing FI but shows a wide scatter in high FI rocks (dyke rocks). The Drachenberg syenites are slightly enriched in Ga relative to the Pomona syenites.

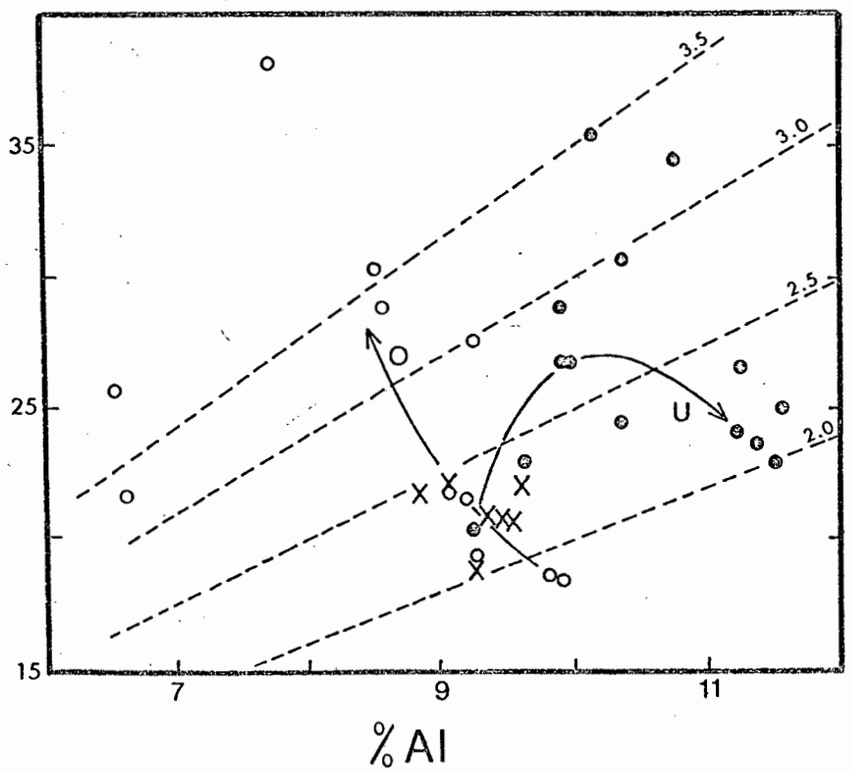

Figure 26. Plot of ppmGa vs %Al for all Luderitz Province rocks. Symbols as in Figure 24.

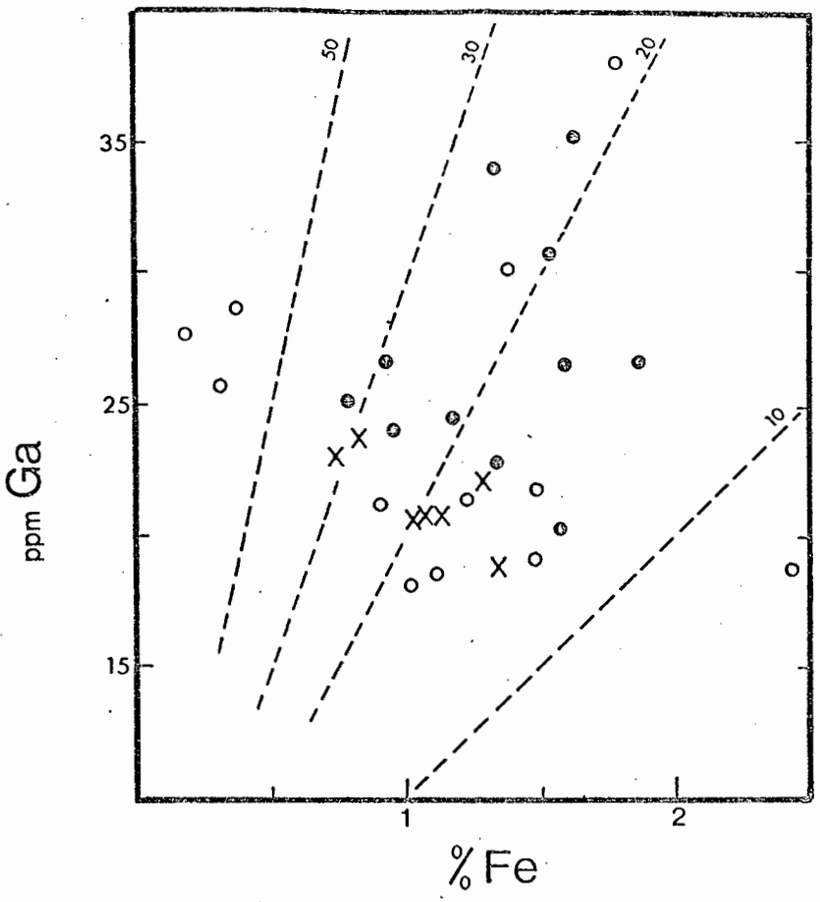

Figure 27. Plot of ppmGa vs $\%Fe^{+++}$ for all Luderitz Province rocks. Symbols as in Figure 24

The Ga/Al ratios increase progressively with increasing FI (Table 16, 17). A plot of Ga vs Al (Figure 26) shows no coherence between these two elements, in fact the correlation is negative. A Ga vs Fe^{3+} plot shows no coherence and Ga/Fe^{3+} ratio varies considerably with FI (Tables 16, 17).

If the extrapolations from Goodman's (1972) data are correct then the increasing Ga/Al ratios indicate fractionation dominated by alkali feldspar, confirming the interpretation of the major element and other trace element data.

6.5.5. Zirconium

Zr increases with fractionation especially in alkaline rock series (Chao and Fleischer, 1960). This feature, and the very high concentrations of Zr in alkaline felsic rocks, is a commonly reported phenomenon (MacDonald and Parker, 1969; Ferguson, 1970; Gill, 1972; Weaver, et al, 1972; Siedner 1965; Upton, 1960; Bowden 1966; Butler and Smith, 1962). This reflects the high solubility of Zr in peralkaline liquids, for which there is experimental evidence (Dietrich, 1968), and petrographic evidence (eudialyte and less frequently zircon are typical late crystallizing interstitial minerals in the Granitberg and Pomona nepheline syenites, tinguaites and syenites).

Zr does not commonly substitute for other common ions but is known to replace Ti in early Fe-Ti oxides as well as entering pyroxene and apatite (Taylor, 1965; Arrhenius et al 1971). In alkaline rocks high Zr has been reported from Na-pyroxenes and arfvedsonite (Vlasov et al 1966).

6.5.5.1. The Undersaturated Suite

Zr is abundant in these rocks and has similar pattern of variation as Rb and Ga, i.e. it is relatively depleted in the Outer Foyaites. Despite this, Zr increases with increasing FI. The Zr abundances in the various rock units can be directly attributed to the presence or absence of Zr-minerals. Thus Zr-minerals are absent in the PCNS and only rarely present in the Outer Foyaite. In contrast the other rocks contain notable amounts of zircon and/or eudialyte-eucolite.

It does not seem possible to account for the Zr distribution without postulating fractionation of either zircon (eudialyte is always a late crystallizing mineral) or Zr-rich mafic mineral during the middle stages of the development of the undersaturated suite.

6.5.5.2. The Oversaturated Suite

Zr does not show the enrichment expected of a peralkaline silicic suite (see above). Zr increases slightly with increasing FI, but is strongly depleted in some of the dyke rocks, only GM339 (2990 ppm) showing notable enrichment (Figure 23).

The only explanation of the Zr distribution pattern is that Zr was removed by fractionation of zircon or Zr-rich mafic minerals. With respect to this suggestion the occurrence of large euhedral zircons in the Hub and Inner Syenites, and the presence of microphenocrysts of zircon in a bostonite at Drachenberg, is perhaps significant.

6.5.6. Niobium

Nb substitutes for Ti and Zr in igneous minerals, but has a tendency to form large complexes with oxygen in the liquid and therefore enriches in residual liquids with fractionation (Taylor, 1965).

Nb therefore shows a coherence with both Ti and Zr although it tends to enrich relative to these elements in residual liquids. Nb is found in Ti-minerals (Fe-Ti oxides, sphene, perovskite) and Zr-minerals. There is no distribution coefficient data for Nb, and the variation of Nb can only be treated qualitatively. Theory predicts that Ti/Nb and Zr/Nb should decrease with increasing fractionation (Taylor, 1965).

6.5.6.1. The Undersaturated Suite

Nb has a similar distribution to Zr, being relatively depleted in the Outer Foyaite in contrast to the dyke rocks and the Pomona foyaite. Therefore, in general, Nb increases with increasing FI (Figure 22).

Zr/Nb has a complex behaviour (Table 15). Nb is enriched relative to Zr in the Outer Foyaite and the Pomona Foyaite but the reverse applies to the tinguaite dykes. The PCNS and Inner Foyaite have Zr/Nb ratios intermediate between these two.

Ti/Nb (Table 15) generally decreases with increasing FI but again the Outer Foyaites are anomalous to this trend.

In general these trends are similar to those shown by other alkaline suites. At Ilimaussaq (Ferguson, 1970) Nb and Zr/Nb increase with differentiation but Ti/Nb decreases. This antipathetic variation of Zr/Nb and Ti/Nb is in part also displayed by the Luderitz Province undersaturated rocks. Perhaps under conditions of extreme fractionation in peralkaline liquids, Zr enrichment relative to Nb operates in contradiction to theoretical predictions.

6.5.6.2. The Oversaturated Suite

Nb increases with increasing FI in this suite (Figure 23) whereas Ti/Nb decreases progressively in both the Pomona dnd Drachenberg syenites (Table 16, 17).

Zr/Nb has a more complex behaviour. It remains fairly constant in the Drachenberg syenites (Table 16, 17) but in the Pomona syenites it increases slightly with increasing FI. The oversaturated dyke rocks have very low ratios in keeping with the low Zr in these rocks (Table 16, 17).

The behaviour of Nb is similar to that recorded for other alkaline-peralkaline silicic suites (MacDonald and Edge, 1970; Weaver, Sceal and Gibson, 1972; Cox et al, 1970). The Zr/Nb variation is not entirely similar to that in other peralkaline suites. At Mayor Island, New Zealand (Ewart et al, 1968) Zr/Nb is nearly constant but high at 16 to 18 in the pantellerites. Butler and Smith (1962) record Zr/Nb of 5,4 to 6,0 for the Pantelleria pantellerites. Weaver et al (1972) show that the coherence between Nb and Zr for trachytes and pantellerites from a number of Rift Valley volcanoes is near perfect. Furthermore, lavas from each volcano have a unique Zr/Nb ratio with no indication of fluctuation with fractionation.

For the Tugtutoq dykes (MacDonald and Edge, 1970; MacDonald and Parker, 1970) Zr/Nb increases with fractionation from 5 to 10, contrary to theoretical predictions. In contrast Ti/Nb varies considerably but generally decreases

with fractionation. The antipathetic variation of these two ratios is similar to that noted by Ferguson (1970) for the undersaturated Ilimaussaq rocks.

It does not seem possible to account for the behaviour of Nb, Ti/Nb and Zr/Nb in the Luderitz Province rocks. The data reviewed here suggests that factors governing Nb and Zr behaviour in melts breakdown in peralkaline liquids. It has been shown that Zr/Nb ratios may remain constant (Rift Valley volcanoes), increase with fractionation (Ilimaussaq, Tugtutoq) or decrease with fractionation (this work). No general rules regarding Zr/Nb behaviour in peralkaline melts can therefore be made.

6.5.7. Thorium

Th is generally present in terrestrial rocks in amounts < 30 ppm and in all igneous rock series it increases with differentiation (Rogers and Adams, 1969). Of the common igneous minerals, Th is noticeably concentrated in apatite, sphene, zircon, Fe-Ti oxides as well as biotite and hornblende. Th variation in any igneous rock series is therefore probably controlled by mafic mineral fractionation.

No distribution coefficient data are available for Th, in fact the location of Th in rock-forming minerals is uncertain. It is possible that in some minerals it does not fill lattice sites but occures interstitially or in submicroscopic defects (Rogers and Adams, 1969).

6.5.7.1. The Undersaturated Suite

The Th distribution has a pattern similar to the Zr distribution in these rocks (Figure 22). Th increases with increasing FI but is depleted in the Outer Foyaite. Compared to the data collected in Rogers and Adams (1969) some of the undersaturated rock have abnormally high Th (> 30 ppm), but Gill (1972) reported 50 ppm Th in the Grønnedal-Ika phonolites so the values reported here may be quite normal for peralkaline undersaturated rocks.

Zr/Th decreases with FI (Table 15) with the two Pomona specimens having very low values for the ratio. There is no regular variation of the K/Th ratio.

Since the distribution of Zr and Th is similar, the Th distribution is probably controlled by fractionation of Zr-bearing minerals. However, the data does not allow any certain predictions to be made.

6.5.7.2. The Oversaturated Suite

Th increases with increasing FI and the siliceous dyke rocks all have 60 ppm Th. The White Mountain Magma series contains up to 50 ppm and more Th and is considered by Rogers and Adams (1969) to be high. On this scale the oversaturated dyke rocks are abnormally enriched in Th. However, data on Th for similar rock suites are few in the literature and it is uncertain whether such enrichment is common or not.

Zr/Th decreases with increasing FI (Table 16, 17) and ratios for the dyke rocks are very low due to the Zr depletion in these rocks. K/Th (Table 16, 17) decreases regularly with increasing FI in the Pomona syenites, being lowest in the dykes. In the Drachenberg syenites K/Th varies considerably.

It is noticeable that the distribution pattern for Th is unlike that for Zr in the oversaturated suite, in contrast to the undersaturated rocks. If the Zr deficiency in the dykes is ascribed to fractionation of zircon, then it would seem that Th does not substitute for Zr in zircon, or perhaps in any other mineral.

6.5.8. Lead

Pb may substitute for both K and Ca in common silicate minerals (feldspars, apatite, micas, plagioclase). However, Pb is concentrated in residual liquids due to marked covalency of the Pb-O bond in comparison to Ca-O and K-O bonds (Taylor, 1965).

Pb^{++} and Sr^{++} are nearly identical in size and should show a strong coherence, but Sr enters K and Ca sites more readily than Pb thus Pb/Sr ratio increases with fractionation.

Wedepohl (1956) has shown that Pb concentrates in micas (up to 70 ppm), alkali feldspar (up to 80 ppm), Fe-Ti oxides (10 to 40 ppm), and plagioclase (< 15 ppm) in that order. However, no distribution coefficients are

available, and Pb abundances in a rock series cannot be evaluated quantitively.

6.5.8.1. The Undersaturated Suite

Pb has a distribution pattern similar to Th, Ga, Zr, Nb, and Rb in this suite, i.e. increases with increasing FI but is relatively depleted in the Outer Foyaites. The Pb/Sr ratio increases with increasing FI (Table 15) although there is some variation especially in the dyke rocks. Despite their depletion in Pb the Outer Foyaites have high Pb/Sr ratios - this ratio is therefore a better indicator of fractionation than Pb abundances alone.

There is little comparable data in the literature. In a trachyte-phonolite suite from Ua Pu, Marquesas Islands (Bishop and Woolley, 1973) Pb/Sr increases from 1,1 in the trachytes to 25,0 in the phonolites. The diagrams of Gill (1972) indicate that Pb/Sr also increases with fractionation in a suite of phonolite dykes. Both these reports confirm the date presented here.

6.5.8.2. The Oversaturated Suite

Pb shows an irregular variation in the syenites and is relatively depleted in the dyke rocks (Figure 23). Pb/Sr increases with increasing FI (Table 16, 17) as is predicted by theory.

Comparison with other oversaturated suites indicates that at Paresis (Sidner 1965) and in the dykes from the Tugtutoq region (MacDonald and Edge, 1970) Pb increases regularly with increasing fractionation and no depletion occurs in the highly fractionated rocks. Calculation of Pb/Sr from the data given by these authors shows that this ratio increases with increasing fractionation as reported here.

6.5.9. Yttrium

Y has a variable and complex behaviour in evolving magmatic rocks, but no distribution coefficient data are available so its behaviour is difficult to interpret. Data quoted by Hermann (1970) indicate that Y is enriched in alkaline rocks compared to basalts, but not necessarily so compared to 'normal'

granites. In an intrusive sequence in alkaline rock complexes, Y tends to enrich with fractionation but may be quite variable and no general rule applies.

Y concentrations in co-existing alkali feldspar and arfvedsonite in a syenite, quoted by Hermann (1970) show that arfvedsonite (170 ppm) holds 10 times more Y than the feldspar. Towell et al (1965) found that the abundance of Y in various minerals in granitic rocks of the Southern California batholith is biotite $\gg$ plagioclase $>$ K-feldspar. For a gabbro the same authors find apatite $\gg$ hornblende $>$ augite $\gg$ plagioclase. This evidence suggests that Y is strongly concentrated in mafic minerals.

6.5.9.1. The Undersaturated Suite

Y abundances are listed in order of increasing FI in Table 15 and are variable with respect to increasing fractionation. Generally Y has a similar distribution pattern to Ga, Rb, Th, Zr etc. in this suite - enriching in the Inner Foyaite and some of the dyke rocks but is relatively depleted in the Outer Foyaite. Other undersaturated alkaline rock suites have similar abundances of Y, except for the Lovozero massif which is enriched in Y (Vlasov et al, 1965).

The fairly constant values of Y and its slight enrichment with fractionation indicate that mafic minerals did not dominate the evolutionary path of these nepheline syenites.

6.5.9.2. The Oversaturated Suite

Y abundances (Table 16, 17) are similar to the undersaturated suite with no regular variation with fractionation. The Drachenberg syenites have slightly higher Y than similar syenites from Pomona. The behaviour of Y in the Luderitz Province silicic rocks contrasts with the much higher concentration, and marked increase of Y with fractionation reported by MacDonald and Edge (1970) for the Tugtutoq dykes.

6.6. COMPARISON BETWEEN THE POMONA AND DRACHENBERG SYENITES

In the preceeding account the Pomona and Drachenberg syenites have been discussed together with the implication that they are consanguineous. Here I point out a few differences between the two complexes.

On major element chemistry there appears to be no difference between the syenites from each complex, but in the discussion on feldspar fractionation, the metaluminous nature of the late differentiates from Drachenberg was noted, in contrast to the peralkaline nature of similar rocks from Pomona.

At this stage all indications are that the syenites from both complexes could have been derived from the same parent (trachytic, or one of more basic character), but that they evolved by slightly different fractionation processes.

On considering trace elements, differences are more marked. The Drachenberg rocks have distinctly lower Sr and Ba and slightly higher Ga. For similar values of FI the ratios Ba/Sr, Ca/Sr, K/Ba are also different. Despite the characterization of FI, the Drachenberg syenites appear to be more "fractionated" than the equivalent Pomona syenites. Yet this is hardly reflected in K/Rb, where, if anything, the Drachenberg rocks have higher K/Rb than the Pomona equivalents.

This indicates that the Pomona and Drachenberg syenites have no immediate common parent. If the syenites are considered part of an alkali basalt - trachyte - rhyolite liquid line of descent, the differences indicated above may not even be resolved to a common alkali basalt parent. Abbott (1967) and Kable (1972), have shown that in a large number of continental and oceanic alkaline suites, K/Rb, K/Ba and other ratios of the "residual" elements, remain remarkably constant during the evolution of the basalt-trachyte spectrum, and only show differentiation with the development of more siliceous, or nepheline-bearing rocks from the trachytes. Therefore it is possible that the element ratios of the syenites reflect the value of these ratios in their basaltic parents.

6.7. COMPARISON BETWEEN THE POMONA AND GRANITBERG UNDERSATURATED ROCKS

Although all the nepheline-bearing rocks have been discussed as a single suite this does not imply that they are of the same evolutionary trend. In this respect it would be worthwhile to compare the undersaturated rocks at Pomona and

Granitberg. However, the outcrop area of nepheline syenites and tinguaites at Pomona is small, and enough samples were not collected to justify a full-scale comparison.

In general the Pomona nepheline syenite, although a coarse grained rock, has a similar chemistry to the tinguaite dyke rocks. Although it contains far less normative nepheline than the Granitberg Outer Foyaites it is chemically more "fractionated" and several of the differences have been noted in the preceding account. With the evidence available suggestions as to the possible different origins of the Pomona and Granitberg rocks would be speculation.

6.8. COMPARISON BETWEEN THE UNDERSATURATED AND OVERSATURATED SUITES

It is important to compare the chemistry of the oversaturated and the undersaturated suites in order to test suggestions that they may arise from a common "trachytic" parent. It has already been established that it is unlikely that the Pomona and Drachenberg syenitic rocks are related to an immediate common parent. In this section the possible relationship of the Granitberg foyaites to the syenites of these two complexes is discussed.

To facilitate comparison, the variation of major and trace elements with FI for the oversaturated suite, is indicated by a field enclosed by a dashed line on the FI vs OXIDE and FI vs ELEMENT plots (Figure 18, 22) for the undersaturated rocks. Where the Pomona and Drachenberg rocks show different trends (e.g. Sr) the field for each complex is delineated.

Only the fields for the saturated syenites are indicated; (a) to avoid confusion on the diagrams, and (b) because these are the rocks important to the problem of consanguinity.

6.8.1. Points of difference

FI is a sensitive measure of the ratio of felsic/mafic minerals in a rock which does not crystallise acmite. In the initial members of the undersaturated trend (PCNS specimens GM128, GM146) with 10 to 17% normative ne, mafic minerals are more abundant than in the syenites, which have less than 1% normative quartz.

If the nepheline syenites were generated by fractionation from a trachyte (syenite) parent then that parent must have been unusually rich in mafic minerals and would be quite unlike any of the syenites (in mineralogy and chemistry) observed at Drachenberg or Pomona.

Thus although the syenites and the initial members of the undersaturated trend have similar FI's they are not strictly comparable. In terms of the trachyte parent model which is being tested, the PCNS specimens are far more "fractionated" than the syenites (since they have developed a considerable amount of nepheline), assuming that fractionation in the trachyte-rhyolite and trachyte-phonolite spectra are of equal efficiency. Indeed, Gill (1972) found normative nepheline a better index of fractionation than FI.

6.8.2. Major elements

Apart from the obvious SiO_2 difference the undersaturated suite is enriched in Na_2O, MgO, $Na_2 + K_2O$ and depleted in K_2O. The differences in the alkalies may not be significant, but the difference in Mg is, especially when the 'real' position of the PCNS in the fractionation scheme is taken into account. If the PCNS is derived by fractionation from the syenites, then the nature of the fractionation must have been one of Mg enrichment. This is possible by early removal of Fe in iron bearing minerals, e.g. magnetite, which requires a high fO_2 environment. Since it has already been pointed out that the PCNS is more abundant in mafic minerals than the syenites, marked fractionation of Fe mafic minerals is untenable. It seems unlikely then that the PCNS are derived from any of the Pomona or Drachenberg syenites.

6.8.3. Trace elements

The syenites have lower Nb, Zr, Ga, Rb, but similar Pb and Th, when compared with the PCNS. Since the abundance of these elements increases with fractionation, consideration of the position of the PCNS relative to the syenites in terms of normative nepheline, reveals little real difference in the amount of these elements in the two rock types.

Ba and Sr in the PCNS is much higher than in both the Drachenberg and the Pomona syenites and this difference is aggravated when comparison is made on the "normative nepheline" basis. Since the studies here and elsewhere (see the discussion on these two elements) report the progressive decrease in Ba and Sr with fractionation in trachyte-phonolite and trachyte-rhyolite suites, the high Ba and Sr in the PCNS cannot be reconciled with the derivation of the latter from the syenites.

The compositions of the rocks from all 3 complexes are plotted in the two conventional KNC and FMA triangular diagrams, Figures 28 and 29. It is clear that each complex has a unique fractionation path although there is considerable convergence in the highly fractionated rocks in the FMA diagram. Altogether, these diagrams support the features evident in the FI plots and the Bailey-MacDonald diagram, and re-emphasise the points discussed above.

6.9. SUMMARY

Each complex in the Luderitz Province has developed independently, and their syenites cannot be related to any common parent presently exposed in the Province. Successive rock types in each complex have evolved through crystal fractionation dominated by alkali feldspar, and supported by minor amounts of mafic mineral fractionation. The chemistry of the dyke rocks, particularly in the oversaturated suites, suggests that their development through crystal fractionation has been modified by vapour phase action during crystallization.

The chemical and petrographic features of the undersaturated suite are analogous to a typical trachybasanite - phonolite evolutionary trend (Coombs and Wilkinson, 1969; Ridley, 1970; Turner and Verhoogen, 1960). The oversaturated suites at Pomona and Drachenberg, although not consanguineous, are similar to typical saturated trachyte - alkali rhyolite suites (e.g. Abbott, 1969; Turner and Verhoogen, 1960).

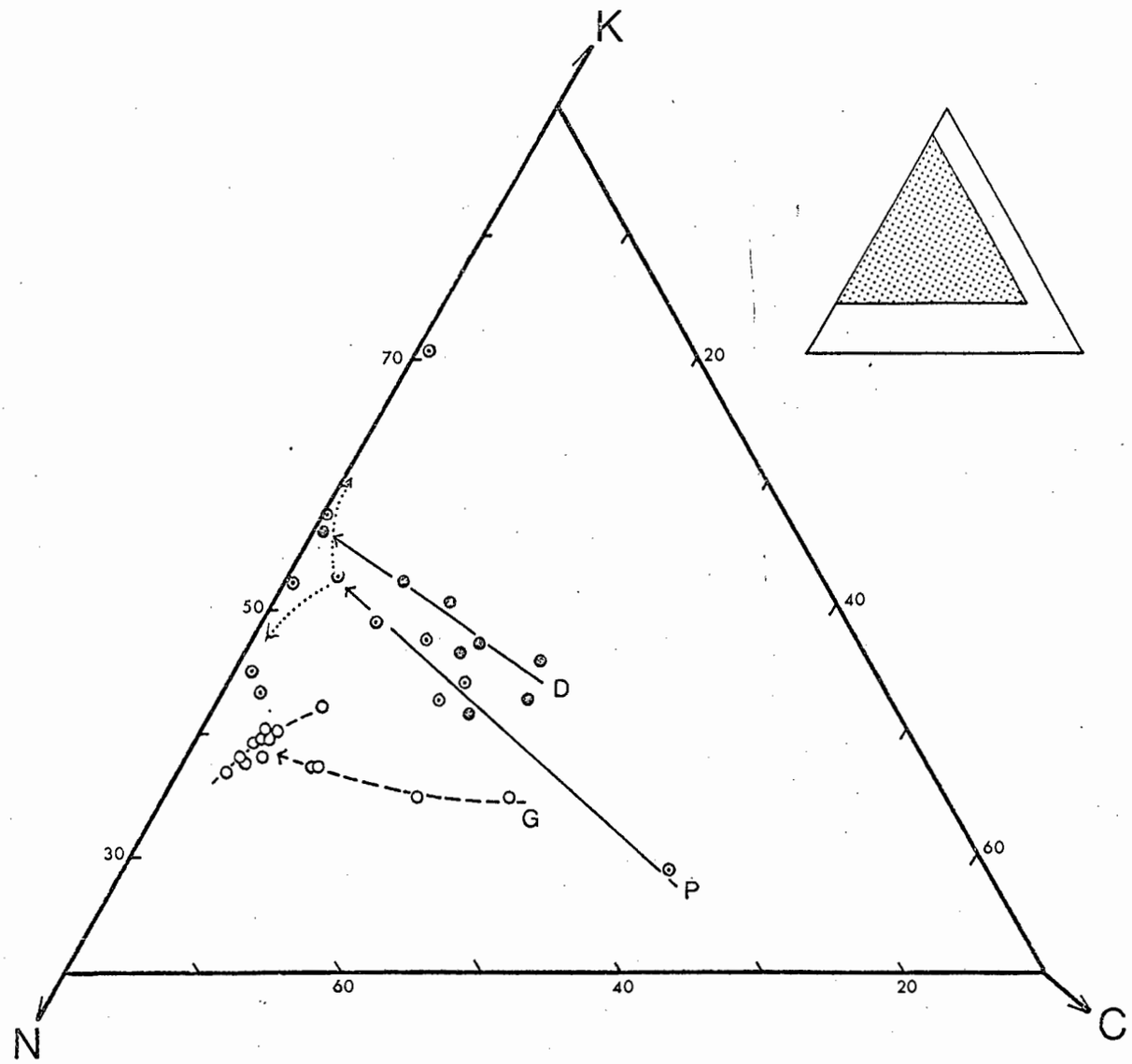

Figure 28. KNC diagram for all Luderitz Province rocks.

o , G - Granitberg and Pomona undersaturated rocks

⊙ , P - Pomona oversaturated rocks

● , D - Drachenberg oversaturated rocks.

Figure 29. FMA diagram for all Luderitz Province rocks. Symbols as in Figure 28.

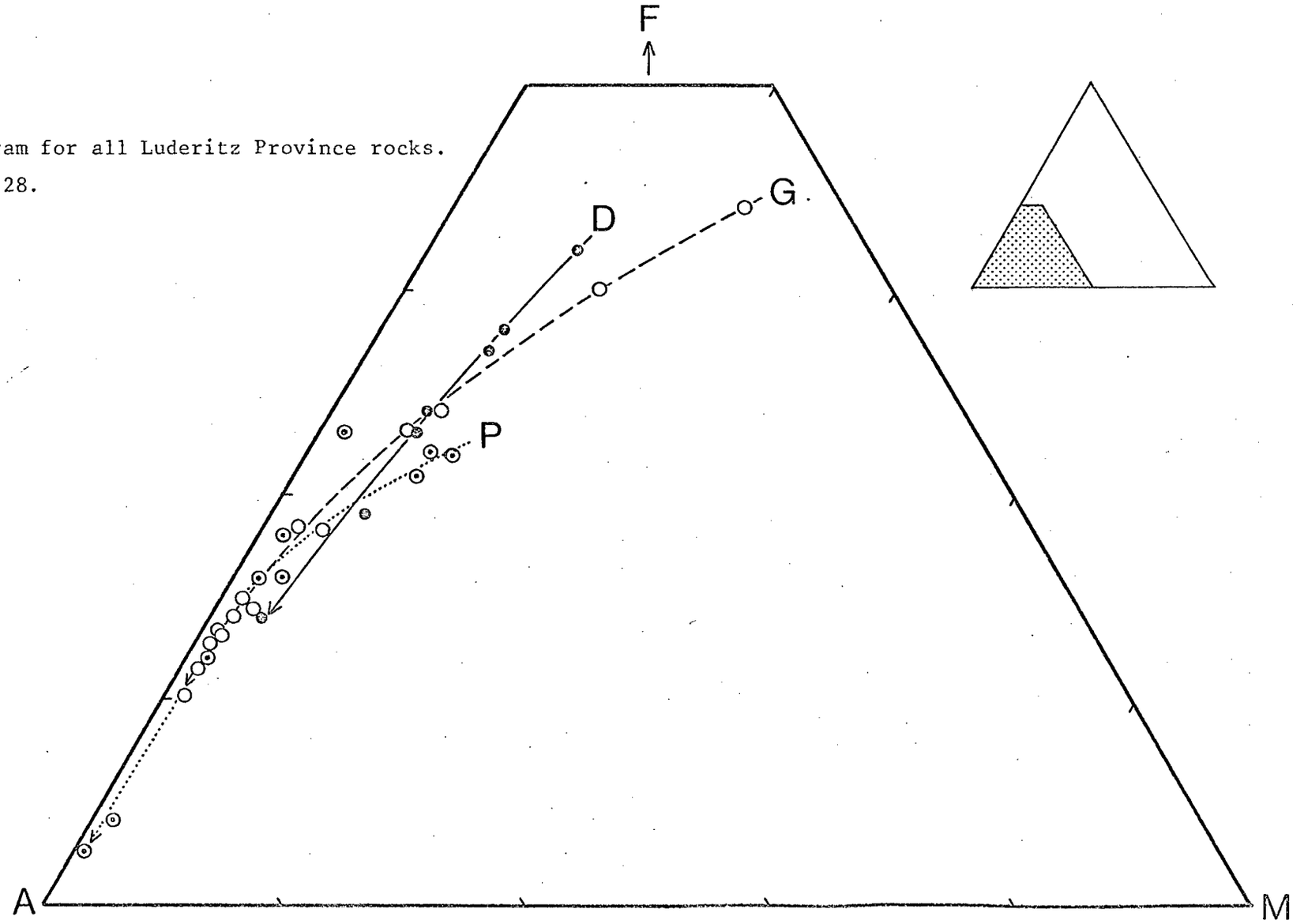

CHAPTER 7

THE MINERALOGY OF THE ALKALINE ROCKS

A microprobe has been used to analyze the mafic minerals and nepheline in carefully selected samples from the undersaturated suite at Granitberg, and the oversaturated suite at Pomona. Since the mineralogy of these two suites is similar, it is interesting to compare the composition of the minerals crystallizing in contrasted peralkaline environments. In addition the analyses may be used together with thermochemical data to estimate important intensive parameters of crystallization - P, T, fO_2, fH_2O, etc.

The microprobe analytical procedures are summarised in the Appendix.

7.1. MAFIC MINERAL REACTION SERIES

The mafic mineralogy of the principal members of the undersaturated suite (Granitberg), and the oversaturated suite (Pomona), is summarised in Figures 30 and 31, the main features of which are discussed below.

7.1.1. The Undersaturated Suite

Biotite and clinopyroxene are present at all stages of the development of the suite. Amphibole is noticeably absent, but has appeared in trace amounts in the early stages of crystallization of the Inner Foyaite, and late in the crystallization of the marginal zone of the Outer Foyaite.

Perovskite is unusual in its appearance in the Inner Foyaite, and to the writer's knowledge, there is no record in the literature of perovskite crystallizing in mildly undersaturated nepheline syenite in apparent equilibrium with alkali feldspar. The perovskite appears to have developed at the expense of Ti-magnetite and sphene.

A marked diversification in what is essentially a simple mineralogy appears in the marginal zone of the Outer Foyaite, where aenigmatite crystallizes at the expense of an Fe-Ti oxide, along with astrophyllite, lavenite, arfvedsonite, and eudialyte-eucolite. The relationship between aenigmatite and astrophyllite is similar to the relationship between aegirine and arfvedsonite.

Figure 30.

Mafic mineral reaction series, Granitberg foyaites.

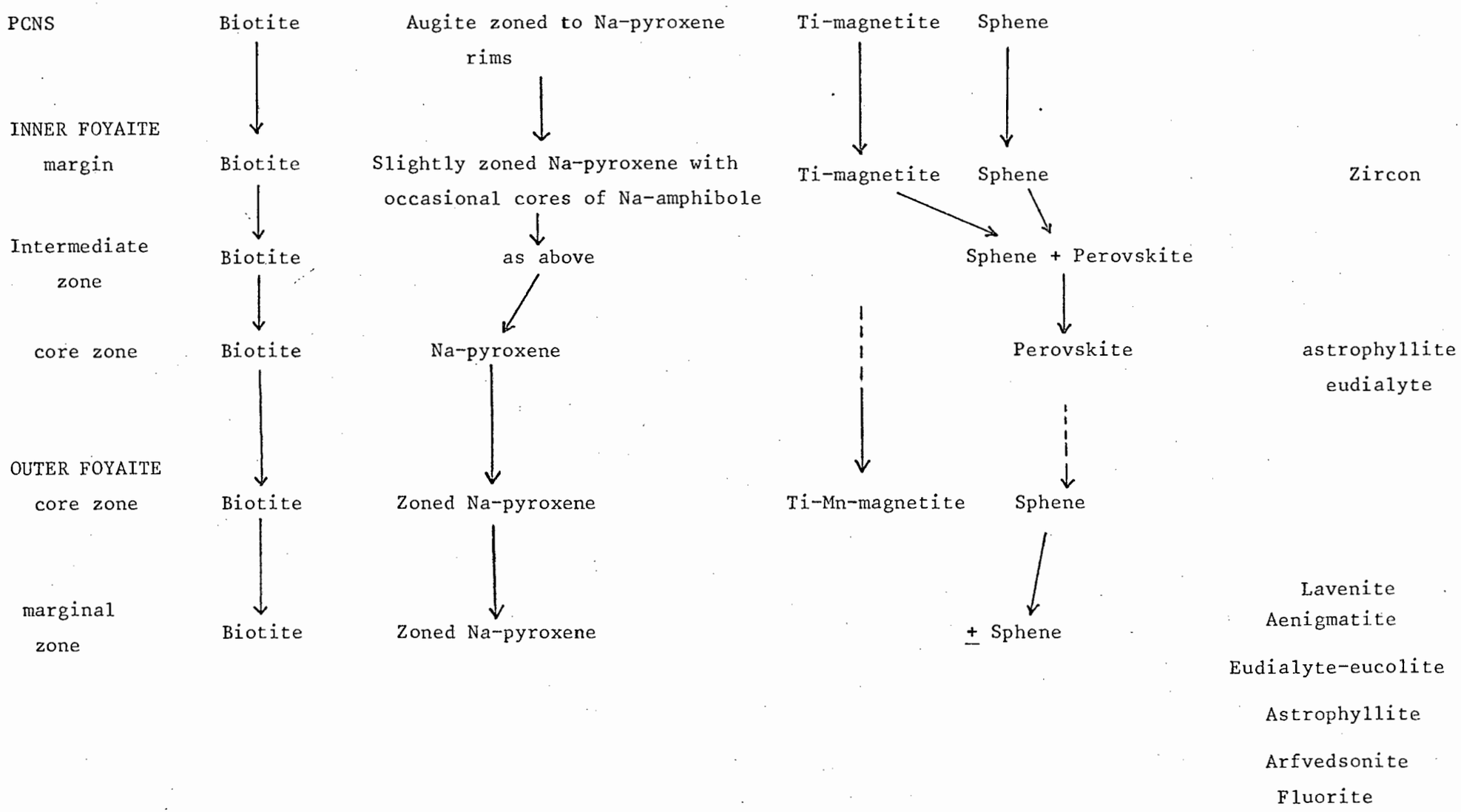

Figure 31.

Mafic Mineral reaction series, Pomona Syenites.

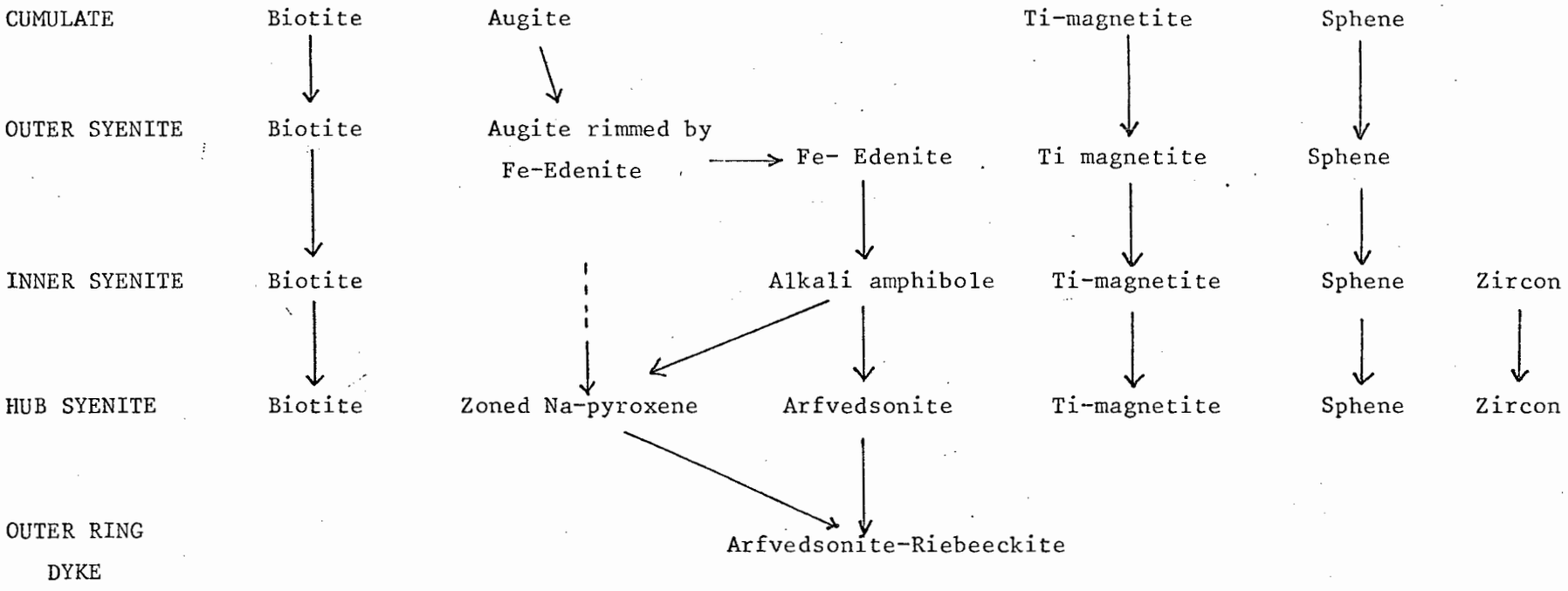

The mineralogy of the undersaturated rocks is typical of miaskitic nepheline syenites, except for the core zone of the Inner Foyaite, and the marginal zone of the Outer Foyaite which have distinct agpaitic affinities (Sorensen, 1960).

7.1.2. The Oversaturated Suite

Biotite is a constant member of all stages in the fractionation scheme, except in the nordmarkite Ring Dyke. Amphibole is important in all rocks other than the cumulate, and is the only mineral in the Ring Dyke. Pyroxene, as augite, appears early, but in the middle stages is replaced by amphibole. It reappears in the Hub Syenite as Na-pyroxene.

Ti-magnetite and sphene are also always present, except in the Ring Dyke. Zircon is abundant in the Inner and Hub Syenites.

7.1.3. Comparison between the Over- and Undersaturated Suites

The most obvious contrasting feature in the two suites is the importance of amphibole in the oversaturated trend, compared to its almost total absence in the undersaturated suite. This appears to be a common phenomenon in peralkaline rocks. In the writer's experience, although alkali amphibole may accompany Na-pyroxene in undersaturated alkaline rocks, it is seldom, if ever, present to the exclusion of alkali pyroxenes. Yet the converse is common in the oversaturated alkaline rocks. If this observation is general, it is difficult to explain. Alkali amphibole crystallizes from melts which precipitate aegirine only under low fO_2 conditions, yet silicic alkaline rocks crystallize at higher fO_2 than do undersaturated liquids (Nash et al, 1969; this work section 8.4.). However if high fO_2 indicates high fH_2O, then the persistence of anhydrous mafic phases in the relatively dry undersaturated liquids is to be expected.

The other feature is the extreme diversification in mineralogy commonly reported in alkaline undersaturated rocks, in contrast to the relatively simple mineralogies of oversaturated peralkaline rocks. Vlasov et al (1966) reports over 130 mineral species and varieties in the Lovozero massif, and similar complex mineralogies are seen in the peralkaline undersaturated intrusions of the Gardar province, S. Greenland (Sorensen, 1960).

It is doubtful whether these differences are due to the undersaturated rocks being more 'fractionated' than their oversaturated counterparts. More likely, the undersaturated environment provides optimum conditions for the stabilization of Zr, Ti, and Nb complexes in the melt, and subsequent crystallization of these elements in a variety of minerals. At Lovozero Zr, Ti, and Nb are major constituents of 37 different minerals (Vlasov et al, 1966).

7.2. BIOTITE

Analyses of biotites are presented in Tables 18, 19. Since no OH or halogen (F, Cl) has been determined the totals of the analyses are low. The formulae are based on a cell of 22 oxygen atoms, and the composition of the biotites, calculated from the octahedrally co-ordinated cations, are expressed in terms of mole % of four compositional end-members - annite, phlogopite, manganophyllite and Ti-biotite. The composition of the biotites in terms of these end-members is illustrated in Figure 32.

The composition of individual biotite grains is remarkably constant over the whole grain area. During analysis slight zoning of Ti, Mn and to a lesser extent Fe and Mg was noted in some grains.

The biotites from both suites are all Al-poor and some Ti has been assigned to the tetrahedral sites with Si and Al. Despite this, the biotites are all peraluminous, in that they contain excess Al over Na + K + Ca, a feature which seems to be common with many analyzed biotites (Deer et al, 1962). Fractionation of biotite can therefore enhance any peralkaline trend, or even generate it, as has been noted by Carmichael (1967). Furthermore this data supports that of Carmichael (1967) in indicating that peraluminous biotites readily crystallize in peralkaline environments.

Ca is not present in biotites to any extent, a feature which is emerging with more microprobe analyses of biotites, and suggests that the Ca recorded in most analyses of bulk separates is due to contamination by apatite inclusions (Mitchell, 1972; Carmichael, 1967).

Mn is especially high in some of the biotites from the Luderitz Province rocks studied here. Weight % MnO ranges from 0,54 to 2,07 in the oversaturated syenites, and from 0,99 to 3,78 in the nepheline syenites. This is far higher than any of the igneous biotites listed in Deer et al (1962), but Nash and

TABLE 18

Microprobe analyses of biotites from nepheline syenites, Granitberg.

	GM146	GM146	GM350	GM350	GM147	GM147	GM137
SiO_2	35,00	34,85	35,15	36,02	34,03	34,46	34,36
TiO_2	3,29	3,10	3,56	3,52	3,88	3,78	3,93
Al_2O_3	13,28	13,60	10,35	10,01	11,91	12,35	12,11
FeO*	25,27	25,12	28,76	27,86	31,36	31,13	31,80
MnO	1,01	0,99	3,60	3,78	3,21	3,25	1,68
MgO	9,04	9,02	5,06	5,84	2,90	3,98	2,72
CaO	0,01	0,01	0,01	0,01	0,01	0,01	0,05
K_2O	9,21	9,16	8,92	9,08	9,07	9,24	8,88
Na_2O	0,28	0,40	0,30	0,32	0,23	0,23	0,18
	96,40	96,26	95,72	96,43	96,62	98,44	95,72

* All Fe as FeO

Number of ions on the basis of 22 oxygens

Si	5,498	5,478	5,746	5,812	5,576	5,522	5,641
Al	2,459	2,520	1,994	1,904	2,300	2,332	2,344
Ti	0,043	0,002	0,260	0,284	0,124	0,146	0,015
Ti	0,346	0,365	0,158	0,143	0,355	0,309	0,470
Mn	0,134	3,303	0,498	0,516	0,466	0,441	0,234
Mg	2,117	2,115	1,233	1,404	0,709	0,951	0,664
Fe	3,320	0,132	3,930	3,759	4,298	4,172	4,366
Ca	-	-	-	-	-	-	0,010
Na	0,085	0,121	0,096	0,100	0,075	0,073	0,057
K	1,846	1,836	1,860	1,869	1,895	1,888	1,859
Ann	56	56	68	65	74	71	76
Phlog	36	36	21	24	12	16	12
MnBi	2	2	8	9	8	8	4
TiBi	6	6	3	2	6	5	8

TABLE 19

Microprobe analyses of biotites from syenites, Pomona

	PM64	PM64	PM157	PM157	PM60	PM127
SiO_2	35,81	35,94	35,45	35,66	37,36	40,68
TiO_2	4,26	4,49	2,95	2,48	3,03	2,87
Al_2O_3	11,75	11,55	11,12	11,32	13,25	10,60
FeO*	19,96	20,41	24,11	23,01	17,65	17,26
MnO	0,57	0,54	0,91	0,95	2,07	1,49
MgO	12,21	11,80	9,56	10,49	12,99	14,63
CaO	0,01	0,03	0,01	0,03	0,01	0,01
K_2O	9,32	9,33	9,24	9,46	9,56	9,43
Na_2O	0,41	0,43	0,26	0,31	0,28	0,19
	94,31	94,52	93,61	93,81	96,21	97,16

* All Fe as FeO

Number of ions on the basis of 22 oxygens

Si	5,606	5,625	5,720	5,715	5,669	6,042
Al	2,168	2,131	2,116	2,140	2,331	1,856
Ti	0,226	0,244	0,164	0,145	0,039	0,102
Ti	0,275	0,284	0,136	0,154	0,346	0,218
Mn	0,075	0,072	0,124	0,129	0,267	0,187
Mg	2,850	2,753	2,300	2,531	2,940	3,240
Fe	2,613	2,671	3,253	3,084	2,239	2,143
Ca	-	0,005	-	0,005	-	-
Na	0,126	0,131	0,082	0,096	0,081	0,055
K	1,861	1,863	1,902	1,933	1,851	1,786
Ann	45	46	56	52	38	37
Phlog	49	48	40	43	50	56
MnBi	1	1	2	2	5	3
TiBi	5	5	2	3	6	4

Wilkinson (1970) reported very rapid zoning toward extremely Mn-rich margins in biotites from Na-syenites in the Shonkin Sag laccolith. The biotites analyzed here are all very homogeneous with respect to Mn, except at the rims in specimens in the Hub Syenite (PM127) and the Inner Foyaite (GM350) where a slight Mn depletion was detected during analysis.

There is a contrasted variation in Fe and Mg in the biotites for the over- and undersaturated suites. In the oversaturated suite the phlogopite component increases with fractionation (as determined by major and trace element data) from the Outer Syenite → Inner Syenite → Hub Syenite. The cumulate, PM64 has a biotite Fe/Fe+Mg intermediate between the Outer and Inner Syenites (Table 27). This variation is illustrated in Figure 32. In contrast the biotites in the undersaturated suite have much higher Fe/Fe+Mg than any of the oversaturated syenites, and the phlogopite component in the biotite decreases with fractionation. No zoning of Fe and Mg occurs in the biotites except in the Inner Foyaite (GM350) which display slightly Mg-rich rims. The significance of the Fe - Mg variation will be discussed in section 7.9.

7.8. AMPHIBOLES

Analyses of the amphiboles are presented in Table 20 with their formulae calculated on the basis of 23 oxygens in the cell. No determinations of OH or F were made, thus the analyses have low totals.

During analysis compositional inhomogeneity was detected in amphiboles from several of the rocks. Fe and Mg are generally constant over the whole grain area, but some grains show slight Fe enrichment at the rim. The minor elements, Ti, Al, and in the more alkali amphiboles, Ca, show more marked variation. No pattern in the inhomogeneity could be detected, except in the arfvedsonite in GM137 which shows a distinct Ca and Al depletion towards the margins of the grains. As in the biotites, Mn is surprisingly constant over the grain area.

The Fe-edenite (PM157) and the alkali amphibole in PM60 are all slightly Al-poor - in all the other amphiboles Al enters both the Z and Y positions. In the Fe-edenite Al > (Na + K) and fractionation of these amphiboles will generate a peralkaline condition in the residual liquid. PM157, in which these amphiboles are found, is not peralkaline, but all

TABLE 20

Microprobe analyses of amphiboles from syenites and nepheline syenites, Granitberg and Pomona

	PM157	PM157	PM60	PM127	PM127	PM66	PM66	GM137	GM137
SiO_2	40,38	40,00	49,28	53,02	54,35	49,54	49,74	47,51	48,10
TiO_2	2,44	2,30	1,03	0,26	0,36	0,68	0,73	2,02	1,83
Al_2O_3	9,09	9,38	3,10	1,80	1,34	1,46	1,38	3,60	3,48
FeO*	19,83	20,12	16,95	15,12	15,09	25,63	27,29	26,39	25,61
MnO	1,03	0,99	3,43	1,87	2,09	4,97	4,84	2,20	2,28
MgO	8,75	8,82	11,56	13,11	13,43	4,99	4,54	3,75	3,95
CaO	10,60	10,52	6,69	6,41	5,30	3,22	3,10	2,55	2,32
K_2O	2,23	2,35	1,42	1,26	1,17	1,17	1,19	1,77	1,85
Na_2O	3,21	3,10	5,16	5,45	5,56	6,18	6,35	7,79	7,83
	97,56	97,58	98,62	98,30	98,68	97,84	99,17	97,60	97,25

* All Fe ans FeO

Number of ions based on 23 oxygens

Si	6,323	6,274	7,409	7,801	7,934	7,807	7,786	7,517	7,599
Al	1,667	1,724	0,549	,199	0,066	0,193	0,214	0,483	0,401
Al				0,112	0,162	0,074	0,040	0,188	0,218
Ti	0,287	0,270	0,116	0,028	0,039	0,081	0,086	0,240	0,217
Mn	0,136	0,131	0,437	0,233	0,257	0,664	0,642	0,295	0,305
Mg	2,041	2,062	2,591	2,875	2,906	1,172	1,059	0,884	0,930
Fe	2,597	2,641	2,131	1,860	1,832	3,378	3,572	3,492	3,384
Ca	1,778	1,767	1,078	1,010	0,824	0,554	0,520	0,432	0,303
K	0,446	0,471	0,273	0,236	0,216	0,235	0,237	2,390	2,398
Na	0,975	0,943	1,505	1,554	1,565	1,888	1,928	0,357	0,373

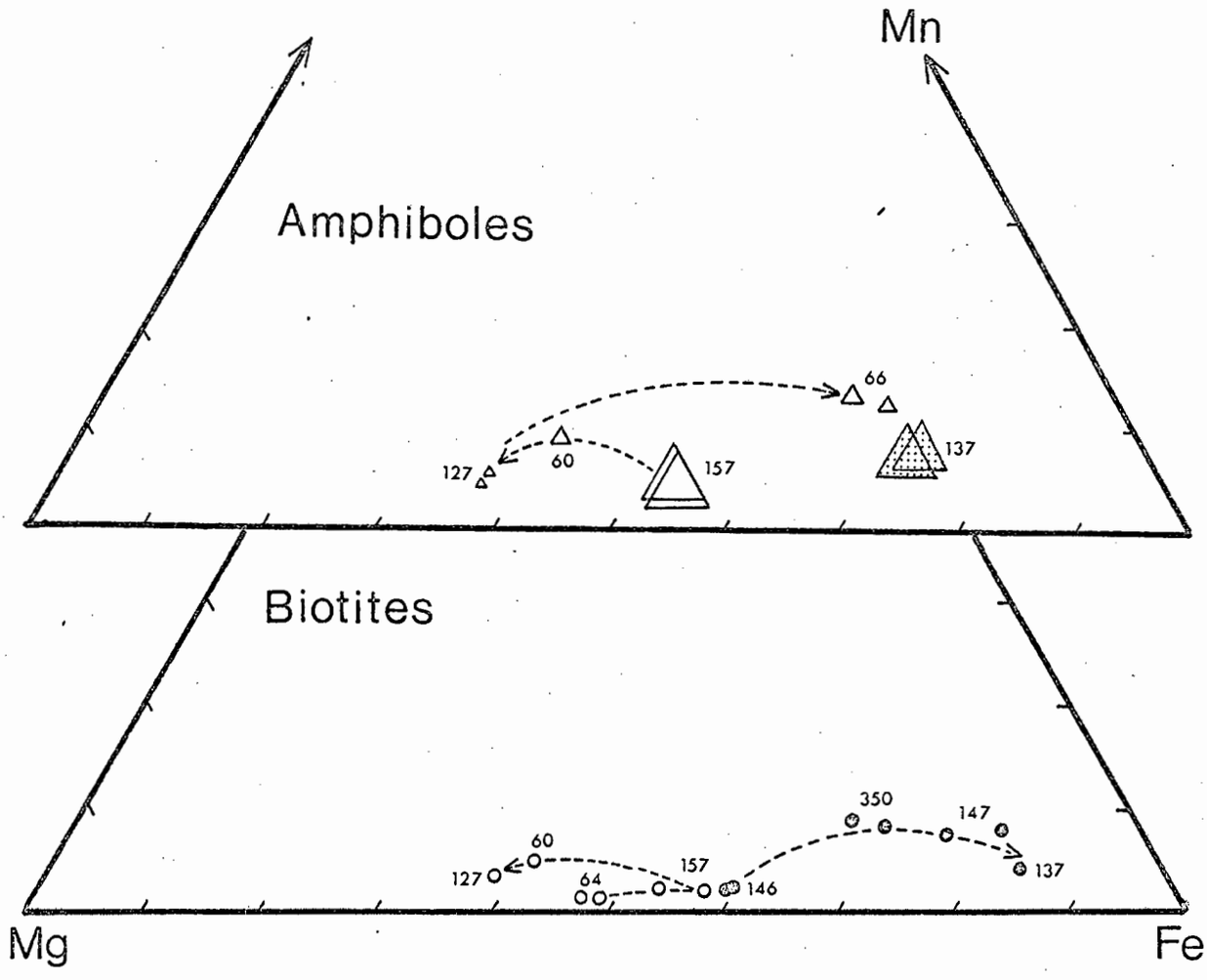

Figure 32. Composition of biotites and amphiboles from Granitberg and Pomona. Amphibole compositions in terms of atomic Mn, Fe, and Mg, with the triangular 'error of closure' proportional to the Ti content. Biotite compositions in terms of Mn, Fe, and Mg only. Numbers refer to rock samples. Dashed arrows indicate direction (but not necessarily the path) of fractionation, as deduced from field and chemical data.

⊙ , △ - undersaturated syenites, Granitberg

o , △ - oversaturated syenites, Pomona

the other rocks (except PM64) are, and in these Al < Na + K. The Na+K/Al ratio in the amphiboles, unlike biotite, appears to be sensitive to the NA+K/Al of the environment in which they crystallize.

Ca in the amphiboles decreases with fractionation, as does Ti, although the arfvedsonite in GM137 has high Ti. This rock is devoid of Fe-Ti oxides and sphene and Ti has entered the mafic silicate minerals instead.

Mn is considerably enriched in the amphiboles, the MnO content increasing with increasing fractionation to nearly 5 Wt% in the arfvedsonites in the nordmarkite ring dyke (PM66). This is far higher than the MnO content of any amphiboles listed by Deer et al (1962). Such high Mn has not even been reported in the amphiboles of the Lovozero massif where Mn is enriched to the extent that it is one of the main mineral-forming elements in 15 minerals (Vlasov et al, 1966).

Fe and Mg variation in the amphiboles is similar to the biotites. The amphiboles become more Mg-rich with fractionation from the Outer Syenite to the Hub Syenite. The arfvedsonite in the nordmarkite ring dyke has low Mg, similar to the arfvedsonite in GM137. The composition of the amphiboles is illustrated in Figure 32.

7.4. PYROXENES

Analyses of clinopyroxenes are presented in Tables 21, 22, with their formulae based on a cell of 6 oxygens. The compositions of the pyroxenes in terms of mole % of the three end-member nolecules, Acmite, Diopside and Hedenbergite are also given. The compositions are also plotted in Figure 33, where the error of closure is proportional to the Mn content of the pyroxenes. Most of the analyzed pyroxenes are zoned toward acmite-rich rims, thus several determinations of the composition of the core and rim were made on individual grains.

Both the Ti and Al contents of the pyroxenes are 'normal' and within the range commonly reported for igneous alkali-pyroxenes (Gomes et al, 1970; Tyler and King, 1967; Stephenson, 1972). Potassium was either very low or not detected in the pyroxenes, a feature also noted by Stephenson (1972). In contrast analyses of bulk separates commonly report considerable amounts of K, greater than 1% in some separates. It would appear that these high K contents

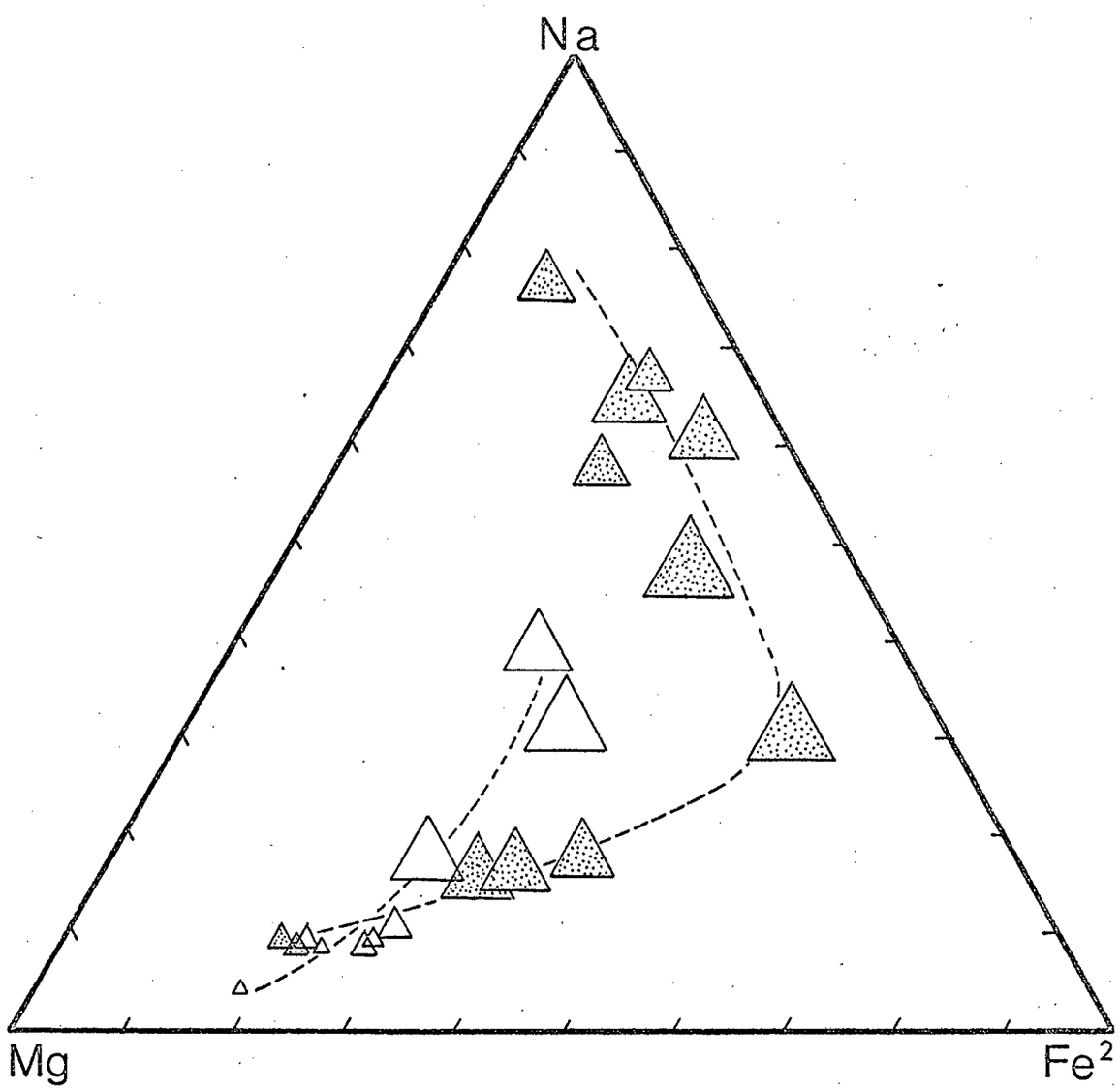

Figure 33. Composition of Na pyroxenes from Pomona and Granitberg in terms of atomic Na, Fe^{++}, and Mg.

- undersaturated syenites, Granitberg

- oversaturated syenites, Pomona

"Triangles of error closure" proportional to Mn content of the pyroxenes.

TABLE 21

Microprobe analyses of clinopyroxenes from nepheline syenites, Granitberg.

	GM146	GM146	GM350	GM350	GM137(c)	GM137(i)	GM137(r)	GM137	GM147(c)	GM147(r)	GM147(c)	GM147(r)
SiO_2	51,12	51,05	51,56	52,28	50,85	50,43	51,23	50,50	50,73	50,75	50,60	50,63
TiO_2	0,46	0,49	0,52	0,57	0,41	0,47	0,56	0,73	0,53	0,45	0,58	0.56
Al_2O_3	2,29	2,30	1,04	1,00	1,33	1,20	0,97	1,00	1,90	1,18	1,97	1,19
FeO*	9,23	9,26	23,84	24,57	17,10	23,52	25,49	26,43	14,52	24,17	15,59	25,37
MnO	0,86	0,82	1,58	1,62	1,81	2,24	1,63	1,22	2,05	2,63	2,13	1,95
MgO	13,02	13,50	2,87	2,08	6,42	1,93	0,88	1,37	8,64	2,26	7,92	1,75
CaO	20,01	20,17	9,34	6,18	19,99	16,10	9,78	9,94	21,11	13,66	20,93	9,42
Na_2O	1,13	1,21	7,36	9,64	2,05	3,52	7,25	8,53	1,87	5,86	1,93	8,20
	98,12	98,80	98,12	97,99	99,97	99,43	97,82	99,73	101,35	100,98	101,67	99,08

* All Fe as FeO. K_2O consistently < 0,01. (c) core; (i) intermediate zone (r) rim.

Number of Cations on the basis of 6 oxygens

Si	1,949	1,936	2,084	2,117	1,988	2,033	2,097	2,048	1,945	2,025	1,942	2,062
Al	0,103	0,103	0,049	0,048	0,061	0,057	0,047	0,048	0,085	0,056	0,089	0,056
Ti	0,013	0,014	0,016	0,017	0,012	0,014	0,017	0,022	0,015	0,014	0,017	0,017
Mn	0,028	0,026	0,054	0,056	0,060	0,077	0,057	0,042	0,066	0,089	0,069	0,067
Mg	0,740	0,763	0,173	0,126	0,374	0,116	0,054	0,083	0,493	0,134	0,451	0,106
Fe	0,294	0,294	0,806	0,832	0,559	0,793	0,872	0,896	0,466	0,806	0,499	0,864
Ca	0,818	0,819	0,404	0,268	0,837	0,696	0,429	0,432	0,864	0,584	0,857	0,411
Na	0,083	0,089	0,577	0,757	0,156	0,275	0,575	0,670	0,139	0,454	0,143	0,647
Di	69,7	70,5	16,8	12,4	37,7	11,8	5,5	8,1	48,1	13,0	44,3	10,3
Hd	22,5	21,3	27,4	12,9	46,6	60,3	36,0	26,3	38,3	42,9	41,7	27,3
Ac	7,8	8,2	55,8	74,7	15,7	27,9	58,5	65,6	13,6	44,1	14,0	62,4

TABLE 22

Microprobe analyses of clinopyroxenes from Syenites, Pomona

	PM64	PM64(c)	PM64(r)	PM157	PM157(c)	PM157(r)	PM127	PM127(c)	PM127(r)
SiO_2	51,39	52,64	51,40	51,27	51,76	51,20	52,37	51,08	50,43
TiO_2	0,25	0,32	0,71	0,48	0,61	0,46	0,13	0,28	0,26
Al_2O_3	1,51	0,92	2,20	1,67	1,86	1,84	0,32	0,67	0,42
FeO*	12,11	7,39	10,37	10,84	9,50	11,89	19,94	13,25	19,36
MnO	0,64	0,39	0,41	0,85	0,85	1,02	2,00	2,07	2,30
MgO	11,91	14,71	12,58	11,32	12,51	10,60	5,64	9,29	5,79
CaO	21,54	22,36	22,19	21,67	21,69	21,04	14,56	21,50	17,60
Na_2O	1,26	0,52	1,13	1,06	1,13	1,29	5,05	2,08	3,98
	101,13	99,91	101,00	99,15	99,91	99,35	100,02	100,19	100,52

* All Fe as FeO; K_2O consistently < 0,01; (c) core; (r) rim.

Number of cations on the basis of 6 oxygens

Si	1,951	1,978	1,922	1,958	1,948	1,959	2,057	1,971	1,997
Al	0,066	0,040	0,097	0,075	0,083	0,083	0,015	0,031	0,019
Ti	0,007	0,009	0,020	0,014	0,017	0,013	0,004	0,008	0,008
Mn	0,020	0,012	0,013	0,027	0,027	0,033	0,066	0,068	0,077
Mg	0,668	0,813	0,701	0,644	0,702	0,605	0,330	0,534	0,342
Fe	0,380	0,229	0,324	0,346	0,299	0,381	0,655	0,427	0,641
Ca	0,868	0,889	0,889	0,887	0,875	0,863	0,613	0,889	0,746
Na	0,092	0,037	0,082	0,079	0,082	0,096	0,384	0,156	0,305
Di	62,5	77,1	67,5	63,3	68,4	59,4	31,5	51,9	32,3
Hd	28,9	19,4	24,6	28,9	23,7	31,2	32,0	32,9	39,0
Ac	8,8	3,5	7,9	7,8	7,9	9,4	36,5	15,2	28,7

are due to impurities or to the fact that K is frequently concentrated along cracks in the grains (A.J. Erlank, personal communication), since microprobe analyses consistently confirm the virtual absence of K from pyroxenes.

One of the outstanding features of the Luderitz Province pyroxenes is their high Mn content, up to 2,63 Wt % MnO in the pyroxenes in the more fractionated rocks. The only record of similar concentrations of Mn in pyroxenes is in Vlasov et al (1966) who report 1,4 Wt % MnO in the aegirines in the Lovozero alkaline massif. Gerasimovskii (1956) records 2,12 % MnO in pyroxenes from miaskitic alkaline rocks, though he does not mention the locality. It is also noticeable that the mafic minerals coexisting with the high Mn-pyroxenes are also enriched in Mn. In the Outer Foyaite the MnO content of Pyroxene biotite, and Ti-magnetite is 2,63; 3,25; and 6,14% respectively.

7.5. AENIGMATITE

Aenigmatite is found in the outer zone of the Outer Foyaite, and analyses are presented in Table 23. Aenigmatite is known to occur in both over- and undersaturated peralkaline rocks, but none has been found in the silicic rocks in the Luderitz Province.

Little variation in the composition of aenigmatite occurs, except amongst the minor elements. Microprobe analyses (this work, and Nicholls and Carmichael, 1969) indicate that K is virtually absent, in contrast to that indicated from bulk separate analyses (Vlasov et al, 1966; Kelsey and McKie, 1964). The K contents in the latter analyses appear to be due to contamination.

The outstanding feature of the aenigmatites analyzed here is their high MnO content (4,3 Wt %) compared to those from Lovozero (2,42 % - Vlasov et al, 1966), from pantellerites and comendites (0,49 to 1,19 % - Nicholls and Carmichael, 1969), and those analyses listed by Kelsey and McKie (1964). The Ti/Fe+Ti ratio for the Granitberg aenigmatites is 17,1, well within the range reported by the latter authors.

The petrography of the aenigmatite-bearing rocks at Granitberg indicates that this mineral does not precipitate from a melt crystallizing Fe-Ti oxides. Similar conclusions were made by Nicholls and Carmichael

TABLE 23

Microprobe analysis of aenigmatite from foyaite GM137, Granitberg

SiO_2	41,61	41,73
TiO_2	8,25	8,07
Al_2O_3	1,13	1,09
FeO*	35,80	35,89
MnO	4,36	4,39
MgO	0,90	0,90
CaO	0,27	0,33
K_2O	0,01	0,01
Na_2O	7,41	7,18
	99,28	98,89
$\frac{100Ti}{Fe + Ti}$	17,1	17,1

* All Fe as FeO

TABLE 24

Analyses of Ti-magnetites

	PM64	PM157	PM127	GM147 **
FeO	31,97	32,42	31,60	47,00
Fe_2O_3*	63,04	60,21	63,43	34,89
MnO	0,90	1,52	0,63	6,14
TiO_2	2,83	4,72	2,23	12,22
Al_2O_3	0,63	0,72	0,02	0,13
Cr_2O_3	0,05	0,03	0,03	n.d.
Na_2O				0,05
SiO_2				0,02
CaO				0,04
MgO				0,04
	99,42	99,62	98,94	100,53

* Fe_2O_3 calculated by the method of Carmichael (1967).

** microprobe analysis; other analyses by XRF.

(1969) for acid alkaline rocks. This antipathetic relationship between aenigmatite and Fe-Ti oxides will be dealt with more fully in section 8.6.

7.6. Fe-Ti OXIDES

Ti-magnetite is the sole primary Fe-Ti oxide crystallizing in both the oversaturated and undersaturated suites. The magnetite is now seen as intergrowths of ilmenite and magnetite, and following Buddington and Lindsley (1964), the ilmenite is considered to represent the original ulvospinel component of the magnetite-ulvospinel solid solution, which has been oxidized on exsolution.

Bulk concentrates of the oxides were made for analysis by X-ray fluorescence. Concentrates of sufficient bulk and purity were obtained only from PM64, PM157, and PM127. Their analyses are presented in Table 24, and have been recalculated to express the composition in terms of mole % Usp according to the rules of Carmichael (1967). This method also allows an estimate of Fe_2O_3 to be made.

In the Outer Foyaite a one-phase oxide mineral occurs. Anisotropism and other properties in reflected light indicated that it was possibly ilmenite. However the microprobe analysis of this oxide indicates that it is an Mn-rich Ti-magnetite. The grains are not compositionally homogeneous, but a satisfactory analysis (Table 24) was obtained by analyzing sufficient spots. No reference to magnetites with Mn contents of similar magnitude could be found in the literature, but Vlasov et al (1966) reported manganilmenite with 13% MnO from the Lovozero massif.

7.7. NEPHELINE

Analyses of nepheline from rocks in the undersaturated suite are presented in Table 25 and their compositions plotted in terms of nepheline-kalsilite-quartz in Figure 34. All the nephelines contain excess SiO_2 which is a reflection of the temperature-dependent solid solution of SiO_2 in members of the nepheline - kalsilite series (Hamilton and MacKenzie, 1960; Hamilton, 1961).

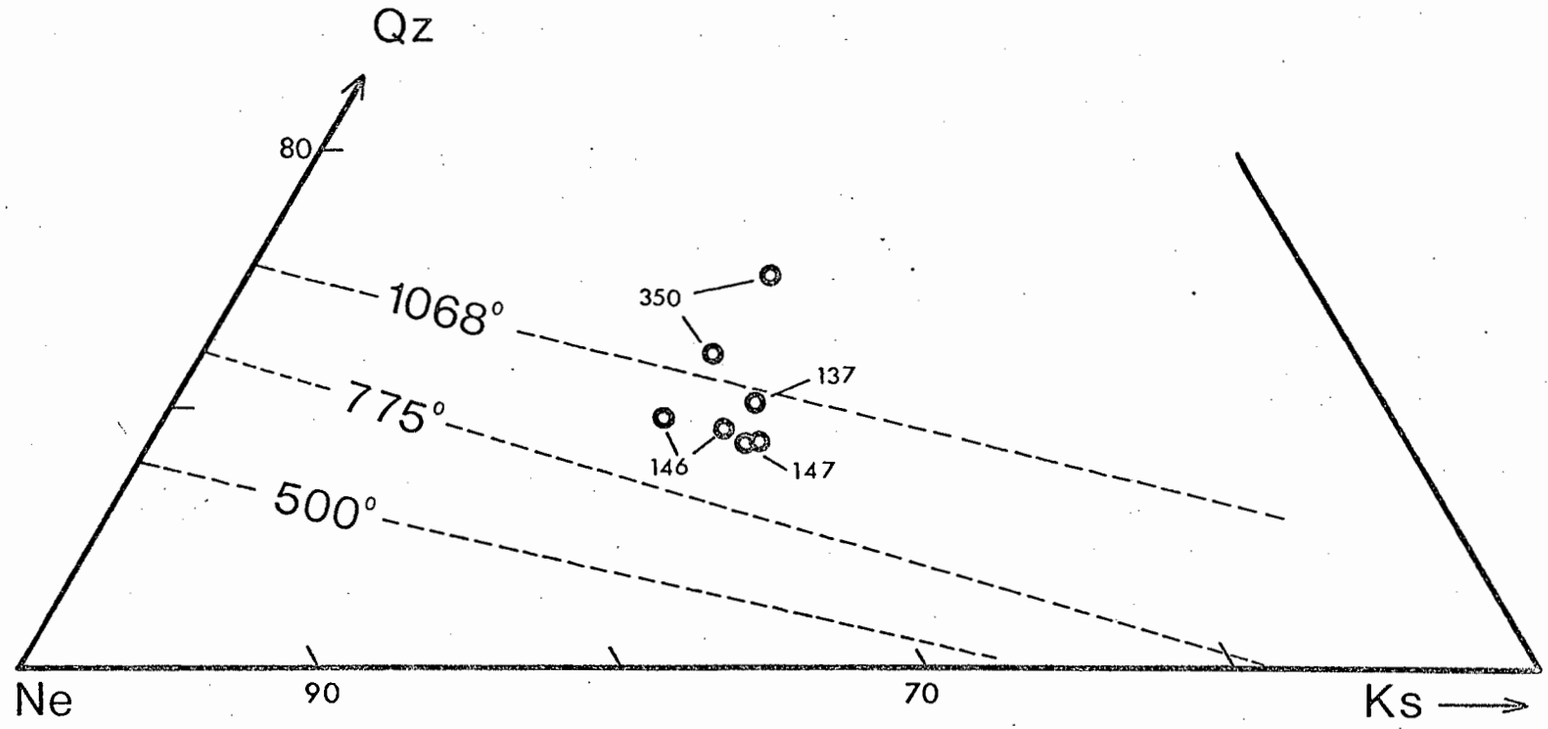

Figure 34. Composition of nepheline from the Granitberg undersaturated syenites, in terms of mole Ne - Ks - Qz. Dashed lines indicate the experimentally determined limits of solid solution of SiO_2 in the nepheline at the indicated temperatures (after Hamilton, 1961).

TABLE 25

Microprobe analyses of nepheline from foyaites, Granitberg

	GM146	GM146	GM350	GM350	GM147	GM147	GM137
SiO_2	46,40	46,13	46,47	46,81	45,60	45,94	46,54
Al_2O_3	32,21	22,44	33,01	32,91	33,63	33,67	33,04
FeO*	0,53	0,49	0,73	0,69	0,42	0,47	0,51
MnO	nd	nd	0,01	0,01	0,01	0,01	0,01
CaO	0,24	0,24	0,01	0,01	0,03	0,03	0,01
K_2O	4,81	5,51	5,29	5,14	5,85	5,80	5,65
Na_2O	15,56	15,19	14,54	14,66	15,26	15,54	15,08
	99,22	100,01	100,13	100,29	100,84	101,50	100,85
Ne	73,83	71,95	70,80	67,48	71,27	71,85	70,39
Ks	16,44	18,77	16,96	17,34	20,01	19,66	19,33
Q_2	9,72	9,27	12,24	15,17	8,71	8,48	10,28

* All Fe as FeO; n.d. - not determined.

TABLE 26

Bulk Alkali-feldspar analyses

	K_2O	Na_2O	
Outer Syenite PM157	5,48	7,01	$Ab_{66}Or_{34}$
Inner Syenite PM60	6,51	6,63	$Ab_{61}Or_{39}$
Hub Syenite PM127	6,70	6,54	$Ab_{60}Or_{40}$
PCNS (phenocrysts) GM146	3,65	9,95	$Ab_{80}Or_{20}$
Inner Foyaite GM350	6,26	7,32	$Ab_{64}Or_{36}$
Outer Foyaite GM147	6,54	8,07	$Ab_{65}Or_{35}$

Excess SiO_2 is generally of the order of 0 to 5 Wt % for the 'plutonic' nephelines and may be as high as 10% for the phonolites. Hamilton (1961) has proposed that temperatures of quenching in nepheline-bearing rocks may be determined using the excess SiO_2 in analyzed nephelines. When the plotted compositions for the Granitberg nephelines are compared to the limits of solid solution for various temperatures (Figure 34), the indicated temperatures are clearly anomalously high for coarse grained rocks, the lowest being in the region of 900° to 950°C. No signs of disequilibrium have been observed, either optically or during analysis. The high SiO_2 content of the nephelines appears therefore, to be due to small errors in the analyses. This underlines Barth's (1963) criticism of this geothermometer.

Apart from excess SiO_2 the nephelines show little variation in the amounts of Ne and Ks molecule. However in accordance with experimental evidence there is a slight increase in the amount of Ks molecule with the determined position of the rocks in the fractionation scheme.

7.8. ALKALI FELDSPAR

The main features of the alkali feldspars in the two suites have been presented in the petrographic descriptions of the various rock types. Na and K determinations were made on bulk separates by X-ray fluorescence, and the results are presented in Table 26. The analyses have already been used with the major element data (see section 6.4.4.), and their significance discussed in the light of feldspar fractionation. In addition a limited X-ray study of the structural state of the feldspars has been conducted. The data is presented and discussed below.

7.8.1. Structural state of the alkali feldspars

The structural state of the potassic phase of the perthites (hereinafter referred to as K-feldspar) in the major rock units of the Granitberg, Pomona, and Drachenberg intrusions was studied by X-ray diffraction procedures. The purpose of the study is twofold:

(a) to attempt to confirm the evidence from other intrusions (see Parsons and Boyd 1971) that the degree of fractionation of a magma in an intrusive sequence controls the structural state of the crystallizing

feldspar;

(b) to establish whether there is any difference in the structural state of the alkali feldspar crystallizing in an undersaturated environment compared to an oversaturated environment.

This study was limited in the number of samples processed by the number of chemical analyses available, and by the number of rock samples whose degree of fractionation could be confidently estimated by association with the analyzed samples. In all, the rather small number of 44 samples were processed.

Of all the physical methods of estimating the structural state of the feldspar the 'three peak' method of Wright (1968) was selected for the following reasons:

(1) the reflections measured are directly related to the unit cell dimensions of the feldspars. Moreover Smith (1970) has concluded that cell dimensions have the greatest significance with respect to order-disorder in alkali feldspar, whereas triclinic geometry has little fundamental significance.

(2) A minimum of sample preparation is necessary in order to ensure sharp, interference-free reflections (both nepheline and plagioclase interfere with the 131 and $1\bar{3}1$ reflections if the obliquity method of Goldsmith and Laves (1954) is used).

7.8.1.1. Results

The normality of the cell dimensions for the K-feldspars were tested as suggested by Wright (1968, p. 93). Most of the feldspars are considered to be 'normal' and the 2θ values for the 060 and $\bar{2}04$ reflections of these feldspars have been used to calculate δ as suggested by Ragland (1970). Both normal and anomalous K-feldspars have been used to construct the plots in Figure 35. Only normal feldspars have been plotted in the Fractionation Index diagrams. (Figure 36).

7.8.1.2. Discussion

Except for DM115 and DM105 all the Drachenberg syenites possess 'anomalous' K-feldspars in the sense used above. Major and trace element

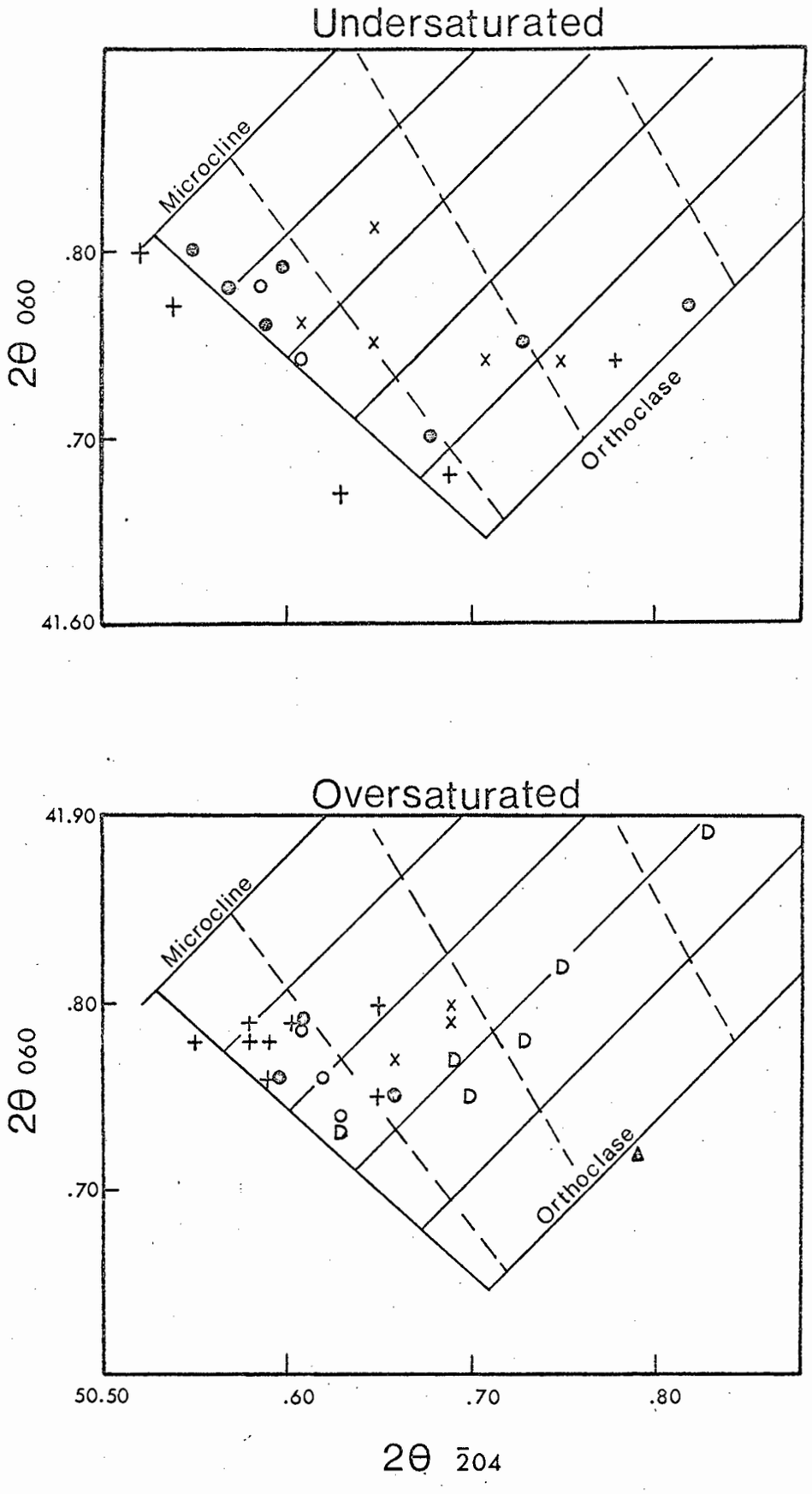

Figure 35. Structural state of K-feldspars from the intrusive complexes. Oversaturated suite: x - Outer Syenite; o - Inner Syenite; ⊙ - Hub syenite; ▲ - Biotite-rich Monzonite; + - dyke rocks; D - Drachenberg Syenites. Undersaturated suite: x - PCNS o - Inner Foyaite; ⊙ - Outer Foyaite; + - tinguaite dykes. Diagram after Wright(1968).

chemistry indicate that DM115 has undergone fairly substantial fractionation, and DM105 is chemically more primitive. There seems therefore to be no significance in the presence of anomolous feldspars in relation to the degree of fractionation of the host rock. More extensive studies may negate this apparent dominance of abnormal feldspars in the Drachenberg syenites.

Considering the Pomona and Granitberg samples, it would appear that anomolous feldspars are more common in the undersaturated than in the oversaturated rocks. Otherwise, except for one sample, (PM64), all the K-feldspars have structural states intermediate between Orthoclase and Maximum Microline.

All the rocks, except PM64, are one feldspar rocks in which the single alkali feldspar is a perthite. In many of the coarse-grained rocks the perthitic intergrowth is very coarse. The plagioclase component is often twinned on the Albite law and has a composition An_6 to An_{15}. The position of the $\bar{2}01$ reflection for normal feldspars can be used to estimate the composition of the potassic phase using the curves given by Wright (1968). Many of the samples gave broad or doubly peaked $\bar{2}01$ reflections, indicating a range in the composition of the potassic phase, and is possibly a reflection of the presence of albite-rich domains as described by Vogel (1970).

Figure 36 shows a plot of Δ vs FI. FI is the Fractionation Index of MacDonald (1969), and is believed to represent the degree of fractionation of the host rock, where strongly fractionated rocks have a high FI. Likewise indicates the structural state of the feldspar and is calculated after the formula given in Ragland (1970). Δ varies from 0,000 for a feldspar of the Orthoclase series, to 1,000 for a feldspar in the Maximum Microline - Low Albite series. For feldspars which have a structural state between the Orthoclase and the Sanidine - High Albite series Δ' is calculated. The larger Δ or Δ' is in the positive sense, the greater the degree of ordering.

From the diagram it can be seen that for the oversaturated rocks, there is a marked positive correlation between FI and Δ, though there exists a large amount of scatter of the plotted points. Certainly as a group the K-feldspars of the quartz bostonites and quartz-feldspar porphyry dyke rocks have higher Δ values, and are therefore more ordered than those of the Pomona Outer Syenites.

For the undersaturated rocks the high incidence of anomalous feldspars allow only a few samples to be plotted, and no firm conclusions can be drawn. There are indications that a positive correlation between δ and FI could be proved in a wider study, but a number of feldspars from rocks with a very high FI have disturbingly low values of δ.

In Figure 35 both normal and anomalous feldspars have been plotted, and the pattern largely confirms those illustrated in Figure 36. Considering the diagram for the oversaturated rocks, it is clear that as a group the Drachenberg syenites not only show a high incidence of anomalous feldspars, but crystallised more disordered feldspars than any other syenites in the oversaturated trend besides PM64. This indicates that the Drachenberg syenites should be considered as an entity, and they are not part of the oversaturated trend as is developed at Pomona and Granitberg.

The most ordered feldspars are to be found in the quartz-bearing dyke rocks, i.e. those rocks which are chemically the most highly fractionated in the oversaturated trend. The one exception to this is PM177, a quartz-feldspar porphyry, the trace element chemistry of which is also exceptional compared to the other dyke rocks. Otherwise, with the limited number of samples studied, the degree of ordering in the K-feldspars increases with the differentiation series: Outer Syenite $\longrightarrow$ Inner Syenite $\longrightarrow$ Hub Syenite $\longrightarrow$ Quartz-bearing dyke rocks.

In the undersaturated rocks the pattern is more confused. The most ordered feldspars are found in the tinguaite dykes and in the Outer Foyaite. The feldspars from the Inner Foyaite have a structural state intermediate between these and the PCNS of the Roof Zone, thus indicating an increase in ordering of the K-feldspars with the differentiation sequence: PCNS $\longrightarrow$ Inner Foyaite $\longrightarrow$ Outer Foyaite. However, both tinguaites and the Outer Foyaite are amongst those rocks which carry the most disordered alkali feldspars. In order to arrive at any sound conclusions regarding structural state - composition correlations in the undersaturated rocks, a statistical treatment of a large number of samples would be required.

7.8.1.3. Comparison with other data

Parsons and Boyd (1971) have produced convincing evidence that the structural state of a K-feldspar is strongly dependent on the relative bulk

composition of the rock in which it is found. They showed that in a number of studied igneous intrusions, the most ordered K-feldspars were found in the most fractionated rocks in the differentiation scheme appropriate to each intrusion.

This limited study indicates that similar conclusions can be applied to the K-feldspars in the rocks in the Luderitz Province. It may be argued that increasing degree of fractionation is a reflection of decreasing temperature of crystallization, and that temperature is the controlling factor. This may be refuted by comparing the structural states of the feldspar in the quartz-bostonites to that of the quartz-feldspar porphyry, PM177. The latter crystallized at a lower temperature than the bostonites, but exhibits a more primitive trace element chemistry, and contains more disordered alkali feldspars. Furthermore, if temperature were the chief controlling factor it would not be expected that maximum microline or near maximum microline (which is a stable phase only below 400°C) (Barth, 1969) be found in tinguaites and foyaites which crystallised at higher temperatures (in the range 700 to 800°C - see section 8.4.).

Likewise, cooling rate appears to have no effect on the ordering processes as the most ordered K-feldspars are found in the fine grained, rapidly cooled dyke rocks, as well as in some of the coarse grained foyaites. There is abundant evidence in the coarse intergrowths of most of the perthites from the syenites and foyaites, that annealing was prolonged and possibly fluxed by volatiles. Ragland (1970) has suggested that such conditions can account for high degrees of ordering in K-feldspars. The evidence from the Luderitz Province appears to contradict this notion.

In their study, Parsons and Boyd (1970) concluded that the nature of the magmatic and volatile environment, at the time feldspar is crystallizing from the magma, is critical in determining whether microline will form, or whether orthoclase will persist during cooling. Their summary of the pertinent literature emphasises the importance of volatiles in the ordering process. Furthermore, they indicate that a peralkaline environment promotes ordering, whereas a peraluminous environment inhibits ordering, conclusions which are supported by the synthesis experiments of Martin (1969a; 1969b).

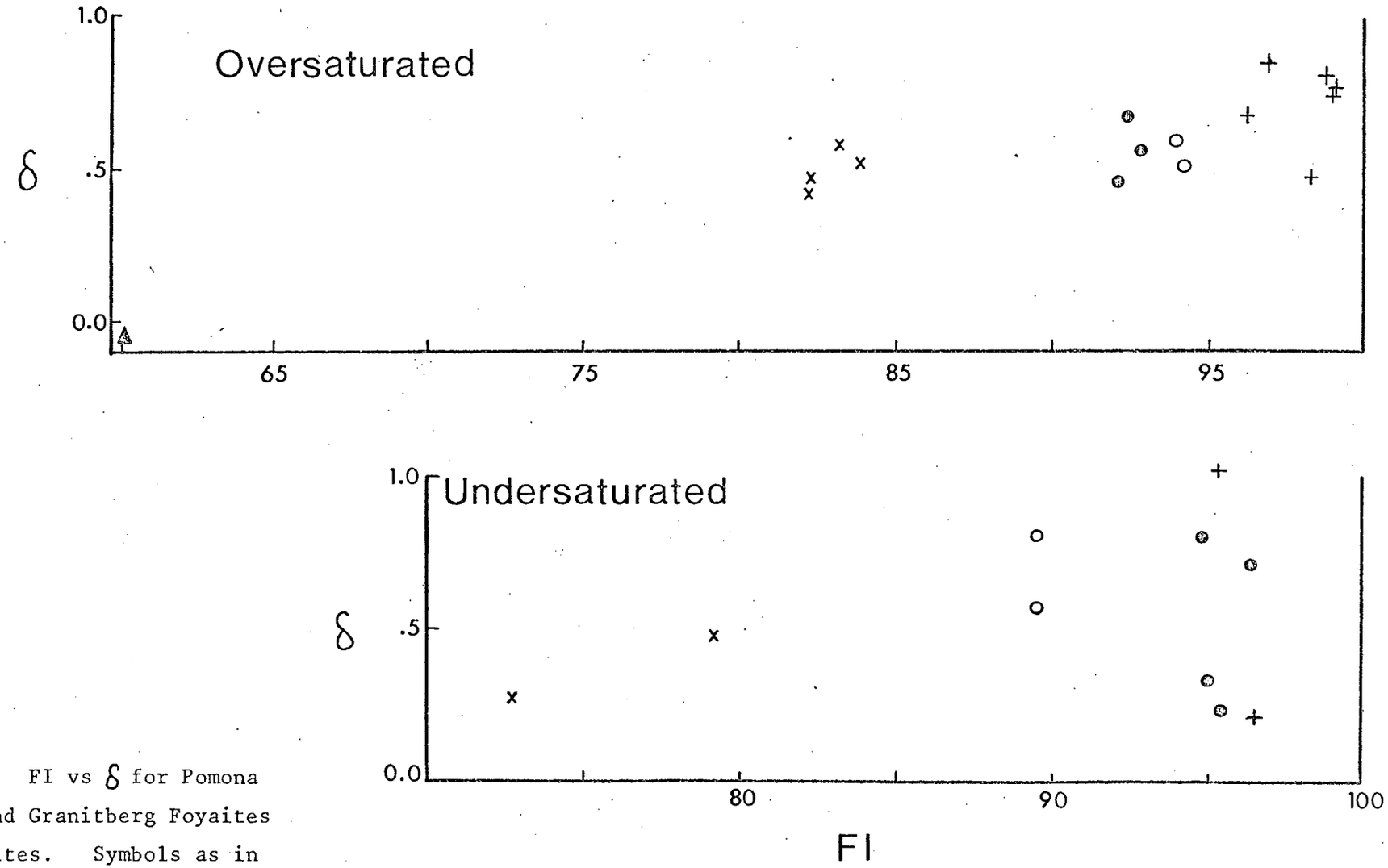

Figure 36. FI vs δ for Pomona Syenites and Granitberg Foyaites and Tinguaites. Symbols as in Figure 35.

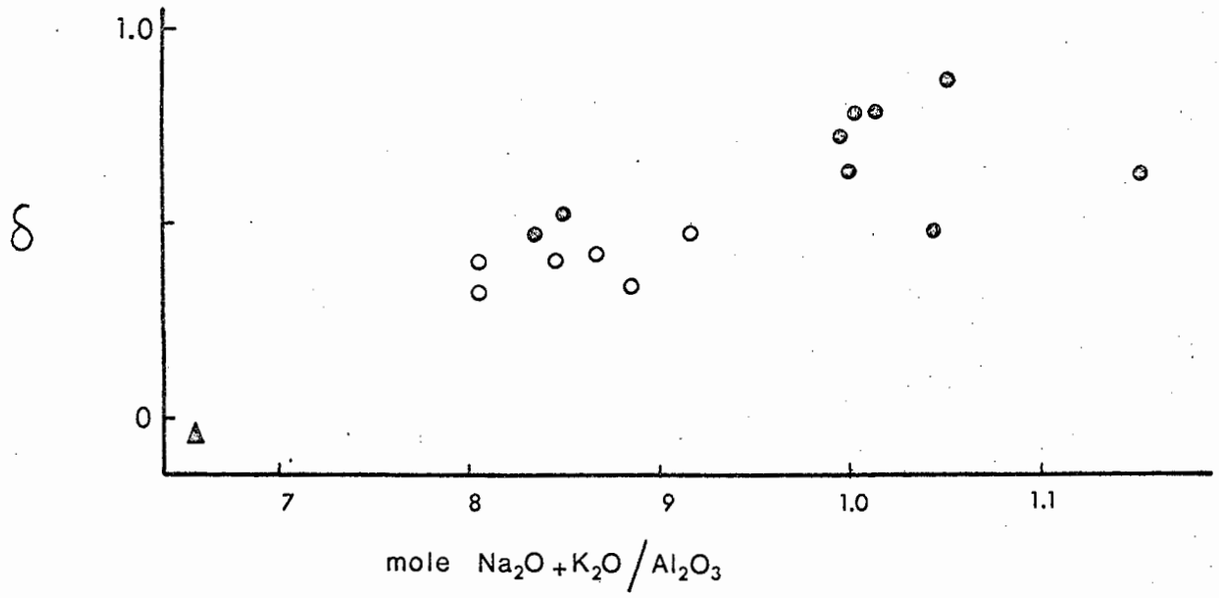

Figure 37. Agpaitic Index vs δ .

o - Drachenberg Syenites

● - Pomona Syenites

These postulates are well supported by the data from the Luderitz Province. The three intrusions can be considered to have experienced similar cooling histories. The Drachenberg rocks are all sub-aluminous and saturated to oversaturated, and display the lowest degree of ordering of all the oversaturated syenites measured. The Pomona syenites, crystallizing in a progressively increasing peralkaline environment, display more ordered K-feldspars and a distinct positive correlation between and the peralkaline index, mole $Na_2O + K_2O/Al_2O_3$ (Figure 37).

It is noteworthy that Parsons and Boyd's (1971) paper concerned itself with intrusive sequences which are largely oversaturated and drew on support from the experimental evidence of Martin (1969a) in presenting their case. The latter work records the relative ease with which low albite was synthesised from gels having compositions on the join $NaAlSi_3O_8$ - $Na_2Si_2O_5$, i.e. in the presence of excess Na and excess Si. Martin (1969b) identified aNa^+/aH^+ in the aqueous phase as being critical to the rate of ordering of the feldspars in his experiments, and apparently the presence of $Na_2Si_2O_5$, when dissociated in the aqueous phase, insured optimum values for these ratios. Furthermore, his work showed that the presence of NaF, NaCl, Na_2CO_3, led not only to less ordered structural states in the feldspars, but affected ordering to varying extents. In the undersaturated environment, aqueous solutions of these salts are likely to be important in the fluid/volatile phase. The occurrence of fluorite, cancrinite, and sodalite in many of the foyaites and tinguaites attests to the variable distribution of F^-, Cl^-, and CO_3^- in the peralkaline undersaturated rocks during crystallization, and hence variable aNa^+/aH^+ and aK^+/aH^+. It thus seems possible to account qualitatively for the ordering - composition relationships illustrated in Figures 35 and 36, in the undersaturated rocks of the Luderitz Province.

7.8.1.4. Summary

(1) All the feldspars studied exhibit structural states intermediate between Orthoclase and Maximum Microline.

(2) Feldspars from the sub-aluminous rocks of the Drachenberg intrusion show a high incidence of anomalous cell dimensions. The structural state of both normal and anomalous feldspars is Orthoclase - the most disordered of any in the oversaturated syenites.

(3) For the Pomona syenites and the oversaturated dyke rocks of the province there is a distinct correlation between the degree of order of the K-feldspars and the degree of fractionation in the host rock.

(4) For the undersaturated rocks, anomalous feldspars are common, and there is no clear correlation between ordering in the feldspars and degree of fractionation in the host rock.

(5) The features exhibited by the feldspars in the province, support the findings of Martin's (1969a, 1969b) experimental work. Ordering is facilitated by peralkaline aqueous solutions in silica oversaturated environments, but may be impeded in the presence of aqueous solutions of alkali halide and carbonate salts.

7.9. MINERAL CHEMISTRY AND CRYSTAL FRACTIONATION

7.9.1. Biotites and Amphiboles

The compositions of the hydrous minerals indicate that during the early stages in the fractionation development of the oversaturated rocks at Pomona, the 'normal' trend of increasing substitution of Fe for Mg with increasing fractionation is reversed. In contrast, in the development of the undersaturated suite, the normal trend of iron enrichment is followed.

Table 27 presents Fe/Fe+Mg data for whole rocks and hydrous minerals in both suites of rocks. In the undersaturated suite, Fe/Fe+Mg in the biotites and the whole rock are the same, and the ratio increases steadily with increasing fractionation. There is no whole rock data for GM137 but the arfvedsonite which coexists with the biotite has an Fe/Fe+Mg ratio distinctly different to the biotite but of similar magnitude.

In the oversaturated suite the coexisting biotite and the amphibole have the same Fe/Fe+Mg ratios, increasing from PM64 to PM157 then decreasing regularly through the Inner Syenite to the Hub Syenite. However the Fe/Fe+Mg ratio in the whole rocks do not reflect this trend, nor are they the same as the ratios observed in the minerals. The whole rock Fe/Fe+Mg ratios only show a slight decrease in the Hub Syenite, otherwise they increase from the cumulate, PM64, to the nordmarkite ring dyke, PM66, the latter having the same ratio as the Inner Syenite.

TABLE 27

Fe/Fe+Mg ratios for whole rock and mafic minerals from Granitberg and Pomona

OVERSATURATED SUITE

SAMPLE	WHOLE ROCK	BIOTITE	AMPHIBOLE	CLINOPYROXENE
PM64	0,76	0,68	-	0,39 - 0,57
PM157	0,80	0,75	0,75	0,49 - 0,59
PM60	0,95	0,64	0,65	-
PM127	0,87	0,60	0,59	0,65 - 0,82
PM66	0,95	-	0,88	-

UNDERSATURATED SUITE

GM146	0,77	0,78	-	0,47
GM350	0,86	0,87	-	0,92
GM147	0,91	0,92	-	0,68 - 0,95
GM137	-	0,94	0,90	0,77 - 0,97

Also of importance is that the whole rock ratio is at all stages greater than the ratio of the coexisting biotite and amphibole.

Data for Na-pyroxenes coexisting with the hydrous minerals are also presented in Table 27. The pyroxenes are zoned, yet in the oversaturated suite they have lower ratios than not only the whole rock, but the hydrous minerals as well. In contrast, in the undersaturated suite, except for the initial member of the trend (GM146), the pyroxenes (or in zoned pyroxenes, the rims) have a higher ratio than both the biotites and the whole rock.

The only other mineral of importance for which no data is reported is an Fe-Ti oxide. No Mg of significance was detected in the analysed Ti-magnetites (Table 24), and the Fe/Fe+Mg ratio for this mineral is effectively unity. If magnetite was the first mineral to crystallize the Fe/Fe+Mg ratio in the liquid would decrease, i.e. the liquid would be relatively enriched in Mg. The data in the undersaturated suite indicate that Fe and Mg are distributed proportionately between liquid and biotite, thus, if the biotite and amphibole crystallized sometime after magnetite, the ratios for these hydrous minerals would reflect the ratio in the liquid at the time of crystallization, i.e. the ratio will be less than the ratio for the whole rock.

From the data in Table 27 it appears that magnetite crystallized early at all stages of fractionation in the oversaturated suite, followed by the mafic silicate minerals. Since PM127 has a lower whole rock ratio than PM60 it would appear that magnetite fractionation occurred during the evolution of the Hub Syenite.

Reports of Mg enrichment in minerals, or even in successive liquids, in a fractionation series are not common. Carmichael (1963) reported Mg-rich pyroxenes in acid glasses and proposed a process similar to that described above to account for their composition. Carmichael (1967) presented more data on acid volcanics, similar to that for the oversaturated suite in Table 27. He also noted that an Fe-Ti oxide appeared before biotite and amphibole in many of these volcanics.

Although early appearance of an Fe-Ti oxide in crystallizing liquids is a common occurrence, precipitation of large amounts of the oxide before the appearance of other mafic phases seems to require unusually high oxidizing conditions (Hamilton et al, 1964). It is also important to note that in leucocratic rocks mafic minerals form only a small percentage of the rock, thus their com-

position will be very sensitive to even moderate amounts of magnetite precipitation. In contrast, extensive magnetite crystallization is required to notably modify the Fe/Mg ratio in a liquid of basaltic composition.

The work of Eugster and Wones (1962) and Wones and Eugster (1965) has shown that a hydrous phase such as biotite is compositionally sensitive to the fO_2 conditions under which it crystallizes. Oxygen fugacity exercises a similar control on the composition and stability of amphibole (Ernst, 1968; Charles, 1973).

In a crystallizing magma where fO_2 is held constant or increases, the Fe/Fe+Mg in the biotite will remain constant or decrease (Wones and Eugster, 1965; Mueller, 1971). This appears to be the situation in the oversaturated suite, and it might be expected that amphiboles will react to constant fO_2 conditions in a similar manner. Since the 'normal' behaviour of fO_2 which is being internally buffered (Carmichael and Nicholls, 1967), is to fall with falling temperature, a constant fO_2 is indicative of an oxidizing trend (Osborn, 1959, 1962). It might be impossible to decide whether Mg-rich biotites are a direct result of high fO_2 conditions during crystallization, or of prior precipitation of abundant magnetite which radically alters the Fe/Mg ratio in the liquid. Since both these processes are a result of high fO_2 the distinction is probably superficial.

In summary, the compositions of the biotites and amphiboles in the oversaturated trend indicate that during the development of the suite, fO_2 remained constant or increased. An Mg-enrichment trend was produced which is reflected in the mineral compositions and, to a lesser extent in the whole rock compositions. The unusual fO_2 conditions resulted in early crystallization of Ti-magnetite, thus there are large differences in the Fe/Fe+Mg ratios of the whole rocks and their mafic minerals.

In the undersaturated suite the Fe/Fe+Mg ratio in the whole rock and the biotites is the same for successive fractions, and the ratio increases steadily with increasing fractionation. The undersaturated suite therefore crystallized under normally evolving fO_2 conditions, and crystallization of abundant Ti-magnetite did not preceed the crystallization of biotite.

7.9.2. Pyroxenes

The presentation of the clinopyroxene analyses in Figure 33 indicates that both suites crystallize similar pyroxenes during the early stages of fractionation, but in later stages, the pyroxene composition trends for each suite diverge considerably. For a given Na content in the pyroxenes, the oversaturated suite crystallizes more Mg-rich pyroxenes than in the undersaturated suite. Figure 38 compares the two pyroxene crystallization trends with other trends reported in the literature. It is clear that the oversaturated trend is Mg-rich in comparison to most other trends.

It has become increasingly clear that Na-pyroxenes in a given rock series conform to a unique path in terms of the compositional end-members, Diopside, Hedenbergite, and Acmite. Stephenson (1972) has recently suggested that in undersaturated rocks the pyroxenes show early enrichment in $NaFe^{+++}$ relative to the $CaMg - CaFe^{++}$ substitution, whereas in oversaturated rocks a marked trend toward hedenbergite is developed before $NaFe^{+++}$ enrichment commences to any extent. This is the reverse of the trend pattern exhibited in the Luderitz Province rocks.

Following the discussion on Mg enrichment in biotites and amphiboles, it appears that the Mg-enrichment in the pyroxenes in the oversaturated syenites can best be explained by considering the fO_2 environment in which they crystallized. A pyroxene crystallizing from a liquid which has been depleted in Fe by magnetite precipitation under high fO_2 conditions will be Mg rich. Wones and Eugster (1965, p. 1262 and figure 13) have indicated that the pyroxene crystallizing with biotite in an oxidizing trend will be Mg rich.

Thus the position of pyroxene crystallization trends in the ternary Di - Hd - Ac plot have little to do with bulk chemical composition of the host rock (i.e. whether it is silica over- or undersaturated), but rather with the fO_2 and temperature of crystallization, and the order in which mafic minerals appear on the liquidus. Stephenson (1972) did note that fO_2 was critical to the early enrichment of $NaFe^{+++}$ in the pyroxenes, but was wrong in suggesting that highly oxidizing conditions are the perogative of nepheline syenites. In this respect it is interesting to note that the fO_2 conditions under which salic undersaturated liquids crystallize, are calculated to be some of the lowest of any igneous liquid (see section 8.4. of this thesis; Nash et al, 1969; Nash and Wilkinson, 1970).

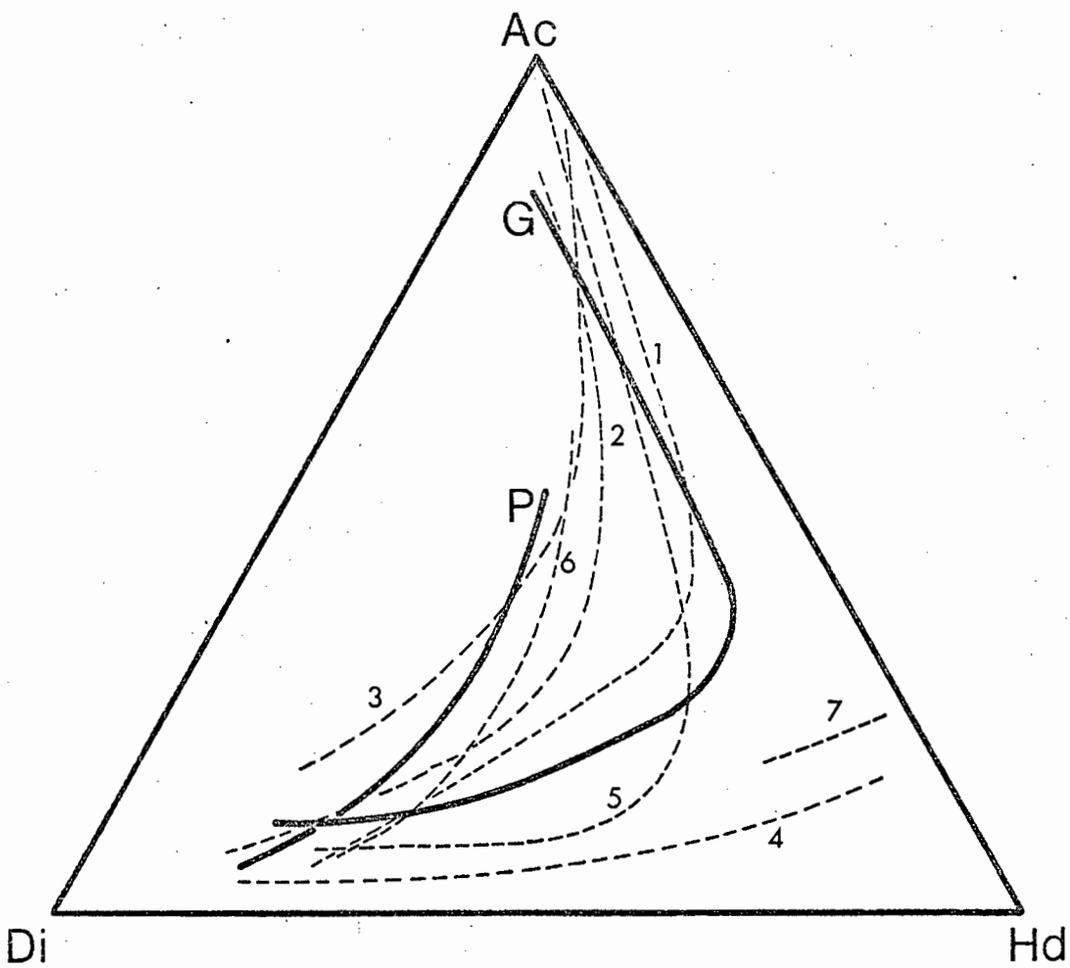

Figure 38. Comparison of Luderitz Province pyroxene composition trends with those from other suites and provinces.

G - Granitberg

P - Pomona

1 - Morutu, Sakhalin (Yagi, 1953)

2 - Uganda (Tyler and King, 1967)

3 - Itapirapua (Gomes et al, 1970)

4 - Alkali basalt-trachyte series (Aoki, 1964)

5, 6 - South Qoroq, Greenland (Stephenson, 1973)

7 - Pantellerites (Carmichael, 1962)

CHAPTER 8

ESTIMATES OF SILICA ACTIVITY, OXYGEN FUGACITY, AND TEMPERATURE OF CRYSTALLIZATION

One of the most useful applications of the compositions of coexisting minerals is their use with standard thermodynamic data in determining pressure, temperature, and the fugacity of any gas phases present during crystallization.

These methods stem from important experimental studies of Wones and Eugster (1965), Eugster and Wones (1962), and Buddington and Lindsley (1964), and from the theoretical considerations of Eugster and Skippen (1967), Nicholls et al, (1971), Carmichael et al, (1970), and Nicholls and Carmichael (1972). Excellent examples of the application of these methods to solving petrological problems are given in these abovementioned papers and in Nash and Wilkinson (1970), Carmichael and Nicholls (1967), Mitchell (1972) and Stormer (1972).

8.1. THE THERMODYNAMIC DATA

Gibbs' free energy data for the minerals and related substances used in this section are listed in Table 28. Most of the data is from Robie and Waldbaum (1968) but some is from other sources, all of which are listed in the table. Some of the data were derived by the writer using a variety of sources and methods. These procedures are outlined below.

For ulvospinel ΔH°_{f298} was calculated from entropy data in Robie and Waldbaum (1968) and ΔG°_{f298} from Verhoogen (1962). ΔG°_{fT} for ulvospinel was then calculated with this data using the free energy function given in Robie and Waldbaum (1968).

The data for annite was calculated in a similar fashion, using ΔG°_{f298} and ΔS°_{f298} from Zen (1973) to estimate ΔH°_{f298}. There is no listing of the free energy function for annite, but at 298.15°K, the free energy function,

$$-\left(\frac{G^{\circ}_{T} - H^{\circ}_{298}}{T}\right) = S^{\circ}_{298}$$

and

$$\Delta\left(\frac{G^{\circ}_{T} - H^{\circ}_{298}}{T}\right) = -\Delta S^{\circ}_{f}$$

These functions vary only slightly with temperature. Between $298^{o}K$ and $1200^{o}K$ for fluorphlogopite

$$\frac{d\left[\Delta\left(\frac{G^{o}_{T} - H^{o}_{298}}{T}\right)\right]}{dT} \sim 0.3 \text{ cal mole}^{-1}\text{deg}^{-1}$$

If we assume a similar variation in the free energy function for annite over the same T range, we can estimate G^{o}_{fT} for annite with reasonable accuracy.

For phlogopite, Bird and Anderson's (1973) estimate of ΔG^{o}_{f298} was used with the entropy value listed in Robie and Waldbaum (1968) to calculate ΔH^{o}_{f298}. ΔG^{o}_{fT} was then calculated using the free energy function for fluorphlogopite after correction to the S^{o}_{298} value for phlogopite.

8.2. ASSUMPTIONS MADE IN THE CALCULATIONS

A. Members of solid solution series are considered to mix ideally, except where there are quantitative expressions for the departure from ideality. Therefore activity, a, is in most cases taken as being equal to the mole fraction, x, with allowances made for an entropy of mixing correction (assuming random mixing) where an atom may occupy more than one site.

e.g.

$$a_{FeSiO_3} = x_{FeSiO_3}$$

$$a_{Mg_2SiO_4} = \left(x_{Mg_2SiO_4}\right)^2$$

$$a_{Mg_7Si_8O_{22}(OH)_2} = \left(x_{Mg_7Si_8O_{22}(OH)_2}\right)^7$$

Recent Mossbauer spectroscopic work has revealed that most atoms have site preferences in the lattices of members of a solid solution series, and random mixing seldom, if ever, occurs. However quantitative expression for departure from ideality in most solid solutions is lacking. Although the

TABLE 28

Free Energy data used in calculations in chapter 8

$-\Delta G^{\circ}_{fT}$

$T^{\circ}K$	800°	900°	1000°	1100°	1200°	1300°	REFERENCE
ACMITE	505,56	492,15	479,6	466,6	453,0		1
AENIGMATITE	1698,3	1658,9	1616,7	1576,0	1534,2		1
ALBITE	793,643	775,802	757,839	739,866	721,521	701,740	2
ANNITE	1007,2	979,3	951,5	925,6	895,9		3
DIOPSIDE	655,841	642,093	628,241	614,389	600,454	586,512	2
FERROSILITE	235,69	229,79	224,08	218,21	212,41		4
ILMENITE	246,742	240,822	234,920	229,003	223,044	217,062	2
MAGNETITE	203,52	196,23	189,11	182,00	174,78	167,57	5
NEPHELINE	422,987	413,761	404,364	394,941	385,121	373,854	2
PEROVSKITE	343,122	336,611	330,130	323,671	317,036	310,335	2
PHLOGOPITE	1250,5	1223,1	1195,1	1165,8	1135,9		3
QUARTZ	182,905	178,680	174,494	170,325	166,175	162,039	2
ORTHOCLASE	803,577	786,047	768,405	749,759	730,413	711,147	2
SILICA GLASS	182,222	178,075	173,943	169,838	165,748	161,684	2
SODIUM DISILICATE	493,4	482,4	471,8	461,1	450,7	439,9	6
SPHENE	531,967	520,907	509,906	498,906	487,773	476,589	2
STEAM	48,644	47,353	46,040	44,709	43,373	42,028	2
TREMOLITE	2487,580	2430,170	2372,150	2314,120			2
ULVOSPINEL	299,97	292,56	285,16	277,70	270,77		3

1. Nicholls and Carmichael (1969)
2. Robie and Waldbaum (1968)
3. See section 8.1.
4. Anderson (1971)
5. Haas and Robie (1973)
6. Kelley (1962)

assumption of ideality produces errors, the mole fractions are always applied to equilibrium equations where the errors in the reactants tend to be cancelled by the errors in the products of the reaction.

B. Where equations expressing the mineralogy of the rock are presented, the phases in the equation (whether solid or gaseous or liquid) are assumed to exist in mutual equilibrium over a range in temperature. In coarse-grained, holocrystalline rocks this assumption is not necessarily valid, but is adequate for the purpose to which it is applied here.

C. In some of the calculations an estimate of P_{H_2O} (or P_{TOTAL} if it is assumed that $P_{TOTAL} = P_{H_2O}$) is necessary. It is possible to estimate P_{TOTAL} using silica activity data of Nicholls et al. (1971). This has not been possible here. P_{TOTAL} may also be calculated from a knowledge of the cover rock thickness at the time of crystallization of an intrusive body, but again this has not been possible. Since the intrusions have all the characteristics of subvolcanic ring complexes, P_{TOTAL} was probably not greater than 1 Kb. For the calculations $P_{TOTAL} = P_{H_2O} = 0.5$ Kb has been assumed.

D. It has been assumed that the fluid phase consists entirely of H_2O, H_2, and O_2. This is certainly incorrect as a number of halogen bearing phases (sodalite, fluorite) have been identified in the rocks, attesting to the presence of F, Cl, CO_2, and possibly SO_2 as well. Without determinations of these substances in the minerals or whole rocks it is impossible to estimate the fugacity of these species. However H_2O is probably the dominant constituent in the fluid phase and the assumption is therefore a valid approximation.

8.3. ESTIMATION OF SILICA ACTIVITY

Several of the equations in the oxygen fugacity calculations involve silica. Since quartz is either absent, or is a product of final crystallization (in the Pomona syenites) an expression for the silica activity in the liquids from which the syenites crystallized is required.

For the nepheline syenites the silica activity is buffered by the reaction:

$$\tfrac{1}{2}NaAlSiO_4 + SiO_2 \rightleftharpoons \tfrac{1}{2}NaAlSi_3O_8 \quad \ldots\ldots\ldots\ldots \quad (1)$$

nepheline glass albite

where for pure phases at equilibrium,

$$\Delta G_r^o = 0$$

$$\log a^{\text{liquid}}_{SiO_2} = \frac{\Delta G_r^o}{2{,}303RT} \quad \ldots\ldots\ldots\ldots \quad (2)$$

Since both nepheline and albite form solid solutions in the rocks in question, equation (2) has to be corrected for the reduced activities of albite in the alkali feldspar solid solution, and nepheline in the nepheline-kalsilite solid solution series.

Equation (2) thus becomes

$$\log a^{\text{liquid}}_{SiO_2} = \frac{\Delta G_r^o}{2{,}303RT} + \tfrac{1}{2}\log a^{\text{feldspar}}_{\text{albite}} - \tfrac{1}{2}\log a^{\text{feldspathoid}}_{\text{nepheline}} \quad \ldots\ldots\ldots \quad (3)$$

At $P > 1$ bar a correction term, $\frac{\Delta V^o}{2{,}303RT} \cdot (P - 1)$, where ΔV^o is the volume change of the solids accompanying the reaction and P is in bars, must be applied to equation (3). Thus

$$\left(\log a^{\text{liquid}}_{SiO_2}\right)_{P = P \text{ bars}} = \frac{\Delta G_r^o}{2{,}303RT} + \frac{\Delta V^o}{2{,}303RT}(P-1) + \tfrac{1}{2}\log a^{\text{feldspar}}_{\text{albite}} - \tfrac{1}{2}\log a^{\text{feldspathoid}}_{\text{nepheline}} \quad \ldots\ldots\ldots \quad (4)$$

For $P < 10$ Kb the pressure correction term is negligible and has been ignored in the sections that follow.

Using data from Nicholls et al. (1971), the determined compositions of alkali feldspar and nepheline for the rocks in question, and the activity coefficients for alkali feldspars calculated from data in Thompson and Waldbaum (1969), the variation of $\log a_{SiO_2}$ with temperature has been calculated and plotted in Figure 39.

GM147 has the highest silica activity for any temperatures, yet in the petrographic sense it is the most silica undersaturated of the nepheline syenites, in terms of normative and modal nepheline, and in Wt% SiO_2. This emphasises one

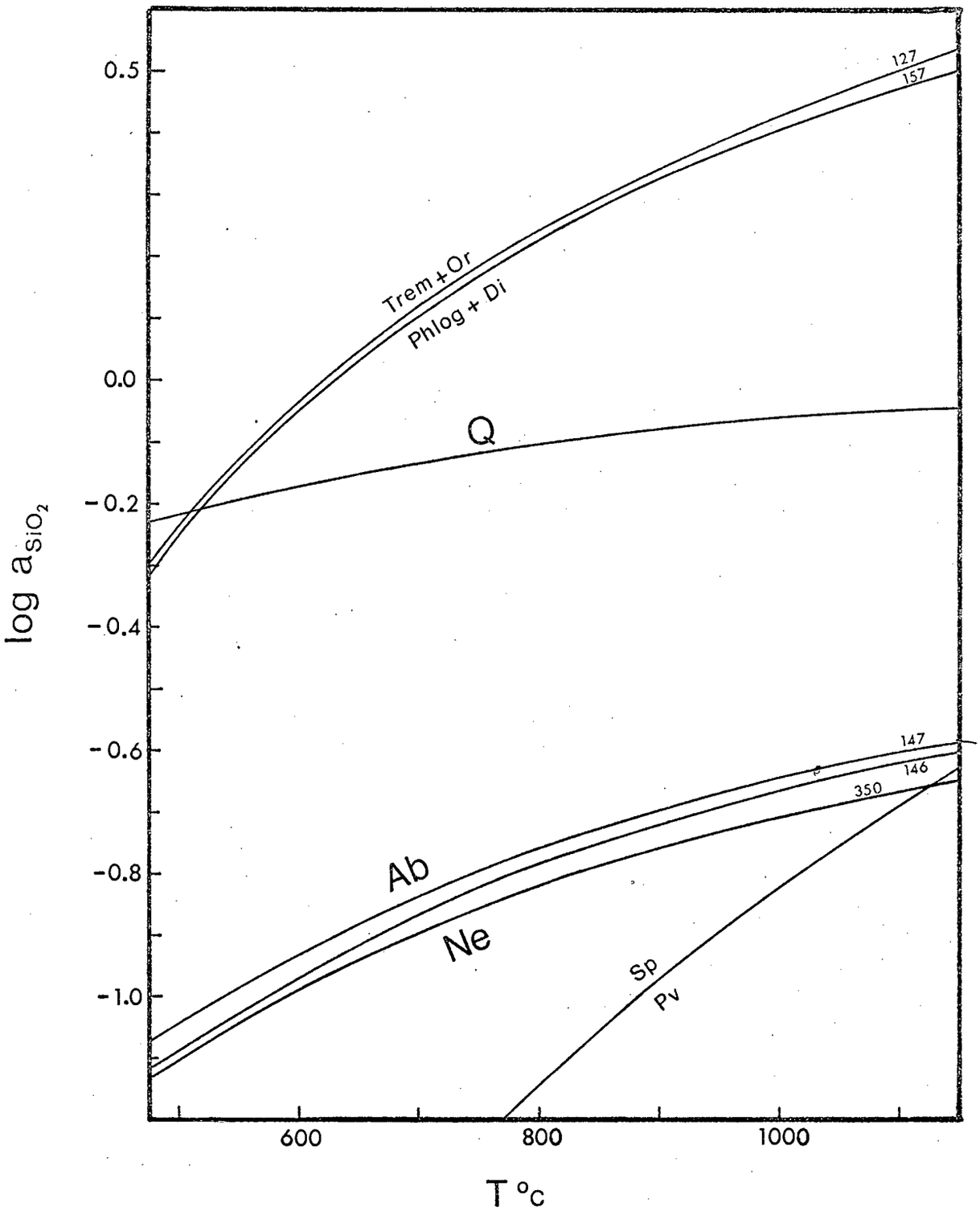

Figure 39. $\log a_{SiO_2}$ vs T for the undersaturated Granitberg syenites (146, 350,147) defined by reaction (1), and for the Pomona oversaturated syenites (127, 157) defined by reaction (6). Curve Q, is for a liquid in equilibrium with quartz. Sp - Pv is the curve defined by the sphene - perovskite buffer (Nicholls et al, 1972)

of the important characteristics of silica activity - that in detail it need not vary sympathetically with any of the common silica undersaturation indicators.

If the mineralogy of any of the undersaturated rocks defines a silica buffer other than reaction (1), then the equations of type (4) for each buffer can be equated and solved simultaneously for P and T (see Nicholls et al., 1971).

The coexistence of sphene and perovskite in the Inner Foyaite (GM350) is one such alternative buffer. The variation of $\log a_{SiO_2}$ with T for this buffer (Nicholls et al, 1971) intersects the nepheline-albite buffer for GM350 at $\log a_{SiO_2} = -0{,}65$ and $T = 1400^{\circ}K$ ($1127^{\circ}C$). This temperature is higher than liquidus temperatures determined for nepheline syenites under mild pressure (1,0 Kb P_{H_2O}) (Sood and Edgar, 1970; Millhollen, 1971), and also higher than the experimentally determined liquidus of etindites ($1118^{\circ}C$ - Tilley and Thompson, 1972) which carry phenocrysts of both sphene and perovskite.

The presence of perovskite in GM350 is therefore unlikely to be due to silica activity alone, and it is shown in section 8.5. of this work that fO_2 plays an equally important part in stabilising perovskite in the foyaite. The sphene-perovskite buffer cannot therefore be used to determine P, T, of equilibration.

The reaction

$$\tfrac{1}{2}NaFeSi_2O_6 + 1/4KFe_3AlSi_3O_{10}(OH)_2 + SiO_2 \rightleftharpoons 1/4Na_2Fe_5Si_8O_{22}(OH)_2 + 1/4KAlSi_3O_8 \quad \ldots\ldots \quad (5)$$

acmite annite glass riebeeckite K-feldspar

represents the common occurrence of a clinopyroxene, biotite and Na-amphibole in undersaturated and saturated syenites, and is a potentially useful silica buffer for these rocks. However free energy data for annite, acmite and especially riebeeckite are too imprecisely known for this buffer to be of much value. The value of $\log a_{SiO_2}$ is very sensitive to variations in ΔG_r°, therefore precise knowledge of ΔG_f° for the phases in the buffer reaction is critical for reliable use of the silica activities for P, T, estimates. Furthermore, riebeeckite has a limited stability range with respect to temperature which limits the application of reaction (5). However the use of other amphibole compositions (e.g. Mg-riebeeckite), with accompanying free energy data, might render reactions similar to (5) useful for alternative silica activity determinations in peralkaline undersaturated rocks.

The absence of nepheline in the Pomona syenites does not allow reaction (1) to be used to estimate silica activity in these rocks. Instead, the reaction

$$1/4KMg_3AlSi_3O_{10}(OH)_2 + \tfrac{1}{2}CaMgSi_2O_6 + SiO_2 \rightleftharpoons 1/4KAlSi_3O_8 + 1/4Ca_2Mg_5Si_8O_{22}(OH)_2 \quad \ldots\ldots \quad (6)$$

phlogopite diopside glass K-feldspar tremolite

expresses the mineralogy of these rocks if the tremolite composition is taken to represent the edenite and alkali amphiboles in the syenites.

Log a_{SiO_2} vs T for this reaction is illustrated in Figure 39, and falls at higher silica activities than reaction (1). Also plotted is the log a_{SiO_2} vs T variation for the reaction

$$SiO_2 \rightleftharpoons SiO_2 \quad \ldots\ldots\ldots\ldots \quad (7)$$

glass quartz

for which

$$\log a^{liquid}_{SiO_2} = \frac{\Delta G^\circ_r}{2{,}303RT} \quad \ldots\ldots\ldots\ldots \quad (7a)$$

which illustrates the variation of silica activity in a liquid in equilibrium with quartz (Nicholls et al., 1971; Carmichael et al., 1970).

Above 510°C the curve for reaction (6) lies above that for reaction (7). This indicates that the syenites are effectively saturated with quartz for any T > 510°C, yet quartz only appears in these rocks during the final stages of crystallization of PM127.

Wones (1970) has indicated that the left hand side of reaction (6) is stable at high temperature and the tremolite-K-feldspar assemblage at low temperature. The thermochemical data for (6) as represented in Figure 39 is in agreement with Wones (1970).

Therefore the reaction as written in (6) is not a reaction valid for quartz-absent assemblages at magmatic temperatures and cannot be used to define the activity of silica for the purposes required here.

It is thus impossible to define the silica activity in the liquids from which the Pomona syenites crystallized. Since they contain no nepheline, and

PM127 only precipitates quartz at the close of its crystallization their silica activities must lie somewhere between those defined by reaction (1) and reaction (7).

8.4. ESTIMATION OF OXYGEN FUGACITY

In section 7.9. the importance of oxygen fugacity in the development of the fractionation series was emphasised. It is possible to make estimates of fO_2 and T of crystallization from the available mineral and thermodynamic data.

Since biotite, alkali feldspar and magnetite are present in nearly all the over and undersaturated rocks, the oxygen fugacity can be defined by the reaction:

$$\underset{\text{annite}}{2KFe_3AlSi_3O_{10}(OH)_4} + \underset{\text{gas}}{O_2} \rightleftharpoons \underset{\text{K-feldspar}}{2KAlSi_3O_8} + \underset{\text{magnetite}}{2Fe_3O_4} + \underset{\text{steam}}{2H_2O} \quad \ldots\ldots\ldots \quad (8)$$

for which

$$\log fO_2 = \frac{\Delta G_r^o}{2{,}303RT} + 2\log a^{\text{feldspar}}_{\text{k-feldspar}} + 2\log a^{\text{Ti-magnetite}}_{\text{magnetite}} + 2\log fH_2O - 2\log a^{\text{biotite}}_{\text{annite}} \quad \ldots\ldots\ldots \quad (9)$$

For pure phases

$$\log fO_2 = -\frac{6876}{T} - 16{,}64 \quad \ldots\ldots\ldots \quad (10)$$

(Nash and Wilkinson (1969) after Wones and Eugster (1965)).
More recently Wones (1972) has given for reaction (8) the expression (for pure phases)

$$\log fO_2 = -\frac{14818}{T} - 8{,}50 \quad \ldots\ldots\ldots \quad (11)$$

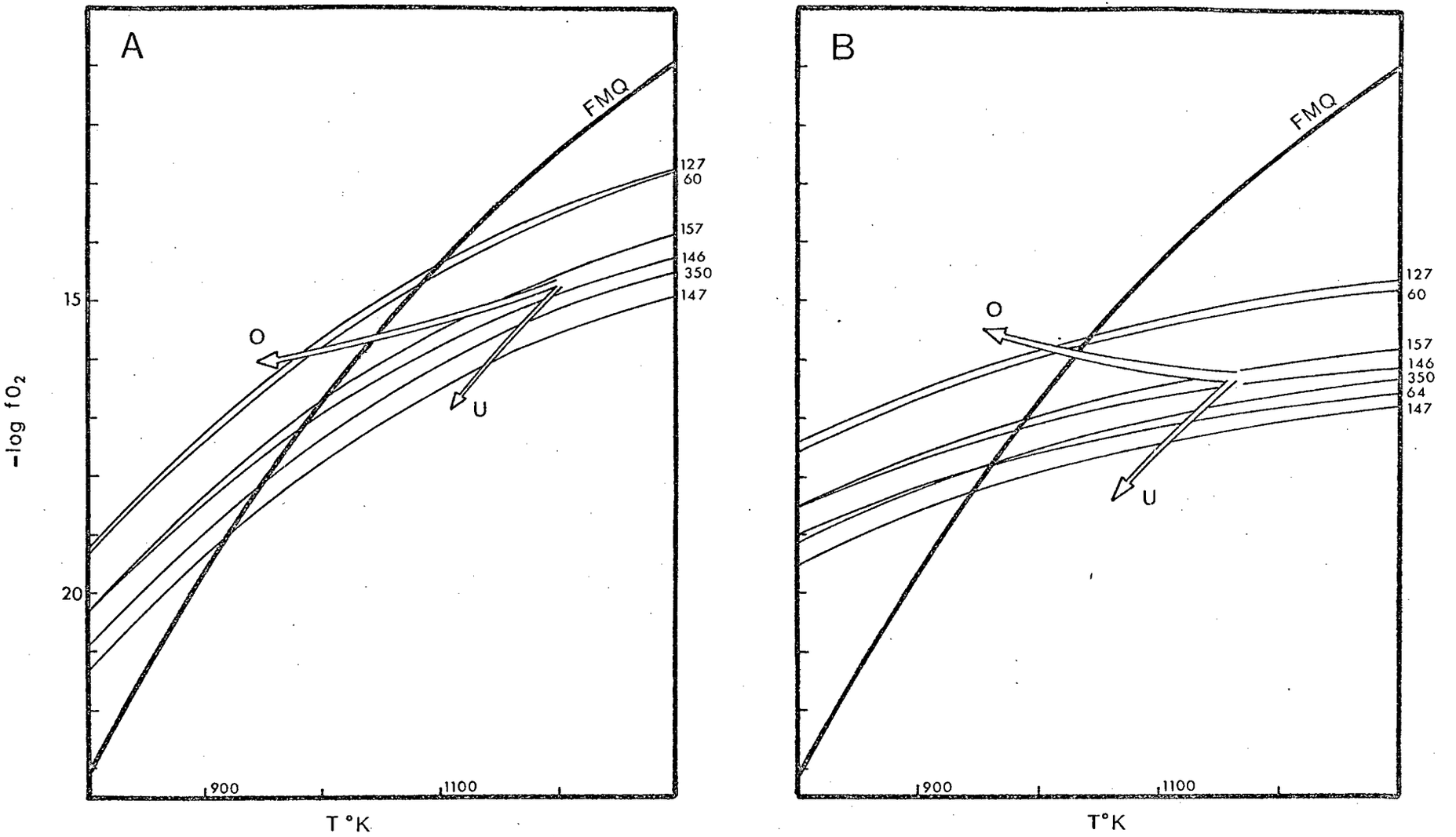

Figure 40. Biotite breakdown curves (reaction (8)) in fO_2 - T space according to reaction (11)(figure A) and reaction (10)(figure B). FMQ is the quartz-fayalite-magnetite buffer curve after Wones and Gilbert(1969). The arrow O, is the hypothetical trend for the Pomona Syenites, and the arrow U, is the Trend for the Granitberg Foyaites.

The variation of log fO_2 with T for (8) has been calculated from expression (10) and (11) with the necessary corrections for the reduced activities of the phases in the reaction. For the logarithm correction terms the compositions of the minerals in each rock were used (with estimates of Ti-magnetite compositions for PM60, GM146 and GM350), and in addition fH_2O was derived from tables of Burnham et al. (1969) assuming $P_{H_2O} = 0,5$ Kb.

The log fO_2-T curves are plotted in Figure 40. Also plotted is the position of the QFM synthetic buffer (Eugster and Wones, 1962) using the expression given by Wones and Gilbert (1969). Although the relative position of the log fO_2-T curves derived from (10) and (11) is the same, their absolute position differs. The curves derived using (11) are steeper and lie at lower values of log fO_2 for $T < 1000^oK$, and at higher log fO_2 for $T > 1000^oK$, than those calculated from (10).

In a liquid or fractional crystallization sequence controlled by an internal buffer (Carmichael and Nicholls, 1967) ($\equiv$ crystallization under constant total composition of Presnall (1966) and Osborn (1959)), the decrease in fO_2 with T is in a manner parallel to the synthetic oxygen buffer curves (Nash and Wilkinson, 1970; Eugster and Wones, 1965). This is the orientation of a line drawn to intersect the curves given by (9) for GM146, GM350 and GM147 at successively lower temperatures (Figure 40). Thus if GM146, GM350, and GM147 are indeed successive liquid fractions (as the mineralogy, chemistry and field relations indicate) derived at successively lower temperatures, then the oxygen fugacity in the fractionating magma from which they were derived, was internally buffered. Moreover the fO_2 conditions under which they subsequently crystallized was also internally buffered. Similar conclusions were also made in section 7.9.1.

Whether or not fO_2 was controlled by crystal-liquid equilibrium, or by the composition of a coexisting fluid phase cannot be determined unequivocally as Carmichael and Nicholls (1967) and Mueller (1971) have indicated. The latter author is of the opinion that in felsic magmas with high H_2O content the mass of mafic minerals is too low to have any significant buffering capacity. Instead, fO_2 is controlled by the interaction of the fluid phase with the melt, i.e. fO_2 is controlled by the variation of the H_2O/H_2 ratio of the dissolved water in the melt.

In contrast, a line drawn to intersect the biotite breakdown curves (reaction (8)) of PM157, PM60 and PM127 at successively lower temperatures cuts

sharply across the QFM synthetic buffer curve (Figure 40). If this line represents a crystallization or fractionation path for these rocks then it indicates crystallization under constant, or even increasing fO_2 conditions. Similar conclusions regarding fO_2 conditions for the crystallization of these rocks were made in section 7.9.1.

Constant, or increasing oxygen fugacity conditions during crystallization or fractionation implies open system conditions, where fO_2 is controlled by the composition of the fluid phase from which oxygen may be subtracted, or to which oxygen may be added from an external source.

If Mueller's (1971) contention, that fO_2 in felsic magmas is controlled by the composition of the fluid phase, is correct, then trends such as that described for the Pomona syenites should be more common in a series of related felsic rocks. In subvolcanic magma chambers (which is the setting envisioned for the Pomona complex), open system conditions can be expected to commonly prevail, with the resultant possible effects on the fluid phase composition and the composition of the phases crystallizing from the magma.

As was discussed in section 7.9.1. there is little record of Mg-enrichment or curtailed Fe-enrichment trends in felsic rock suites. This rarity may be more apparent than real. There are few published accounts of fO_2 estimates in a suite of related felsic liquids as described here. More investigations into fO_2 conditions of crystallization of felsic magmas may reveal that conditions of constant oxygen fugacity do commonly prevail.

If two or more oxygen fugacity buffer assemblages can be identified in a rock, then the two buffers may be used to give unique fO_2 and T estimates of equilibration. If the minerals constituting the buffers are extensively zoned, then the fO_2 and T interval of crystallization may be defined. A fine example of this approach is Nash and Wilkinson's (1970) account of the Shonkin Sag laccolith.

The mineralogy of the syenites allows the following reaction to be written:

$$KFe_3AlSi_3O_{10}(OH)_2 + 3SiO_2 \rightleftharpoons KAlSi_3O_8 + 3FeSiO_3 + H_2O \quad \ldots\ldots\ldots\ldots \quad (12)$$

annite glass K-feldspar ferrosilite steam

for which

$$\log fH_2O = \frac{-\Delta G_r^o}{2{,}303RT} + \log a^{\text{biotite}}_{\text{annite}} + 3 \log a^{\text{liquid}}_{SiO_2} - \log a^{\text{feldspar}}_{\text{K-feldspar}} - 3 \log a^{\text{pyroxene}}_{\text{ferrosilite}} \quad .. \quad (13)$$

If H_2O, H_2 and O_2 are the only gas phases present then

$$K_w = \frac{fH_2O}{fH_2 . f^{\frac{1}{2}}O_2} \quad ..... \quad (14)$$

and if $P_{TOTAL} = P_{H_2O} + P_{H_2} = 0.5$ Kb ..... (15)

then

$$fH_2O = \frac{P_{TOTAL} . K_w . f^{\frac{1}{2}}O_2 . \gamma H_2 . \gamma H_2O}{K_w . f^{\frac{1}{2}}O_2 . \gamma H_2 + \gamma H_2O} \quad ..... \quad (16)$$

(Eugster and Wones, 1962). If we substitute fH_2O obtained from (13) into (16) then we may calculate fO_2.

In this manner the fO_2-T variation for each of the rocks was calculated. For the nepheline syenites log a_{SiO_2} is that calculated from equations (1;3). For the Pomona syenites log a_{SiO_2} was estimated. Log $a_{\text{ferrosilite}}$ is the log of the mole fraction of ferrosilite in the clinopyroxenes compositions recalculated in terms of Wo, En, and Fs. The equilibrium constant for water, Kw, is taken from the equation given by Zen (1973), and the activity coefficients of H_2O and H_2 (γH_2O, γH_2) are from Burnham et al. (1969) and Shaw and Wones (1964) respectively.

This procedure for estimating fO_2 is very unsatisfactory as Kw is very large and $fH_2 \gg fO_2$. Thus fO_2 is insensitive to large variations in fH_2O at the moderate pressures considered here. Shaw (1967, p. 535) has shown that at P = 1 Kb and T = 1000°K, fO_2 in the region of 10^{-23} to 10^{-17} bars (typical of many magmatic liquids under these P,T conditions) varies only slightly with variation in fH_2O. Furthermore, variation of fH_2O with variation in the composition of the species in (12) is not reflected in fO_2 especially at high fH_2O. Nevertheless fO_2-T curves from (13, 14, 15 and 16) have been calculated. They are not smooth and the "best fit" curve has been plotted in Figure 41, where they give satisfactory intersections with the biotite breakdown curves (reaction (8)). The fO_2 -T co-ordinates of the inter-

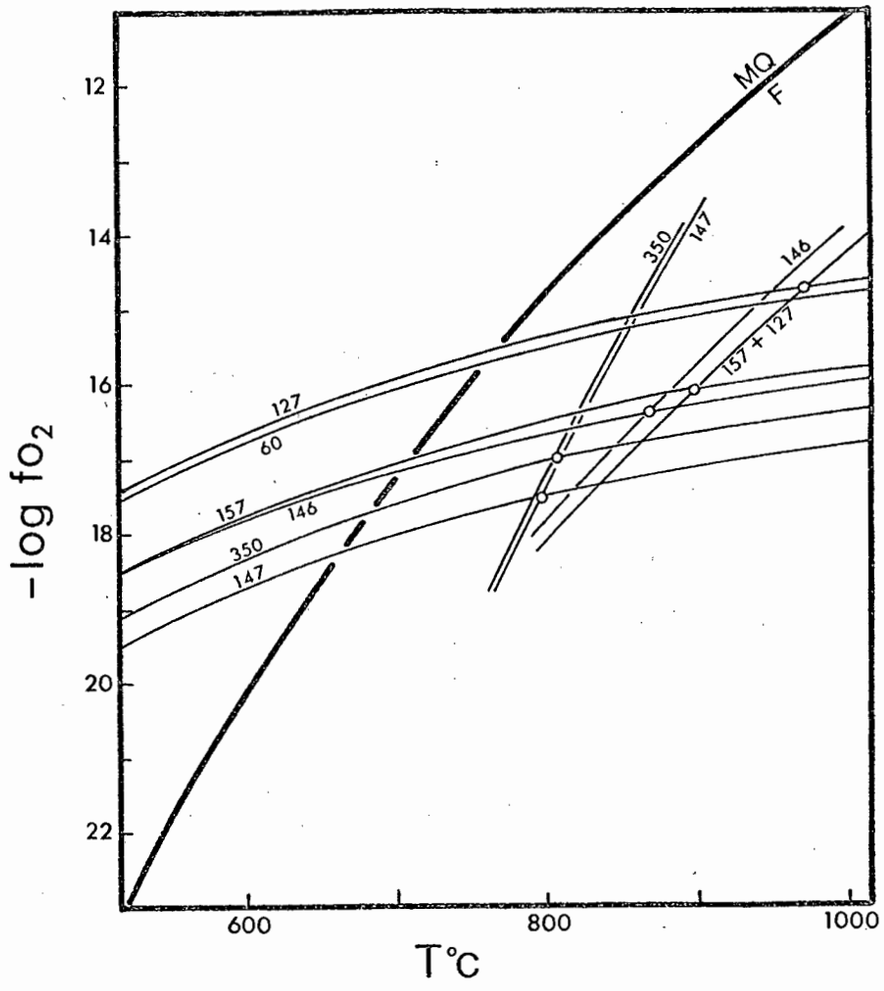

Figure 41. T - fO_2 equillibration data defined by the intersection of curves calculated for reactions (9) and (13).

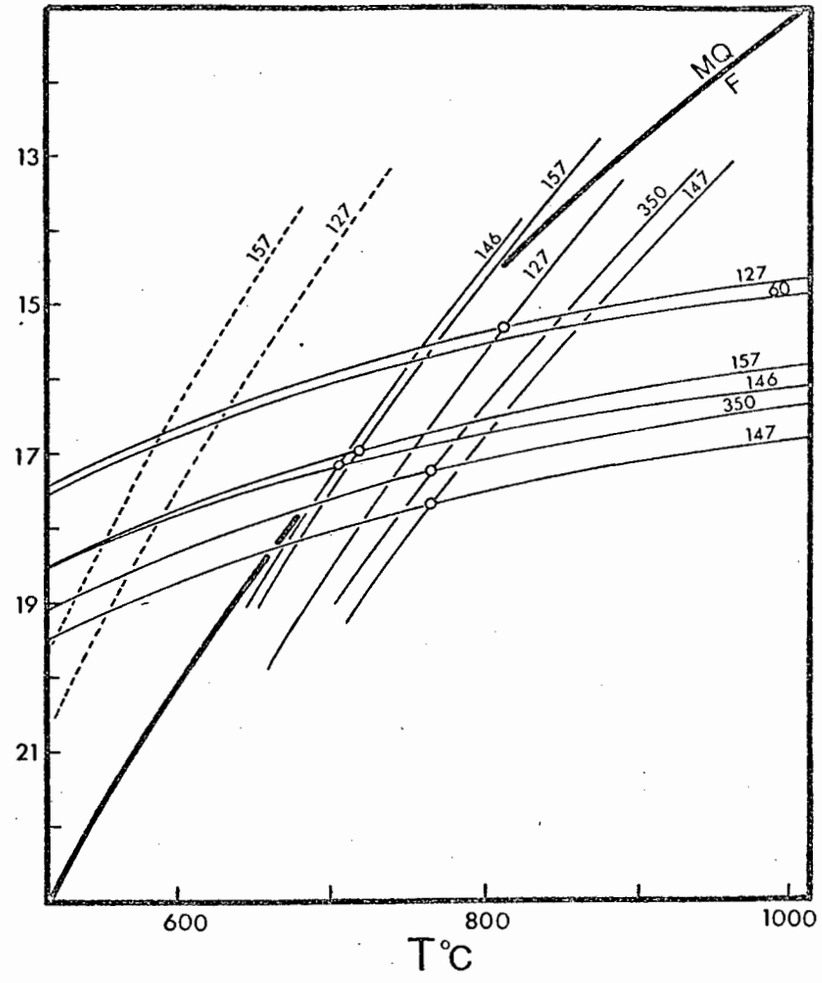

Figure 42. T - fO_2 equillibration data defined by intersection of curves for reactions (9) and (18). Solid curves for (18) assumes silica activity defined by the Ne-Ab buffer. Dashed curve for (18) assumes silica activity defined by the SiO_2 glass-crystals buffer (reaction (7)).

sections of the curves for each rock is listed in Table 29.

An alternative fO_2 buffer is the reaction:

$$6FeSiO_3 + O_2 \rightleftharpoons 2Fe_3O_4 + 6SiO_2 \quad \ldots\ldots\ldots\ldots (17)$$

ferrosilite gas magnetite glass

for which

$$\log fO_2 = \frac{\Delta G^o_r}{2{,}303RT} + 2\log a^{\text{Ti-magnetite}}_{\text{magnetite}} + 6 \log a^{\text{liquid}}_{SiO_2} - 6 \log a^{\text{pyroxene}}_{\text{ferrosilite}} \quad \ldots\ldots\ldots\ldots (18)$$

Two sets of curves relating fO_2 to T for (17) have been calculated for the Pomona syenites. One set was calculated using reaction (1) to define the silica activity, and the other set uses reaction (7). For the nepheline syenite $\log a_{SiO_2}$ is defined by reaction (1).

The curves are plotted together with the curves for the biotite breakdown reaction in Figure 42, and the co-ordinates of intersection are listed in Table 29.

The interpretation of the temperature and oxygen fugacity equilibration data in Table 29, in terms of the crystallization history is complex. The rocks in question are coarse grained and holocrystalline with the constituent minerals, apart from Na-pyroxene, showing slight or no zoning. It is therefore reasonable to assume that the T, fO_2 data represent conditions close to the final crystallization ($>$ 75 to 80% crystals) especially as the composition of the rim of the zoned pyroxenes were used to calculate the logarithm correction term for reduced activity of $FeSiO_3$ in equations (13) and (18).

The one exception is GM146, which is a porphyritic rock and whose phenocryst (nepheline, alkali feldspar, clinopyroxene, biotite and Ti-magnetite) compositions were employed in the calculations. The equilibration data for this rock therefore represent conditions prevailing between the liquidus and final crystallization.

TABLE 29

T - fO_2 equilibration data

SAMPLE	1		2	
	T°C	$\log fO_2$*	T°C	$\log fO_2$*
GM146	880°	-16,5	703°	-17,2
GM350	822°	-17,0	782°	-17,2
GM147	815°	-17,5	782°	-17,2
PM157	910°	-16,1	720°-555°	-17,0 to -18,2
PM60	-	-	-	-
PM127	987°	-14,7	815°-640°	-15,3 to 16,4

Column 1 data for intersection of (10) and (12)

Column 2 data for intersection of (10) and (17)

* fO_2 in bars

Referring to Table 29 the intersection data in columns 1 and 2 for GM350 and GM147 is in fair agreement and indicating that crystallization was essentially complete at temperatures of 780 to 810°C. GM147 however grades into an agpaitic outer zone whose final products of crystallization are astrophyllite and arfvedsonite. The experimentally determined stability of the latter mineral (Ernst, 1968) indicates that in the agpaitic zone crystallization was complete only at temperatures below 700°C (see section 8.6.1.). This does not preclude the possibility that most of the liquid was crystallized at the temperatures of equilibration.

The data in column 2 for GM146 is probably anomalous as it was derived from phenocryst data for which these temperatures appear far too low.

The agreement between columns 1 and 2 (Table 29) for the oversaturated syenites is also poor. The column 1 data for PM157 are reasonable for a trachytic liquid although the fO_2 values can be considered a bit low. In column 2 is the range within which final crystallization occurs according to reaction (17). It seems possible that the silica activity for PM157 is close to those defined by reaction (1), thus indicating a final crystallization temperature of about 700 to 720°C. Temperatures of this order must however be regarded as the absolute minimum for a trachytic liquid under moderate pressure.

For PM127 the column 1 temperatures appear anomously high. Mg-riebeeckite-arfvedsonite is a major mafic mineral in PM127 and final crystallization, at least, must have been in the stability field of this amphibole. For the oxygen fugacity conditions indicated here, the experimental work of Ernst (1968) suggests temperatures less than 880°C for crystallization of > 75% of the liquid. However the presence of blue, fibrous amphibole (probably riebeeckite) with quartz in the interstices between feldspar laths in PM127, sugg-sts that the interstitial liquid crystallized in the stability field of riebeeckite. This means temperatures $< 600°C$ and $fO_2 < 10^{-21}$ bars (Ernst, 1968).

CONCLUSIONS

Equilibration data for GM146 indicate that it was emplaced in a partially crystalline state (< 25% crystals) at about 880°C. The data for GM350 and GM147 give temperatures of final crystallization (> 80% crystals) in the region of 780 to 810°C, but the agpaitic facies of GM147 was probably only completely crystalline

TABLE 30

Comparative Solidus Temperatures

Reference	This work	1	2	3	3	4	5	6	7
Pressure (Kb)	0,5	1,0	1,0	0,5	1,0	0,5	0,5	0,5	0,5
PCNS	850^{o}-880^{o}	-	850^{o}	-	-	-	-	-	-
Inner Foyaite	780^{o}-810^{o}	-	750^{o}	-	-	-	-	-	-
Outer Foyaite	780^{o}-800^{o}	450^{o}	750^{0}	-	-	-	840^{o}-860^{0}	810^{o}	805^{o}
Outer Syenite	880^{o}-910^{o}	-	-	850^{o}-950^{o}	760^{o}-870^{o}	910^{o}-920^{o}	-	-	-
Hub Syenite	anomalous	-	-	950^{o}+	820^{o}+	-	-	-	-

1. Sood and Edgar (1970)
2. Hamilton and MacKenzie (1965)
3. McDowell and Wyllie (1971)
4. Bowen and Tuttle (1958)
5. Millhollen (1972)
6. Barker (1965)
7. Yoder and Tilley (1962)

TABLE 31

Possible temperature - oxygen fugacity limits of crystallization for Pomona syenites and Granitberg foyaites.

	GM146	GM350	GM147	PM157	PM127
Liquidus Temp.*	880°	950°	930°	1050°	
> 80% crystals Temp.	820°	780°	780°	900°	880°
solidus Temp.		-	650°	720°	
Liquidus $\log fO_2$	-14,3	-14,5	-15,2	-13,5	
$\log fO_2$ (> 80% crystals)	-17,3	-17,7	-18,0	-16,1	-15,1
solidus $\log fO_2$			-21,0	-17,0	

* Temperature in degrees C.

at 650 to 700°C. Final crystallization of PM157 occurred at 900 to 910°C with the possibility of complete crystallization occurring only at temperatures as low as 700°C. The data for PM127 is anomalous but mineralogy suggests that the liquid was mostly crystallized at 880°C though the interstitial liquid probably only crystallized at <600°C.

In Table 30 the temperatures of crystallization are compared to those derived by other workers, mostly from experimental systems. There is considerable variation in the reported solidus temperatures, and the temperatures estimated here for the Luderitz Province rocks agrees well with those from experiment. Below 1,5 Kb P_{H_2O}, dP/dT of the solidus is small (McDowell and Wyllie, 1971) thus small variations in the pressure of crystallization produce large variations in the temperature. The composition of the gas phase is also important. Diluting an aqueous fluid phase with CO_2 may elevate the solidus by over 100°C (Millhollen, 1971). It is not unexpected then, that such large variations in the solidus temperatures assembled in Table 30 exist.

It is also possible to estimate the liquidus temperatures for the syenites if the melting interval is known. Most syenites and nepheline syenites have melting intervals of about 150°C (Barker, 1965; Millhollen, 1971; McDowell and Wyllie, 1971), although Sood and Edgar (1970) recorded melting intervals of 450°C for some Ilimaussaq agpaitic rocks. This does not necessarily imply a high liquidus temperature since the agpaitic rocks appear to have solidi of less than 650°C (Sood and Edgar, 1970; this work).

Table 31 therefore summarises the probable temperature and oxygen fugacity limits of crystallization, for the rocks under discussion. It has not been possible to place complete fO_2 limits on the oversaturated syenites as fO_2 has not been buffered in these rocks and extrapolation from the equilibration data is impossible.

Figure 43 summarises the fO_2 - T data for the alkaline rocks studied here in comparison with similar data obtained by other workers. The data for the Granitberg foyaites and Pomona syenites fall well within the limits delineated by Nash et al (1969) for the trachyte-phonolite spectrum.

In general phonolites equilibrate at distinctly lower oxygen fugacities than acid lavas. it is a common misconception that alkaline undersaturated rocks that contain aegirine, crystallize under high fO_2 conditions. Figure 43 clearly refutes this notion. It is also significant that equilibration data for carbon-

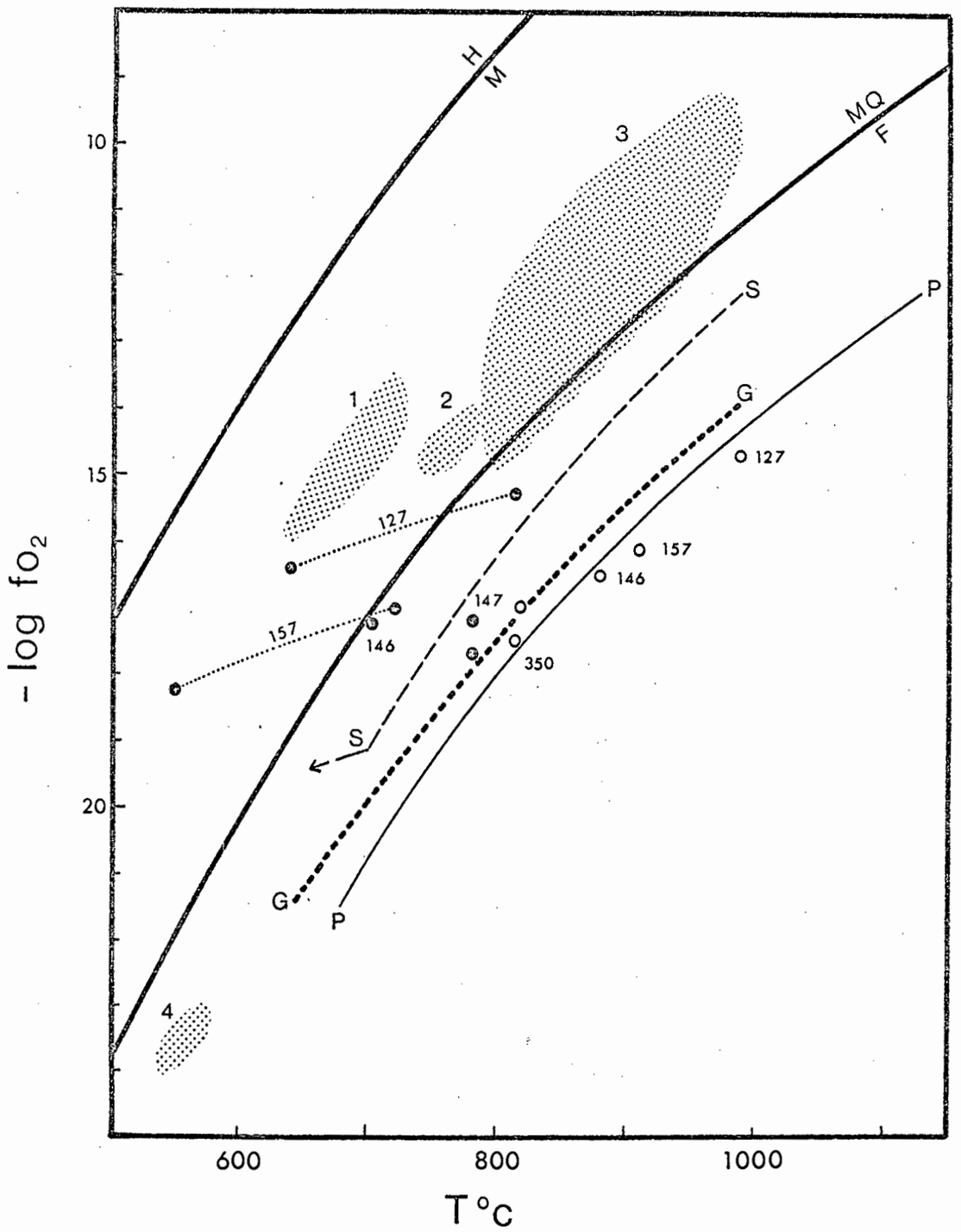

Figure 43. Comparison of T - fO_2 equillibration data for igneous rocks. Open circles - data for Pomona and Granitberg from Figure 41; Filled circles - data from Figure 42. G - G - cooling curve for Granitberg foyaites. S - S - cooling curve for the Shonkin Sag laccolith (Nash and Wilkinson, 1970). P - P - lower limit for phonolites (Nash et al, 1969) HM - synthetic hematite-magnetite buffer curve (Eugster and Wones, 1962); FMQ - synthetic quartz-fayalite-magnetite buffer curve (Wones and Gilbert, 1969). Shaded areas:

1 - Nevada ash flows (rhyolite) (Lipman, 1971)

2 - New Zealand ash flows (Ewart et al, 1971)

3 - Calc alkaline rhyolites and pumices (Heming and Carmichael, 1973; Lowder, 1970)

4 - Carbonatites (Prins, 1972).

atites (Prins, 1972) falls within the fO_2 limits, although at lower T, obtained for nepheline syenites - rocks with which carbonatites are commonly associated.

8.5. THE OCCURRENCE OF PEROVSKITE IN THE INNER FOYAITE

The occurrence of perovskite in the Inner Foyaite at Granitberg has already been described (section 3.4.5.3.(c)) but is summarised below.

The Inner Foyaite is a zoned body with a foliated marginal zone, an intermediate zone, and a core zone. In the marginal zone, euhedral sphene coexists with Ti-magnetite and there is petrographic evidence for a possible reaction relationship between the two. In the intermediate zone Ti-magnetite occurs very rarely, and then only in the cores of some biotite and pyroxene crystals - indicating that it crystallized early, but was later resorped by the liquid. The sphene crystals are anhedral and corroded, indicating that during the later stages of crystallization they too became unstable in the liquid. Small euhedral crystals of perovskite are scattered through the rock and are enclosed by the late-crystallizing feldspathoid minerals. It appears that as sphene was being resorped by the liquid, perovskite was precipitated as a stable phase in its place. There is no direct evidence of a reaction relationship between the two. In the core zone both sphene and an Fe-Ti oxide (except occasional grains enclosed by other mafic minerals) are absent, but perovskite is common.

It appears that in relatively mildly undersaturated liquids, with silica activities well above those defined by the sphene-perovskite buffer (Nicholls et al, 1971), perovskite is stabilized in the liquid at relatively low temperatures (700° to $800^{\circ}C$) by increasing peralkalinity in the liquid.

The equilibrium coexistence of perovskite and alkali feldspar has already been discussed (section 8.3.), and it has been shown that the two minerals may coexist at temperatures greater than $1127^{\circ}C$ at a silica activity of $\log a_{SiO_2} = -0,66$, far above the inferred liquidus of a foyaite under moderately low pressure. Therefore, in the case of the Inner Foyaite, silica activity alone cannot explain the presence of perovskite in the foyaite.

The reaction relationship between sphene and an Fe-Ti oxide in the peralkaline environment of the Inner Foyaite can be expressed by the reaction:-

$$2FeTiO_4 + 2CaMgSi_2O_6 + 2Na_2Si_2O_5 + 2/3KAlSi_3O_8 + 2/3H_2O + 2SiO_2 + O_2 \rightleftharpoons 2CaTiSiO_5$$

ulvospinel diopside glass orthoclase steam glass gas sphene

$$+ 4NaFeSi_2O_6 + 2/3KMg_3AlSi_3O_{10}(OH)_2 \quad \ldots\ldots \quad (19)$$

acmite phlogopite

where $Na_2Si_2O_5$ is a measure of the peralkalinity in the liquid. For pure phases, at equilibrium

$$\log fO_2 = \frac{\Delta G^o_r}{2{,}303RT}$$

However, log fO_2 must be corrected for the reduced activities of the phases in solid solution series in the conventional manner. In addition the activity of silica is that of the albite-nepheline buffer forGM350 (see section 8.3.), the activity of $Na_2Si_2O_5$ is assumed tobe unity, as is the activity of $CaTiSiO_5$ (sphene is assumed pure), and the P_{H_2O} is assumed to be 500 bars.

If the reaction of sphene with the liquid, and the subsequent crystallization of perovskite, can be expressed by the equation:-

$$4/3CaTiSiO_5 + 2Na_2Si_2O_5 + 4/3KFe_3AlSi_3O_{10}(OH)_2 + 8/3SiO_2 + O_2 \rightleftharpoons 4/3CaTiO_3 + 4/3H_2O$$

sphene glass annite glass gas perovskite steam

$$+ 4NaFeSi_2O_6 + 4/3KAlSi_3O_8 \quad \ldots\ldots \quad (20)$$

acmite orthoclase

then, at equilibrium,

$$\log fO_2 = \frac{\Delta G^o_r}{2{,}303RT} + \text{correction terms} \quad \ldots\ldots\ldots \quad (21)$$

The same activities for the various phases used in (19) were applied in the correction terms for (21). In addition perovskite was considered pure (unit activity).

Figure 44 is a plot of log fO_2 vs T for reactions (19) and (20). The sphene-perovskite equilibrium curve (20) intersects the ulvospinel-sphene curve

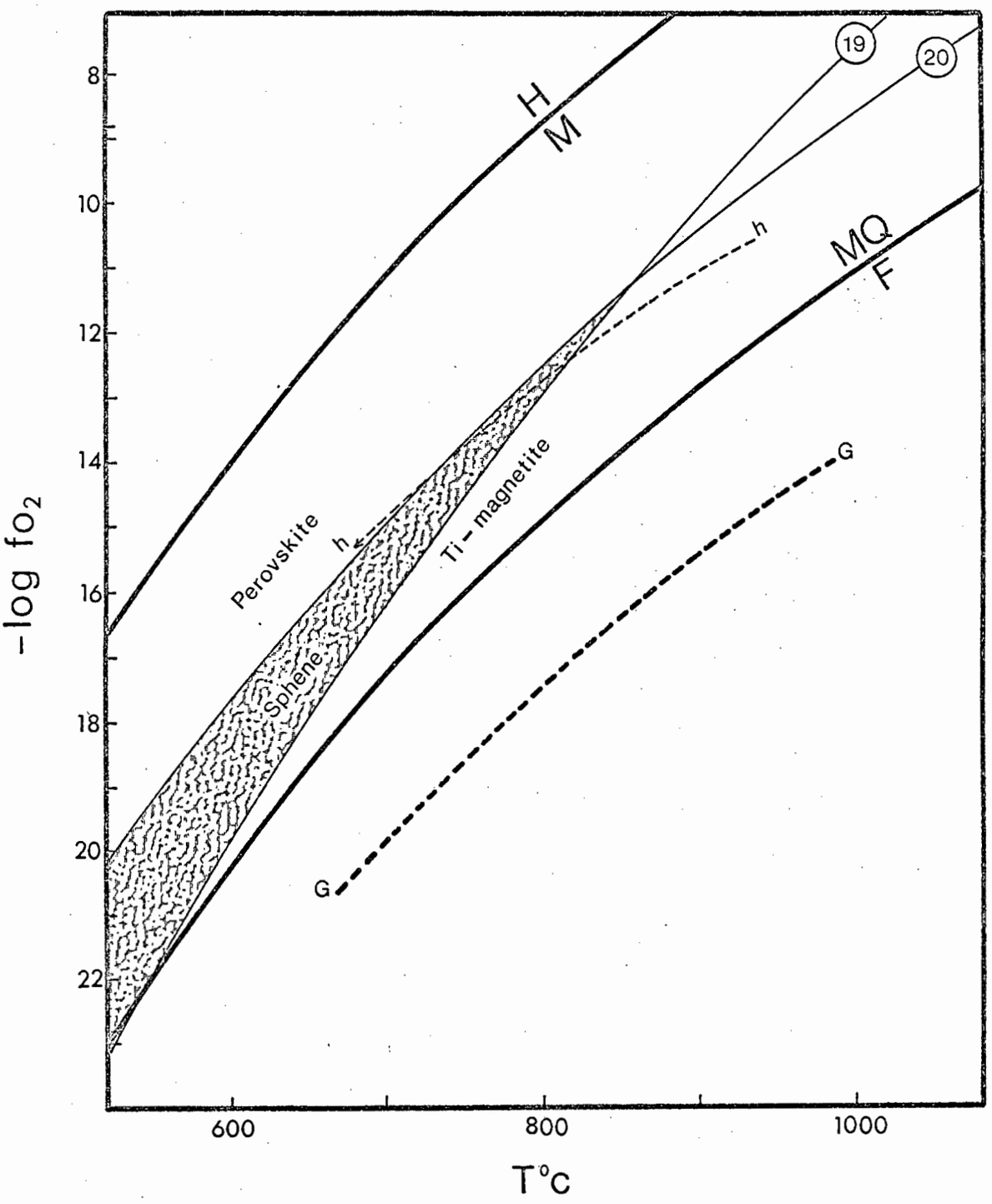

Figure 44. Relative stabilities of Ti-magnetite, sphene, and perovskite in undersaturated peralkaline liquids (see section 8.5. of the text for explanation). G-G is the cooling curve of the Inner Foyaite; h-h is the same cooling curve relative to the sphene stability field (shaded) if the latter is constrained to lie below the FMQ buffer curve.

(19) at T = 867°C and log $fO_2 = -11,2$. Also plotted is the T - fO_2 range of crystallization of GM350 derived from reactions (8), (12), and (17), which lies somewhat below the two curves. What is important is the relative position of the two curves, and that they intersect each other, not their absolute position. Since there is no way in assessing the peralkalinity of the liquid, i.e. the value of $a_{Na_2Si_2O_5}$, the absolute position of the curves remains uncertain. Increasing the activity of sodium disilicate will shift the two curves to lower values of fO_2, but will not change their positions relative to one another. By suitable choice of $a_{Na_2Si_2O_5}$ the curves could be constrained to lie in the T - fO_2 region of crystallization of GM350.

The area defined by the intersection of the two curves (shaded in Figure 44) is the stability field of sphene to the exclusion of both an Fe - Ti oxide and perovskite. Therefore, at any temperature below 867°C, with increasing oxygen fugacity, successive assemblages in which an Fe-Ti oxide, then sphene, then perovskite is the only Ti-bearing phase can be crystallized. Above 867°C perovskite + Ti-magnetite are stable at low fO_2, and perovskite + sphene at higher fO_2.

8.5.1. The crystallization of GM350

The crystallization path of GM350 in relation to the curves of reaction (19) and (20) is indicated in Figure 44. This path intersects, at successively lower temperatures, first the ulvospinel-sphene reaction curve, then the perovskite-sphene reaction curve, given that by suitable choice of the activity of sodium disilicate, the reaction curves would lie below the QFM buffer, in the cooling path of GM350. This suggests that the order of crystallization in GM350 was early precipitation of Ti-magnetite + other phases, resorption of magnetite and precipitation of sphene + other phases, and towards the close of crystallization, resorption of sphene and precipitation of perovskite.

Most likely the curves of (19) and (20) lay above the cooling path of GM350 in fO_2 - T space, during the early stages of crystallization. With increasing peralkalinity in the residual liquid, the curves moved to lower and lower values of fO_2, and first the sphene-ulvospinel curve, then the sphene-perovskite curve is intersected by the cooling path of GM350.

The dependence of perovskite stability on peralkalinity and oxygen fugacity suggests that the Inner Foyaite intrusive body was zoned with respect to either, or both of these conditions. There is no evidence that sphene ever crystallized in the core zone, thus the crystallization of the liquid in this zone could have lain entirely in the perovskite stability field. This indicates that either fO_2, or peralkalinity, or both, were higher in the core of the intrusion than in the intermediate or marginal zones.

The relative stability of sphene and perovskite in magmatic rocks has been the target of speculation. Verhoogen (1962) argued that perovskite is favoured by low silica activity and high oxygen fugacity. Carmichael and Nicholls (1967) calculated oxygen fugacities for a variety of igneous rocks, and indicated that perovskite-bearing lavas crystallized at higher fO_2 than do sphene-bearing lavas. Smith (1970) found the converse, and proposed that perovskite-bearing assemblages equilibrate at lower fO_2 than sphene assemblages. Smith (1970) also concluded that the stability of sphene and perovskite is not only dependent on silica activity, but also on fO_2. This fact is well illustrated by the crystallization of GM350, although this work supports the arguments of Verhoogen (1962) and Carmichael and Nicholls (1967), rather than those of Smith (1970). To the latter's conclusions as to the factors influencing the relative stabilities of sphene and perovskite, can be added the importance of peralkalinity.

8.6. THE STABILITY OF AENIGMATITE IN PERALKALINE UNDERSATURATED ROCKS

Nicholls and Carmichael (1969) found that the stability of aenigmatite in peralkaline acid liquids is controlled by the reaction of Fe-Ti oxides with the peralkaline liquid. They noted that the stability of aenigmatite could therefore be defined by the reactions:

$$\underset{\text{magnetite}}{4Fe_3O_4} + \underset{\text{glass}}{6Na_2Si_2O_5} + \underset{\text{glass}}{12SiO_2} + \underset{\text{gas}}{O_2} \rightleftharpoons \underset{\text{acmite}}{12NaFeSi_2O_6} \quad \ldots\ldots \quad (22)$$

for which

$$\log fO_2 = \frac{\triangle G^o_r}{2{,}303RT} + 12\log a^{\text{pyroxene}}_{\text{acmite}} - 4\log a^{\text{magnetite}}_{\text{magnetite}} - 6\log a^{\text{glass}}_{Na_2Si_2O_5} - 12\log a^{\text{glass}}_{SiO_2} \ldots \quad (23)$$

at equilibrium, and

$$\underset{\text{aenigmatite}}{Na_2Fe_5TiSi_6O_{20}} + \underset{\text{glass}}{Na_2Si_2O_5} + \underset{\text{gas}}{O_2} \rightleftharpoons \underset{\text{acmite}}{4NaFeSi_2O_6} + \underset{\text{ilmenite}}{FeTiO_3} \quad \ldots (24)$$

for which, at equilibrium,

$$\log fO_2 = \frac{\triangle G^o_r}{2{,}303RT} + 4\log a^{\text{pyroxene}}_{\text{acmite}} + \log a^{\text{ilmenite}}_{\text{ilmenite}} - \log a^{\text{glass}}_{Na_2Si_2O_5} - \log a_{\text{aenigmatite}} \quad \ldots (25)$$

The antipathetic relationship between aenigmatite and an Fe-Ti oxide observed in the agpaitic zone of the Outer Foyaite is equally well described by these equations provided allowances are made for the reduced activity of silica. Ilmenite is rare in silica undersaturated rocks, and aenigmatite probably arises through reaction of Ti-magnetite, rather than by reaction (24). Nevertheless (24) is a close approximation of the natural conditions, and its use allows direct comparison with the data obtained by Nicholls and Carmichael (1969).

Log fO_2 - T curves defined by reactions (23) and (25) are plotted in Figure 45. In the calculation of these curves, aenigmatite, ilmenite and magnetite are assumed pure, the activity of sodium disilicate is assumed to be unity, and the activity of silica is that defined by the nepheline-albite buffer (Nicholls et al, 1971). Two sets of curves have been plotted - one set assumes unit activity of acmite, and the other set assumes an activity for acmite of 0,25. As found in the acid environment the curves intersect each other and define an area where both aenigmatite and acmite crystallize to the exclusion of Fe-Ti oxides (Nicholls and Carmichael, 1969). The absolute position of the two curves in fO_2 - T space is not known since there are large errors in the free energy estimates of acmite, and especially aenigmatite.

Also indicated on Figure 45 is the intersection of the curves for varying activities of sodium disilicate at the two assumed activities of acmite. The lower termination of the no-oxide field is considered to be the stability field of Na-amphiboles (Nicholls and Carmichael, 1969). This also appears to be the case for undersaturated liquids, since there is ample petrographic evidence at Granitberg that liquids which crystallized acmite and aenigmatite, eventually crystallized arfvedsonite and astrophyllite.

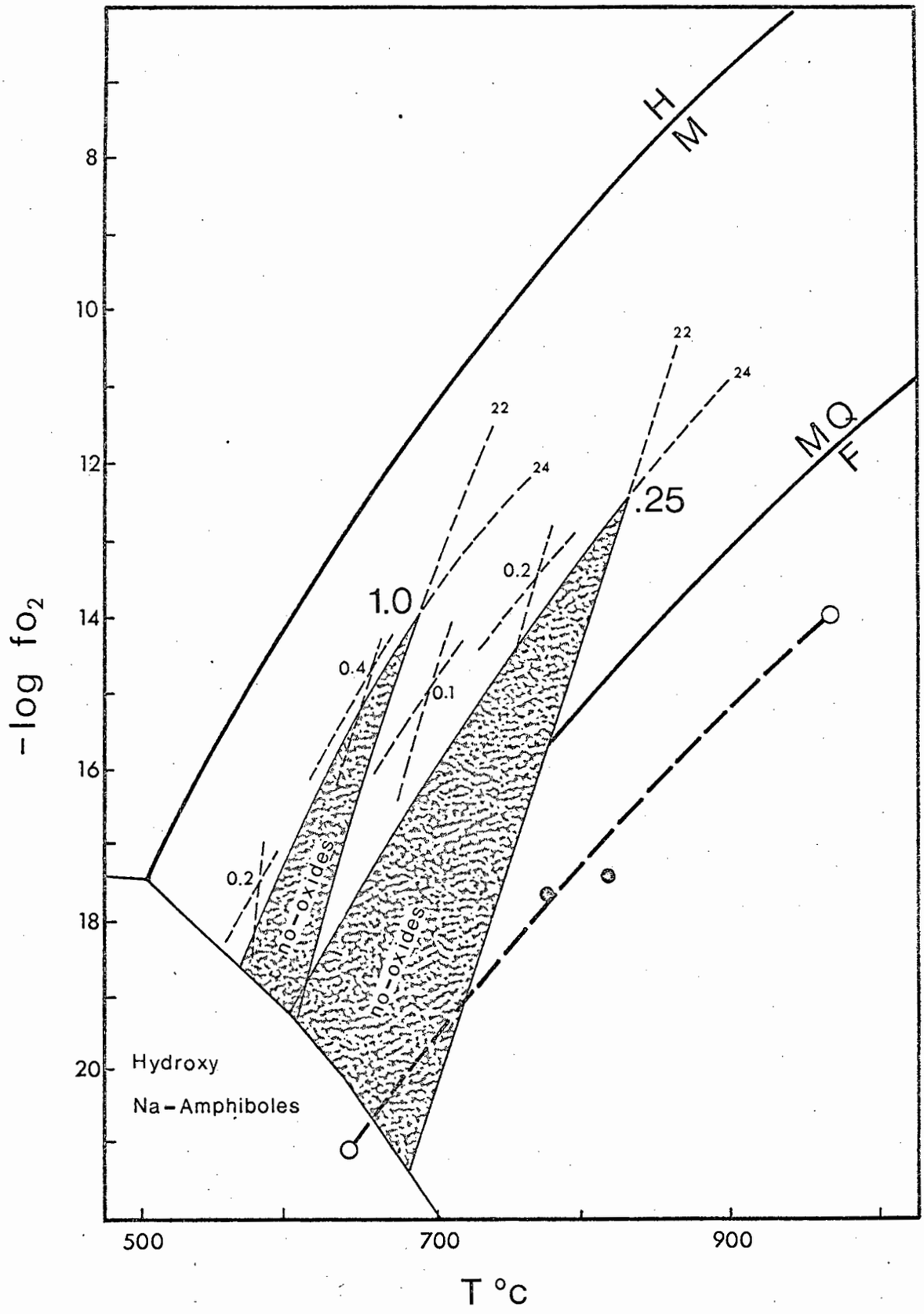

Figure 45. No-oxide fields in T - fO_2 space where aenigmatite and aegirine crystallize at the expense of an Fe-Ti oxide in peralkaline undersaturated liquids. Dashed curves (22) and (24) refer to equations in section 8.6. of the text. The heavy dashed curve is the probable cooling curve for the agpaitic zone of the Outer Foyaite. The two filled circles are equilibration data for GM147 from Figures 41 and 42. All other features are explained in the text.

TABLE 32

UNDERSATURATED (this work)			OVERSATURATED Nicholls and Carmichael (1969)	
	T°C	$-\log fO_2$	T°C	$-\log fO_2$
a (acmite)* = 1.0			a (acmite) = 1.0	
a (Nds)** = 1.0	685°	14,2	840°	11,2
a (Nds) = 0.4	650°	14,9	730°	13,3
a (Nds) = 0.2	577°	17,6	660°	15,3
a (acmite) = 0.5			a (acmite) = 0.5	
a (Nds) = 1.0	753°	13,4	1025°	9,1

fO_2 in bars

* a (acmite) activity of acmite in clinopyroxene

** a (Nds) activity of Sodium disilicate in the liquid

The important difference between the no-oxide field in oversaturated liquids and the field in undersaturated liquids, is that in the latter, the field is far more restricted. This is illustrated in Table 32 where the intersection of the two curves in terms of fO_2 and T are compared for various activities of acmite and sodium disilicate.

Nicholls and Carmichael (1969) believed that the no-oxide would initially be rather small, but would shift and grow in fO_2 - T space during crystallization as the peralkalinity in the residual liquid (as indicated by the activity of $Na_2Si_2O_5$) increased. Thus the field would rise to meet a liquid, cooling down a path approximately parallel to the synthetic oxygen buffers. The liquid, on entering the no-oxide field, would precipitate acmite and aegirine at the expense of any Fe-Ti oxides.

A similar situation applies to undersaturated liquids, but the indications are that the no-oxide field in this environment is restricted to rather narrow limits in fO_2 - T space. This is because of the opposite effects that the activity of $Na_2Si_2O_5$ and the activity of acmite in the pyroxene, exercise on the field. During crystallization, the tendency for the no-oxide field to rise due to increase in the peralkalinity of the melt, is offset by the increased activity of acmite in the pyroxene being precipitated, which surpresses the no-oxide field. This may be seen in Figure 45 where the intersection labelled '0,1' (which is for $a_{acmite} = 0,25$ and $a_{Na_2Si_2O_5} = 0,1$) lies very close to the field defined by unit activity for both acmite and sodium disilicate. Therefore, during the whole course of crystallization the no-oxide field may only shift by $50^{o}C$ and one unit of log fO_2, and is as likely to decrease in size, as it is to increase.

8.6.1. Crystallization in the agpaitic zone of the Outer Foyaite

The no-oxide field as defined above, allows the petrographic features of the agpaitic rocks in the Outer Foyaite at Granitberg to be fully explained in terms of a crystallization path in fO_2 - T space. Since the crystallization path lies below the QFM buffer curve (see section 8.4.) the position of the no-oxide field, as indicated in Figure 45, is probably incorrect. This is not surprising considering the assumptions made and the poor free energy data for aenigmatite and acmite.

Initially the agpaitic liquid crystallizes Ti-magnetite, an Na-poor

pyroxene, and possibly a little biotite, together with nepheline and orthoclase. With increasing crystallization the peralkalinity of the liquid increases as does the activity of the acmite in the pyroxene. The no-oxide field shifts into a position where it is intersected by the cooling path of the liquid, the Ti-magnetite reacts with the liquid, and aenigmatite is precipitated together with aegirine and the felsic minerals. Some of the magnetite is enclosed by the other mafic minerals and is unable to react with the liquid, and is preserved to the close of crystallization.

Although it is indicated in reaction (24) that aenigmatite arises by reaction of ilmenite with the liquid, the presence of skeletal grains of magnetite enclosed by the aenigmatite indicates the reaction:

$$2Na_2Fe_5TiSi_6O_{20} + Na_2Si_2O_5 + 2SiO_2 + 3O_2 \rightleftharpoons 6NaFeSi_2O_6 + 2Fe_2TiO_4 \quad \ldots\ldots \quad (26)$$

aenigmatite glass glass gas acmite ulvospinel

which is probably very similar to (24) in the complex conditions of a natural magma.

The euhedral and abundant nature of the aenigmatite in the agpaitic zone indicates that the no-oxide zone was intersected early in the crystallization of these rocks. With further cooling, the cooling path remains in the no-oxide field and eudialyte-eucolite crystallizes, zirconium being unable to enter an Fe-Ti oxide. Just before final crystallization the residual liquid enters the stability field of Na-amphibole. Here astrophyllite and arfvedsonite crystallize, the latter as large semi-poikilitic grains. A reaction relationship between aenigmatite and astrophyllite is also evident, as their respective formulae would suggest. Astrophyllite can be considered the hydrated equivalent of aenigmatite, and possibly has a stability similar to riebeeckite-arfvedsonite solid solutions in terms of temperature and oxygen fugacity.

The crystallization of arfvedsonite with a low Mg content suggests that final crystallization took place at $T = 620^{\circ}$ to $650^{\circ}C$, and log $fO_2 = -21$ to -22 bars (Ernst, 1968). This is some $150^{\circ}C$ lower than the temperatures indicated in section 8.4. for $> 80\%$ crystallization. If the liquidus lies in the region 900° to $950^{\circ}C$ then the agpaitic rocks would have a crystallization interval of over $300^{\circ}C$. If the results of the melting experiments of Sood and Edgar (1970) are typical of agpaites, then such a large interval is not unexpected.

CHAPTER 9

PETROGENISIS AND TECTONIC IMPLICATIONS

Numerous petrogenitic schemes have been proposed to account for the presence of peralkaline rocks in the earth's crust, and few have stood the tests of modern petrology. Limestone assimilation (Shand, 1922[45] and 1930; Daly, 1933) was considered, but not favoured by Kaiser (1926) as an explanation for the origin of the alkaline rocks at Granitberg. Kaiser's beliefs are today vindicated by the results of modern petrology which discounts the Daly-Shand theory as a viable major process in alkaline rock genesis (see Wyllie and Watkinson, 1970). The other major theories for alkaline rock genesis are partial melting of the lower crust with alkali concentration by volatile action (Currie, 1970; Bailey, 1964 and 1970; Bailey and Schairer, 1966); and differentiation from basic or ultrabasic parental magma (Turner and Verhoogen, 1960).

The mechanism of partial melting might be necessarily invoked to explain volume relationships for some continental alkaline provinces, e.g. the Rift Valley provinces and the Younger Granites of Nigeria. Unless strontium isotope data is available this process remains largely speculative. For the Early-Cretaceous provinces on either side of the South Atlantic (Uruguay, Angola, Brazil, Damaraland, and Luderitz - see Marsh (1973)), the nature of the volcanism and its tectonic setting in time and space, is more consistent with derivation by differentiation of mantle-derived basic magmas.

One reason for the proliferation and complexity of petrogenetic schemes, is the attempt to explain the derivation of alkali silicate and carbonatitic magmas from a common parent. Thus Verwoerd (1968) favoured the derivation of such rocks by from a basaltic parent by volatile concentration, immiscibility, and wall-rock reaction. In the same sphere falls Ferguson and Currie's (1971) proposal using immiscibility relationships in lamprophyric liquids to produce carbonatite, nepheline syenite, and members of the melteigite-urtite series. However, carbonatites and members of the melteigite-urtite series are not present in the Luderitz Province, and such schemes can be considered superfluous in the context of this Province. A simpler genetic scheme is therefore indicated.

There is abundant evidence from the continents and oceans that trachytes and trachybasanites evolve through crystal fractionation from alkali basalt and

basanite parental magmas (Coombs and Wilkinson, 1969; Turner and Verhoogen, 1960; McBirney and Williams, 1969; Abbott, 1969; Ridley, 1970; Wright, 1971; Mukherjee, 1967;). In the related Damaraland Province, the Okonjeje Complex (Simpson, 1954; H. Fesq, personal communication) is an excellent example displaying the relationship between alkaline salic liquids and their probable basic parent magmas.

Experimental evidence (Green, 1970; Green and Ringwood, 1967) indicates that alkali olivine basalts and olivine basanites are generated at depths in excess of 35 km. Although tholeiitic magmas may also be generated at similar depths, extensive and lengthy periods of eruption characterised by tholeiites and their oversaturated differentiation products, suggests generation at shallower depths. At the time of emplacement of the majority of complexes (120 to 135 my) the nature of the volcanism in Damaraland, Brazil, and most likely in the Luderitz Province as well, was tholeiitic (Siedner and Miller, 1968; Amaral et al, 1966; Melfi, 1967). Thus some mechanism is necessary to tap alkali basalts and basanites from deeper levels and transport these magmas rapidly into the upper crust to avoid mixing and hybridization with tholeiitic material.

The writer has recently summarised age data for complexes in alkaline Provinces from both sides of the Atlantic (Marsh, 1973), and has shown that there is excellent agreement between the time of emplacement of many of the complexes, and the time of Gondwanaland rifting and the formation of the proto Atlantic as determined by others (Le Pichon and Hayes, 1971; Dietz and Holden 1970).

It seems unlikely that rifting parallel to the present-day coastline penetrated to the levels of alkali basalt derivation (> 35 km), since there is no evidence of alkali magmatism in a continuous or semi-continuous belt parallel to the coast. Instead, the alkaline complexes in the various provinces in Africa and South America form lineaments, which strike at high angles to the coastline, and the writer has recently suggested that their orientation and disposition are related to transform directions (Marsh, 1973). Transform directions are continental extensions of transform fracture zones (Francheteau and Le Pichon, 1972) which are fundamental features of the oceanic crust (Wilson, 1965), and their associated volcanism is distinctly alkaline (Gass, 1972).

It is not proposed that the alkaline complex lineaments are the result of fractures penetrating the entire crust. Rather, the base of the crust and the upper mantle, weakened by generation of large amounts of tholeiitic magma was ruptured along the continuation of the transform fractures at the time of

the Africa-South America split and allowed access to the levels of alkali basalt generations. Since pre-existing lines of weakness in the continental crust are held to be responsible for the initiation and siting of the fracture zones (Wilson, 1965), it is not unreasonable to assume that these weaknesses, now reactivated, allowed rapid and easy passage of the alkali basaltic magma into the upper crust. Thereafter, differentiation and emplacement of the ring complexes took place from high-level magma chambers.

In detail, the complexes in the lineaments fall with considerable scatter about any extension of the transform fractures. It would be naive not to expect this, as crustal structures will tend to modify the magma ascent path in the upper crust.

The complexes of the Luderitz Province are too few to define any lineament, although it has been shown that they do define a transform direction (Marsh, 1973). Kaiser (1926, p. 313, 316) found that the dominant trend for the Luderitz Province dyke swarm is 060°, and therefore parallels the trend of the transform direction for this province.

For the well developed provinces in Damaraland and Brazil, the regional basement trends lie parallel to the transform directions. However, in Uruguay, and in the Luderitz Province, the basement trends parallel the coast and therefore strike at right angle to the transform direction for these two provinces. This could well explain why the Damaraland and Brazil Provinces are more 'mature' (in size and in number of complexes) than the Luderitz and Uruguay Provinces. In Angola there is a 30° difference between the basement and transform direction trends, yet the Angola Province comprises over 30 alkaline complexes (Rodrigues, 1970). However, the complexes show a considerable scatter about the transform direction and this could be an interference effect - the transform direction controls the gross regional position of the province, whereas the basement trends control the local distribution of the individual complexes.

Given that the transform fractures are responsible for activating and tapping alkali basaltic magmas below the passive edges of the continents, then the evidence presented above suggests that the appearance of this magma and its differentiates in the upper crust is influenced by the regional basement structures there. Where these structures parallel the transform directions the magmas find easy access to the upper crust, and vice-versa. This might explain why the Damaraland lineament has no relation in Southern Brazil; the basement structures there parallel the coastline and thus strike at right angles to the trans-

form direction. Similar reasoning might answer the question as to why alkaline complex lineaments are associated with some transform fractures and not others.

The origin and evolution of the Luderitz Province and the other Early Cretaceous Provinces in Africa and South America are therefore intimately involved with the early development of the South Atlantic ocean. It is not unexpected then that the trachyte - alkali rhyolite and the trachybasanite - phonolite suites of the Luderitz Province are similar in chemistry and genesis to similar suites from oceanic environments. This emphasises that the alkaline magmatism in these provinces considered as a whole, is in many respects markedly different to the Rift Valley provinces in East Africa.

The hypothesis presented here differs from the mantle plume theory of Rhodes (1972), and the volcanic cycle postulate presented by Cox (1972) for the Karroo magmatism of south-eastern Africa. Doubts as to the validity of the former have already been expressed (Marsh, 1973). These doubts are somewhat vindicated by recent questioning as to whether plumes are fixed in the mantle (McElhinny, 1973) or whether they exist at all.

see Turnock & Onions Nature 246 1973 337

The Kaoko lavas in South West Africa have received only superficial attention, and it is uncertain whether a cycle as envisaged by Cox (1972) could be inferred for these rocks. It seems that a cycle was initiated (H. Fesq, personal communication), but was subsequently disrupted by rifting and the opening of the Atlantic. A more intensive study of all aspects of Karroo volcanicity on the south-west coast of Africa is needed to solve the complex development of the Luderitz and Damaraland Provinces.

ACKNOWLEDGEMENTS

This study was aided financially by the generosity of the Council for Scientific and Industrial Research and the University of Cape Town.

I am indebted to Professor F.C.M. Mathias, recently retired from the Department of Geology, U.C.T., whose enthusiastic teaching of mineralogy and igneous petrology during my undergraduate years aroused my interest in the alkaline igneous rocks. I am grateful to Professor E.S.W. Simpson of the Geology Department, who provided time, energy, and the facilities that made this study possible.

Field work was conducted with the generosity of the Consolidated Diamond Mines of South West Africa, Ltd., and in this respect the interest of Dr C.G. Stocken and the staff of the Geology Department at Oranjemund is appreciated.

The analytical work presented in this thesis is the result of the constant availability of facilities and advice in the Department of Geochemistry, U.C.T. In particular I must acknowledge the generous help given at all times by Dr Tony Erlank and Mr James Willis, as well as Mr Dick Rickard who introduced me to the electron microprobe.

Thanks are also due to Dr Alan Moore who bravely waded through much of the initial draft, and to many others in the Division of Earth Sciences for the many discussions, sometimes arguments, which their patience allowed. Thanks are, however, not enough for the gentle and patient support of my Lily of the Valley.

APPENDIX

WHOLE ROCK CHEMICAL ANALYSES

All analyses were conducted in the Department of Geochemistry by X-ray fluorescence procedures using a PW1540 (manual) and a PW1220 (semi-automatic) spectrometers. Na was determined on 4 grams of powder ground to -300 mesh and pressed into briquettes. Si, AL Al, Ti, Ca, K, Mg, Fe, and P were determined on fusion discs prepared after the method of Norrish and Hutton (1969). In addition, FeO was determined by titrimetric methods using the potassium dichromate procedure outlined by Shapiro and Brannock (1956). The method was calibrated by analyzing departmental and international rock standards at frequent intervals during the determinations. Trace elements were determined on 4 gram pressed powder briquettes.

Analytical conditions for the trace and major element determinations are set out in Table A. Adopted values for international and departmental rock standards used in the analyses, are set out in Tables B and C. Precision data for the analytical techniques are contained in Table D.

Raw data was processed using computer programs written in the department of Geochemistry. These programs calculate working curves from the standards, and make the necessary corrections for spectral line interference, dead time, and matrix effects (Trace elements). For the latter, Birk's values for the mass absorption coefficient, calculated from major element data, were used.

Some of the analyses presented in this thesis have totals that are lower than is normally acceptable. Several of the samples were re-analyzed with little or no improvement to the results. In addition the samples were analyzed with a large number of others, most of which gave satisfactory totals. It therefore seems unlikely that the 'error' is due to instrumental drift, but the other possibilities are:

(1) the presence of non-determined elements. The major element totals do not include trace element abundances, which may make up 0,5% of the total sample weight. In addition, F and Cl were not determined and could be present to the extent of several thousand ppm;

(2) during preheating the samples were ignited at 850°C to avoid fusion of the undersaturated rocks and reaction with the silica crucible.

Volatiles may therefore have been only partially driven off with the resultant low LOI values, and low totals.

X-RAY DIFFRACTION PROCEDURES

X-ray diffraction scans were made with a PW1540 unit using Cu K radiation with a nickel filter. Alkali feldspar concentrates were mixed with $KBrO_3$ (internal standard), ground to -250 mesh and pressed into briquettes. $KBrO_3$ has three sharp reflections close to the relevant feldspar peaks. These are:

(a) the 101 reflection at 20,212° which calibrates the $\bar{2}01$ feldspar peak;

(b) the 202 reflection at 41,088° which calibrates the $\bar{2}04$ feldspar peak;

(c) the 122 reflection at 51,476° which calibrates the 060 feldspar peak.

Three scans (or more) were made over each of the following angular distances - 19,5° to 22,5°; 40,5° to 42,5°; and 50,0° to 52,0°. Peak positions were estimated to 0,01°. Positions from repeated scans never differed by more than $\pm$ 0,02° from the average, and for most samples this was $\pm$ 0,01°. Nine scans of one sample, DM105, were made in order to estimate the precision of the procedure. The results are set out in Table E and are considered satisfactory.

MICROBROBE ANALYTICAL PROCEDURE

Minerals were analyzed for Si, Ti, Al, Fe, Mn, Mg, Ca, Na, K, with a Cambridge Microscan 5 microprobe in the Department of Geochemistry, University of Cape Town, using a variety of natural silicate mineral standards. The raw data was corrected and reduced using ABFAN, a computer program written by Boyd, Finger, and Chayes (1968) (Ann. Rept. Dir. Geophys. Laboratory, Washington, 1967 - 1968, 210 - 215).

K_α lines for the nine elements were measured at 15Kv with a total beam current of 0,15 X 10^{-6} amps. For Si, Al, Mg, Na an RAP analyzing crystal was used, and for Ti, Fe, Mn, Ca, and K, a Quartz crystal was used.

Table A

Analytical conditions: Major elements

	Ti	Ca	K	Si	Al	Mg	P	Na	Fe	Mn
TUBE	Cr →								Au →	
Kv	50 →									
mA	20 →			32 →					20 →	
COUNTER	FLOW →									
COLLIMATOR	Course	Fine	Course →						Fine →	
CRYSTAL	LiF →			Pet →		ADP	Germanium	Gypsum	Lif →	

Analytical conditions: Trace elements

	Pb	Th	Nb	Zr	Y	Rb	Sr	Ga	Ba
TUBE	W →							Mo	Cr
Kv	50 →							80	50
mA	20 →		30 →					25	20
COUNTER	Scintillation →							Flow + Sc.	Flow
COLLIMATOR	Fine →								
CRYSTAL	LiF (220) →		LiF (420) →					LiF(200)	Lif (220)

TABLE B

Adopted values for X-ray fluorescence standards: Major elements

STANDARD	SiO_2	TiO_2	Al_2O_3	Fe_2O_3*	MnO	MgO	CaO	K_2O	Na_2O	P_2O_5
G-1									3,321	
GSP	67,942	0,666	15,269	4,302	0,042	0,989	2,030	5,584		0,292
BR	39,434	2,705	10,530	13,348	0,213	13,723	14,184	1,445		1,052
W-1	52,693	1,071	14,955	11,104	0,174	6,639	10,971	0,641	2,150	0,140
AGV-1	60,162	1,051	17,345	6,832	0,096	1,541	5,037	2,957		0,489
S-1	60,013	0,484	9,369	8,271	0,405	4,094	10,157	2,650		0,221
GH	76,324	0,081	12,586			0,054	0,654	4,813		0,021
USBS99									10,730	
OK272									5,290	

* All Fe as Fe_2O_3

TABLE C

Adopted values for X-ray fluorescence standards: Trace elements

STANDARD	Th	Pb	Nb	Zr	Y	Sr	Rb	Ga	Ba
G-1	50	48	21,7	219	11,9	252	210	18,0	1089
GSP	108	55	25,4	543	25,4	234	252		
BR			115	240	27,6	1350	45		
BCR	7	15	11,3	192	33,4	1015	47,3		
KNIPPA-1			83,4	83,4	24,5	334	27,9		
G-2	25	28							
W-1								16,0	158
ZnGaCu								91,8	
ZnGaCuHf								96,3	
6624									214

TABLE D

Precision data for X-ray fluorescence analysis: data for eleven individually prepared and analyzed aliquotts of sample GM 146.

	MEAN ($\bar{x}$)	STANDARD DEVIATION (s)	COEFFICIENT OF VARIATION ($\frac{s}{\bar{x}}$)%
SiO_2	53,42	0,29	0,54
TiO_2	1,27	0,12	0,97
Al_2O_3	18,28	0,07	0,38
Fe_2O_3*	6,62	0,05	0,81
MnO	0,232	0,003	1,293
MgO	2,24	0,17	7,74
CaO	3,03	0,04	1,26
K_2O	4,88	0,03	0,60
Na_2O	7,49	0,13	1,74
P_2O_5	1,01	0,014	1,42
H_2O	0,08	0,02	24,99
LOI	0,58	0,04	7,47
Ba	1598,6	12,0	0,75
Ga	22,89	0,30	1,32
Nb	199,1	3,4	1,74
Zr	843,6	8,9	1,05
Y	34,2	3,1	9,1
Sr	1596,3	12,2	0,7
Rb	151,8	5,2	3,4

TABLE E

X-RAY DIFFRACTION PRECISION DATA SAMPLE : DM 105

	$\bar{2}01$	060	$\bar{2}04$
	21.07	41.78	50.65
	21.05	41.78	50.68
	21.04	41.80	50.70
	21.04	41.75	50.69
	21.08	41.78	50.70
	21.03	41.80	50.68
	21.03	41.75	50.70
	21.03		
	21.05	41.77	50.69
	21.07	41.78	50.73
$\bar{x}$	21.05	41.78	50.69
s	.02	.02	.02

LIST OF ANALYZED SAMPLES

GRANITBERG

GMA 1	
GMA 2	Feldspathic sandstones
GMA 3	
GMA 4	
GMA 5	
GMA 6	Metasomatized sandstones
GMA 7	
GMA 8	
GMA 9	
GM 77	Tinguaite dyke, E of Granitberg
GM 88	Shonkinite, NE Contact zone
GM 128	PCNS, Roof Zone
GM 129	Outer Foyaite
GM 130	Foyaite, Roof Zone
GM 131	Inner Foyaite, W of jeep track, Roof Zone
GM 136	Outer Foyaite
GM 142	Outer Foyaite
GM 146	PCNS, Roof Zone
GM 147	Outer Foyaite
GM 160	Tinguaite dyke, SE of Granitberg
GM 169	Pulaskite, West ridge contact zone
GM 171	Outer Foyaite
GM 174	Alkali granite, West Ridge
GM 175	Alkali granite, West Ridge
GM 232	Nordmarkite, SW contact zone
GM 339	Grorudite sheet, NE of Granitberg

GM 340	Quartz-bostonite dyke, SE of Granitberg
GM 350	Inner Foyaite, W of jeep track, Roof Zone

POMONA

PM 53	Nepheline syenite, W of Signalberg
PM 55	Outer Syenite, W of Schlueberg
PM 60	Inner Syenite, SE of Signalberg
PM 61	Tinguaite dyke, SE of Signalberg
PM 63	Syenite porphyry, W of Signalberg
PM 64	Biotite-rich monzonite, S of Signalberg
PM 66	Outer Ring Dyke nordmarkite, S of Schlueberg
PM 127	Hub Syenite, Signalberg
PM 156	Quartz-bostonite, W of Schlueberg
PM 157	Outer Syenite, SW of Schlueberg
PM 177	Quartz-feldspar porphyry, E of Schlueberg

DRACHENBERG

DM 105	Coarse porphyritic syenite, Black Cap Hill
DM 106	Fine porphyritic syenite, Black Cap Hill
DM 110	Syenite, S of Drachenberg
DM 111	Quartz-feldspar porphyry
DM 115	Quartz syenite, W of Drachenberg
DM 124	Quartz monzonite, SW of Black Cap Hill
DM 125	Syenite, NW of Black Cap Hill
DM 126	Biotite-rich syenite, W of Drachenberg

REFERENCES

Abbott, M.J. (1967) K and Rb in a continental alkaline igneous rock suite. Geochim. Cosmochim. Acta, 31, 1035-1041.

Abbott, M.J. (1969) Petrology of the Nandewar Volcano, N.S.W., Australia. Contr.Mineral. and Petrol., 20, 115-134.

Ahrens, L.H., Pinson, W.H., and Kearns, M.M. (1952) The association of rubidium and potassium and their abundance in igneous rocks and meteorites. Geochim. Cosmochim. Acta, 2, 229-242.

Amaral, G., Cordani U.G., Kawashita, K., and Reynolds, J.H. (1966) Potassium-argon dates of basaltic rocks from Southern Brazil. Gaochim. Cosmochim. Acta, 30, 159-180.

Anderson, A.L. (1963) Contact syenitization in the Yellowjacket District, Lemhi County, Idaho. Am.J.Sci., 261, 826-838.

Arrhenius, G., Everson, J.E., Fitzgerald, R.W., and Fujita, H. (1971) Zirconium fractionation in Apollo 11 and Apollo 12 rocks. In Proc. 2nd Lunar Conf. (ed. A.A. Levinson), 1, 169-176, M.I.T. Press.

Bailey, D.K. (1964) Crustal Warping - a possible tectonic control of alkaline magmatism. J. Geophys. Res., 69, 1103-1111.

Bailey, D.K. (1969) The stability of acmite in the presence of H_2O. Am. J. Sci., Schairer vol. 267-A, 1-17.

Bailey, D.K. (1970) Volatile flux, heat focussing, and the generation of magma. Geol, J. Special Publication 2, 177-186.

Bailey, D.K., and Schairer, J.F. (1964) Feldspar-liquid equilibria in peralkaline liquids - the orthoclase effect. Am. J. Sci., 262, 1198-1206.

Bailey, D.K., and Schairer, J.F. (1966) The system Na_2O-Al_2O_3-Fe_2O_3-SiO_2 at 1 atmosphere, and the petrogenesis of alkaline rocks. J. Petrol., 7, 114-170.

Bailey, D.K., and MacDonald, R. (1969) Alkali feldspar fractionation trends and the derivation of peralkaline liquids. Am. J. Sci., 267, 242-248.

Bailey, D.K., and MacDonald, R. (1970) Petrochemical variations among mildly peralkaline (comendite) obsidians from the oceans and continents. Contr. Mineral. and Petrol., 28, 340-352.

Barbieri, M., Fornaseri, M., and Penta, A. (1968) Rubidium and potassium relationships in some volcanoes of Central Italy. Chem. Geol., 3, 189-197.

Barker, D.S. (1965) Alkalic rocks of Litchfield, Maine. J. Petrol., 6, 1-27.

Barth, T.F.W. (1963) The composition of nepheline. Schweiz. Mineral. Petrol. Mitt., 43, 153-164.

Barth, T.F.W. (1969) Feldspars. Wiley Interscience, New York.

Beetz, W. (1924) On a great trough-valley in the Namib. Trans. Geol. Soc. S. Afr., 27, 1-38.

Berlin, R., and Henderson, C.M.B. (1968) A reinterpretation of Sr and Ca fractionation trends in plagioclase from basic rocks. Earth Planet. Sci. Lett., 4, 79-83.

Berlin, R., and Henderson, C.M.B. (1969) The distribution of Sr and Ba between the alkali feldspar, plagioclase and groundmass phases of porphyritic trachytes and phonolites. Geochim. Cosmochim Acta, 33, 247-255.

Beswick, A.E. (1973) An experimental study of alkali metal distribution in feldspars and micas. Geochim. Cosmochim. Acta, 37, 183-208.

Bird, G.W., and Anderson, G.M. (1973) The free energy of formation of magnesian cordierite and phlogopite. Am.J. Sci., 273, 84-90.

Bishop, A.C. and Woolley, A.R. (1973) A basalt-trachyte-phonolite series from Ua Pu, Marquesas Islands, Pacific Ocean. Contr. Mineral. and Petrol 39, 309-326.

Bottinga, Y., and Weill, D.F. (1970) Densities of liquid silicate systems calculated from partial molar volumes of oxide components. Am.J. Sci., 269, 169-182.

Bottinga, Y., and Weill, D.F. (1972) The viscosity of magmatic silicate liquids: a model for calculation. Am. J. Sci., 272, 438-475.

Bowen, N.L. (1928) the evolution of the igneous rocks. Dover Publications Inc., New York, 332p.

Buddington, A.F., and Lindsley, D.H. (1964) Iron-titanium oxide minerals and synthetic equivalents. J. Petrol., 5, 310-357.

Burnham, C.W. (1967) Hydrothermal fluids at the magmatic stage. In: Geochemistry of hydrothermal ore deposits (ed. H.L. Barnes), 34-76. Holt, Rinehart, and Winston, New York.

Burnham, C.W., Holloway, J.R., and Davis, N.F. (1969) Thermodynamic properties of water to 1000°C and 10 000 bars. Geol. Soc. Am. Special Paper 132.

Burton, J.D., and Culkin, F. (1972) Gallium. In Handbook of Geochemistry (ed. K.H. Wedepohl), 2/3, Springer Verlag, New York.

Butler, J.R., Bowden, P., and Smith, A.Z. (1962) K/Rb ratios in the evolution of the Younger Granites of Northern Nigeria. Geochim. Cosmochim. Acta, 26, 89-100.

Carmichael, I.S.E. (1963) The occurrence of magnesian pyroxenes and magnetite in porphyritic acid glasses. Mineral. Mag., 33, 394-403.

Carmichael, I.S.E. (1964) Natural liquids and the phonolitic minimum. Geol. J. 4, 55-60.

Carmichael, I.S.E. (1967) The iron-titanium oxides of salic volcanic rocks and their associated ferromagnesian silicates. Contr. Mineral. and Petrol., 14, 36-64.

Carmichael, I.S.E., and Mackenzie, W.S. (1963) Feldspar-liquid equilibria in pantellerites: an experimental study. Am. J. Sci., 261, 382-396.

Carmichael, I.S.E., and Nicholls, J. (1967) Iron-titanium oxides and oxygen fugacities in volcanic rocks. J. Geophys. Res., 72, 4665-4687.

Carmichael, I.S.E., Nicholls, J., and Smith, A.L. (1970) Silica activity in igneous rocks. Am. Mineral., 55, 246-263.

Clark, S.P., editor (1966) Handbook of physical constants. Geol. Soc. Am. Memoir 97.

Charles, R.W. (1973) The phase equilibria of intermediate compositions on the pseudobinary richterite-ferrorichterite (abstract). EOS, 54, 478.

Chao, E.C.T., and Fleischer, M. (1960) Abundance of zirconium in igneous rocks. 21st Int. Geol. Congr., 1, 106-131.

Coombs, D.S., and Wilkinson, J.F.G. (1969) Lineages and fractionation trends in undersaturated volcanic rocks from the East Otago Volcanic Province (New Zealand) and related rocks. J. Petrol., 10, 440-501.

Cox, K.G. (1972) The Karroo volcanic cycle. J. Geol. Soc., 128, 311-336.

Cox, K.G., Gass, I.G., and Mallick, D.I.J. (1970) The peralkaline volcanic suite of Aden and Little Aden, South Arabia. J. Petrol., 11, 433-461.

Currie, K.L. (1970) An hypothesis on the origin of alkaline rocks suggested by the tectonic setting of the Monteregian Hills. Can.Mineral., 10, 411-420.

Currie, K.L., and Ferguson, J. (1972) A study of fenitization in mafic rocks with special reference to the Callander Bay complex. Can. J. Earth Sci., 9, 1254-1261.

Currie, K.L., and Ferguson, J. (1971) A study of fenitization around the alkaline carbonatite complex at Callander Bay, Ontario, Canada. Can. J. Earth Sci., 8, 498-517.

Daly, R.A. (1933) Igneous rocks and the depths of the earth. McGraw-Hill, New York.

Davidson, A. (1970) Nepheline - K-feldspar intergrowths from Kaminak Lake, N.W. Territories. Can. Mineral., 10, 191-206.

Deans, T., Garson, M.S., and Coats, J.S. (1971) Fenite-type Na-metasomatism in the Great Glen, Scotland. Nature Phys. Sci., 234, 145-148.

Deer, W.A., Howie, R.A., and Zussman, J. (1962) Rock forming minerals: Volume 2: Chain Silicates. John Wiley and Sons, New York.

Deer, W.A., Howie, R.A., and Zussman, J. (1962) Rock forming minerals, Volume 3: Sheet Silicates. John Wiley and Sons, New York.

Deer, W.A., Howie, R.A., and Zussman, J. (1962) An introduction to the rock forming minerals. Longmans Green and Co. Ltd., London.

De Villiers, J. (1971) The younger Precambrian. In: Seventh, eighth, and ninth Annual Repts., P.R.U., Univ. of Cape Town, 48-51.

Dietz, R.S., and Holden, J.C. (1970) Reconstruction of Pangea: breakup and dispersion of the continents, Permian to Present. J. Geophys. Res., 75, 4939-49

Dupuy, C. (1968) Rubidium et caesium dans biotite, sanidine et verre des ignimbrites de Toscane (Italie). Chem. Geol., 3, 281-291.

Erlank, A.J. (1968) The terrestrial abundance relationship between potassium and rubidium. In: Origin and distribution of the elements (ed. L.H. Ahrens), 87-888, Pergamon Press, Oxford.

Ernst, W.G. (1968) Amphiboles. Springer Verlag, New York.

Eugster, H.P., and Shippen, G.B. (1967) Igneous and metamorphic reactions involving gas equilibria. In: Researches in Geochemistry, vol. 2 (ed. P.H. Abelson), 492-520, John Wiley and Sons, New York.

Eugster, H.P., and Wones, D.R. (1962) Stability relations of the ferrugineous biotite, annite. J. Petrol., 3, 82-155.

Ewart, A., Green, D.C., Carmichael, I.S.E., and Brown, F.H. (1971) Voluminous low-temperature rhyolitic magmas in New Zealand. Contr. Mineral. and Petrol. 33, 128-145.

Ewart, A., Taylor, S.R., and Capp, A.C. (1968) Geochemistry of the pantellerites of Mayor Island, New Zealand. Contr. Mineral. and Petrol., 17, 116-140.

Ewart, A., Taylor, S.R., and Capp, A.C. (1968) Trace and minor element geochemistry of the rhyolitic volcanic rocks, Central North Island, New Zealand. Total rock and residual liquid data. Contr. Mineral. and Petrol., 18, 76-104.

Ferguson, J. (1970) The differentiation of agpaitic magmas: the Ilimaussaq intrusion, South Greenland. Can. Mineral., 10, 335-349.

Ferguson, J., and Currie, K.L. (1971) Evidence of liquid immiscibility in alkaline ultrabasic dykes at Callander Bay, Ontario. J. Petrol., 12, 561-586.

Fleischer, M. (1965) Some aspects of the geochemistry of Yttrium and the Lanthadnides. Geochim. Cosmochim Acta, 29, 755-772.

Francheteau, J., and Le Pichon, X. (1972) Marginal fracture zones as structural framework of continental margins in the South Atlantic Ocean. Bull. Am. Assoc. Petroleum Geologists., 56, 991-100%.

Gass, I.G. (1972) Proposals concerning the variation of volcanic products and processes within the oceanic environment. Phil. Trans. Roy. Soc. London, A271, 131-140.

Gerasimovskii, V.I. (1956) Geochemistry and mineralogy of nepheline syenite intrusions. Geochemistry, 5, 494-510.

Gill, R.C.O. (1972) Chemistry of peralkaline dykes from the Grønnedal-Ika area, S. Greenland. Contr. Mineral. and Petrol., 34, 87-100.

Goldsmith, J.R., and Laves, F. (1954) The microcline stability relations. Geochim. Cosmochim. Acta, 5, 1-19.

Goodman, R.J. (1972) The distribution of Ga and Rb in coexisting groundmass and phenocryst phases of some basic volcanic rocks. Geochim. Cosmochim. Acta. 36, 303-318.

Green, D.H. (1970) A review of the experimental evidence on the origin of basaltic and nephelinitic magmas. Phys. Earth Planet. Interiors, 3, 221-235.

Green, D.H., and Ringwood, A.E. (1967) the genesis of basaltic magmas. Contr. Mineral. and Petrol., 15, 103-190.

Haas, J.L., and Robie, R.A. (1973) Thermodynamic data for wustite, $Fe_{0,947}O$, magnetite, Fe_3O_4, and hematite, Fe_2O_3 (abstract). EOS, 54, 483.

Hallam, G.D. (1964) The geology of the coastal diamond deposits of Southern Africa. In: The geology of some ore deposits in southern Africa., 2, 671-728.

Hamilton, D.L. (1961) Nepheline as crystallization temperature indicators. J. Geol. 69, 321-329.

Hamilton, D.L., Burnham, C.W., and Osborn, E.F. (1964) The solubility of water and effects of water fugacity and water content on crystallization in mafic magmas. J. Petrol., 5, 21-39.

Heier, K.S. (1966) Some crystallochemical relations of nephelines and feldspars on Stjernoy, N. Norway. J. Petrol., 7, 95-113.

Heinrich, E.W. (1966) The geology of carbonatites. Rand McNally and Co., Chicago.

Heming, R.F., and Carmichael, I.S.E. (1973) High temperature pumice flows from the Rabaul Caldera, Papua New Guinea. Contr. Mineral. and Petrol., 38, 1-20.

Herrmann, A.G. (1970) Yttrium and the Lanthanides. In: Handbook of Geochemistry (ed. K.H. Wedepohl), 2/2, Springer Verlag, Berlin.

Holland, J.G., and Brown, G.M. (1972) Hebriddean tholeiitic magmas: a geochemical study of the Ardnamurchan cone sheets. Contr. Mineral. and Petrol., 37, 139-160.

Jackson, E.D. (1967) Ultramafic cumulates in the Stillwater, Great Dyke, and the Bushveld intrusions. In: Ultramafic and related rocks (ed P.J. Wyllie), 20-38.

Kable, E.J.D. (1972) Some aspects of the geochemistry of selected elements in basalts and associated lavas. Unpbl. Ph.D. thesis, Univ. of Cape Town.

Kaiser, E. (1926) Die diamantenwuste Sudwestafrikas. Volume 1, Dietrich Reimer, Berlin.

Kaiser, E. (1926) Die Diamantenwuste Sudwestafrikas. Volume 2, Dietrich Reimer, Berlin.

Kelley, K.K. (1962) Heats and free energies of formation of anhydrous silicates. U.S. Bureau of Mines Rept. of Invest. 5901, 32p.

Kelsey, C.H., and McKie, D. (1964) The unit cell of aenigmatite. Mineral. Mag., 33, 986-1001.

Kennedy, G.C. (1955) Some aspects of the role of water in rock melts. Geol. Soc. Amer. Spec. Paper 62, 489-504.

King, L.C. (1951) South African Scenery. 2nd Ed. Oliver and Boyd, Edinburgh.

Korringa, M.K., and Noble, D.C. (1971) Distribution of Sr and Ba between natural feldspars and igneous melt. Earth Planet. Sci. Lett., 11, 147-151.

Kroner, A. (1972) Preliminary resume of the geology of the Gariep geosyncline in

Kesler S.E. (1968) Mechanisms of magmatic assimilation at a marble contact, Northern Haiti, Lithos, 1, 219-229

the Orange River area. In: Seventh, eighth, and ninth Ann. Repts. P.R.U. Univ. of Cape Town., 51-57.

Le Maitre, R.W. (1968) Chemical variation within and between volcanic rock series - a statistical approach. J. Petrol., 9, 220-252.

Le Pichon, X., and Hayes, D.E. (1971) Marginal offsets, fracture zones and the early opening of the South Atlantic. J. Geophys. Res., 76, 6283-6293.

Lovering, T.G. (1969) Distribution of minor elements in samples of biotite from igneous rock. In: Geological Survey research, 1969: U.S. Geol. Survey Prof. Paper 650-B, 101-106.

Lowder, G.G. (1970) The volcanoes and caldera of Talasea, New Britain: Mineralogy. Contr. Mineral. and Petrol. 26, 324-340.

McBirney, A.R., and Williams, H. (1969) Geology and petrology of the Galapagos Islands. Geol. Soc. Amer. Memoir 118, 197p.

MacDonald, R. (1969) The petrology of alkaline dykes from the Tugtutoq area, S. Greenland. Bull. Geol. Soc. Denmark, 19, 257-282.

MacDonald, R., and Edge, R.A. (1970) Trace element distribution in alkaline dykes from the Tugtutoq region, S. Greenland. Bull. Geol. Soc. Denmark, 20, 38-58.

MacDonald, R., and Parker, A. (1969) Zirconium in alkaline dykes from the Tugtutoq region, S. Greenland. Bull. Geol. Soc. Denmark, 20, 59-63.

MacDonald, R., Bailey, D.K., and Sutherland, D.S. (1970) Oversaturated peralkaline glassy trachytes from Kenya. J. Petrol., 11, 507-517.

McDowell, S.D., and Wyllie, P.J. (1971) Experimental studies of igneous rock series: The Kungnat syenite complex of southwest Greenland. J. Geol. 79, 173-194.

McElhinny, M.W. (1973) Mantle plumes, paleomagnetism and polar wandering. Nature Phys. Sci., 241, 523-524.

McKie, D. (1966) Fenitization. In: Carbonatites (ed. O.F. Tuttle and J. Gittins) Interscience, New York.

Marsh, J.S. (1973) Relationships between transform directions and alkaline igneous rock lineaments in Africa and South America. Earth. Planet. Sci. Lett., 18, 317-323.

Martin, H. (1965) The Precambrian geology of South West Africa and Namaqualand. Precambrian Research Unit, Univ. of Cape Town, 159p.

Martin, R.F. (1969a) The hydrothermal synthesis of low albite. Contr. Mineral. and Petrol. 23, 323-339.

Martin, R.F. (1969b) The effect of fluid composition on structural state of alkali feldspars. Trans. Am. Geophys. Union, 50, 350.

Melfi, A.J. (1967) Potassium-argon ages for core samples from Southern Brazil. Geochim. Cosmochim. Acta, 31, 1079-1089.

Millhollen, G.L. (1971) Melting of nepheline syenite with H_2O and H_2O+CO_2, and the effect of dilution of the aqueous phase on the beginning of melting Am. J. Sci., 270, 244-254.

Mitchell, R.H. (1972) Composition of nepheline, pyroxene and biotite in ijolite from the Seabrook Lake complex, Ontario, Canada. N. Jb. Miner. Mh., 9, 415-422.

Mitchell, R.H. (1973) Composition of olivine, silica activity, and oxygen fugacity in kimberlite. Lithos, 6, 65-82.

Mueller, R.F. (1971) Oxidative capacity of magmatic components. Am. J. Sci., 270, 236-243.

Mukherjee, A. (1967) Role of fractional crystallization in the descent: basalt - trachyte. Contr. Mineral. and Petrol., 16, 139-148.

Nash, W.P., Carmichael, I.S.E., and Johnson, R.W. (1969) The mineralogy and petrology of Mount Suswa, Kenya. J. Petrol., 10, 409-439.

Nash, W.P., and Wilkinson, J.F.G. (1970) Shonkin Sag laccolith, Montana. 1: mafic mineralogys and estimates of temperature, pressure, oxygen fugacity, and silica activity. Contr. Mineral. and Petrol., 20, 268-294.

Nicholls, J., and Carmichael, I.S.E. (1967) Iron-titanium oxides and oxygen fugacities in volcanic rocks. J. Geophys. Res., 72, 4665-4687.

Nicholls, J., and Carmichael, I.S.E. (1969) Peralkaline acid liquids: a petrological study. Contr. Mineral. and Petrol., 20, 268-294.

Nicholls, J., and Carmichael, I.S.E. (1972) The equilibration temperature and pressure of various lava types with spinel and garnet peridotite. Am. Mineral., 57, 941-959.

Nicholls, J., Carmichael, I.S.E., and Stormer, J.C. (1971) Silica activity and P_{Total} in igneous rocks. Contr. Mineral. and Petrol., 33, 1-20.

Noble, D.C. (1968) Systematic variation of major elements in comendite and pantellerite glasses. Earth Planet. Sci. Lett., 4, 167-172.

Noble, D.C. (1970) Loss of sodium from crystallized comendite welded tuffs of the Miocene Grouse Canyon member of the Belted Range Tuff, Nevada. Bull. Geol. Soc. Amer., 81, 2677-2688.

Noble, D.C. Haffty, J., and Hedge, C.E. (1969) Strontium and magnesium contents of some natural peralkaline silicic glasses and their petrogenetic significance. Am. J. Sci., 267, 598-608.

Noble, D.C., Korringa, M.K., and Haffty, J. (1971) Distribution of calcium between alkali feldspar and glass in some highly differentiated silicic volcanic rocks, Am. Mineral., 56, 2088-2097.

Nolan, J. (1966) Melting relations in the system $NaAlSi_3O_8$-$NaAlSiO_4$-$NaFeSi_2O_6$-$CaMgSi_2O_6$-H_2O and their bearing on the genesis of alkaline undersaturated rocks. Geol. Soc. London Quart. J., 122, 119-158.

Norrish, K., and Hutton, J.T. (1969) An accurate X-ray spectrographic method for analysis of a wide range of geological samples. Geochim. Cosmochim. Acta, 33, 431-453.

Osborn, E.F. (1959) Role of oxygen pressure in the crystallization and differentiation of basaltic magmas. Am. J. Sci., 257, 609-647.

Osborn, E.F. (1962) Reaction series for subalkaline igneous rocks based on different oxygen pressure conditions. Am. Mineral., 47, 211-226.

Parsons, I., and Boyd, R. (1971) Distribution of potassium feldspar polymorphs in intrusive sequences. Mineral. Mag., 38, 293-311.

Pearce, T.H. (1968) A contribution to the theory of variation diagrams. Contr. Mineral. and Petrol., 19, 142-157.

Philpotts, A.R., and Hodgson, C.J. (1968) Role of liquid immiscibility in alkaline rock genesis. 23rd Int. Geol. Congr., 2, 175-188.

Philpotts, J.A., and Schnetzler, C.C. (1970) Phenocryst matrix partition coefficient for K, Rb, Sr, and Ba with application to anorthosite and basalt genesis. Geochim. Cosmochim. Acta, 34, 307-322.

Presnall, D.C. (1966) The join forsterite-diopside-iron oxide and its bearing on the crystallization of basaltic and ultramafic magmas. Am. J. Sci., 264, 753-809.

Poldervaart, A., and Parker, A.B. (1964) The crystallization index as a parameter of igneous differentiation in binary variation diagrams. Am. J. Sci., 262, 281-289.

Puchelt, H. (1972) Barium. In: Handbook of Geochemistry (ed. K.H. Wedepohl), 2/3, Springer Verlag, Berlin.

Ragland, P.C. (1970) Composition and structural state of the potassic phase in perthites as related to petrogenesis of a granite pluton. Lihtos, 3, 167-189.

Rhodes, J.M. (1969) On the chemistry of potassium feldspars in granitic rocks. Chem. Geol., 4, 373-392.

Rhodes, R.C. (1972) Structural geometrey of sub-volcanic ring complexes as related to pre-Cenozoic motions of continental plates. Tectonophysics, 12, 111-117.

Ridley, W.I. (1970) The petrology of the Las Canadas volcanoes, Tenerife, Canary Islands. Contr. Mineral. and Petrol., 26, 124-160.

Rogers, J.J.W.,and Adams, J.A.S. (1969) Thorium. In: Handbook of Geochemistry (ed. K.H. Wedepohl), 2/1, Springer Verlag, Berlin.

Robertson, J.K., and Wyllie, P.J. (1971) Experimental studies on rocks from the Debouille Stock, Northern Maine, including melting relations in the water defficient environment, J. Geol., 79, 549-571.

Robie, R.A., and Waldbaum, D.R. (1968) Thermodynamic properties of minerals and related substances at 298, 15°K (25,0°C) and one atmosphere (1,013 bars) pressure, and at higher temperature. U.S. Geol. Surv. Bulletin 1259.

Scharbert, H.G. (1966) The alkali feldspars from microsyenite dykes of southern Greenland. Mineral. Mag., 35, 903-919.

Shand, S.J. (1915) The alkaline rocks of South West Africa. Geol. Mag., 11, 575.

Shand, S.J. (1945) The present status of Daly's hypothesis on the alkaline rocks. Am. J. Sci. (Daly Volume), 243-A, 495-507.

Shand, S.J. (1930) Limestone and the origin of feldspathoidal rocks: an aftermath of the Geological Congress. Geol. Mag., 67, 415-427.

Shapiro, L., and Brannock, W.W. (1956) Rapid analysis of silicate rocks. U.S. Geol. Surv. Bulletin 1036-C.

Shaw, D.M. (1968) A review of K-Rb fractionation trends by co-variance analysis. Geochim. Cosmochim. Acta, 32, 573-601.

Shaw, H.R. (1963) Obsidian - H_2O viscosities at 1000 and 2000 bars in the T range 700°C to 900°C. J. Geophys Res., 68, 6337-6343.

Shaw, H.R. (1967) Hydrogen osmosis in hydrothermal experiments. In: Researches in

Geochemistry (ed. P.H. Abelson), 2, 521-541, John Wiley and sons, New York.

Shaw, H.R., and Wones, D.R. (1964) Fugacity coefficients for hydrogen gas between 0°C and 1000°C for pressures to 3000 atm.. Am. J. Sci., 262, 918-929.

Siedner, G. (1965) Geochemical features of a strongly fractionated alkali igneous suite. Geochim. Cosmochim. Acta, 29, 113-137.

Siedner, G., and Miller, G.A. (1968) K-Ar age determinations on basaltic rocks from South West Africa, and their bearing on continental drift. Earth Planet. Sci. Lett., 4, 451-458.

Simpson, E.S.W. (1954) The Okonjeje Igneous complex. Trans. Geol. Soc. S. Afr., 57, 125-172.

Smith, A.L. (1970) Sphene, perovskite and coexisting Fe-Ti oxide minerals. Am. Mineral., 55, 264-269.

Smith, J.V. (1970) Physical propertouies of order - disorder structures with especial reference to the feldspar minerals. Lithos, 3, 145-160.

Sood, M.K., and Edgar, A.D. (1970) Melting relations of undersaturated alkaline rocks from the Ilimaussaq intrusion and Grønnedal-Ika complex, South Greenland, under water vapour and controlled partial oxygen pressures. Medd. Grønland, 181, No. 12.

Sørensen, H. (1960) On the agpaitic rocks. 21st Int. Geol. Congr., 13, 319-327.

Sørensen, H. (1968) Rhythmic igneous layering in peralkaline intrusions. An essay review on Ilimaussaq (Greenland), and Lovozero (Kola, USSR). Lithos, 2, 261-283.

Stormer, J.C. (1972) Mineralogy and petrology of the Raton-Clayton volcanic field, NE New Mexico. Bull. Geol. Soc. Amer., 83, 3299-3322.

Stormer, J.C., and Carmichael, I.S.E. (1971) The free energy of sodalite and the behaviour of chloride, fluoride and sulfate in silicate magmas. Am. Mineral., 56, 292-306.

Tanner, P.W.G., and Tobisch, O.T. (1972) Sodic and ultra-sodic rocks of meta-somatic origin from part of the Moine Nappe. Scott. J. Geol., 8, 151-178.

Taylor, S.R. (1965) The application of trace element data to problems in petrology. Phys. Chem. of the Earth, 6, 123-213.

Stephenson D. (1972) Alkali clinopyroxenes from nepheline syenites of the South Qôroq Centre, south Greenland Lithos, 5, 187-201.

Thompson, J.B., and Waldbaum, D.R. (1969) Mixing properties of sanidine crystalline solutions: III, calculations based on two phase data. Am. Mineral., 54, 811-838.

Thompson, R.N., and MacKenzie, W.S. (1967) Feldspar-liquid equilibria in peralkaline acid liquids: an experimental study. Am. J. Sci., 265, 714-734.

Thornton, C.P., and Tuttle, O.F. (1960) Chemistry of igneous rocks: I. Differentiation Index. Am. J. Sci., 258, 664-684.

Tilley, C.E., and Thompson, R.N. (1972) Melting relations of some ultra-alkaline volcanics. Geol. J., 8, 65-70.

Towell, D.G., Winchester, J.W., and Spirn, R.V.V. (1965) Rare-earth distributions in some rocks and associated minerals of the batholith of Southern California. J. Geophys. Res., 70, 3485-3496.

Turner, F.J. (1968) Metamorphic petrology - mineralogical and field aspects. McGraw-Hill Inc. New York.

Turner, F.J., and Verhoogen, J. (1960) Igneous and Metamorphic Petrology. McGraw-Hill Inc. New York.

Tuttle, O.F., and Bowen, N.L. (1958) Origin of granite in the light of experimental studies in the system $NaAlSi_3O_9$ - $KAlSi_3O_8$ - SiO_2. Geol. Soc. Am. Memoir 74, 153p.

Upton, B.G.J. (1960) The alkaline igneous complex of Kungnat Fjeld South Greenland. Bull. Grønlands Geol. Unders., 27, 145p.

Upton, B.G.J. (1964) Geology of Tugtutoq and neighbouring islands, South Greenland, Pt IV. The nepheline syenites of the Hviddal composite dyke. Bull. Grønlands Geol. Unders., 48, 49-80.

Verhoogen, J. (1962) Oxidation of Iron-titanium oxides in igneous rocks. J. Geol., 70, 168-181.

Verhoogen, J. (1962) Distribution of titanium between silicates and oxides in igneous rocks. Am. J. Sci., 260, 211-220.

Verwoerd, W.J. (1966) Fenitization of basic igneous rocks. In: Carbonatites (ed. O.F. Tuttle and J. Gittins) Interscience, New York.

Verwoerd, W.J. (1968) The carbonatites of South Africa and South West Africa. Geol. Surv. S. Afr. Handbook 6.

Vlasov, K.A., Kuzmenko, M.Z., and Eskova, E.M. (1966) The Lovozero Alkali Massif. Oliver and Boyd, Edinburgh.

Von Brunn, V. (1967) Acid and basic igneous rock associations west of Helmeringhausen, South West Africa. Unpubl. Ph.D. thesis Univ. of Cape Town.

Von Brunn, V. (1969) Igneous rocks of the Nagatis and Sinclair Formations northeast of Luderitz, South West Africa. Bull. P.R.U. Univ. of Cape Town, 7.

Vogel, T.A. (1970) Albite-rich domains in K-feldspars. Contr. Mineral. and Petrol. 25, 138-143.

Wadsworth, W.J. (1973) Magmatic sediments. Mineral Sci. and Eng., 5, 25-35.

Wagner, P.A. (1910) About an occurrence of nepheline syenite in Luderitz, German South West Africa. Centralblatt. f. Mineral., 721.

Watkinson, D.H., and Wyllie, P.J. (1971) Experimental study of the composition join $NaAlSiO_4$ - $CaCO_3$ - H_2O and the genesis of alkaline rock carbonatite complexes. J. Petrol., 12, 357-378.

Weaver, S.D., Sceal, J.S.C., and Gibson, I.L. (1972) Trace element data relevant to the origin of trachytic and pantelleritic lavas in the East African Rift System. Contr. Mineral. and Petrol., 36, 181-194.

Williams, R.J. (1971) Reaction constants in the system Fe - MgO - SiO_2 - O_2 at 1 atm between 900° and 1300°C. Am. J. Sci., 270, 334-360.

Wilson, J.T. (1965) A new class of faults and their bearing on continental drift. Nature, 207, 343.

Wright, J.B. (1971) The phonolite - trachyte spectrum. Lithos, 4, 1-5.

Wright, T.L. (1968) X-ray and optical study of alkali feldspar: II. An X-ray method for determining the composition and structural state from measurements of 2θ values for three reflections. Am. Mineral., 53, 88-104.

Wones, D.R. (1972) Stability of biotite; a reply. Am. Mineral. 57, 316-317.

Wones, D.R., and Eugster, H.P. (1965) Stability of biotite: experiment, theory and application. Am. Mineral., 50, 1228-1272.

Wones, D.R., and Gilbert, M.C. (1969) The fayalite-magnetite-quartz assemblage between 600° and 800°C. Am J. Sci. 267A, 480-488.

Wyllie, P.J., and Watkinson, D.H. (1970) Phase equilibrium studies bearing on genetic links between alkaline and subalkaline magmas with special reference to the limestone assimilation hypothesis, Can. Mineral., 10, 362-374.

Yoder, H.S., and Tilley, C.E. (1962) Origin of basalt magmas: an experimental study

of natural and synthetic rock systems. J. Petrol., 3, 342-532.

Zen, E-an (1973) Thermochemical parameters of minerals from oxygen buffered hydrothermal equilibrium data: method, application to anni[illegible] and almandine. Contr. Mineral. and Petrol., 39, 65-80.

ADDENDUM

Aoki, K. (1964) Clinopyroxenes from the alkaline rocks of Japan. Am. Miner., 49, 1199-1223.

Carmichael, I.S.E. (1962) Pantelleritic liquids and their phenocrysts. Mineral. Mag., 33, 86-113.

Christophe Michel-Levy, M. (1962) Reproduction artificielle de quelques mineraux riches on zirconium (zircon, eudialyte, catapleite, elpidite): comparison avec leurs conditions naturelles de formation. Bull. Soc. Franc. Mineral. Crist., 84, 265-269.

Lipman, P.W. (1971) Iron-titanium oxide phenocrysts in compositionally zoned ash flow sheets from southern Nevada. J. Geol., 79, 438-456.

Prins, P. (1972) Composition of magnetite from carbonatite. Lithos, 5, 227-246.

Rodrigues, B. (1970) Tectonic alignments related with alkaline intrusions in Angola and Brazil. 2nd Gondwana Symposium, CSIR, Pretoria, 457-460.

Wones, D.R. (1970) Amphibole - biotite relations (abstract) Am. Mineral., 55, 295-296.

Yagi, K. (1953) Petrochemical studies on the alkalic rocks of the Morutu district, Sakhalin. Bull. Geol. Soc. Amer., 64, 769-810.

Drachenberg Syenite Complex

SCALE 1:10,000

0 1/2 1 km

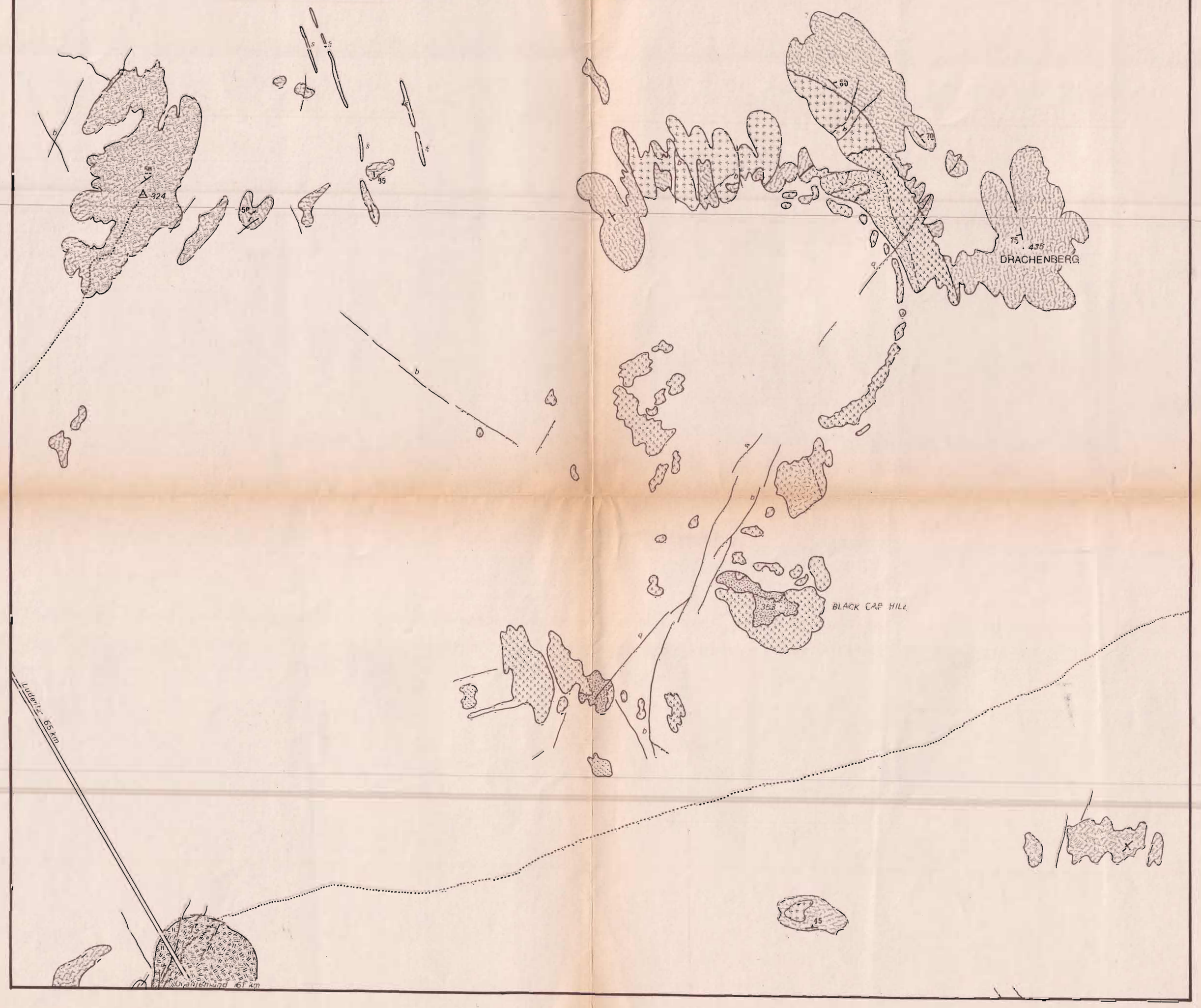

- SAND, minor gravels, calcrete — Tertiary to Recent

Drachenberg Syenite Complex — Early Cretaceous ?

- Quartz-feispar porphyry dykes
- Bostonite dykes
- Syenite porphyry
- Various SYENITES, NORDMARKITE
- BIOTITE-RICH SYENITE
- Fine and coarse grained PORPHYRITIC SYENITES
- QUARTZ MONZONITE

Pre-Gariep — > 900 my.

- Quartz veins
- GRANITE
- METASEDIMENTS – quartz schists, phyllite, garnet hornfelses

- Dip of foliation
- Main road
- Jeep track
- Δ324 Trig beacon (height in metres)
- ·435 Spot height (metres)

N

mapped 7/71, drawn 1/73 By J.S.M.

Pomona Syenite Complex

SCALE 1:10,000

0 1/2 1 km

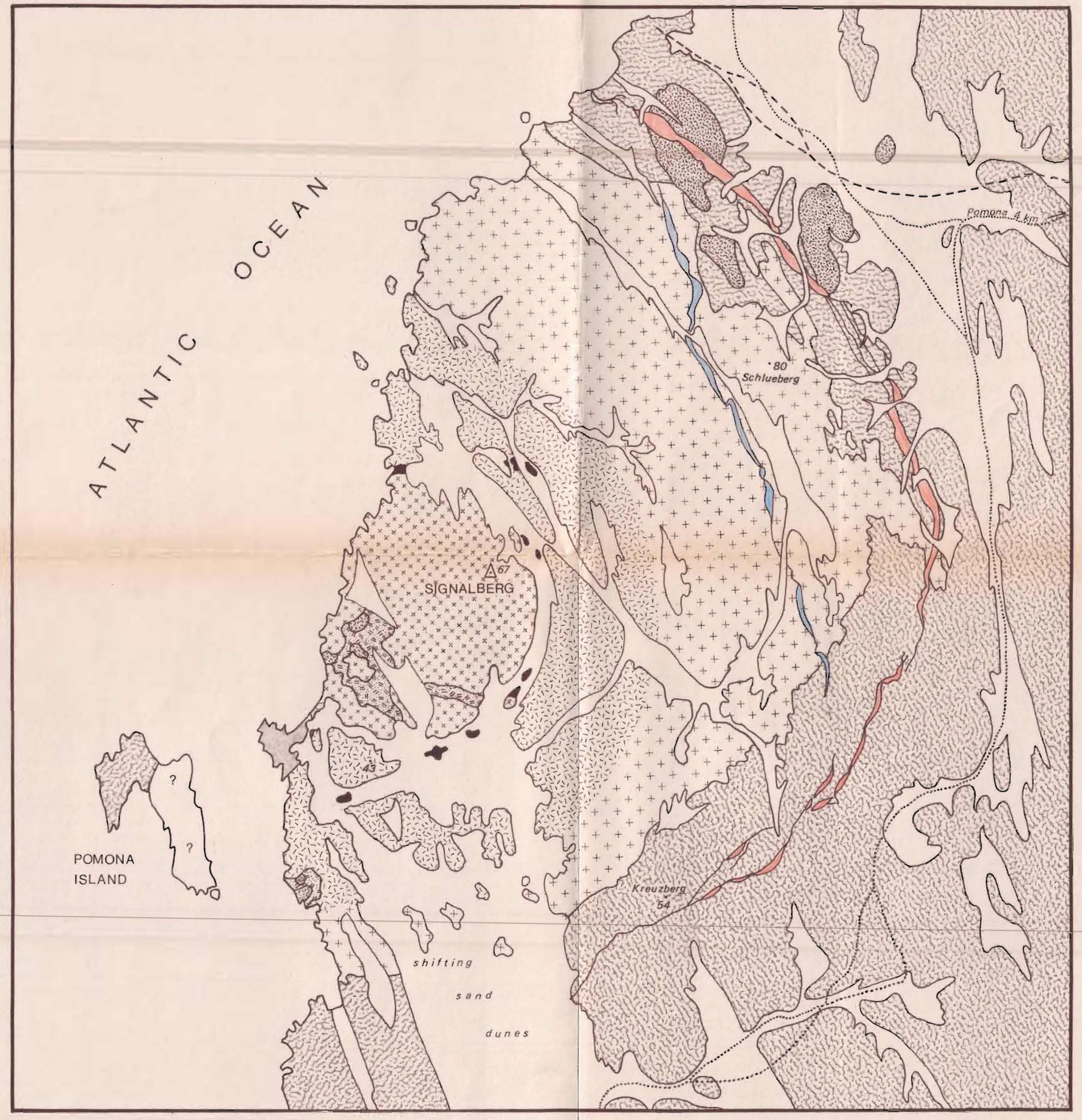

- SAND, minor gravels — Tertiary to Recent
- Bostonite dyke
- OUTER RING DYKE – nordmarkite
- POMONA FOYAITE
- SYENITE PORPHYRY
- Agglomerate, breccia with associated quartz-feldspar pophyry in the NE
- HUB SYENITE – nordmarkite
- OUTER SYENITE
- INNER SYENITE
- BIOTITE-RICH MONZONITE

Pomona Syenite Complex — Early Cretaceous ?

- Various GNEISSES, SCHISTS — Kheis ? > 1850 my.

- ---- Abandoned railway line
- ..... Jeep track
- △67 Trig beacon (height in metres)
- ·43 Spot height (metres)

T.N

mapped 5/70 and 7/71, drawn 1/73 by J.S.M.